BIOPROSPECTING MICROALGAE AS POTENTIAL SOURCES OF "GREEN ENERGY"—CHALLENGES AND PERSPECTIVES (REVIEW)

© 2012 S. K. Ratha, R. Prasanna

Division of Microbiology, Indian Agricultural Research Institute, New Delhi — 110012, India
e-mail: radhapr@gmail.com

Microalgae and cyanobacteria are potential foods, feeds, sources of high-value bioactive molecules and biofuels, and find tremendous applications in bioremediation and agriculture. Although few efforts have been undertaken to index the microalgal germplasm available in terms of lipid content, information on suitability of strains for mass multiplication and advances in development of methods for extraction and generating biofuel are scarce. Our review summarizes the potential of microalgae, latest developments in the field and analyzes the "pitfalls" in oversimplification of their promise in the years to come. Microalgae represent "green gold mines" for generating energy; however, the path to success is long and winding and needs tremendous and concerted efforts from science and industry, besides political will and social acceptance for overcoming the limitations. The major advantages of second generation biofuels based on microalgal systems, include their higher photon conversion efficiency, growth all around the year, even in wastewaters, and production of environment friendly biodegradable biofuels.

Microalgae are microscopic photosynthetic organisms that are found in marine and freshwater environments, besides being prevalent in soil and air. They include unicellular, microscopic (2—200 μm), polyphyletic, highly diverse, non-cohesive, oxygen evolving autotrophic organisms which grow by photosynthesis. The term algae has no formal taxonomic standing and is defined as thallophytes (plant body lack of roots, embryos, vascular system, stems and leaves) that have chlorophyll-a as their primary photosynthetic pigment and lack a sterile covering of cells around the reproductive organs [1].

The number of algal species has been estimated to be one to ten million, and most of them are microalgae. It has been estimated that about 200000—800000 species of microalgae exist, of which about 35000 species are described. Over 15000 novel compounds originating from algal biomass have been chemically determined [2]. Most of these microalgal species produce unique products like carotenoids, antioxidants, fatty acids, enzymes, polymers, peptides, toxins and sterols [3]. Their photosynthetic mechanism is similar to land plants, but due to their simple cellular structure and submergence in an aqueous environment, in most cases, where they have an efficient access to water, CO_2 and other nutrients, they are generally more efficient in converting solar energy to biomass than terrestrial plants and are efficient CO_2 fixers. They account for ~50% of global organic carbon fixation.

The evolutionary history and taxonomy of microalgae is complex due to constant revisions as a result of new genetic and ultrastructural evidence. The main criteria for categorizing microalgae are pigmentation, life cycle and basic cellular structure [1]. Algae are classified into 11 divisions comprising 2 prokaryotic divisions — Cyanophyta/Cyanobacteria and prochlorophyta (although the prokaryotic cyanobacteria are frequently included as algae) and 9 eukaryotic divisions (Glaucophyta, Rhodophyta, Heterokontophyta, Haptophyta, Cryptophyta, Dinophyta, Euglenophyta, Chlorarachniophyta and Chlorophyta) [4]. Many algae can switch from phototrophic to heterotrophic growth, and some can also grow mixotrophically [5].

Overview of applications of microalgae. The use of microalgae by human populations goes back to around thousands years ago. The first reported use of "microalgae" by humans is that by the Chinese who utilised *Nostoc* and other edible cyanobacteria as an emergency food source some 2000 years ago. But the mass culture of microalgae began shortly after World War II in the USA, Germany and Japan as a potential source of food in a world experiencing a population explosion. Since then, mass culturing of microalgal species have been variously explored in the treatment of wastewater and control of water pollution, for atmosphere regeneration in biospheres (i.e., spacecraft), as renewable fuels for transportation (biodiesel), as a source of high value natural health products (nutraceuticals) and lately in the mitigation of greenhouse gases (GHG) and the production of hydrogen as a fuel source [6].

Microalgae are potentially a great source of natural compounds that could be used as ingredients for preparing foods and enhancing the nutritional food content of humans and animals. Research initially focused on algal biomass as a source of protein and the

Table 1. Selected microalgal species with their products and application areas

Genus/group	Product	Application areas	References
Spirulina (*Arthrospira platensis*)/Cyanobacteria	Phycocyanin, biomass	Health food, cosmetics	[12]
Aphanizomenon flos-aquae/Cyanobacteria	Phycocyanin, biomass	Pharmaceuticals, nutrition	[13]
Lyngbya majuscula/Cyanobacteria	Immunomodulators	Pharmaceuticals, nutrition	[14]
Anabaena/Cyanobacteria	Bioactive metabolites/ hydrolytic enzymes	Agriculture and industry	[10, 11]
Chlorella minutissima/Chlorophyta	Eicosapentaenoic acid, Polyunsaturated fatty acids	Food additive, nutraceuticals	[2]
Chlorella vulgaris/Chlorophyta	Biomass	Health food, food supplement, feed surrogates	[12]
Prototheca moriformis/Chlorophyta	Ascorbic acid	Nutrition	[13]
Dunaliella salina/Chlorophyta	Carotenoids, β-carotene	Health food, food supplement, feed	[14]
Haematococcus pluvialis/Chlorophyta	Carotenoids, astaxanthin, leutein	Health food, pharmaceuticals, feed additives	[8, 14, 15]
Muriellopsis sp./Chlorophyta	Carotenoids, lutein	Health food, food supplement, feed	[14]
Isochrysis galbana /Chlorophyta	Fatty acids	Animal nutrition	[16]
Euglena gracilis/Euglenophyta	Biotin	Nutrition	[17]
Crypthecodinium cohnii/Dinophyta	Lipids, fatty acids	Pharmaceuticals, fuel production	[18]
Nannochloropsis /Eustigmatophyceae	Lipids, fatty acids	Pharmaceuticals	[19]
Odontella aurita/Bacillariophyta	Fatty acids	Pharmaceuticals, cosmetics, baby food	[16]
Phaedactylum tricornutum/Bacillariohyta	Lipids, fatty acids	Nutrition, fuel production	[20, 21]
Porphyridium cruentum /Rhodophyta	Polysaccharides	Pharmaceuticals, cosmetics, nutrition	[22]

systematic examination of algae for biologically active compounds and pharmaceuticals. The high protein content of various microalgal species is one of the main reasons to consider them as unconventional sources of protein. As their cells are capable of synthesizing all amino acids, they can provide the essential ones to humans and animals. They also represent a valuable source of nearly all essential vitamins (e.g., A, B1, B2, B6, B12, C, E, nicotinate, biotin, folic acid and pantothenic acid) [7]. Vitamins improve the nutritional value of algal cells but their quantity fluctuates with environmental factors, the harvesting treatment and the method of drying the cells [9]. They are also rich in pigments like chlorophyll (0.5% to 1% of dry weight), carotenoids (0.1% to 0.2% of dry weight on average and up to 14% of dry weight for β-carotene of *Dunaliella*) and phycobiliproteins. Carbohydrates in microalgae can be found in the form of glucose, starch and polysaccharides. Their overall digestibility is high, which is why there is no limitation to using dried whole microalgae in foods or feeds. The average lipid content of algal cells varies between 1% and 70% but can reach 90% of dry weight under certain conditions [8]. More recently, algae have been used successfully to produce biodiesel, polyunsaturated fatty acids (PUFA), such as docosahexaenoic and eicosapentaenoic acids. Different compounds with anti-bacterial, anti-viral

and anti-fungicidal activity can be found in these types of organisms [8−11]. The most frequently used microalgae belong to Cyanophyceae (cyanobacteria/blue-green algae), Chlorophyceae (green algae), Bacillariophyceae (including the diatoms) and Chryssophyceae (including golden algae). A list of selected microalgal species with their products and applications is given in Table 1.

Significance of biofuels. Energy is an indispensable factor to sustain our economic growth and quality of living standards. A rapidly growing world population and rising consumption of fossil fuels is increasing the demand for both food and biofuels [23], which can lead to energy shortage. Producing biofuels requires huge amounts of both fossil energy and food resources, which will intensify conflicts among these resources. Global warming is caused by indiscriminate use of resources, in particular of fossil fuel for a variety of human needs and is largely responsible for climate change. The current definition of progress is largely confined to economic well being of humankind dictated by access to modern technologies, which are driven by modern energy carriers. Along with the increased demands of the burgeoning populations, the production and use of fossil fuel based energy sources has led to the degradation of the environment.

Among the GHG, which are responsible for global warming, CO_2 is the most prominent one. According to information given in World Energy Outlook-2009 of the International Energy Agency (IEA), the energy sector contributes 84% of global CO_2 emissions and 64% of the world's GHG emissions. If no action is initiated, the contributions will increase to about 91% of the global CO_2 emissions by 2030 and the share in GHG emissions is likely to reach 71%. In an absolute sense, energy-related emissions are expected to increase from 28.8 Gt in 2007 to 40.2 Gt in 2030. To limit the global average temperature increase of $2°C$, the concentration of GHG in the atmosphere has to be stabilized at a level of around 450 ppm CO_2. The energy sector contribution is expected to be very significant to achieve this target. According to the IEA, in this scenario, the global energy-related CO_2 emissions are expected to peak at 30.9 Gt by 2020 and decline thereafter to 26.4 Gt in 2030. Enhancing the energy efficiency is expected to be the largest contributor to abatement of CO_2 emissions till 2030 [24].

Biofuel can be broadly defined as solid, liquid, or gas fuel consisting of/or derived from biomass. In 1900, Rudolph Diesel first demonstrated the use of biodiesel from a variety of crops. However, the widespread availability of inexpensive petroleum during the 20th century determined otherwise. Now, biofuels are a key focus of developmental efforts globally. Biofuels are ecofriendly, fossil energy independent, carbon neutral, non-toxic, biodegradable and renewable resources [23, 25, 26]. Their use leads to a decrease in the harmful emissions of carbon monoxide, hydrocarbons and SO_x emissions, with a consequent decrease in the greenhouse effect. Biofuels can play an essential part in reaching targets to replace petroleum based transportation fuels with a viable alternative, and in reducing long-term CO_2 emissions, if environmental and economic sustainability are considered carefully. They can be direct and immediate replacements for the liquid fuels used in transport and can be easily integrated to the logistic systems that are operating today. In recent years, the use of liquid biofuels in the transport sector has shown rapid global growth, driven mostly by policies focused on achievement of energy security, and mitigation of GHG emissions [27].

Types of biofuels. Oil seeds/cells of many plants/algae have been extensively evaluated as sources of biofuels. Biofuels are derived from food crops such as sugarcane, sugar beet, maize (corn), sorghum, rapeseed, sunflower, soybean and palm, although other forms of biomass can be used, and may be preferable. The most significant concern is the efficiency and sustainability of these first generation biofuels. In contrast, the second generation biofuels are derived from non-food feedstock [28, 29]. They are extracted from microalgae and other microbial sources, lignocellulosic biomass, rice straw and bioethers, and are a better option for addressing the food and energy security and envi-ronmental concerns. However, the lack of enough land space to grow crops for food and feed as well as for biofuels on one hand, and the need to retain the forests and other land uses that sequester carbon in huge quantities, on the other is a complex issue. According to one estimate, to replace worldwide petroleum use with biofuel, 10.8 million square miles of farmland with the highest yielding biofuel crops are needed, but unfortunately, we have only 5.8 million square miles of farmland on earth. A major criticism often leveled against biomass, particularly against large-scale fuel production, is that it will consume vast swaths of farmland and native habitats, drive up food prices, and result in little reduction in GHG emissions. However, this so-called ''food vs. fuel'' controversy appears to have been exaggerated in many cases [30]. Credible studies show that with plausible technology developments, biofuels could supply some 30% of global demand in an environmentally responsible manner without affecting food production. As a matter of fact, average biodiesel production yield from microalgae can be 10−20 times higher than the yield obtained from oleaginous seeds and/or vegetable. The search for renewable carbon neutral energy sources has spurred research and development (R&D) in this area globally, into various forms of solar energy transformations like solar thermal, photovoltaic, photocatalysis, and photosynthetic processes. Out of this, biofuel derived from cellulose and lipid materials of higher plants, has drawn considerable commercial entrepreneurship in recent times. Corn, sugar cane, jatropha etc. (Fig. 1) have been used as feedstock for production of fuels like ethanol and biodiesel. Brazil, USA and Europe already produce significant quantities of biofuel based on these feedstock. Algae as a feedstock is emerging at the forefront of biofuel research with the increasing awareness of global energy uses and production limitations of agriculture based oilseed crops. Khan with co-workers [31] undertook a methodical analysis of a maximum algal oil production rate from a theoretical perspective. They found that a theoretical maximum of $354\,000$ l ha^{-1} $year^{-1}$ of unrefined oil, as against reported estimates of $40\,700-53\,200$ l ha^{-1} $year^{-1}$ of unrefined oil. However, the full potential of microalgae is yet untapped.

Present scenario of biofuels. The twenty-first century has brought forward two major obstacles in the path of advancement of human civilization, namely clean environment to live in and eco-friendly, sustainable source of energy to fuel the modernization. According to a World Bank report (2008), 6.5 billion liters of biodiesel was produced worldwide in 2006, 75% of which by the European Union and 13% by the USA. The current contribution of biodiesel to global transportation fuel consumption is, however, only 0.14% and the favorable policies of major countries in the world are expected to increase this contribution by 5 times by 2020. The use of renewable energy source is becoming increasingly necessary to mitigate the de-
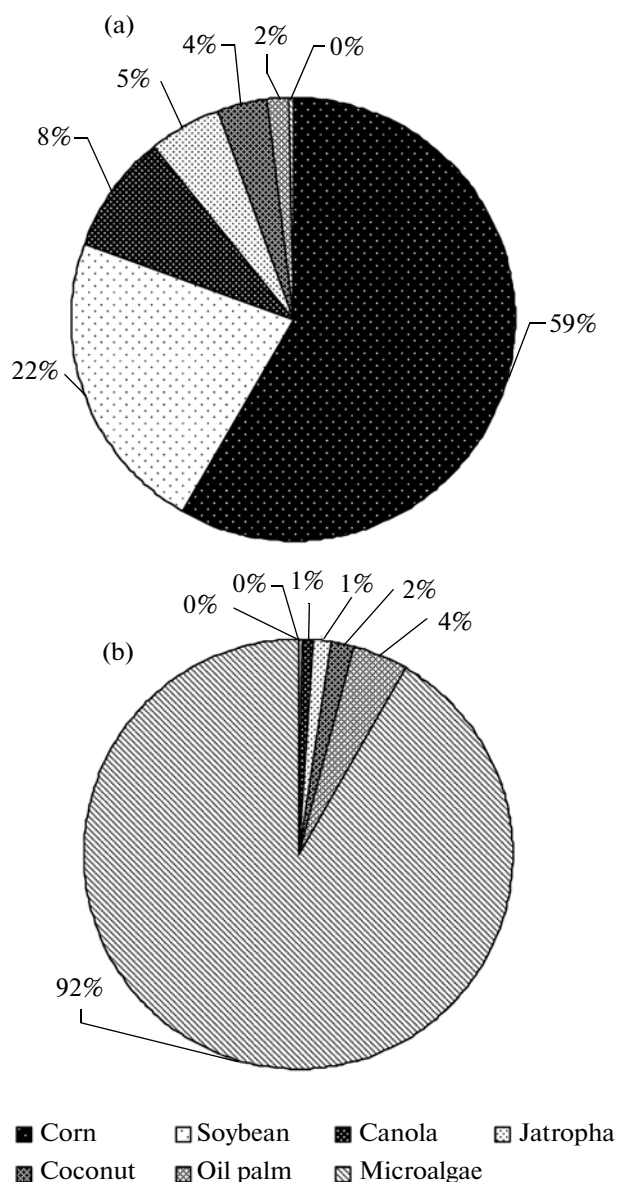
(a)

(b)

■ Corn   □ Soybean   ▦ Canola   ▨ Jatropha
▩ Coconut   ▨ Oil palm   ▨ Microalgae

Fig. 1. Comparison of different crops and microalgae in terms of area (a, in ha) required for oil crop production and oil yield (b, in l/ha).

pletion of fossil fuels and increasing global warming. It is estimated that there will be a 60% increase in global energy requirement by 2030 over its present consumption level. Out of this 45% will be accounted by India and China alone [28].

However, diversion of agricultural or forest land for the cultivation of biofuel crops, has drawn strong criticism of late, due to its impact on food supply and net carbon footprint. Under these circumstances, photosynthetic organisms of microalgae species, which have productivity many orders higher than the conventional biofuel crops, do not require agricultural land and can sequester CO_2, have seen intense R&D inputs in the last few years for their commercialization. In re-

cent years, with the boom in oil prices, some firms have already invested money in US, Israel, Australia and New Zealand for setting up pilot scale operations in algae cultivation and extraction of value added products including biodiesel. India started its biofuel initiative in 2003. This approach differs from other nations' in its choice of raw material for biofuel production—molasses for bioethanol and non-edible oil for biodiesel. Cyclicality resulted in a fuel ethanol program from sugar and molasses which suffered from inconsistent production and supply. However, except for sporadic R&D efforts on culturing and characterization, no major initiatives have been undertaken in scaling up and studying the economics of deriving biofuel from appropriate algae species in the Third world countries.

Microalgae as biofuels. The last few decades have seen a growing interest in using microalgae, cyanobacteria and other photosynthetic bacteria as potential producers of biorenewable fuels, such as biodiesel, biohydrogen and biogas. Biodiesel production from microalgae is a relatively novel concept. Microalgae (as opposed to other plants) are a natural choice for maximum-yield biofuels because they (1) intrinsically offer the greatest flux tolerance and photosynthetic efficiency as a consequence of a minimum of internally competitive plant functions (2) have fast reproductive cycles, (3) have limited nutrient requirements, and (4) can readily be exposed to temporal and spectral irradiation distributions and intensities that are not encountered in nature but are optimal for bioproductivity via cleverly crafted photonic systems. Alternative approaches for biofuel generation have identified aquatic microalgae as fast-growing species. Some microalgae exhibit carbon fixation rates and solar conversion efficiencies an order of magnitude greater than those of typical land-based plants [32]. Exploitation of microalgae for bioenergy generation (biodiesel, biomethane, biohydrogen), or combined applications for biofuels production and CO_2 mitigation, by which CO_2 is captured and sequestered, are under research [33–42]. An integrated strategy was proposed to enhance the economics, cost effectiveness and environmental sustainability by combining the benefits of biofuel production, CO_2 mitigation, waste heat utilization, waste water treatment and novel bioproduct production using the microalgal cultivation processes [43–46].

Several reviews on the commercial applications of microalgae are available [3, 47] especially those focusing particularly on biofuel [38, 48–51]. However, a critical evaluation of the prospects of microalgae as sources of biofuels is scarce.

Technologies for use of microalgae as sources of biofuels. Microalgae are found in diverse environmental conditions and habitats where light and water are available—lacustrine, brackish, freshwater, hypersaline, wastewater maturation ponds, dams, rivers, ma-
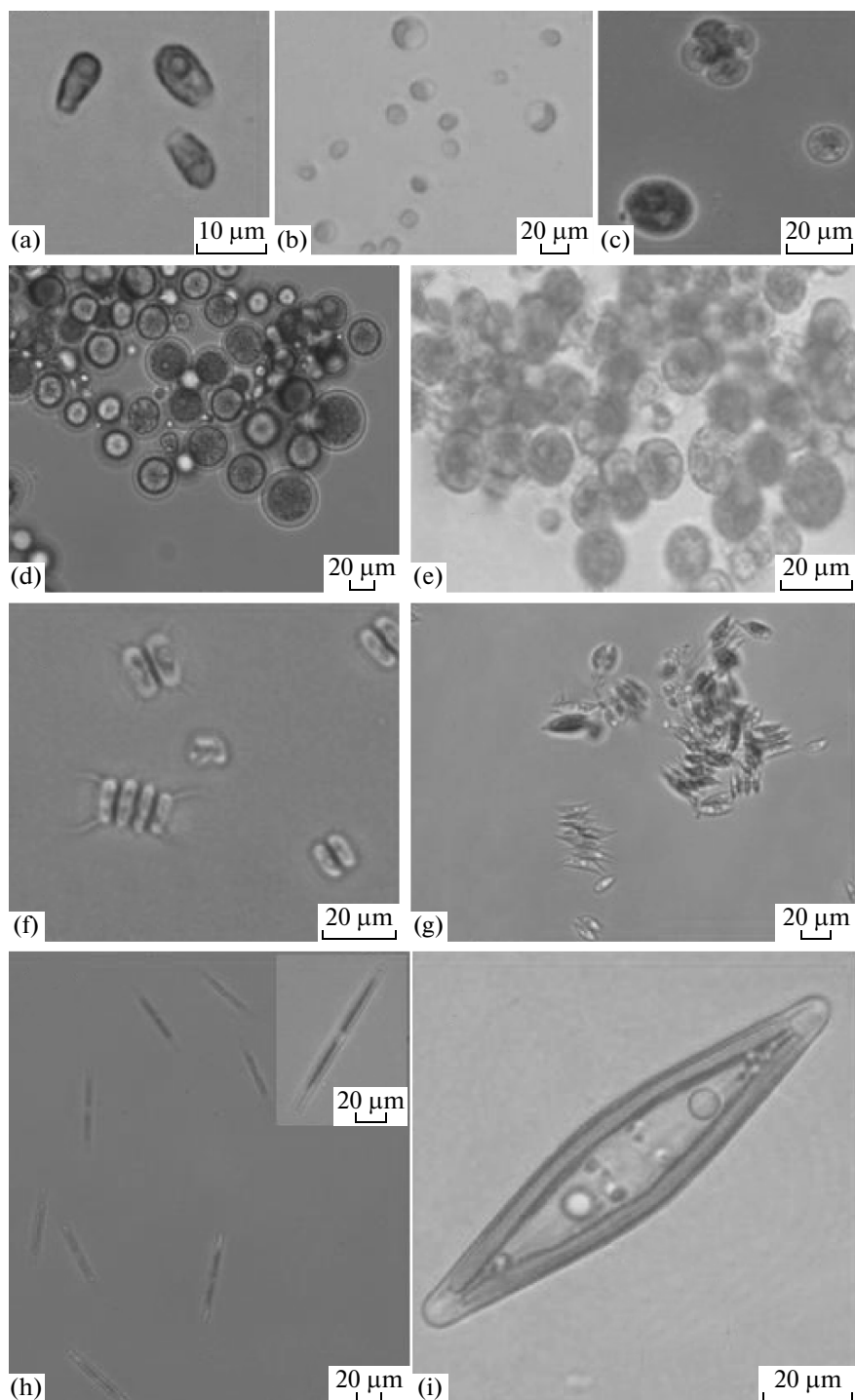
Fig. 2. Light micrographs of potential microalgal species for biofuel production: a — *Chlamydomonas* sp.; b, c — *Chlorella* sp.; d, e — *Chlorococcum* sp.; f, g — *Scenedesmus* sp.; h — *Pinnularia* sp.; i — *Navicula* sp.

rine and coastal areas. Fig. 2 provides an insight into their morphological diversity. Due to selection pressure and changing environmental conditions, there is a wide range of microalgal species worldwide found in extreme environments and these natural ecosystems have immeasurable value as sources of hyper-lipid producing microalgae [52]. In bioprospecting, it is important to collect microalgal samples temporally and spatially so as to determine if there are any successional tendencies in the habitat. Microalgal biomass has shown exhibit clear temporal and spatial patterns during the heterogeneous conditions of the open and

closed phases in estuaries. The microalgae are found as a mixed consortium and their population dynamics is complex in any habitat [53]. Different types of microalgal strains require different habitats.

The crucial step is to search, collect and identify hyper-lipid producing strains. Selection of productive strains, fast-growing, optimized for the local climatic conditions is very important for the success of any algal mass culture and particularly for high-value products such as biodiesel. It is also important to evaluate harvesting costs at the time of choosing the species. Low-cost harvesting requires large cell size, high specific gravity compared to the medium and reliable autoflocculation for successful biofuel production [54].

The idea of using microalgae as a source of transportation fuel is not new. It was first proposed in the 1950s [55] and, since the 1970s, several publicly funded research programs in different countries (USA, Australia, Japan) have investigated microalgae cultivation for producing renewable liquid fuels [36, 56–58]. Although the net energetics of the process appeared in some cases favorable, the projected costs for algal oil were several-fold higher than fossil oil prices, even with the most optimistic assumptions [36]. From 1978 to 1996 the U.S. Department of Energy invested more than US$ 25 million in the Aquatic Species Program (ASP) to develop renewable transportation fuels from microalgae [36]. The major focus of the program was to isolate high lipid content microalgae that could be cultivated in open ponds using CO_2 from coal fired power plants for wide-scale renewable fuel (biodiesel) production. The major conclusions were (1) oil accumulation in the algal cell attained through nitrogen deficiency does not increase oil productivity, since the higher oil content is more than offset by the lower productivities attained under nutrient shortage; (2) given the low cost requirements associated with fuel production, there is little prospect for any alternative (i.e., closed reactors) to the open pond design for large-scale production of microalgae; (3) maintaining mono-specific cultures of laboratory selected organisms in open ponds for more than a few weeks or months is very difficult because these are not robust enough to withstand contamination under field conditions. To overcome the latter limitation, it was suggested to allow native species to take over the culture. This solution, however, would conflict with the approach of genetically modifying microalgae attempted in ASP to reach higher, hopefully near-theoretical, conversion efficiencies of sunlight into biomass and to accumulate high levels of neutral lipids.

One of the biggest challenges in algae culture for biodiesel is to find a suitable strain with high lipid content and growth rate. Microalgae, by contrast, have received scant attention. The productivity of microalgae in nature, on an aerial basis, exceeds that of terrestrial plants by approximately one order of magnitude. The biodiversity of microalgae is large but the most of it remains biochemically and metabolically unexplored. To date, only very few number of species have been cultivated at industrial scale.

It is worthwhile to review in some detail the history of research and development on bioproducts from microalgae. Agriculture began more than 5.000 years ago. Industrial microbiology was a global business by the mid-twentieth century. By contrast, the first attempts at large-scale cultivation of microalgae began only 50 years ago. Their potential for bioenergy production was not recognized until the 1970s, and the resources devoted to this potential have been trivial by comparison to those lavished upon alternatives. Major advances in the biochemistry of microalgae were made in the 1980s and 1990s. Models of bioenergy production based on laboratory results showed great promise, and significant funding flowed into further studies, especially in Japan and the USA. However, with the increasing importance of microalgae in biodiesel production, several countries are vying with each other in the race for developing a suitable cost effective technology, by identifying the right alga, its cultivation and biodiesel production.

Sampling and isolation techniques. The microalgal sampling and selection process is well established although it requires specialized equipment and may be time-consuming [53]. Collection is mainly depends up on both biotic and abiotic factors, parameters measured onsite, type of aquatic system and sampling equipment. The equipment required for microalgal sampling includes a knife, mesh net (2 μm mesh), scooping jar, vials for collecting samples, scalpels, water analyzer kit measuring dissolved CO_2 and O_2 analyzer with a data logger, light meter, GPS, salinity meter, multiprobe system (measuring pH, temperature, turbidity, conductivity and light intensity simultaneously). Heavy duty equipment includes a suitable vehicle for rough terrain with enough space for the collected samples. There is no definite sampling procedure documented in literature though researchers can follow simple and cheap methods of collecting microalgal samples. Ideally samples can be collected from the natural substrata by chipping, scrapping, and by brushing from rock surfaces and bottom sediments. The brushing method was reported to be effective and reproducible method of collecting microalgal cells and also that it does not damage them. Sampling in deep freshwater lakes and dams requires systematic sampling, whereby water samples are scooped from at least three depth levels to the bottom of the lake or dam. This will allow selection of microalgae which prefer different light intensities. Bottom sediments are also major habitats of benthic microalgae and therefore should be collected together with pieces of detritus and mud. Stringent regimes and protocols need to be exercised when sampling. Therefore an all encompassing sampling regime is essential to undertake collection and isolation of microalgae from aquatic environments.

The isolation of microalgae from nature has a long history. The first microalga to be isolated and grown in pure culture was the freshwater microalga, *Chlorella vulgaris*. Over the next several decades, hundreds of species were gathered and maintained in very small quantities to form permanent culture collections, but very few species were cultivated in volumes of 50 ml or more. The chemical composition of microalgae could not be studied until the 1930s, when a new technique for "large-scale cultivation" made it possible to collect sufficiently large samples for analysis [59]. A key consideration is the choice of algal strain. There are many screening programs around the globe surveying algal species in different locations for suitable strains, very often building on the pioneering studies in the aquatic species program (ASP) during the 1980s and 1990s and a culture collection of more than 3000 strains were maintained. On the basis of oil content and high growth rate 300 species were screened [60]. Japan committed about US$ 117 million [61] to conduct research on microalgal CO_2 utilization in the 1990s in a program entitled Research Institute of Innovative Technology for the Earth, funded by the Ministry of International Trade and Industry through the New Energy Development Organization. Like the ASP, the program focused on both species collection and characterization [62–64] and development of cultivation technology and it has maintained marine microalgal culture collection comprising 1393 strains.

Isolation of microalgae into culture can be done by means of either the traditional methods or advanced methods or a judicious mix of both. The traditional methods are well established. Some species, often called weeds, are easy to isolate and cultivate, whereas others are difficult or seemingly impossible to grow. The first step towards successful isolation is the naturally occurring environmental conditions, which depends up on the nature of environment, quality of water, temperature, salinity etc. The second step is aimed towards the elimination of contaminants. The collection method is sometimes crucial for success, because damaged or dead cells lead to failure.

The most common method for single-cell isolation is by micropipette, although automation is more advantageous. Micropipette isolation is usually performed with a Pasteur pipette or a glass capillary having a straight or bent or curved tip. The goal of micropipette isolation is to pick up a cell from the sample, deposit it without damage into a series of sterile droplets, until a single algal cell, free of all other protists, can be confidently placed into the culture medium. Subsequently, the sample can be examined microscopically in a glass or plastic dish, in a multiwell plate, or on a microscope slide. However, the microalgal droplets can be placed on agar to reduce evaporation but this step depends on the size of the cells. Furthermore, the single cell can be pipetted and discharged into the sterile rinsing droplet and before the cell can settle, it should be picked up and transferred.

Skill of the technique is important not to shear or damage the cell. For flagellates, cessation of swimming sometimes indicates damage. For diatoms, broken frustules can refract light differently than for intact cells. Leakage of protoplasm is an obvious sign of severe damage. Rogerson and co-workers, [65] employed repeated introduction and ejection of cells, suspended in a 1% crude papain solution, into and from a micropipette to generate ca. 10% naked cells of *Coscinodiscus asteromphalus*. These naked cells were re-isolated via micropipette into fresh medium. The traditional method of micropipette isolation can be successfully employed with certain precautions. Ultraclean droplets for rinsing are necessary, because the tiny cells cannot be easily distinguished from particulate material present, especially when working with seawater.

Screening of microalgae. The screening stage of bioprospecting focuses on isolation and identification of algal species capable of substantial lipid production, targeting organisms with rapid growth rate and tolerance to environmental parameters. The conventional method used for lipid determination involves solvent extraction and gravimetric determination. A major disadvantage of the conventional method is that it is time-consuming, labor-intensive and has a low throughput screening rate. Moreover, approximately 10–15 mg of wet weight of cells must be cultured for the extraction and derivatization [66]. Consequently, there is greater interest on a rapid in situ measurement of the lipid content [67]. Nile red (9-diethylamino-5H-benzo[a]phenoxazine-5-one), a lipid- soluble fluorescent dye, has been commonly used to evaluate the lipid content of animal cells and microorganisms [65] and especially microalgae [67, 68]. Nile red possesses several characteristics advantageous to in situ screening. It is relatively photostable, intensely fluorescent in organic solvents and hydrophobic environments. The emission maximum of Nile red is blue-shifted as the polarity of the medium decreases, [67, 69, 70] which allows one to differentiate between neutral and polar lipids at the excitation and emission wavelengths. Elsey et al. [71] showed the technical emission spectra for Nile red in various solvents. The peak emission intensity of Nile red in hexane is located near 576 nm when excited at 486 nm. The chloroform and ethanol peaks excitation were recorded at 600 and 632 nm, respectively [68]. In acetone Nile red is excited at 488–525 nm and the fluorescent emission is measured at 570–600 nm using various instruments [67]. Measurement of neutral lipids using the Nile red application requires the instrument to be calibrated using the stain dissolved in an organic solvent and account for the nonlinear intensity emission with respect to time. Measurements of lipid per unit cell require a calibration curve that correlates fluorescence to lipid content, whether determined gravimetrically or by use of lipid standards [68]. Thick cell walls of microalgae inhibit the permeation of Nile red and may indicate the

absence of oil, even though gravimetric analysis shows high yields of neutral lipids. It has been noted that the permeation of Nile red dye is also variable among algal species, requiring the use of high levels of DMSO (20–30% vol./vol.) and elevated temperatures of 40°C [72]. Stockenreiter et al., [73] observed that analysis of microalgae lipid content with Nile red fluorescence along with imaging flowcytometer (Flow CAM^R) offers the unique advantages of estimating the lipid content of each cell without the physical separation of algal cells.

Alternatively, the lipophilic fluorescent dye BODIPY 505/515 (4,4-difluoro-1,3,5,7-tetramethyl-4-bora-3a,4adiaza-s-indacene) has recently been used as a vital stain to monitor algal oil storage within viable cells. Lipid bodies are stained green and chloroplasts appear red and are visualized in live oleaginous (oil-containing) algal cells [73]. The advantage of BODIPY 505/515 is that high lipid yielding cells may be identified and isolated microscopically using a micromanipulator system, flow cytometry or a fluorescence-activated cell sorter [72]. Subsequently, pure cultures may be propagated from the isolated viable cells. BODIPY 505/515 has been shown to have a narrower emission spectrum than Nile red, making it potentially more useful for confocal imaging, where fluorescence contrast enhancement of lipid bodies is important for image resolution [73]. Unlike Nile red, BODIPY 505/515 has the advantage that it does not bind to cytoplasmic compartments other than lipid bodies and chloroplasts. A recent study [74] demonstrated the use of Fourier transform infrared microspectroscopy (FTIR) to determine lipid and carbohydrate content of freshwater microalgae. FTIR was shown to be an efficient and rapid tool for monitoring lipid accumulation of microalgae. This study has reported highly significant correlations between the FTIR- and Nile red-based lipid measurements. For the purposes of bioprospecting for high lipid yielding microalgae, a rapid throughput of sample processing is required. The semi-quantification of neutral lipids using Nile red or BODIPY 505/515 and fluorescence microscopy allows for an initial rapid screening and visualization of lipid globules. FTIR spectroscopy may be used thereafter to quantify the yield of lipids. Once the high lipid producing microalgae have been identified, isolated and purified, a further step in the screening would be to determine the photosynthetic efficiency of the culture.

Subsequent to screening, understanding the physiology of the algal isolate is imperative. Pulse Amplitude Modulated (PAM) chlorophyll- a fluorescence measurements are widely used as a simple, rapid, and non-invasive method to assess the physiological state of microalgae. It is also a valuable tool to assess the optimum growth conditions required to maximize the biomass yield and to quantify the effect of nutrient or other extreme environmental stresses (salinity, temperature, photosynthetically active radiation, PAR

and pH) on the algal culture. Neutral lipid synthesis is stimulated under nutrient depleted or limited conditions. Many microalgae have the ability to produce triacylglycerols (TAG) which comprise almost 80% of dry cell weight as a storage lipid [3, 38] under nutrient or other environmental stress. The PAM fluorometer parameters (electron transport rate, maximum quantum efficiency of Photosystem II [FV/Fm], and non-photochemical quenching) may be used as indicators of nutrient stress and consequently the possibility of neutral lipid synthesis and can be a valuable instrument in the screening process. Neutral lipid synthesis is likely to occur during the stationary phase of growth due to nutrient limitation [39]. The screening process of microalgae bioprospecting has to be comprehensive in assessing the lipid producing potential as well as the kinetics of growth and tolerance. The success of downstream processing is dependent on reliable biochemical and physiological screening tools such as the BODIPY 505/515 lipid stain, FTIR spectroscopy and PAM fluorometry.

Realizing the importance of microalgae in biodiesel production, several countries like China, Taiwan, Germany, France, Brazil, Australia, Canada, New Zealand, Italy and Israel are vying with each other in the race for developing a suitable cost effective technology by identifying the right alga, its cultivation and biodiesel production. A list of microalgae strains with potential to be used for the production of oils for biofuel is presented in Table 2.

Effect of different parameters on microalgal oil production. The yield of biodiesel from microalgae depends on both the biomass concentration of the cultures and the oil content of individual cells [8, 38, 98, 99]. One option for enhancing the metabolic flux into lipid biosynthesis is by applying artificial physiological stresses and producing biodiesel from microalgae that accumulate high amounts of oil.

Oleaginous algae produce only small quantities of TAG under optimal growth or favorable environmental conditions [100]. The interest in microalgae for oil production is due to the high lipid content of some species, and to the fact that lipid synthesis, especially of the non-polar TAG, which are the best substrate to produce biodiesel, can be modulated by varying growth conditions. The total content of lipids in microalgae may vary from about 1–85% of the dry weight, with values higher than 40% being typically achieved under stress conditions [8, 38, 101]. The lipid content in some microalgae could be modified by various growth conditions such as nitrogen deprivation [39, 52, 95, 102, 103], silicon deficiency [104, 105], phosphate limitation [23], high salinity [106] and some heavy metal stress such as cadmium [107].

Factors such as temperature, irradiance and, most markedly, nutrient availability have been shown to affect both lipid composition and lipid content in many algae [48, 107, 108]. Research is going on to identify

Table 2. List of microalgal strains (with their oil content) having potential for biofuel production

Microalgae	Oil content, % dry wt	Reference
Ankistrodesmus sp.	28–40	[75]
Botryococcus braunni	25–86	[33, 36, 69, 76]
Chaetoceros calcitrans	40	[52]
Chaetoceros muelleri	34	[52]
Chlamydomonas reihardtii	25	[77]
Chlorella emersonii	63	[78]
Chlorella minutissima	56–57	[79, 78]
Chlorella protothecoides (autotrophic/ heterotrophic)	15–55	[80]
Chlorella pyrenoidosa	55	[70, 80, 81, 82]
Chlorella vulgaris	19–56	[41, 52, 70, 78, 83, 84]
Chlorella zofingiensis	79	[83]
Chlorella sp.	28–48	[36, 38, 52]
Chlorococcum littorale	34	[85]
Chlorococcum sp.	19	[52]
Crypthecodinium cohnii	20	[38]
Cyclotella sp.	42	[36]
Cylindrotheca sp.	16–37	[38]
Dunaliella primolecta	23	[38]
Dunaliella salina	28	[81]
Dunaliella tertiolecta	15–42	[37, 41, 78, 86]
Haematococcus pluvialis	25	[87]
Hantzschia sp.	66	[36]
Isochrysis sp.	25–33	[36, 38, 88]
Monallanthus salina	20	[38]
Nannochloris sp.	63	[36]
Nannochloropsis sp.	31–80	[36, 38, 52]
Nanochloropsis oculata	36–60	[52, 89]
Nanochloropsis salina	72	[90, 91]
Neochloris oleoabundans	35–65	[38, 78, 92]
Nitzschia sp.	28–50	[38, 93]
Phaeodactylum tricornutum	20–30	[36, 38]
Pseudochlorococcum sp.	52	[94]
Scenedesmus dimophus	16–40	[78]
Scenedesmus obliquus	31–55	[78]
Scenedesmus sp.	21–45	[36, 52]
Schizochytrium sp.	50–77	[38]
Stichococcus sp.	9–59	[36, 95]
Tetraselmis suecica	15–32	[36, 82, 89, 96]
Thalassiosira pseudonana	21–31	[97]

the environmental/abiotic factors which cause stress. Among chemical environmental stimuli, nutrient starvation (nitrogen and phosphate), salinity and pH of growth medium are the most investigated. It is important to take into consideration physical/environmental stimuli—temperature and light intensity, growth phase and/or aging of the culture. The point of concern is to identify stimuli which can enhance oil/lipid accumulation in microalgae without affecting their growth rate. A number of algal strains, with good potential for making biodiesel have been identified, which include *Botryococcus* sp., *Chlorella* spp., *Chlamydomonas* sp., *Scenedesmus* sp., *Crypthecodinium* sp., *Nannochloropsis* sp., *Nannochloris* sp. etc.

Nutrients. The strategy of enhancing lipid production of microalgae by controlling the nutritional or cultivation conditions (e.g., temperature, pH, and salinity) is aimed at channeling metabolic flux generated in photobiosynthesis into lipid biosynthesis. Nutrient starvation has so far been the most commonly employed approach for directing metabolic fluxes to lipid biosynthesis of microalgae. In this scenario, microalgae accumulate lipids as a means of storage under nutrient limitation when energy source (i.e., light) and carbon source (i.e., CO_2) are abundantly available and when the cellular mechanisms for the photobiosynthesis are active. While a number of nutrients such as phosphorus and iron deficiency have been reported as being able to cause cell growth cessation and channel metabolic flux to lipid/fatty acid biosynthesis, nitrogen is the most commonly reported nutritional limiting factor triggering lipid accumulation in microalgae. Nitrogen starvation has been observed to lead to lipid accumulation in a number of microalgal species. For instance, *Chlorella* usually accumulates starch as storage material. However, it was observed by Illman et al. [103] that *C. emersonii*, *C. minutissima*, *C. vulgaris*, and *C. pyrenoidosa* could accumulate lipids of up to 63%, 57%, 40%, and 23% of their cells on a dry weight basis, respectively, in low-N medium. Under nitrogen-deficient conditions, *Neochloris oleoabundans* was reported to be able to accumulate 35–54% lipids of its cell dry weight and its TAG comprised 80% of the total lipids [109]. Yamaberi et al., [110] also observed that TAG accumulated in *Nannochloris* sp. cells could be 2.2-fold more than in the cells in nitrogen sufficient cultures. Li et al. [39] showed that sodium nitrate was the most favourable nitrogen source for cell growth and lipid production of *N. oleoabundans* among the three tested nitrogen-containing compounds, i.e., sodium nitrate, urea, and ammonium bicarbonate. It was observed that lipid cell content decreased with the increase of sodium nitrate in the medium in the range of 3–20 mM concenteration. The trend that lower nitrogen source concentration in medium led to higher lipid cell content was hypothetically explained by the fact that nitrogen would have exhausted earlier at low cell density when the initial concentration of nitrogen source in medium was low. As a result, cells started to accumulate lipid when light had good penetration (at low cell density), when individual cells were exposed to a large quantity of light energy, resulting in more metabolic flux generated from photosynthesis to be channeled to lipid accumulation on an unit biomass basis.

Nutrient deficiency (particularly nitrogen and silicon) has been regarded as the most efficient approach to increase lipid content in algae. Enhanced lipid accumulation (TAG) in various algal taxa and numerous species has been observed under nitrogen limitation. As green algae require more nitrogen source for growth, nitrogen limitation is considered more beneficial for increasing lipid content in them. Spoehr and Milner [102] demonstrated that a nitrogen starved *C. pyrenoidosa* culture was able to accumulate up to 85% lipid in its biomass, while the typical content of exponential cultures was only about 5%. An increase of lipid content up to 70% of the dry biomass has been reported with several species in response to limiting nitrogen supply in batch cultures, with TAG mainly containing saturated and monounsaturated fatty acids forming the bulk (up to 80%) of the lipid fraction in the starved cells [108, 110]. However, a large variability exists in the response to nitrogen deficiency. Generally, diatoms, which have relatively high log-phase lipid content, do not respond to nitrogen starvation by increasing their lipid content [1, 90]. Green microalgae show a variety of responses, from several-fold increase from log-phase values (e.g., in *C. pyrenoidosa*), to no change or even a slight reduction (e.g., in some *Dunaliella* spp. and in *Tetraselmis suecica*) [110]. Within the same genus (e.g., *Chlorella*) some strains were found to accumulate starch under nitrogen starvation, whereas others accumulated neutral lipids.

A stronger stimulation of lipid production occurs in response to conditions of nitrogen limitation, which potentially can occur in all known microalgae. Nitrogen-starved cells can contain four times lipid content as compared with N-sufficient cells [91, 110, 111], and optimization of the lipid production of pond bioreactors therefore depends on their operators' ability to induce N-limitation in the resident algal cells reliably and consistently. Resource-ratio theory and the principles of ecological stoichiometry provide additional new insights into the control of algal biomass and lipid production in pond bioreactors [112, 113]. As demonstrated by Rhee [114], the nutrient limitation status of microalgae can be directly controlled by regulating the ratio of nitrogen and phosphorus (N : P). A transition between N- and P-limitation of phytoplankton growth typically occurs in the range of N : P supply ratios between ca. 20 : 1 to ca. 50 : 1 by moles [114]. Such shifts between N- and P-limitation have extremely important implications for algal biofuel production because diverse species of microalgae grown under nitrogen-limited conditions (i.e. low N : P supply ratios) can exhibit 3 times more the lipid content than cells grown under conditions of phosphorus limitation

(high N : P supply ratios) [113]. Total phosphorus and nitrogen concentration in the nutrient feed to pond bioreactors should therefore impact algal biodiesel production, because the N : P ratio of incoming nutrients will strongly influence algal biomass production [99] as well as the cellular lipid content. An inverse relationship was observed between N : P and cellular lipids [115], and a positive, hyperbolic relationship observed between N : P and microalgal biomass [99]. Thus, it can be concluded that optimal lipid yield (in terms of mass of lipid produced per unit of bioreactor volume per day) occurs at intermediate values of the N : P supply ratio. From the strong apparent interactions between the effects of nitrogen and carbon dioxide availability on microalgal lipids, and the effects of N : P supply ratios on volumetric lipid production, it can be surmised that this might be even greater if the bioreactors are simultaneously provided with supplemental CO_2 [99].

Other types of nutrient deficiency that promote lipid accumulation include phosphate and sulfate limitation. Phosphate limitation was observed to cause enhancement of lipid accumulation of *Monodus subterraneus* [105]. With a decrease in phosphate availability, the cellular total lipid content of starved cells increased, mainly due to the drastic increase in TAG levels. In the absence of phosphate, the proportion of phospholipids reduced from 8.3% to 1.4% of total lipids, and the proportion of TAG increased from 6.5% to 39.3% of total lipids. Studies have shown that sulfur deprivation enhanced the total lipid content in the green algae *Chlorella* sp. and *C. reinhardtii* [116].

In diatoms, silicon is an important nutrient that affects cellular lipid metabolism. For example, silicon-deficient *Cyclotella cryptica* cells had higher levels of neutral lipids (primarily TAG) and higher proportions of saturated and mono-unsaturated fatty acids than silicon-replete cells [117].

Micronutrients. In recent years, the function of micronutrients in microalgal growth and lipid accumulation has been investigated by many researchers. Micronutrients, including metals (iron, manganese, zinc, cobalt, copper, molybdenum, nickel, and cadmium) and the metalloid selenium, influence microalgal growth and lipid accumulation, because of their role as limiting micronutrients. Iron has a key function in regulating phytoplankton biomass in oligotrophic waters near the Equator and further south [118]. Furthermore, iron deficiency has also been reported to stimulate lipid accumulation in microalgae *C. vulgaris*, which accumulated up to 56.6% lipid of biomass by dry weight under the optimal condition of 1.2×10^{-5} M $FeCl_3$ [98].

Temperature. Temperature has a significant effect on the fatty acid composition of algae. A general trend towards increasing fatty acid unsaturation with decreasing temperature and increasing saturated fatty acids with increasing temperature has been observed in many algae and cyanobacteria [48, 119].

Light intensity. Algae exhibit remarkable changes in their gross chemical composition, pigment content and photosynthetic activity during growth at various light intensities. Typically, low light intensity induces the formation of polar lipids, particularly the membrane polar lipids associated with the chloroplasts, whereas high light intensity decreases total polar lipid content with an increase in the amount of neutral storage lipids, mainly TAG [97, 120].

Growth phase and physiological status. Lipid content and fatty acid composition are also subjected of variability during the growth cycle. In many algal species examined, an increase in TAG is often observed during stationary phase. For example, in the chlorophyte *Parietochloris incise*, TAG increased from 43% (total fatty acids) in the logarithmic phase to 77% in the stationary phase [121] and in the marine dinoflagellate *Gymnodinium* sp., the proportion of TAG increased from 8% in the logarithmic phase to 30% in the stationary phase of growth [122]. Coincident increases in the relative proportions of both saturated and mono-unsaturated 16 : 0 and 18 : 1 fatty acids and decrease in the proportion of PUFA in total lipids were also associated with growth-phase transition from the logarithmic to the stationary phase.

Salinity. Takagi et al. [123] observed that TAG content increased in a marine alga, *Dunaliella*, under high salinity conditions. An initial NaCl concentration higher than 1.5 M was found to markedly inhibit cell growth. However, when the initial NaCl concentration increased from 0.5 M (equal to seawater) to 1.0 M, it resulted in higher intracellular lipid content (67%) in comparison with 60% for initial salt concentration. Addition of 0.5 or 1.0 M NaCl at mid-log phase or at the end of log phase during cultivation further increased the lipid content to 70%.

A commonly suggested procedure is to use a two-stage cultivation strategy, dedicating the first stage for cell growth/division in nutrient-sufficient medium and the second stage for lipid accumulation under nutrient starvation or other physiological stress. A well formulated medium such as proposed by Li et al. [42] would achieve the two-stage lipid production "naturally" as the cells will be able to grow quickly before the exhaustion of the limiting substrate (N, in this particular case) and then switch to lipid accumulation under N starvation conditions. Furthermore, a hybrid closed photobioreactor/open pond microalgal cultivation system [89] was suggested to be potentially the appropriate engineering solution accommodating the two-stage strategy with the photobioreactors dedicated to nutrient-rich inoculum build-up and the open ponds to low-nutrient lipid accumulation. It was also pointed out that employment of low-nutrient media in open ponds is not only beneficial for lipid accumula-

tion and contamination control, but also environmentally friendly.

Nevertheless, deficiency of these nutrients may slowdown photosynthesis of microalgal cells one way or the other, resulting in lowered overall lipid productivity. Many of the commonly used limiting nutrients are essential for photosynthesis of microalgae and the depletion of which may severely impede the photosynthesis responsible for generating the metabolic flux for lipid production. For instance, it was observed in studies that chlorophyll, the essential pigment for light capturing in the biosynthesis of green alga *N. oleoabundans*, was consumed for cell growth when nitrogen was exhausted from the medium, resulting in a sharp drop of chlorophyll cell content [39]. Phosphorus is essential to the cellular processes related to bioconversion of energy (e.g., photophosphorylation). Of particular relevance, photosynthesis requires large amounts of proteins (notably Rubisco) and proteins are synthesized by phosphorus-rich ribosomes [124]. As a result, channeling metabolic flux to lipid biosynthesis by the means of phosphate starvation may have a severe impact on photosynthesis. There is apparently a dilemma in the biochemical engineering strategy i.e., the very reason that stimulates lipid accumulation in cells may result in severely impeded cell growth and photosynthesis and hence lowered overall lipid productivity. This dilemma could likely be solved by employing metabolic engineering approaches.

Recent studies have also indicated that the diversity of primary producer systems is often positively linked to biomass production and lipid accumulation. Stockenreiter et al. [73] showed that lipid production increased with increasing diversity, in both natural and laboratory microalgal communities and the underlying reason seemed to be resource use complementarity. Such ecology related dynamics can provide a cost-effective and resource conserving technique to improve biofuel production.

Genetic engineering approaches. Although biotechnological processes based on transgenic microalgae are still in their infancy, researchers and companies are considering the potential of microalgae as green cell-factories to produce value-added metabolites and heterologous proteins for pharmaceutical applications. The commercial application of algal transgenics is beginning to be realized and algal biotechnology companies are being established. It was predicted that microalgae, due to the numerous advantages they present, could offer a powerful tool for the production of commercial molecules in the near future. The fast growing interests in the use of transgenic microalgae for industrial applications is powered by the rapid developments in microalgal biotechnology. The genome sequencing projects of the red alga *Cyanidioschyzon merolae* [124], the diatoms *Thalassiosira pseudonana* [125] and *Phaeodactylum tricornutum* [126] and the unicellular green alga *Ostreococcus tauri* [127] have

been completed. Nuclear transformation of various microalgal species is now a routine; chloroplast transformation has been achieved for green, red, and euglenoid algae, and further success in organelle transformation is likely as the number of sequenced plastid, mitochondrial, and nucleomorph genomes continues to grow [128]. Various genetic transformation systems have been developed in green algae such as *Chlamydomonas reinhardtti* and *Volvox carteri* [129].

The fast pace of developments in microalgal biotechnology permit the isolation and use of key genes for genetic transformation. The key enzyme in regulating fatty acid synthesis, acetyl-CoA carboxylase (ACC), was first isolated from the microalga *Cyclotella cryptica* in 1990 by Roessler [118] and then successfully transformed by Dunahay et al. [130] and Sheehan et al. [39] into the diatoms *C. cryptica* and *Navicula saprophila*. The ACC gene, *acc*1, was overexpressed with the enzyme activity enhanced to 2—3-fold. These experiments demonstrated that ACC could be transformed efficiently into microalgae, although no significant increase of lipid accumulation was observed in the transgenic diatoms [129]. It also suggests that overexpression of ACC enzyme alone might not be sufficient to enhance the whole lipid biosynthesis pathway [36]. Even though there is no success story with respect to lipid overproduction of microalgae using the genetic engineering (GE) approach up to now, a solid understanding towards the global TAG biosynthesis pathway, which is generally accepted to be identical throughout all species except the differences in the location of reactions and the structure of some key enzymes, has been established.

Large scale cultivation. Photobioreactors are different types of tanks or closed systems in which algae are cultivated. Algal cultures consist of a single or several specific strains optimised for producing the desired product. Water, necessary nutrients and CO_2 are provided in a controlled way, while oxygen has to be removed. Algae receive sunlight either directly through the transparent container walls or via light fibres or tubes that channel it from sunlight collectors. A great amount of developmental work to optimise different photobioreactor systems for algae cultivation has been carried out and is reviewed in Carvalho et al. [131], and Hankamer et al. [132]. It has also been suggested to grow heterotrophic algae in conventional fermentors instead of photobioreactors for production of high-value products [18]. Instead of light and photosynthesis, heterotrophic algae rely on utilizable carbon sources in the medium for their carbon and energy generation.

Open pond systems. Open pond systems are shallow ponds in which algae are cultivated. Nutrients can be provided through runoff water from nearby land areas or by channeling the water from sewage/water treatment plants. The water is typically kept in motion by paddle wheels or rotating structures, and some mixing

Table 3. Comparison between open pond and photobioreactor system for mass cultivation of algae Modified from [133, 134]

Parameter or issue	Open ponds and raceways	Photobioreactors
Space requirement	High	Low
Water loss	Very high, may also cause salt precipitation	Low
CO_2 loss	High, depending on pond depth	Low
Oxygen concentration	Usually low enough because of continuous spontaneous outgassing	Build-up in closed system requires gas exchange devices (O_2 must be removed to prevent inhibition of photosynthesis and photooxidative damage)
Temperature	Highly variable, some control possible by pond depth	Cooling often required (by spraying water on Photo bioreactor (PBR) or immersing tubes in cooling baths)
Shear	Low (gentle mixing)	High (fast and turbulent flows required for good mixing, pumping through gas exchange devices)
Cleaning	No issue	Required (wall-growth and dirt reduce light intensity), but causes abrasion, limiting PBR life-time
Contamination risk	High (limiting the number of species that can be grown)	Low
Biomass quality	Variable	Reproducible
Biomass concentration	Low, between 0.1 and 0.5 g l^{-1}	High, between 2 and 8 g l^{-1}
Production flexibility	Only few species possible, difficult to switch	High, switching possible
Process control and reproducibility	Limited (flow speed, mixing, temperature only by pond depth)	Possible within certain tolerances
Weather dependence	High (light intensity, temperature, rainfall)	Medium (light intensity, cooling required)
Startup	6—8 weeks	2—4 weeks
Capital investment	Low	Very high
Operating costs	Low (paddle wheel, CO_2 addition)	Very high (CO_2 addition, pH-control, oxygen removal, cooling, cleaning, maintenance)
Harvesting cost	High, species dependent	Lower due to high biomass concentration and better control over species and conditions
Current commercial applications	5000 t of algal biomass per year	Limited to processes for high added value compounds or algae used in food and cosmetics

can be accomplished by appropriately designed guides. Algal cultures can be defined (one or more selected strains), or are made up of an undefined mixture of strains. For an overview of systems used, see Borowitzka [9].

Comparison of the different production systems. The high capital cost associated with producing microalgae in closed culture systems is the main challenge for commercialization of such systems [8]. Open systems do not require expenses associated with sterilization of axenic algal cultures. However, this leads to high risk of contamination of the culture by bacteria or other unwanted microorganisms. A common strategy therefore to achieve monocultures in an open pond system is to keep them at extreme culture conditions such as high salinity, nutrition or alkalinity [12]. Consequently, this strictly limits the species of algae that can be grown in such systems. To our knowledge, based on

available literature, currently only *Dunaliella* (high salinity), *Spirulina* (high alkalinity) and *Chlorella* (high nutrition) have been successfully grown in commercial open pond systems [12]. The necessity for a large cultivation area has been pointed out as a limitation in using open ponds to grow microalgae for mitigating the CO_2 released from power generating plants. It has been estimated that a raceway pond requires 1.5 km^2 to fix the CO_2 emitted from a 150 MW thermal power plant [132]. The large area requirements are partly due to the comparable lower productivity of open pond systems. It was pointed out that improving the control of limiting parameters in open ponds such as culture medium, temperature and contamination and thereby increasing productivity could be accomplished by using a transparent cover over the ponds, such as a greenhouse. Selection of a suitable production system clearly depends on the purpose of the production facility.

For example, closed bioreactors will not be suitable for wastewater treatment, because the costs for treating wastewater in this system will be too high in relation to the low value added during the production process. On the other hand, high quality/value products that are produced only in small amounts might require production in bioreactors. A comparison of the different production systems is presented in Table 3.

Carbon dioxide mitigation and sequestration. To use microalgae to fix CO_2 released from power plants via the exhaust gas and thereby mitigate the amount of carbon released into the atmosphere is an attractive idea. However, there are several major challenges before this idea becomes practical. It is known that growth of algae is negatively influenced by increasing CO_2 [135]. Strains that grow well at CO_2 concentrations of 5−10% show a drastic decrease in their growth rate above 20% [136]. An important task therefore has been to identify strains that can cope with very high CO_2 concentrations and also have high growth rates. Screening has yielded strains that grow well in CO_2 concentrations between 30% and 70% saturation [137]. Also, results by Olaizola [18] indicate that by controlling the pH changes in the culture and releasing CO_2 to the algae on demand, growth could be sustained even at 100% CO_2. Another important property that would need to be optimized is the ability of algal strains to have high thermal stability. It has been suggested that the hot flue gases introduced in the algal cell cultures may influence the temperature [138].

There is a worldwide awareness about global warming as a result from the rising levels of different greenhouse gases such as CO_2 released from the burning of fossil fuels. Different methods have been suggested as to how CO_2 could be sequestered or immobilised through filtering or other mechanical/chemical processes and subjected for long-term storage to avoid release into the atmosphere. In this respect, the idea of biological sequestering by growing algae and take advantage of their photosynthetic machinery of capturing carbon dioxide has been suggested by many researchers as an alternative method of reducing the amount of CO_2 released in the atmosphere [36, 38, 41, 89, 139−141].

The Aquatic Species Program (ASP) funded from 1978 through 1996 by the Office of Fuels Development started out as a project investigating the possibilities of using algae to sequestering CO_2 emissions from coal power plants [36]. The main direction of the program over time became focused on the specific application of developing a production of high-quality diesel from algae utilizing the CO_2 in the exhaust gas from these plants. The project screened for algae that could produce high amount of oils as well as could grow at severe conditions regarding temperature, pH and salinity. In Europe, the Emissions Trading Scheme is one of the policies introduced across Europe to tackle emissions of carbon dioxide and other greenhouse gases and combat the serious threat of climate change. Aquatic species could benefit from trading given their potential to mitigate and/or sequester carbon and this would contribute to the economics of production.

Globally, a lot more needs to be done before the utilization of microalgae can become a reality. An urgent need exists to set up facilities comprising "banks" for maintenance of algal germplasm useful as sources of biofuels, and trained manpower (biologists, engineers and technocrats) needs to be developed for effective utilization of these valuable sources of "green energy".

REFERENCES

1. Brennan, L. and Owende, P., *Renew. Sust. Energy Rev.*, 2010, vol. 14, no. 2, pp. 557−577.

2. Cardozo, K.H.M., Guaratini, T., Barros, M.P., Falcão, V.R., Tonon, A.P., Lopes, N.P., Campos, S., Torres, M.A., Souza, A.O., Colepicolo, P., and Pinto, E., *Comp. Biochem. Physiol. Part C: Toxicol. Pharmacol.,* 2007, vol. 146, no. 1−2, pp. 60−78.

3. Spolaore, P., Joannis-Cassan, C., Duran, E., and Isambert, A., *J. Biosci. Bioeng.*, 2006, vol. 101, no. 2, pp. 87−96.

4. Graham, L.E. and Wilcox, L.W., *Algae*. New Jersey, USA: Prentice Hall, 2000.

5. Barsanti, L. and Gultieri, P., *Algae − Anatomy, Biochemistry and Biotechnology*. Boca Raton, Florida: CRC Press, 2006.

6. Benemann, J. and Oswald, W.J., *Systems and Economic Analysis of Microalgae Ponds for Conversion of CO_2 to Biomass*, Final Report, Pittsburgh: Pittsburgh Energy Technology Center, 1996, 201 p.

7. Soletto, D., Binaghi,L., Lodi, A., Carvalho, J.C.M., and Converti. A., *Aquaculture*, 2005, vol. 243, no. 1−4, pp. 217−224.

8. Becker, W., *Handbook of Microalgal Culture*, Ed. Richmond, Oxford: Blackwell, 2004, pp. 312−351.

9. Borowitzka, M.A., *J. Biotechnol.*, 1999, vol. 77, no. 1−3, pp. 313−321.

10. Ötles, S. and Pire, R., *J. AOAC Int.*, 2001, vol. 84, no. 6, pp. 1708−1714.

11. Prasanna, R., Jaiswal, P., and Kaushik, B.D., *Indian J. Microbiol.,* 2008, vol. 48, no. 1, pp. 89−94.

12. Prasanna, R., Sood, A., Jaiswal, P., Nayak, S., Gupta, V., Chaudhary, V., Joshi, M., and Natarajan, C., *Appl. Biochem. Microbiol.,* 2010, vol. 46, no. 2, pp. 133−147.

13. Lee, Y.K., *J. Appl. Phycol.*, 2001, vol. 13, no. 9, pp. 307−315.

14. Benedetti, S., Benvenuti, F., Pagliarani, S., Francogli, S., Scoglio, S., and Canestrari, F., *Life Sci.* 2004, vol. 75, no. 19, pp. 2353−2362.

15. Singh, S., Kate, B.N., and Banerjee, U.C., *Crit. Rev. Biotechnol.*, 2005, vol. 25, no. 3, pp. 73−95.

16. Running, J.A., Severson, D.K., and Schneider, K.J., *J. Ind. Microbiol. Biotechnol.*, 2002, vol. 29, no. 2, pp. 93−98.

17. Del Campo, J.A., Garcia-Gonzales, M., and Guerrero, M.G., *Appl. Microbiol. Biotechnol.*, 2007, vol. 74, no. 5, pp. 1163−1174.

18. Olaizola, M., *Biomol. Eng.*, 2003, vol. 20, no. 4−6, pp. 459−466.

19. *Pulz, O.* and Gross, W., *Appl. Microbiol. Biotechnol.,* 2004, vol. 65, no. 6, pp. 635−648.

20. Survase S.A., Bajaj, I.B., and Singhal, R.S., *Food Technol. Biotechnol.,* 2006, vol. 44, no. 3, pp. 381−396.

21. Jiang, Y. and Chen, F., *J. Indust. Microbiol. Biotechnol.*, 1999, vol. 23, no. 6, pp. 508−513.

22. Zittelli G.C., Lavista, F., Bastianini., A., Rodolfi, L., Vincenzini, M., and Tredici, M.R., *J. Biotechnol.*, 1999, vol. 70, no. 1−3, pp. 299−312.

23. Yongmanitchai, W. and Ward, O.P., *Appl. Environ. Microbiol.*, 1991, vol. 57, no. 2, pp. 419−425.

24. Acein Fernandez, F.G.A., Hall, D.O., Guerrero, E.C., Rao, K.K., and Grima, E.M., *J. Biotech.*, 2003, vol. 103, no. 2, pp. 137−152.

25. Fuentes, M.M.R., Sanchez, J.L.G., Sevilla, J.M.F., Fernandez, F.G.A., Perez, J.A.S., and Grima, E.M., *J. Biotech.,* 1999, vol. 70, no. 1−3, pp. 271−288.

26. Chisti, Y.*, Trends Biotech.*, 2008, vol. 26, no. 3, pp. 126−131.

27. Reddy, S.B., Balachandra, P., and Kristle Nathan, H.S., *Energy Policy*, 2009, vol. 37, no. 11, pp. 4645−4657.

28. Mata, T.M., Martins, A.A., and Caetano, N.S., *Renew. Sust. Energy Rev.*, 2010, vol. 14, no. 1, pp. 217−232.

29. Lee, D.H., *Bioresour. Technol.*, 2011, vol. 102, no. 1, pp. 43−49.

30. IEA, *Bioenergy Project Development and Biomass Supply − Good Practice Guidelines*, Paris: International Energy Agency, 2007, 66 p.

31. Khan, A.S., Rashmi, Hussain, M.Z., Prasad, S., and Banerjee, U.C., *Renew. Sust. Energy Rev.* 2009, vol. 13, no. 9, pp. 2361−2372.

32. Sims, R.E.H., Mabee,W., Saddler, J.N., and Taylor, M., *Bioresource Technol.* 2010, vol. 101, no. 6, pp. 1570−1580.

33. Righelto, R.. and Spracken, D.V., *Science*, 2007, vol. 317, no. 5840, pp. 902.

34. Weyer, K.M., Bush, D.R., Darzins, A., and Willson, B.D., *Bioenergy Res.*, 2010, vol. 3, no. 2, pp. 204−213.

35. Gordon, J.M. and Polle. J.E., *Appl. Microbiol. Biotechnol.*, 2007, vol. 76, no. 5, pp. 969−75.

36. Banerjee, A., Sharma, R., Chisti,Y., and Banerjee, U.C., *Crit. Rev. Biotechnol.*, 2002, vol. 22, no. 3, pp. 245−79.

37. Miao, X., Wu, Q., and Yang, C.Y., *J. Anal. Appl. Pyrolysis*, 2004, vol. 71, no. 2, pp. 855−863.

38. Scragg A.H., Morrison, J., and Shales S.W., *Enzyme Microb. Technol.* 2003, vol. 33, no. 7, pp. 884−889.

39. Sheehan, J., Dunahay, T., Benemann, J., and Roessler, P., NREL/TP-580-24190. *Close-Out Report*, National Renewable Energy Laboratory, 1998.

40. Tsukahara, K. and Sawayama, S., *J. Japan Petrol. Instit.*, 2005, vol. 48, no. 5, pp. 251−259.

41. Chisti, Y. *Biotechnol. Adv.*, 2007, vol. 25, no. 3, pp. 294−306.

42. Li, Y.Q., Horsman, M., Wang, B., Wu, N., and Lan, C.Q., *Appl. Microbiol. Biotechnol.*, 2008, vol. 81, no. 4, pp. 629−636.

43. Chen, W., Zhang, C., Song, L., Sommerfield, M., and Hu, Q., *J. Microbiol. Meth.* 2009, vol. 77, no. 1, pp. 41−47.

44. Costa, M.C., Mota, S., Nascimento, R.F., and Dos Santos, A.B., *Bioresour. Technol.*, 2010, vol. 101, no. 1, pp. 105−110.

45. Sydney E.B., Wilerson, S., Carvalho, J.C., Thomaz-Soccol, V., Larroche, C., Pandey, A., and Soccol, C.R., *Bioresour. Technol.* 2010, vol. 101, no. 15, pp. 5892−5896.

46. *Costa, J.A.V.* and Morais, M.G., *Bioresour. Technol.*, 2011, vol. 102, no. 1, pp. 2−9.

47. Li, Y., Horsman, M., Wu, N., Lan, C.Q., and Dubois-Calero, N., *Biotechnol. Prog.*, 2008, vol. 24, no. 4, pp. 815−820.

48. Chinnasamy, S., Bhatnagar, A., Claxton, R., and Das, K.C., *Bioresour. Technol.*, 2010, vol. 101, no. 17, pp. 6751−6760.

49. Wang, L., Li, Y.C., Chen, P., Min, M., Chen, Y.F., Zhu, J., and Ruan, R.R., *Bioresour. Technol.*, 2010, vol. 101, no. 8, pp. 2623−2628.

50. Pittman, J.K., Dean, A.P., and Osundeko, O., *Bioresour. Technol.*, 2011, vol. 102, no. 1, pp. 17−25.

51. Raja, R., Hemaiswarya, S., Kumar, N.A., Sridhar, S., and Rengasamy, R., *Crit. Rev. Microbiol.,* 2008, vol. 34, no. 2, pp. 77−88.

52. Hu, Q., Sommerfeld, M., Jarvis, E., Ghirardi, M., Posewitz, M., Seibert, M., and Darzins, A., *Plant J.*, 2008, vol. 54, pp. 621−639.

53. Sharma, Y.C., Singh, B., and Upadhyay, S.N., *Fuel*, 2008, vol. 87, no. 12, pp. 2355−2373.

54. Singh, A., Nigam, S., and Murphy, D.J.D., *Bioresour. Technol.*, 2010, vol. 102, no. 14, pp. 26−34.

55. Scott, S.A., Davey, M.P., Dennis, J.S., Horst, I., Howe, C.J., Lea-Smith, D.J., and Smith, A.G., *Curr. Opin. Biotechnol.*, 2010, vol. 21, no. 3, pp. 277−286.

56. Rodolfi, L., Zittelli, C.G., Bassi, N., Padovani, G., Biondi, N., Bonini, G., and Tredici, M. R., *Biotechnol. Bioeng.*, 2009, vol. 102, no. 1, pp. 100−112.

57. Anandraj, A., Perissinotto, R., Nozais, C., and Stretch, D., *Estuar. Coast. Shelf Sci.*, 2008, vol. 79, no. 4, pp. 599−606.

58. Borowitzka, M.A., *J. Appl.Phycol.*, 1997, vol. 9, no. 5, pp. 393−401.

59. Oswald, W.J. and Golueke, C.G., *Adv. Appl. Microbiol.*, 1960, vol. 2, pp. 223−262.

60. Research Institute of Innovative Technology for the Earth, Research Projects, 2008, http://www.rite.or.jp/English.

61. Packer, M., *Energy Policy*, 2009, vol. 37, no. 9, pp. 3428−3437.

62. Ketchum, B.H. and Redfield, A.C., *Biol. Bull.*, 1938, vol. 75, no. 1, pp. 165−169.

63. Barclay, W., Johansen, J., Chelf, P., Nagle, N., Roessler, P., and Lemke, P., *Microalgae Culture Collection 1986−87*, Golden, Colorado, USA, Solar Energy Research Institute, SERI/SP-232-3079, 147 p.

64. Masutani, S.M. and Nakamura, T., Review and Analysis of Japanese CO_2 Disposal Research Programs. Final Report. U.S. Department of Energy, № DE-AF26-98FT00720, Federal Energy Technology Center, 2000, pp. 1−72.

65. Rogerson, A., DeFreitas, A.S.W., and McInnes, A.C., *Trans. Am. Microsc. Soc.*, 1986, vol. 105, no. 1, pp. 50−67.

66. Nishikawa, N., Koyu, H.N., Hirano, A., Ikuta, Y., Hukuda, Y., Negoro, M., Kaneko, M., and Hada., M., *Energy Conver. Mgmt.*, 1992, vol. 33, no. 5−8, pp. 553−560.

67. Murakami, M. and Ikenouchi, M., *Energy Conver. Mgmt.*, 1997, vol. 38, Suppl., pp. 493−498.

68. Akoto, L., Pel, R., Irth, H., Brinkman, U.A.T., and Vreuls, R.J.J., *J. Anal. Appl. Pyrol.* 2005. vol. 73, no. 1, pp. 69−75.

69. Cooksey, K.E., Guckert, J.B., Williams, S.A., and Callis, P.R., 1987. *J Microbiol. Meth.*, 1987, vol. 6, no. 6, pp. 333−345.

70. Xiong, W., Li, X.F., Xiang, J.Y., and Wu, Q.Y., *Appl. Microbiol. Biotechnol.*, 2008, vol. 78, no. 1, pp. 29−36.

71. Elsey, D., Jameson, D., Raleigh, B., and Cooney, M.J., *J. Microbiol. Meth.* 2007, vol. 68, no. 3, pp. 639−642.

72. Huang, G.H., Chen, F., Wei, D., Zhang, X.W., and Chen., G., *Appl. Energy*, 2009, vol. 87, no. 1, pp. 38−46.

73. Stockenreiter, M., Graber, A.K., Haupt, F., and Stibor, H., *J. Appl. Phycol.*, 2011, DOI 10.1007/s10811-010-9644-1.

74. Cooper, M.S., Hardin, W.R., Petersen, T.W., and Cattolico, R.N., *J. Biosci. Bioeng.*, 2010, vol. 109, no. 2, pp. 198−201.

75. Dean, A.P., Sigee, D.C., Estrada, B., and Pittmann, J.K., 2010. *Biores. Technol.*, 2010, vol. 101, no. 12, pp. 4499−4507.

76. Benemann, J.R., Goebel, R.P., Weissman, J.C., and Augenstein, D.C., *Microalgae as a Source of Liquid Fuels. Final Technical Report to US Department of Energy*. Washington DC: US Department of Energy, 1982.

77. Samorì, C., Torri, C., Samorì, G., Fabbri, D., Galletti, P., Guerrini, F., Pistocchi, R., and E., Tagliavini, *Bioresour. Technol.* 2010, vol. 101, no. 9, pp. 3274−3279.

78. Li, Y., Han, D., Hu, G., Summerfield, M., and Hu, Q., *Biotechnol. Bioeng.,* 2010, vol. 107, no. 2, pp. 258−268.

79. Gouveia, L. and Oliveira, A.C., *J. Ind. Microbiol. Biotech.*, 2009, vol. 36, no. 2, pp. 269−274.

80. Bhatnagar, A., Bhatnagar, M., Chinnasamy, S., and Das, K.C., *Appl. Biochem. Biotechnol.*, 2010, vol. 161, no. 1−8, pp. 523−536.

81. Huang, G.H., Chen, G., and Chen, F., *Biomass Bioeng*, 2009, vol. 33, no. 10, pp. 1386−1392.

82. Guzmán, H.M., Valido, A.J., Duarte, L.C., and Presmanes, K.F., *Aquacult. Int.*, 2010, vol. 18, no. 2, pp. 189−199.

83. Tang, D., Han, W., Li, P., Miao, X., and Zhong, J., *Bioresour. Technol.*, 2011, vol. 102, no. 3, pp. 3071−3076.

84. Liu, J., Huang, J., Sun, Z., Zhong, Y., Jiang, Y., and Chen. F., *Bioresour. Technol.*, 2011, vol. 102, no. 1, pp. 106−110.

85. Chinnasamy, S., Ramakrishnan, B., Bhatnagar, A., and Das K.C. *Int. J. Mol. Sci.*, 2009, vol. 10, no. 2, pp. 518−532.

86. Ota, M., Watanabe, H., Kato, Y., Watanabe, M., Sato, Y., Smith, Jr., R.L., and Inomata, H., *J. Sep. Sci.*, 2009, vol. 32, no. 13, pp. 2327−2335.

87. Chinnasamy, S., Bhatnagar, A., Hunt, R.W., and Das, K.C., *Bioresour. Technol.*, 2010, vol. 101, no. 9, pp. 3097−3105.

88. Zhekisheva, M., Boussiba, S., Khozin-Goldberg, I., Zarka, A., and Cohan, Z., *J. Phycol.*, 2002, vol. 38, no. 2, pp. 325−331.

89. Valenzuela-Espinoza, E., Millan-Nunez, R., Nunez-Cebrero, F., *Aquacult. Eng.*, 2002, vol. 25, no. 4, pp. 207−216.

90. Huntley, M.E. and Redalje, D.G., *Mitigat. Adapt. Strat. Global Change*, 2007, vol. 12, no. 4, pp. 573−608.

91. Shifrin, N.S. and Chisholm, S.W., J. *Phycol.*, 1981, vol. 17, no. 4, pp. 374−384.

92. Boussiba, S., Vonshak, A., Cohen, Z., Avissar, Y., and Richmond, A., *Biomass*, 1978, vol. 12, no. 1, pp. 37−47.

93. Tornabene, T.G., Holzer, G., Lien, S., and Burris, N., *Enzyme Microb. Technol.*, 1983, vol. 5, no. 6, pp. 435−440.

94. Kyle, D.J. and Gladue, R.M., *Int. Patent Appl.* Patent Cooperation Treaty Publication, WO 91/144271, 1991.

95. Li, Y., Han, D., Sommerfeld, M., and Hu, Q., *Bioresour. Technol.*, 2011, vol. 102, no. 1, pp. 123−129.

96. Lewin, R.A. Golden, Production of Hydrocarbons by Micro-Algae: Isolation and Characterization of New and Potentially Useful Algal Strains, Colorado, USA: Solar Energy Research Institute, SERI/CP-231-2700, 1985, pp. 43−51.

97. Zittelli G.C., Rodolfi, L., Biondi, N., and M.R., Tredici, *Aquaculture*, 2006, vol. 261, no. 3, pp. 932−943.

98. Brown M.R., Dunstan, G.A., Norwood, S.J., and Miller, K.A., *J. Phycol.* 1996, vol. 32, no. 1, pp. 64−73.

99. Liu, Z.Y., Wang, G.C., and Zhou, B.C., *Bioresour. Technol.*, 2008, vol. 99, no. 11, pp. 4717−4722.

100. Smith, V.H., Sturm, B.S.M., deNoyelles, F.J., and Billings, S.A., *Trends Ecol. Evol.*, 2009, vol. 25, no. 5, pp. 301−309.

101. Courchesne N.M.D., Parisien, A., Wang, B., and Lan., C.Q. *J. Biotechnol.,* 2009, vol. 14, no. 1−2, pp. 31−41.

102. Spoehr, H.A. and Milner, H.W., *Plant Physiol.*, 1949, vol. 24, no. 1, pp.120−149.

103. Illman, A.M., Scragg, A.H., and Shales, S.W., *Enzyme Microb. Technol.,* 2000, vol. 27, no. 8, pp. 631−635.

104. Lynn, S.G., Kilham, S.S., Kreeger, D.A., and Interlandi, S.J., *J. Phycol.*, 2000, vol. 36, no. 3, pp. 510−522.

105. Reitan K.I., Rainuzzo, J.R., and Olsen, Y., *J. Phycol.*, 1994, vol. 30, no. 6, pp. 972−979.

106. Khozin-Goldberg, I., and Cohn, Z., *Phytochem.*, 2006, vol. 67, no. 7, pp. 696–701.

107. Rao, A.R., Dayananda, C., Sarada, R., Shamala, T.R., and Ravishankar, G.A., *Bioresour. Technol.*, 2007, vol. 98, no. 3, pp. 560–564.

108. Guschina, I.A. and Harwood, J.L., *Prog. Lipid Res.*, 2006, vol. 45, no. 2, pp. 160–186.

109. Roessler, P.G., *Plant Physiol.*, 1990, vol. 92, no. 1, pp. 73–78.

110. Yamaberi, K., Takagi, M., and Yoshida, T., *J. Mar. Biotechnol*, 1998, vol. 6, no. 1, pp. 44–48.

111. Borowitzka, M.A. *Micro-Algal Biotechnology,* Eds. M.A. Borowitzka and Borowitzka, L.J., Cambridge: Cambridge University Press., 1988, pp. 257–287.

112. Griffiths, M.J. and Harrison, S.T.L., *J. Appl. Phycol.,* 2009, vol. 21, no. 5, pp. 493–509.

113. Sterner, R. and Elser, J., *Ecological Stoichiometry: The Biology of Eelements from Molecular to Biosphere*. Princeton, New Jersey: Princeton University Press, 2002.

114. Rhee, G.Y., *Limnology Oceanography*, 1978, vol. 23, no. 1, pp. 10–25.

115. Geider, R.J. and La Roche, J., *Eur. J. Phycol.*, 2002, vol. 37, no. 1, pp. 1–17.

116. Richardson, B., Orcutt, D.M., Schwertner, H.A., Cara, L.M., and Hazel, E.W., *Appl. Microbiol.*, vol. 18, no. 2, pp. 245–250.

117. Sato, N., Hagio, M., Wada, H., and M. Tsuzuki, *Recent Advances in the Biochemistry of Plant Lipids*. Eds., Harwood, J. L., and Quinn, P.J., London: Portland Press Ltd., 2000, pp. 912–914.

118. Roessler, P.G., *Arch. Biochem. Biophys.*, 1988, vol. 267, no. 2, pp. 521–528.

119. Behrenfeld, M.J., Worthington, K., Sherrell, R.M., Chavez, F.P., Strutton, P., McPhaden, M., and Shea, D.M., *Nature,* 2006, vol. 442, no. 7106, pp. 1025–1028.

120. Converti, A., Casazza, A.A., Ortiz, E.Y., Perego, P., Borghi, M.D., *Chem. Eng. Process*, 2009, vol. 48, no. 6, pp. 1146–1151.

121. Khotimchenko, S.V. and Yakovleva, I.M., *Phytochem.*, 2005, vol. 66, no. 1, pp. 73–79.

122. Bigogno, C., Khozin-Goldberg, I., Boussiba, S., Vonshak, A., and Cohen, Z., *Lipids,* 2002, vol. 37, no. 2, pp. 209–216.

123. Takagi, M., Karseno, and Yoshida, T., *J. Biosci. Bioeng.*, 2006, vol. 101, no. 3, pp. 223–226.

124. Mansour, M.P., Volkman, J.K., and Blackburn, S.I., *Phytochem.*, 2003, vol. 63, no. 2, pp. 145–153.

125. Nozaki, H., Takano, H., Misumi et al., *BMC Biology*, 2007, vol. 5, no. 1, pp. 28.

126. Armbrust V.E., Berges, J.A., Bowler, C. et al., *Science*, 2004, vol. 306, no. 5693, pp. 79–86.

127. Bowler, C., Allen, A.E., Badger, J.H. et al., *Nature*, 2008, vol. 456, no. 7219, pp. 239–244.

128. Derelle, E., Ferraz, C., Rombauts, S. et al., *Proc. Natl. Acad. Sci. USA.*, 2006, vol. 103, no. 31, pp. 11647–11652.

129. Walker, T.L., Collet, C., and Purton, S., *J. Phycol.*, 2005, vol. 41, no. 6, pp. 1077–1093.

130. Dunahay, T.G., Jarvis, E.E., and Roessler, P.G., *J. Phycol.* 1995, vol. 31, no. 6, pp. 1004–1012.

131. Carvalho A.P., Meireles, L.A., and Malcata, F.X., *Biotechnol. Prog.,* 2006, vol. 22, no. 6, pp.1490–1506.

132. Hankammer, B., Lehr, F., Rupprecht, J., Mussgnug, J.H., Posten, C., and Kruse, O*., Physiol. Plant.,* 2007, vol. 131, no. 1, pp. 10–21.

133. Karube, I., Takeuchi, T., and Barnes, D., *Advances in Biochemical Engineering-Biotechnology*, *Modern Biochemical Engineering*, Ed. T. Scheper, Berlin, New York: Springer Verlag. 1992.

134. Pulz, O., *Appl. Microbiol. Biotechnol.*, 2001, vol. 57, no. 3, pp. 287–293.

135. Harun, R., Singh, M., Forde, G. M., and Danquat, M.K., *Renew. Sust. Energy Rev.* 2010, vol. 14, no. 3, pp. 1037–1047.

136. Lee S.J. and Lee, J.P., *Biotechnol. Bioprocess Eng.*, 2003, vol. 8, no. 6, pp. 354–359.

137. Watanabe, Y., Ohmura N., and Saiki, H., *Energy Conver. Mgmt.*, 1992, vol. 33, no. 5–8, pp. 545–552.

138. Sung, K.D., Lee, J.S., Shin, C.S., Park, S.C., and Choi, M.J., *Bioresour.Technol.*, 1999, vol. 68, no. 3, pp. 269–273.

139. Ono, E. and Cuello, J.L., *Biosystems Eng.*, 2007, vol. 96, no. 1, pp. 129–134.

140. Hall, D.O. and House, J.I., *Energy Conv. Manage.* 1993, vol. 34, no. 9–10, pp. 889–896.

141. Benemann, J.R., *Energy Conver. Mgmt.*, 1979, vol. 38, supl. 1, pp. S475–S479.

MICROALGAE BIOFUEL POTENTIALS (REVIEW)

© 2012 Y. Ghasemi*, **, S. Rasoul-Amini*, ** ,***, A. T. Naseri**, N. Montazeri-Najafabady*, **,
M. A. Mobasher*, **, F. Dabbagh*, **

*Department of Pharmaceutical Biotechnology, Faculty of Pharmacy, Shiraz University of Medical Sciences,
P.O.Box 71345-1583, Shiraz, Iran*
**Pharmaceutical Sciences Research Center, Shiraz University of Medical Sciences, P.O.Box 71345-158, Shiraz, Iran*
***Department of Medicinal Chemistry, Faculty of Pharmacy, Shiraz University of Medical Sciences,
P.O.Box 71345-1583, Shiraz, Iran*
e-mail: ghasemiy@sums.ac.ir

With the decrease of fossil based fuels and the environmental impact of them over the planet, it seems necessary to seek the sustainable sources of clean energy. Biofuels, is becoming a worldwide leader in the development of renewable energy resources. It is worthwhile to say that algal biofuel production is thought to help stabilize the concentration of carbon dioxide in the atmosphere and decrease global warming impacts. Also, among algal fuels' attractive characteristics, algal biodiesel is non toxic, with no sulfur, highly biodegradable and relatively harmless to the environment if spilled. Algae are capable of producing in excess of 30 times more oil per acre than corn and soybean crops. Currently, algal biofuel production has not been commercialized due to high costs associated with production, harvesting and oil extraction but the technology is progressing. Extensive research was conducted to determine the utilization of microalgae as an energy source and make algae oil production commercially viable.

The world's demand for energy is steadily increasing. Global demand for petroleum is predicted to increase 40% by 2025 [1]. So, the use of an alternative fuel becomes necessary. Biofuels are a wide range of fuels which are in some way derived from biomass. The term covers solid biomass, liquid fuels and various biogases. It is expected to expand biofuels to 36 billion gallons by 2022. Third generation biofuels ("advanced biofuel" or biodiesel from microalgae) are a promising alternatives to other biofuels but there are still vagueness to be investigated. Their energy output per land unit is at least 30 times higher than for 2nd generation biofuels [2]. Biodiesel defined as a mixture of monoalkyl esters derived from fatty acids of oil crop or animal fats is biodegradable, and nontoxic. Biodiesel in conventional diesel engines reduces emissions of unburned hydrocarbons, carbon monoxide, sulfates, polycyclic aromatic hydrocarbons and nitrated polycyclic aromatic hydrocarbons. Microalgae appear to be the only source of renewable biodiesel that is capable of meeting the global demand for transport fuels [3]. Each of the three biochemical fractions of microalgae (lipids, carbohydrates, and proteins) can be converted into fuels. The lipids of some species are hydrocarbons, similar to those found in petroleum, while those of other species resemble seed oils, can be converted to a synthetic diesel fuel (ester-fuel) by transesterification. Carbohydrates are commonly converted to ethanol by fermentation. Alternatively, all three fractions can be converted to methane gas by anaerobic digestion [4]. Oil content of some microalgae may exceed 80% of the dry weight of algae biomass. Even microalgae of low oil content can produce ten times the amount of the most productive terrestrial biodiesel feedstocks. Algae are said to yield about 1.200—10.000 gallons of oil/acre, compared to 48 and 18 gallons/acre for soy and corn, respectively [5, 6]. The major threshold for producing microalgal biodiesel is the high cost of raw material (US$2.4/l microalgal oil), which is 3—4 times higher than plant oil. Algae can be grown in ponds, closed photobioreactors or in plastic tanks called bioreactors. Over 90% of the world's commercial microalgae production uses shallow, open, paddle wheel mixed, raceway type ponds but closed photobioreactors represent only about 1%. The approximate number of companies directly involved in producing fuels from the algae is increasing with a high rate as 50 in 2008 to 75 in early 2009, 100 in mid 2009 and 150 at the end of 2009. Only about 10000 metric tons of microalgal biomass (dry matter basis) is produced annually in commercial operations, with a typical selling price of from 5000 to over 100.000$ US per dry t of biomass. When formulated into finished consumer products, this biomass generates a turnover of several billion dollars per year. This article focuses on microalgae as a potential source of biofuel, cultivation, biofuel opportunities and attempts towards commercial algal fuel production [5].

WHY BIOFUEL? WHY ALGAL BIOFUEL?

The remaining global reserves of crude oil are continuously declining. Based on the available data, the world will run out of crude oil in 24 to 57 years from today [7]. It was estimated that by 2050 biomass could provide nearly 38% of the world's direct fuel use and 17% of the world's electricity [8]. A major criticism against large-scale biofuel production is that it will occupy vast farm land and native habitats, drive up food prices, and result in little reduction in CO_2 emissions. At the moment, only biodiesel and bioethanol are produced on an industrial scale which are derived from food crops such as sugarcane, sugar beet, maize (corn), sorghum and wheat which is known as first generation biofuel. The basic feedstocks for the production of first-generation biofuels are often grains, which yield starch that is fermented into bioethanol, or seeds, which are pressed to yield vegetable oil that can be used in biodiesel. Second generation biofuels use biomass to liquid technology, including cellulosic biofuels (grassoline) from nonfood crops, including waste biomass, the stalks of wheat, corn, or wood. These biofuels are inherently more efficient than first generation technologies because they use more of the plant to produce fuel [3]. Third-generation biofuels "advanced biofuels" are derived from algae [3]. For 2010 it is expected to have 100 000 gallons of algal biofuel production which will increase to 6 billion gallons in 2025 [9]. It is said that in 2020, 30% of algae production goes to oil fraction [10]. Algal biofuels have a tremendous variety. Algal biomass may be used directly as a solid biofuel to generate heat, steam and electricity or converted to gaseous biofuels, such as biogas and biohydrogen. Algal biomass rich in starch can be easily fermented to liquid biofuels such as bioethanol and biobutanol. Algal oils can be converted to diesel, gasoline and jet fuel using existing technology [5]. Currently biodiesel is used for blending (2−10%) with crude oil without the need for any modifications in existing engines since that makes no difference in vapour pressure, viscosity, density, and octane/cetane number. Algae can produce 267 l of ethanol (assuming a 40% starch content) and 190 l of biodiesel/ dry t [11]. Microalgae containing 30% oil by weight of dry biomass could yield almost 587 000 l/ha or 5.000−15 000 gallons/year [10]. However, up to now, the commercial production of biofuels from microalgae has not been realised on an industrial scale in a cost-efficient manner. Several problems have arisen during the large scale production, including high investment costs for production facilities and energy demand for harvesting biomass of low concentration [12]. Microalgal biofuels are 4−10 times as expensive to produce as petroleum-derived fuels or other biodiesels [5].

STRAIN SELECTION

Looking for the microalgal strains with the combination of high oil content and a rapid growth rate is the start of biodiesel production. A limited number, about 4000 species have been identified, which can be divided into several groups including cyanobacteria (Cyanophyceae), green algae (Chlorophyceae), diatoms (Bacillariophyceae), yellow-green algae (Xanthophyceae), golden algae (Chrysophyceae), red algae (Rhodophyceae), brown algae (Phaeophyceae), dinoflagellates (Dinophyceae) and 'pico-plankton'(Prasinophyceae and Eustigmatophyceae) [13]. The three most prevalent groups of algae targeted for biodiesel production include the diatoms that make up a majority of phytoplankton in salt and brackish waters, green algae common in many freshwater systems, blue-green algae (Cyanophyceae), which are actually bacteria that contain chloroplasts and are important to nitrogen fixation in aquatic systems, and finally the golden algae species able to store carbon as oil and complex carbohydrates [14−16]. They have oil levels between 20 and 75% by weight of dry biomass (Table 1). In general, lower oil strains grow faster than high oil strains [17]. Microalgae containing 30% oil grow 30 times faster than those containing 80% oil [18]. Another challenge is that microalgae usually accumulate oil under stress conditions with slow growth rate. The composition of microalgal fatty acids has a significant effect on the fuel properties of biodiesel produced. The proper percentage of saturated and unsaturated fatty acid is very important to microalgae as a biodiesel feedstock [10].

For strain selection, some factors are: lipid content, more the distribution of free fatty acids and triglycerides not only the total lipids; resistance to environmental conditions changes, competition from other microalgae species and/or bacterial; nutrients availability; ease of biomass separation and processing; possibility of obtaining other valuable chemicals. Even when the species are not quite deasirable for the purpose in commercial use, the utilization of genetic engineering may be a solution [21]. Type of metabolism is also important for strain selection. Microalgae may assume many types of metabolisms (autotrophic, heterotrophic, mixotrophic, photoheterotrophic) and are capable of a metabolic shift as a response to changes in the environmental conditions [22]. Generally, heterotrophic cultivation has been found to increase the total lipid content in algae compared to phototrophically grown cells. Mixotrophic, perform photosynthesis as the main energy source, though both organic compounds and CO_2 are essential. Amphitrophy, a subtype of mixotrophy, means that organisms are able to live either autotrophically or heterotrophically, depending on the concentration of organic compounds and light intensity available. For species that can utilize both light energy and chemical substrates, this mode of cultivation offers a superior alternative to phototrophic and heterotrophic growth. Photoheterotrophic, also known as photoorganitrophy, photoassimilation, photometabolism, describes the metabolism in which light is required to use organic com-

Table 1. Lipid content of some microalgae [18, 19]

Microalgae species	Lipid content, % dry waight biomass	Microalgae species	Lipid content, % dry waight biomass
Ankistrodesmus species	28—40	*Euglena gracilis*	14—20
Anabaena cylindrica	4—7	*Ellipsoidion* sp.	27
Botryococcus braunii	25—86	*Haemotococcus pluvialis*	25
Chaetoceros muelleri	33	*Hantzschia* species	66
Chlamydomonas species	23	*Isochrysis galbana*	21.2
Cllorella emersonii	25—63	*Monallantus salina*	20—22
Chlorella minutissima	57	*Nannochloropsis* sp.	20—56
Chlorella protothecoides	14—57	*Neochloris oleoabundans*	35—65
Chlorella sorokiniana	22	*Nitschia closterium*	27.8
Chlorella vulgaris	14—56	*Nitschia frustulum*	25.9
Crypthecodinium cohnii	20—51	*Pavlova lutheri*	35
Cyclotella species	42	*Phaeodactylum tricornutum*	20—30
Dunaliella primolecta	23	*Prostanthera incisa*	62
Dunaliella salina	28.1	*Prymnesium parvum*	22—39
Dunaliella tertiolecta	36—42	*Pyrrosia laevis*	69.1
Skeletonema costatum	13—51	*Spirulina plantensis*	16.6
Scenedesmus dimorphus	16—40	*Stichococcus* species	33
Scenedesmus quadricauda	19.9	*Tetraselmis suecia*	15—23
Schizochytrium sp.	50—77	*Thalassiosira pseudonana*	20
Selenastrum species	21.7	*Zitzschia* sp.	45—47

pounds as carbon source. The photoheterotrophic and mixotrophic metabolisms are not well distinguished, in particular they can be defined according to a difference of the energy source required to perform growth and specific metabolite production [5].

MICROALGAE CULTIVATION

When inoculating a batch of microalgae, subculture is usually used to ensure continuous growth and division of cells. Water, air and carbon dioxide stream should be filtered to reduce contamination risk. Cultivation can be conducted in batch, semi-batch, and continuous systems. Batch culture consists of a single inoculation of cells in container of media over several days of growth period until the cell density reaches a maximum/desirable level ready to be transferred to larger culture volumes to continue growth before reaching the stationary phase. The semi-batch system allows a portion of the culture to be harvested and replenished with fresh medium. In a continuous system, two types of culture can be used: turbidostat and chemostat culture. In a turbidostat culture, when the density reaches a preset level, fresh medium is added to the culture as the cells continue to divide and grow. In the chemostat culture, a slow but steady flow of fresh medium is continually introduced into the culture while excess culture overflows and collected. Two

types of reactors have been developed to cultivate algae: open system (such as raceway ponds) and closed system (such as photobioreactors).

Open pond systems. Such systems can be excavated and used unlined or lined with impermeable materials, or they can be built up with walls. Sometimes unlined ponds are used to reduce costs, but they suffer from silt suspension, percolation, heavy contamination, and their use is limited to a few algal species and to particular soil and environmental conditions [23]. Raceway ponds are open, outdoor ponds that are made of circulating loop channels and are typically shallow (less than 0.3 m deep) and unlined. Open pond has moderate surface-to-volume ratio of 3—10/m [24]. Paddle wheels are used to circulate the suspended algae throughout the raceway channels. Cooling is mostly done by evaporation, and the pond is illuminated solely by sunlight. The raceway pond can be run continuously with growth medium and carbon dioxide feed continuously added to the pond while algal broth is harvested at the end of the circulation loop. Production in the pond usually takes 6—8 weeks to mature and typically yields only 0.1—0.2 g/l algae [25]. Open ponds are dependent on weather because temperature and light intensity vary throughout the day and year. Low temperatures (<17°C) reduce algal growth rate while high temperatures (>27°C) kill algal cells. If cultivation is a success, high biomass yields are mostly

seasonal. Tank size also influences algal growth. Smaller outdoor ponds produce higher algal yield than a larger pond. The open pond system can be converted to an indoor system by covering the pond with a layer of plastic or glass [23]. Raceway pond is the most commonly used design as an open culture system [5]. Open ponds are only suitable for a small number of algal species that can tolerate extreme environmental conditions. The size of commercial ponds varies from 0.1 to 0.5 ha. Raceway ponds are widely used for the commercial cultivation of *Spirulina*, *Haematococcus* and *Dunaliella* [26]. The productivity of raceways is almost 10 times higher than unmixed algae ponds. Open systems can be easily scaled up to several acres for individual ponds. Currently, 98% of commercial algae are produced in open systems [27]. Circular ponds are the other type of open pounds used mainly in Asia for the production of *Chlorella*. These ponds are mixed by a centrally located rotating arm (similar to those used in wastewater treatment). Thin layer, inclined ponds consist of slightly inclined shallow trays, over which a very thin layer of algae flows to the bottom where the culture is collected and returned to the top. Mild mixing or wave producer such as paddlewheel, waterjet or air pump systems can be used to make a water velocity typically at 30 cm/s (much higher velocities require excessive amounts of mixing energy) [28]. Unmixed open systems are not true algae production ponds because production is not maximized and the biomass produced is rarely harvested. Even when the biomass from unmixed ponds is harvested, their chemical byproducts interfere with utilization for biofuels [29].

Photobioreactors (PBRs). PBRs were developed to overcome the problems associated with open pond systems. They can be located indoors and provided with artificial light or natural light via light collection and distribution systems or outdoors to use sunlight directly [30]. PBRs can be classified on the basis of both design and mode of operation. Reactors can be tilted at different angles and can use diffuse and reflected light, which plays an important role in productivity. Materials such as plastic or glass sheets, collapsible or rigid tubes, must lack toxicity, have high transparency, high mechanical strength, high durability, chemical stability and low cost [31]. Closed systems like photobioreactors have higher efficiency and biomass concentration (2–5 g/l), shorter harvest time, reduce contamination risk, and allow greater selection of algal species used for cultivation and higher surface-to-volume ratio (25–125/m) than open ponds [32]. Light can be radiated inside the bioreactor with optical fibers or submerged lamps, or provided externally by fluorescent lights or the sun. The photobioreactor has a photolimited central dark zone and a better lit peripheral zone close to the surface [5]. Carbon dioxide enriched air is sparged into the reactor creating a turbulent flow which circulates cells between the light and dark zones and assists the mass transfer of carbon dioxide and oxygen gases. The frequency of light and dark zone cycling is depended on the intensity of turbulence, cell concentration, optical properties of culture, diameter of tube, and the external irradiance level [5]. Regulation of carbon dioxide and dissolved oxygen levels in the photobioreactor is another key element to algal growth. Challenges with closed system photobioreactors include overheating, build up of photolimited zones in the inner zone, photoinhibition in the peripheral zones, cell structure damage due to hydrodynamic stresses, and growth on the reactor wall [5, 23, 33] and cost. The scale-up of bioreactors increases the percentage of dark zone and reduces algal growth. The highest cost for closed system is the energy cost associated with the mixing mechanism [34]. A small scale bioreactor can be easily incorporated into a pilot plant as an indoor or outdoor system. The most popular photobioreactors are as follows: tubular systems [35–38]; helical PBRs [30]; plastic bag systems [28]; well systems; pyramid photobioreactors; airlift photobioreactors [39]; annular photobioreactors [40]; column photobioreactors [39–41]; bubble column photobioreactors [41]; vertical column photobioreactors [36, 42]; flat Plate PBRs [38, 43, 44]; stirred tank photobioreactors [41]; rectangular tanks [45]; immobilized bioreactors [46–50]; hybrid systems [51].

In conclusion, PBR and open ponds should not be viewed as competing technologies, but the real competing technology will be genetic engineering [31]. PBR can be operated in batch or continuous mode. There are several advantages of using continuous bioreactors instead of the batch mode (Table 2) [52]: continuous bioreactors provide a higher degree of control than do batch, growth rates can be regulated and maintained for extended time periods and biomass concentration can be controlled by varying the dilution rate, because of the steady-state of continuous bioreactors, results are more reliable and easily reproducible and the desired product quality may be more easily obtained.

Fermenters. They are similar to bioreactors in that they are closed or semi closed systems used for the production of biomass. However, fermentors utilize an organic source of carbon (sugar) as the source of energy and carbon instead of light and photosynthesis. Fermentors can usually achieve much higher biomass than a photobioreactor, but the cost per unit weight is usually much higher due to cost of supplying the fixed carbon source [28].

Closed photobioreactors are recommended for scaling up of microalgae because they can be erected over any open space, can operate at high biomass concentration, can keep out atmosphere contaminants and can save water, energy, and chemicals compared to some other open culture systems. The biomass productivity of photobioreactors can average 13 times more than that of a traditional raceway pond. A combination of open ponds and closed photobioreactors is probably the most logical choice for cost-effective cul-

Table 2. Open pond cultivation of microalgae vs. photobioreactors [33, 53, 54]

Factor	Open pond	Photobioreactor
Required space	High	For PBR itself low
Water loss	Very high, may also cause salt precipitation	Low
CO_2-loss	High, depending on pond depth	Low
Oxygen concentration	Usually low enough because of continuous spontaneous outgassing	Build-up in closed system requires gas exchange devices (O_2 must be removed to prevent inhibition of photosynthesis and photo oxidative damage)
Temperature	Highly variable, some control possible by pond depth	Cooling often required (by spraying water on PBR or immersing tubes in cooling baths)
Shear	Usually low (gentle mixing)	Usually high (fast and turbulent flows required for good mixing, pumping through gas exchange devices)
Cleaning	No issue	Required (wall-growth and dirt reduce light intensity), but causes abrasion, limiting PBR lifetime
Contamination risk	High (limiting the number of species that can be grown)	Medium to low
Biomass quality	Variable	Reproducible
Biomass concentration	Low, between 0.1 and 0.5 g/l	High, generally between 0.5 and 8.0 g/l
Production flexibility	Only few species possible, difficult to switch	High, switching possible
Process control and reproducibility	Limited (flow speed, mixing, temperature only by pond depth)	Possible within certain tolerances
Weather dependence	High (light intensity, temperature, rainfall)	Medium (light intensity, cooling required)
Start-up	6–8 weeks	2–4 weeks
Capital costs	High ~ US$100000 per ha	Very high ~ US$250000 to 1000000 per ha (PBR plus supporting systems)
Operarting costs	Low (paddle wheel, CO_2 addition)	Higher (CO_2 addition, oxygen removal, cooling, cleaning, maintenance)
Harvesting costs	High, species dependent	Lower due to high biomass concentration and better control over species and conditions

tivation of high yielding strains for biodiesel [53]. In the first stage, the microalgal strain with high oil content is grown in photobioreactors to produce biomass. In the second stage, the microalgae enter an open raceway with nutrient limitations and other stressors to promote biosynthesis of oil.

Once an algal culture reaches maturity, the biomass is harvested from the culture medium. Biomass harvesting may be one of the more contaminating processes in the production of algae-based biofuels. There are three systemic components of the harvesting process: biomass recovery, dewatering, and drying. The costs of harvesting can be a significant proportion of the total algal production costs, ranging from 20 to 30% [55]. In order to produce energy from algae as economically as possible, the cheapest way of concentrating the algal biomass low enough for oil pressing is essential. The technically simplest option is the use of settling ponds which is filled with a fully grown algae culture and drained at the end of that day, leaving a concentrated biomass volume at the bottom, which is stored for further processing [56]. There are other efficient techniques for recovering algal biomass, the implementation of which may vary depending on existing pond conditions or PBR design. They are as follows: Flocculation (induced in various ways, such as chemical flocculation, bioflocculation, electroflocculation); dissolved air floatation; centrifugation, filtration, decantation and vacuuming, dewatering, and drying [3, 19, 55, 57–59].

BIOFUEL POTENTIALS

Algae for biofuels have been studied for many years for production of hydrogen, methane, triglycerides for biodiesel, hydrocarbons and ethanol. Methane was the
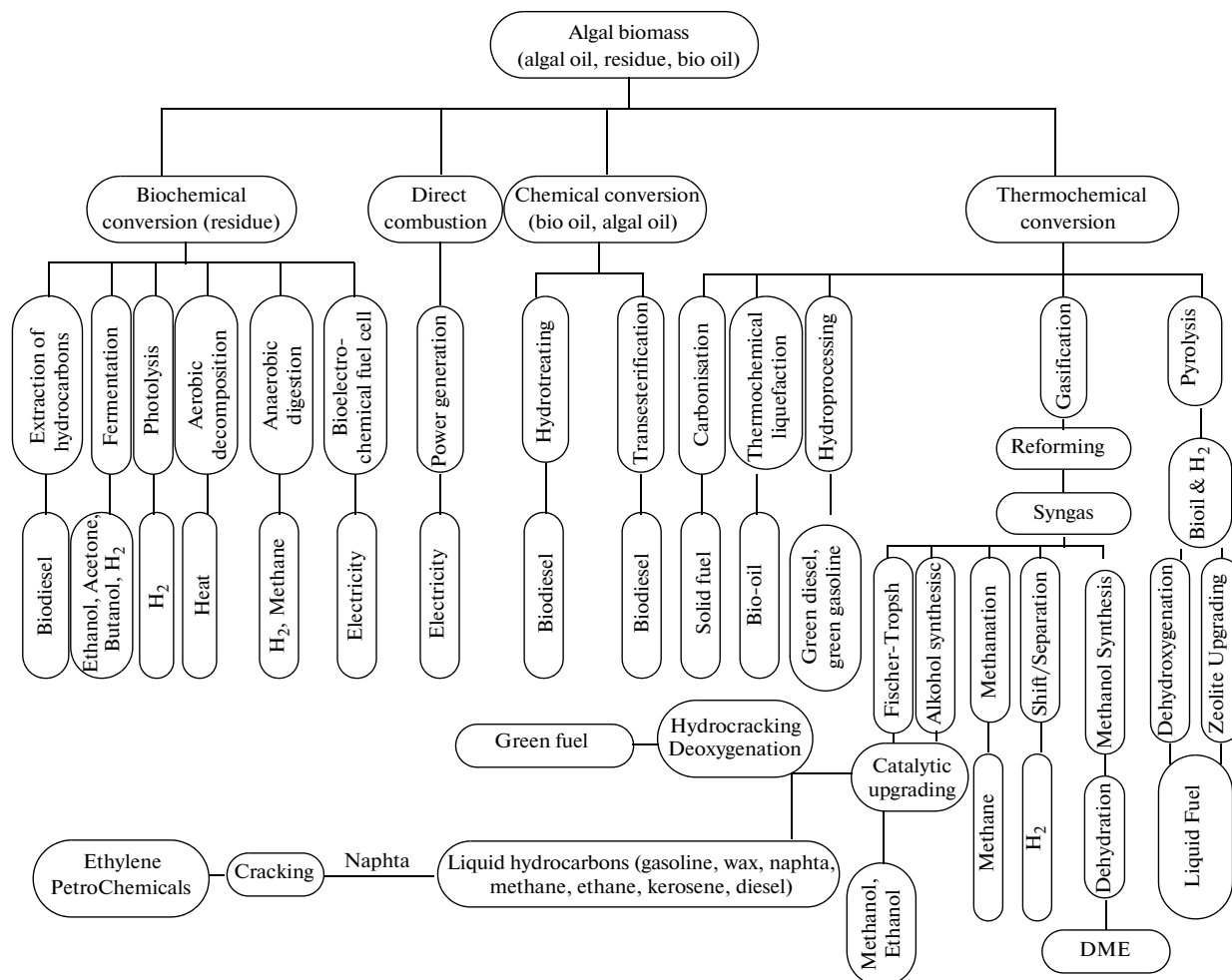
Fig. 1. Algae biomass transformation to energy [3].

focus of the early work in microalgae biofuels production. Since the 1980s, after the first oil shocks and higher value of liquid transportation fuels focused are on algae oil, specifically biodiesel production. Conversion processes of algal biomass (or components of biomass) into several possible biofuels and coproducts are of varying efficiency depending on reaction temperature, pressure, heating rate, and catalyst type, as well as algal species and quality of biomass. If oil extraction is done on algae the product would be algal oil. If thermochemical pretreatment is done on algal biomass bio-oil will be derived that is different from algal oil. They will play as intermediate products in determining which processs may be used to get different kind of fuels [3, 60] (Fig. 1).

Hydrocarbon. Hydrocarbons are fuels such as gasoline, diesel, and jet fuel that do not contain oxygen but carbon and hydrogen. Bioderived hydrocarbon fuels are products of thermochemically converted algal oil or bio-oil and are sometimes referred to green or renewable gasoline, diesel, naptha and jet fuels. Methane (CH_4), ethane (C_2H_6), and propane (C_3H_8) are

the most famous ones [3]. *Botryococcus braunii* is well known for its ability to produce hydrocarbons which have been loosely described as equivalent to the "gasoil fraction of crude oil" [61]. Like petroleum, these hydrocarbons can be turned into gasoline, kerosene and diesel. While other algal species usually contain less than 1 percent hydrocarbons, in *B. braunii* they typically occupy 20−60% of its dry matter, with a maximum of >80%. Depending on the strain, these hydrocarbons are either C_{30} to C_{37} alkenes or C_{23} to C_{33} odd numbered alkenes [62]. These hydrocarbons are mainly accumulated on the outside of the cell, making extraction easier than when the cell wall has to be passed to reach the organics inside the cell. *B. braunii* lives in freshwater, but can also adapt to large range of (sea) salt concentrations. *B. braunii*'s main disadvantage is that it grows very slowly (doubling time is 72 h) [27]. This is >20 times slower than fast-growing algae, therefore only low-investment growth systems like raceway ponds are interesting [63].

Lipids and biodiesel. Lipids (trigelicerides, isoprenoids, phospholipids and glycolipids) are one of

the main components of microalgae. Depending on the species and growth conditions 2–60% of total cell dry matter, as membrane components, storage products, metabolites and storages of energy can be lipid. In comparison with plant oil, algal oil is unsaturated to a larger degree, making it less appropriate for direct combustion in sensitive engines. Triglycerides and free fatty acids can be converted into biodiesel [64]. Triglyceride production rates in algae are 45–220 times higher than terrestrial plants [65]. The global biodiesel market is estimated to reach 37 billion gallons by 2016, growing at an average annual growth of 42%, being Europe the major biodiesel market for the next decade or so, closely followed by US market [66].

Carbohydrates and ethanol. Algal carbohydrates typically are complex mixtures of mono-, poly-, and oligosaccharides, with pentoses and hexoses. Cellulose (aglucan) and glycoproteins are in the cell walls. Algae species starch contents can be over 50%. With new technologies, cellulose and hemicellulose can be hydrolysed to sugars [67], creating the possibility of converting an even larger part of algal dry matter to ethanol. Algae have some beneficial characteristics compared to woody biomass. Most notable is the absence of lignin in algae. Furthermore, algae composition is generally much more uniform and consistent than biomass from terrestrial plants, because algae lack specific functional parts such as roots and leaves. Other algal species, with high starch contents (9 and 69%) [4] are promising feedstock for ethanol production. Currently bioethanol is produced by fermenting sugars, which in the case of corn are derived from hydrolyzing starch. It is estimated that approximately 5000–15.000 gallons of ethanol/acre/ year can be produced by algae which is 10 to 30 times higher than corn starch ethanol systems (400–500 gallons of ethanol/acre/year) [68]. Bioethanol can be used as a biofuel which can replace part of the fossil-derived petrol. Butanol is another kind of alcohol that can be produced by algae. The butanol fermentation process was first commercialised in the UK in 1916. However, it was largely abandoned in the 1950s because it was cheaper to derive butanol from mineral oil. As an automotive fuel, butanol has a number of advantages over ethanol, including lower vapor pressure resulting in fewer evaporative emissions, the ability to be distributed via pipeline as opposed to truck or train, and a higher energy density. Because biobutanol can be produced using the same feedstocks as ethanol, and with a very similar production process, the final product separation process (distillation and dehydration) would be problematical [3].

Hydrogen. Hydrogen is an important fuel with wide applications in fuel cells, liquefaction of coal, and upgrading of heavy oils. Different production process of hydrogen from biomass was described in Fig. 2. Hydrogen can be produced by dark and photo fermentation of organic materials and photolysis of water by special microalgal species [69]. Hydrogen can be applied in mobile applications with only water as exhaust product and no NOx emissions when used in a fuel cell. Currently, hydrogen gas is produced by steam reformation of fossil fuels. Biohydrogen production from microalgae has been known for more than 65 years and was first observed in the green alga *Scenedesmus obliquus* and later identified in many other photosynthetic species such as cyanobacteria [70]. Most studies on algal hydrogen production have been carried out using the green alga *Chlamydomonas reinhardtii*. A major advantage of hydrogen production is that hydrogen does not accumulate in the culture and quickly released into the gas phase not to be at levels toxic to the cells [71]. Efforts to improve biohydrogen production using photosynthetic bacteria and algae mainly rely on engineering of two enzymes, nitrogenase and hydrogenase, which evolve H_2 during catalysis [72]. Biological hydrogen production is also performed in two stages of different atmospheric conditions, the first stage for cell growth followed by the second stage for hydrogen evolution. Nitrogen starvation is often used at the end of the growth stage as an efficient metabolic stress to induce the activity of nitrogenase. A nitrogen-free gas phase such as argon plus carbon dioxide gives a high hydrogen evolution rate [73]. Other algal species such as *Chlorococcum littorale* and *Platymonas subcordiformis* are also investigated for hydrogen evolution [74]. Some algae can make hydrogen directly from sunlight and water, although only in the complete absence of oxygen [75]. Direct biophotolysis is done by green algae and can produce H_2 directly from water and require high intensity of light and O_2 can be poisonous to the system. In direct biophotolysis sunlight and organisms containing either hydrogenase or nitrogenase and closed photobioreactor are used. Unlike nitrogenase, hydrogenase is not cut up within the cell, a low partial pressure of oxygen must be maintained, either by in situ removal or a sweeping gas. Indirect biophotolysis performs by the normal oxygenic photosynthetic processes of microalgae to produce carbohydrate before producing hydrogen through dark anaerobic photosynthetic mechanisms [76]. The use of carbohydrates as intermediates separates the production of oxygen and hydrogen, so avoiding an obstacle of direct photolysis. This can provide spatial separation that lowers costs. The second, dark anaerobic stage is essentially to convert carbohydrate into hydrogen, carbon dioxide and organic acids. In the third stage an oxygenic photosynthetic mechanisms are used to produce hydrogen. Indirect biophotolysis processes are the paths followed by cyanobacteria. Because of the high rates of H_2 production, *Anabaena* species have been subjected to intense study. Hydrogen production has also been investigated by other species, including *Nostoc muscorum*, *N. spongiaeforme*, *Westiellopsis prolifica*, *Oscillotoria Miami* BG7, *Aphanothece halophytico* [77, 78]. Studies indicate that maximum yield for hydrogen production through green-algae of about 98 kg H_2 ha^{-1} day^{-1} [79].
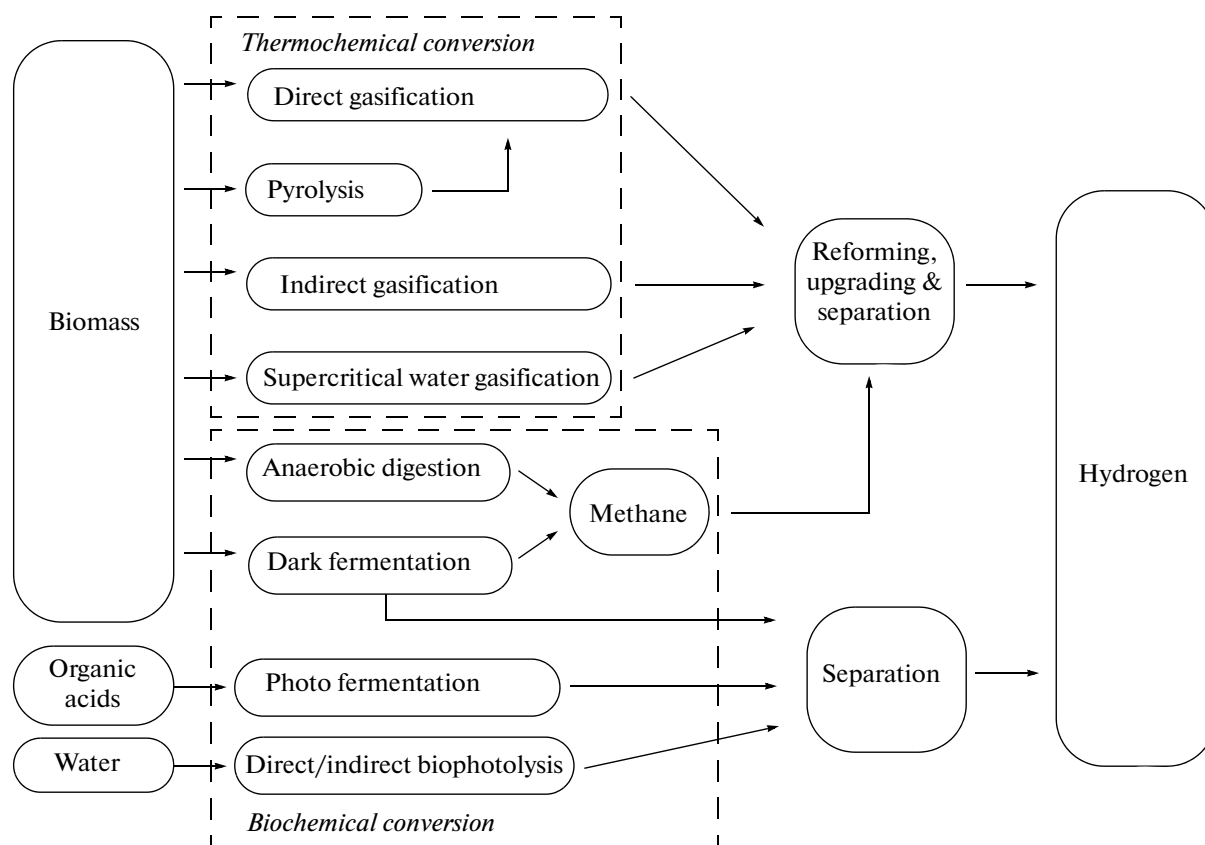
Fig. 2. Hydrogen pathways from biomass and biochemistry [82].

Biogas/biomethane. In biochemical conversion which breaks down sugars using enzymatic anaerobic digestion is more famouse. It can produce a mixture of methane and carbon dioxide with small amounts of hydrogen, hydrogen sulphide and ammonia.

Algae can be digested by bacteria in anaerobic digesters. To optimize biogas yields from anaerobic digestion, the carbon/nitrogen (C/N) balance in the feedstock should be in a range of 25–30. The technical feasibility of anaerobic digestion will also depend on the size of the operation (a minimum of around 150 dry t of biomass per year is required to feed a very small digester), and possibly the availability of additional high-carbon feedstocks, such as waste paper [80]. It has to be mentioned that biomethane production from microalgae currently is not competitive with biomethane production from maize or other crops because the production of biomass is expensive and production capacity is far too low today to feed the demand of commercial biogas plants [53]. The anaerobic digestion of algae can achieve methane yields of about 250 $m^3 t^{-1}$ of algae [81]. There is other ways to produce methane from biomass. The off-gas from the FT reactor is used for bio-gas production through methanation. During methanation, CO and CO_2 react with H_2 to produce methane (CH_4) and water. Another pathway for bio-gas production is biomass gasification in

supercritical water, but the composition of the syngas makes this route less favourable for bio-gas production. Depending on the gasification temperature, gasification in supercritical water is more suitable for hydrogen production [82].

Bio-oil and bio-syngas. When biomass is processed under high temperature at the absence of oxygen, products are produced as three phases: the vapor phase, the liquid phase, and the solid phase. The liquid phase is a complex mixture called bio-oil. Up-grading of the product including hydrodeoxygenation and Zeolite upgrading, both converting the bio-oil into a fuel which can be used directly in diesel engines. Bio-oils can also be blended into diesel fuels using expensive surfactants, thus reducing undesirable viscosity characteristics [65].

Gasification processes provide the opportunity to convert renewable biomass feedstocks into clean fuel gases or synthesis gases. The synthesis gas includes is principally CO, H_2, methane, and lighter hydrocarbons, H_2O, PM, tar, alkali vapors, nitrogen and sulfur compounds, and depending on the process used, can contain significant amounts of CO_2 and N_2, the latter mostly from air. High temperature (>1200°C) oxygen-gasification processes produce syngas with very low concentrations of hydrocarbons and higher concen-
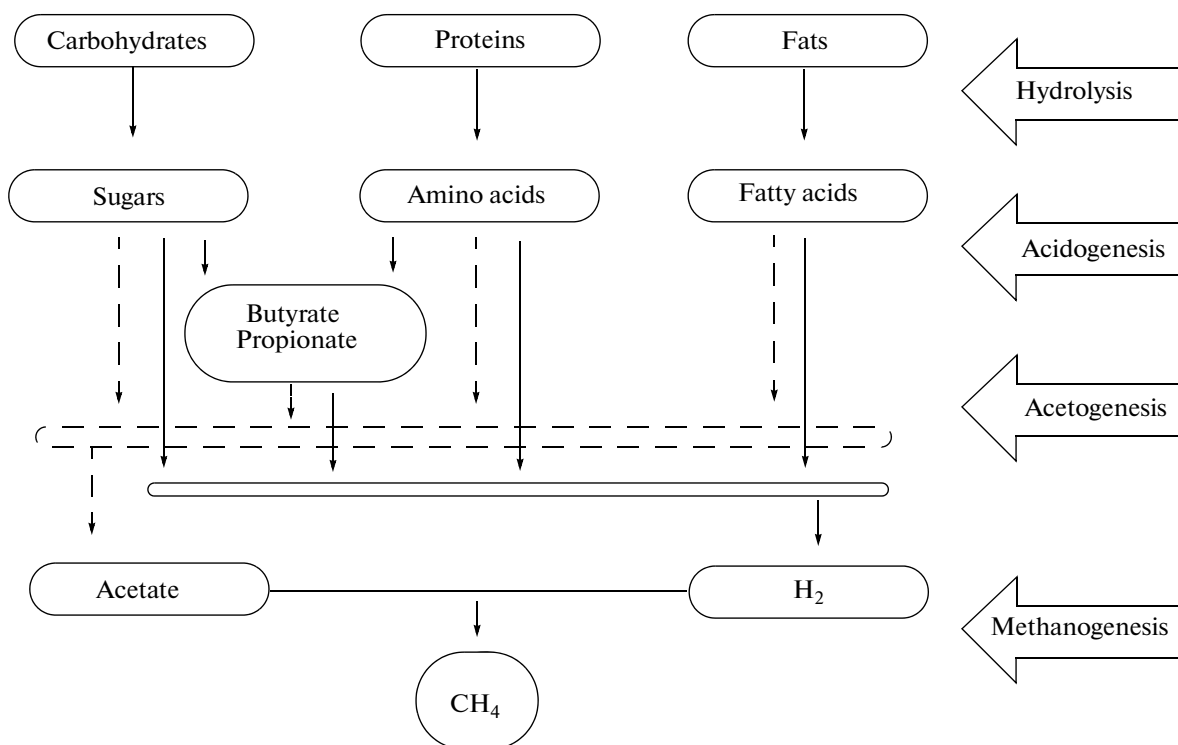
Fig. 3. Degradation steps of anaerobic digestion process [85].

trations of CO and H_2. It is possible to produce diesel fuel from bio-syngas by Fisher-Tropsch synthesis (FTS). The FTS-based gas to liquids technology includes three processing steps, namely syngas generation, syngas conversion, and hydroprocessing. The current commercial applications of the FT process are geared to the production of the valuable linear alpha olefins and of fuels such as liquefied petroleum gas (LPG), gasoline, kerosene, and diesel. Biomass can be converted to bio-syngas by noncatalytic, catalytic, and steam gasification processes [84] (Figs. 3, 4).

Dimethyl ether (DME). DME (CH_3OCH_3) is a synthetic fuel derived from coal, natural gas, or biomass. DME has traditionally been produced in a two-step process where syngas from coal or natural gas was converted into methanol followed by its dehydration [86]. DME offers several advantages over conventional diesel and other transportation fuels. It can be used directly in diesel engines where it produces lower NO_x and SO_x emissions than conventional diesel. The disadvantages of DME are due to its physical properties. The relatively low viscosity causes leaking in pumps and fuel injectors [83].

CONVERSION PATHWAYS FOR BIOFUEL

When biomass is pretreated thermochemically it produces intermediate products bio-oil and residue. Bio-oil must therefore be converted to biofuel under different conditions. Residue can be biochemically or thermochemically converted to a gaseous fuel or a solid, nutrient-rich bioproduct. Conversion pathways include transesterification (chemical, enzymatic), biochemical conversion (fermentation, anaerobic digestion), thermochemical conversion (gasification, pyrolysis, liquefaction) and hydroprocessing. Pyrolysis, gasification, and hydrocracking (use of high-pressure, high-temperature catalysts and hydrogen to produce hydrocarbons) hold promise for creating biomass-based petroleum equivalents, i.e., biocrude, biogasoline, and biodiesel fuels that would be virtually indistinguishable from, and even have advantages over, their petroleum-based counterparts [85].

Transesterification. Transesterification (also called alcoholysis) is the reaction of a fat or oil with an alcohol to form esters and glycerol. There is nothing unique about the transesterification of algal oil compared with that of conventional vegetable oils. Feedstocks obtained from oil pressing (e.g., screw or hydraulic presses) and extraction (e.g., hexane) should be degummed by treating the oil for 4 to 8 h with 300 to 3000 ppm phosphoric acid (depending on the natural levels of gums present) followed by washing with water. Oils can be converted via acid-catalyzed, alkali- or base-catalyzed, or enzymatic transesterification. Alcohols that can be used in the transesterification process are methanol, ethanol, propanol, butanol and amyl alcohol. Methanol and ethanol are used most frequently, especially methanol because of its low cost and its physical and chemical advantages (polar and
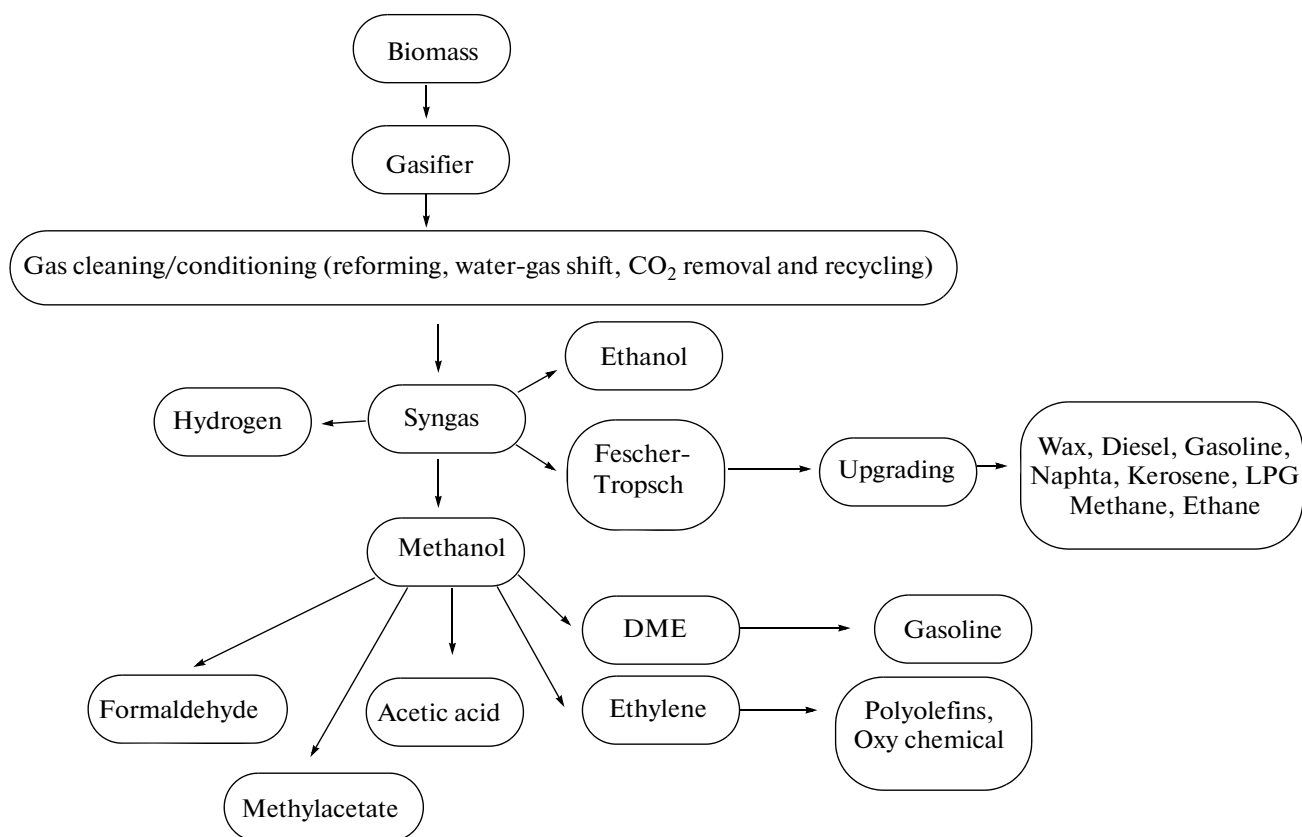
Fig. 4. Syngas products [86].

shortest chain alcohol). This reaction can be catalyzed by alkalis, acids, or enzymes. The alkalis include NaOH, KOH, carbonates and corresponding sodium and potassium alkoxides such as sodium methoxide, sodium ethoxide, sodium propoxide and sodiumbutoxide. Sulfuric acid, sulfonic acids and hydrochloric acid are usually used as acid catalysts. Lipases also can be used as biocatalysts. Alkali-catalyzed transesterification is much faster than acid-catalyzed transesterification and is most often used commercially. An acid catalyst is used when the oil has high acid value. Transesterification can be performed continuously or using a batch process. The main byproducts of transesterification are fatty acid methyl ester (FAME) or fatty acid ethyl ester and glycerol. During conversion, glycerol is periodically or continuously removed from the reaction solution in order to drive the equilibrium reaction toward completion [14]. After transesterification of triglycerides, the products are a mixture of esters, glycerol, alcohol, catalyst and tri-, di- and monoglycerides. Obtaining pure esters is not easy, since there are impurities in the esters, such as di- and monoglycerides. The most important parameters that influence the transesterification reaction are: reaction temperature, ratio of alcohol to vegetable oil, type of acyl donor and acceptor, type and amount of catalyst, mixing intensity, quality (purity, free fatty acid content) of

starting materials and water content [5]. Biodiesel is recovered by repeated washing with water to remove glycerol and methanol. Use of lipases offers important advantages, but is not currently feasible because of the relatively high cost of the catalyst [87]. The recovery of glycerol is easy, and purification of the FAME is usually not required. Additionally, the separation of the product and enzyme is facilitated. Lipases obtained from: *Rhizomucor miehei, Rhizopus oryzae, Candida antarctica, Candida rugosa, Pseudomonas cepacia* and *Thermomyces lanuginosa*, but the commercial immobilized lipase from *C. antarctica* (Novozym 435) is the most commonly used enzyme. Instead of using methanol, the lipase-catalyzed synthesis of FAME can also be performed using alternative alcohol donors such as methyl (alkyl) acetate or dimethyl carbonate. The process of such a biodiesel synthesis is irreversible because the intermediate compound (carbonic acid monoacyl ester) immediately decomposes to carbon dioxide and an alcohol [88]. In this process triacetin, instead of glycerol, is produced [89, 90] which can be applied in the synthesis of alkyl esters. Improvement of the enzymatic synthesis of biodiesel can be achieved through the application of *tert*-butanol as a solvent for enzymatic reaction or washing with a solvent for enzyme regeneration [91]. The world's first large-scale biodiesel plant using enzyme technology is operating in Chi-

na with a capacity of 20000 metric t per year using *tert*-butanol as co-solvent, which protects the enzyme and enables very high productivity [92]. For the production of biodiesel using microalgae feedstocks, transesterification can be done in 3 ways: conventional [93, 94], supercritical [84] and in situ [95]. Although the conventional and supercritical transesterification routes involve prior extraction of the microalgae oil from the biomass before the biodiesel production process, the in situ method facilitates the transesterification of the microalgae lipids directly from the biomass, without the need for initial stripping. Lepage and Roy [96] proposed the direct transesterification of human milk and adipose tissue without prior extraction or purification for improved recovery of fatty acids. This reaction was done with alcohol (e.g., methanol) and acid catalyst (e.g., acetyl chloride) followed with heating at $100°C$ for 1 h under sealed cap. Rodriguez-Ruiz et al. [97] applied this method to microalgal biomass and modified the approach to include hexane in the reaction phase in order to avoid a final purification step. Moreover, Rodriguez-Ruiz and coworkers found that the entire reaction could be shortened to 10 min. Finally, Carvalho and Malcata [98] found that when applying direct transesterification using an acid catalyst (i.e. acetyl chloride), the efficiency of the reaction is increased when a second less polar solvent such as diethyl ether or toluene was mixed with the methanol to modify the polarity of the reaction medium. Supercritical transesterification approach (simultaneous extraction/transesterification) can also be applied for algal oil extracts. Extraction is efficient at the modest operating temperatures, for example, at less than $50°C$, thus ensuring maximum product stability and quality. Additionally, supercritical fluids can be used on whole algae without dewatering, thereby increasing the efficiency of the process.

Biochemical fermentation/anaerobic digestion. Anaerobic fermentation is the more common biochemical approach to convert algal biomass to butanol, methanol, acetone and also converts residue to biogas for biofuel. Byproducts of the fermentation process are CO_2, methane, water, and several acids, including acetic and lactic acids. Methane is suitable for electricity and heat; whereas other liquid byproducts, such as acetone, are suitable for recycling as eutrophied process water. Anaerobic digestion is not currently a popular pathway for algal residue conversion. The three main bottlenecks to digest microalgae are [99]:

— low biodegradability of microalgae depending on both the biochemical composition and the nature of the cell wall;

— high cellular protein content results in ammonia release which can lead to potential toxicity;

— presence of sodium for marine species can also affect the digester performance.

When the cell lipid content does not exceed 40%, anaerobic digestion of the whole biomass appears to be the optimal strategy on an energy balance basis, for the energetic recovery of cell biomass [99]. Methane fermentation is the consequence of a series of metabolic interactions among various groups of microorganisms. The first group of microorganisms secretes enzymes which hydrolyze polymeric materials to monomers such as glucose and amino acids, which are subsequently converted to higher volatile fatty acids, H_2 and acetic acid. In the second stage, hydrogen-producing acetogenic bacteria convert the higher volatile fatty acids like propionic and butyric acids to H_2, CO_2, and acetic acid. Finally, the third group, methanogenic bacteria convert H_2, CO_2, and acetate, to CH_4 and CO_2 [100].

Thermochemical conversion. Endothermochemical conversion involves the consumption of energy to convert a fuel source (biomass) into a different chemical state (oil and residue). Exothermochemical conversion (releasing energy) via combustion to generate power that is not within the scope of this review. The thermochemical conversion processes involve heating of biomass at high temperatures. There are two basic approaches. The first is combustion and gasification of biomass and its conversion to hydrocarbons. The second approach is to liquefy biomass directly by high-temperature pyrolysis, high-pressure liquefaction and ultra-pyrolysis [3].

Combustion. Combustion is the burning of biomass in air. It converts the chemical energy stored in the biomass into heat, mechanical power, or electricity using different process equipment. Combustion produces hot gases at temperatures around 800 to $1000°C$. This is an older method of utilizing biomass for obtaining energy [3].

Gasification. Gasification is a thermochemical process that, in the near absence of oxygen, converts organic material into a combustible gas called synthesis gas (syngas). Syngas, comprised of mainly of CO, CO_2, H_2, CH_4, water and tar vapors (long-chain aliphatics), and ash particles, contains 70—80% of the energy originally present in the biomass feedstock. With proprietary catalysts, syngas yields fuel gases H_2, ethanol, methanol, and DME. Gas components can be used in turbines and boilers or as feed gas for the production of liquid alkanes by Fischer-Tropsch (FT) synthesis. Gasification processes can be classified into two categories: conventional gasification and supercritical water gasification. Conventional gasification is to decompose dry biomass at high temperature (800—$1000°C$ or higher), pressure, and the absence of oxygen to the materials, which are further decomposed into small molecular combustible gas, usually with the help of gasification catalysts. Conventional gasification also requires dry biomass with moisture content not higher than 15—20%. Supercritical water gasification, on the other hand, relies on the existence of supercritical water to cause the hydrolysis of biomass components to produce smaller molecules [101],

whereas supercritical water (hydrothermal) gasification occurs at 347°C with a metal catalyst or at 697°C with a carbonaceous or alkali catalyst. Due to the different reaction mechanisms, supercritical water gasification owns some unique advantages over conventional gasification. Firstly, supercritical water gasification is suitable for recovery of energy from wet biomass, avoiding the energy-intensive drying process. Secondly, supercritical water has some specific features such as high solubility of biomass components and products, which could achieve homogeneous reaction and allows simple separation of the gas products from liquid phase at the end of the reaction [101]. Thirdly, supercritical water gasification requires more moderate conditions than that of conventional gasification. The most significant problem with FTS in gasification is the cost of clean-up and tar reforming. Tars are high molecular weight molecules that can develop during the gasification process. The tars must be removed because they cause coking of the synthesis catalyst and any other catalysts used in the syngas cleanup process. Tar formation can be minimized or avoided via entrained-flow gasification at high temperatures [102]. While this technology requires sub-millimeter sized particles, algae may have a unique advantage in this process. Reforming is a process in which biomass is gasified in the presence of another reactant such as steam, steam-oxygen or steam-air. Gases with low calorific value are generally formed when there is direct contact with air, as this results in dilution with nitrogen. Medium energy gases result when oxygen is used or when air is used but the gasifier is heated indirectly. High-energy gases result at lower temperatures and high pressures which favour the production of methane and other light hydrocarbons [103]. Tars in the product gas are problematic because they condense in exit pipes and on particulate filters leading to blockages and clogged filters. They also cause clogging of fuel lines and injectors in internal combustion engines. There are currently three basic pathways to overcome the tar-related problems:

• fluidised-bed gasification + catalytic reforming;

• fluidised-bed gasification + solvent-based tar removal;

• entrained-flow gasification at high temperatures.

FT processes form long chain hydrocarbons from catalytic combination of CO and H_2. In case of high temperature gasification (1200°C to 1600°C), it leads to few hydrocarbons in the product gas, and a higher proportion of CO and H_2. If the ratio of H_2 to CO (syngas or biosyngas) is 2 : 1, FT synthesis could be an option to convert syngas into high quality synthetic biofuels which are fully compatible with conventional fossil fuel engines. FT processes use catalysts based on iron, cobalt, ruthenium, and potassium, and have been extensively characterized, operate at high pressures (2.50–4.50 MPa) and temperatures (between 220°C and 450°C). The process can co-produce electricity, heat, and a liquid fuel. However, the multistage process requires high capital cost resulting in considerably high cost of biofuels thus making the process economically unviable [3].

Pyrolysis. Pyrolysis, also known as thermal cracking, is a thermochemical process to convert dry biomass to liquid (termed bio-oil or bio-crude), solid, and gaseous fractions by heating the biomass in absence of oxygen with the aid of a catalyst. It involves heating in the absence of air or oxygen and cleavage of chemical bonds to yield small molecules. Pyrolytic chemistry is difficult to characterize because of the variety of reaction paths and the variety of reaction products that may be obtained from the reactions that occur. This process is applied at temperatures above 430°C (500–600°C, 0.1–0.5 MPa). When the off-gases are cooled, liquids condense to produce oil. This organic oil is often referred to pyrolysis oil or bio-oil. Slow pyrolysis produces a black, tarry oil residue, while fast pyrolysis outputs dark-brown, low viscosity oil. The yields for fast pyrolysis vary extensively from 18 to 80% efficiency. Carbon monoxide, alkanes, alkenes, charcoal, phenol-formaldehyde resins, carboxylic acid and wastewater are common byproducts of pyrolysis. Catalysts have been used in many studies, largely metallic salts, to obtain paraffins and olefins similar to those present in petroleum sources. Pyrolysis can be used to produce predominantly bio-oil if flash pyrolysis is used, enabling the conversion of biomass to bio-crude with an efficiency of up to 80% [104]. Upgrading bio-oils can be achieved by lowering the oxygen content and removing alkalis by means of hydrogenation and catalytic cracking of the oil [105]. Hydrogenation is mainly employed for the production of methane by hydro-gasification. Synthesis gas reacts with hydrogen to yield methane. The shredded biomass may directly be converted with the hydrogen-containing gas to a gas containing relatively high methane concentrations in the first-stage reactor. A few studies have been carried out on the production of fuel oil from microalgae by pyrolysis [106, 107]. Yields of 18 and 24% high-quality bio-oil were obtained by fast pyrolysis of *C. protothecoides* and *Microcystis aeruginosa* at temperature of 500°C [107], which has a potential for commercial application of large-scale production of liquid fuels. It was also noticed [108] that *C. protothecoides* was preferable for pyrolysis over *Spirulina platensis* [109]. The quantity and quality of the pyrolysis products depend on various parameters, such as reaction temperature, pressure, heating rate, reaction time, etc. Lower process temperature and longer vapor residence times favor the production of charcoal, whereas high temperature and long vapor residence time increase the gas yields. Moderate temperature and short vapor residence time are optimum for higher liquid yields [110]. The pyrolysis process may be endothermic, or exothermic, depending on the temperature of the reacting system. The pyrolysis processes can be slow, fast and flash. Slow pyrolysis is a conventional process whereby

the heating rate is kept slow (approximately 5–7°C/min) [111]. This slow heating rate leads to higher char (particulates) yields than the liquid and gaseous products. Fast pyrolysis is considered a better process than conventional, slow pyrolysis. In this, the heating rates are kept high, about 300 to 500°C/min and the liquid product yield is higher. Fluidized-bed reactors are best suited for this process as they offer high heating rates, rapid devolatilization and also are easy to operate. Reactors such as entrained flow reactors, circulating fluidized-bed reactors, rotating reactors, etc. are used for this purpose. This is an improved version of fast pyrolysis, whereby high reaction temperature is obtained within a few seconds. The heating rates are very high, about 1000°C/min with reaction times of few to several seconds. This is carried out at atmospheric pressure. Because there is rapid heating of the biomass, for better yields smaller particle size are favored. Flash pyrolysis can be categorized as.

1. Flash hydro-pyrolysis: at the presence of hydrogen, at 20 MPa.

2. Solar flash pyrolysis: solar energy is used.

3. Rapid thermal process: involves very short residence time of 30 ms to 1.5 s and is carried out at temperatures between 900 and 950°C to eliminate the side reactions in the system, with high yields of the desired product.

4. Vacuum flash pyrolysis: with a vaccum to stop the secondary decomposition reactions, giving higher liquid yields, and reduces gas production because of the quick removal of the liquid from the system.

5. Catalytic biomass pyrolysis: to improve the quality of the oil (the oil from pyrolysis processes is generally unsuitable) [84, 112].

Liquefaction. Liquefaction, a thermochemical pretreatment process that converts organic material to bio-oil at low temperature and high pressure (N_2 at 2–3 MPa to control evaporation) using a catalyst in the presence of hydrogen in just a matter of hours or even minutes. However, it is worth noting that liquefaction is a relatively expensive process due to the use of hydrogen. Conversion is conducted at 300°C, accommodating high moisture content biomass. With the help of a catalyst, the process utilizes the high activity of water in subcritical conditions to decompose biomass materials down to those with a higher energy density or higher value chemicals. Liquefaction can be employed to convert the wet biomass (≥60% moisture) without first reducing the moisture content, thereby avoiding energy-intensive drying of biomass especially algae. The oil product of liquefaction can be treated to yield green diesel or green jet fuel. Process residue can either be burned (i.e., exothermal direct combustion) or converted (e.g., via fermentation) into animal feed or fertilizer. Byproducts include CO_2 and some recalcitrant residue. Bio-oils produced by the thermochemical pretreatment processes of pyrolysis and liquefaction need to be upgraded before they can be used as renewable hydrocarbon biofuels. The mixture is then treated with CH_2Cl_2 catalyst, which causes the separation of biodiesel from an aqueous phase [3].

Cracking. Cracking is a process that breaks ("cracks") the heavier, higher boiling petroleum streams produced by atmospheric or vacuum distillation into lighter molecular weight materials such as gasoline, diesel fuel, jet fuel and kerosene. Often, after cracking, streams may be hydrotreated (reduces nitrogen and aromatic content) or undergo desulfurization. There are two basic types of cracking processes, those using heat and pressure (thermal cracking) to break molecular bonds, and those using a catalyst (catalytic cracking on bio-oil) to facilitate the cracking process. Catalytic cracking is similar to thermal cracking except a catalyst facilitates conversion of the heavier to lighter products and requires less severe operating conditions than thermal cracking. Hydrocracking (on glycerol) is a combination of catalytic cracking and hydrogenation, using high pressure, high temperature, a catalyst, and hydrogen. It is typically used for feedstocks that are difficult to process by either catalytic cracking or reforming. Hydrocracking converts sulfur and nitrogen compounds to hydrogen sulfide and ammonia. Catalytic purification and hydrocracking (breaking apart the triglycerides, otherwise known as splitting) are together known as hydroprocessing. Water, carbon dioxide, and hydrogen are the main process byproducts. Hydrotreating (removing the oxygen, or otherwise known as decarboxylation for aqueous sugar stream) and hydrogenation (saturating the double bonds) can be done through the process. Hydroprocessing includes hydrocracking and hydrotreating. Hydroprocessing (350°C to 450°C and a pressure from 4.8 MPa to about 15.2 MPa and a liquid hourly space velocity of 0.5 to 5.0 per h, depending on feedstock) in the presence of catalysts is used to upgrade a crude, intermediary feedstock to a market-ready fuel product. Both algal oil and bio-oil can be accommodated by hydroprocessing to hydrocarbon biofuel such as green or renewable diesel, jet fuel, gasoline, or other light fuel. The key components of upgrading are catalytic purification (by hydrodeoxygenation, hydrodenitrogenation, hydrodesulfurization, and hydrodemetallization) and hydrogenation through catalytic hydrocracking. Hydroprocessing potentially requires large quantities of water and energy to implement the purification and hydrocracking processes. Hydrocracking is to produce diesel while catalytic cracking to produce gasoline. The reactions are catalyzed by dual-function catalysts: zeolite catalysts for the cracking function (to reduce the oxygen content and improve the thermal stability) and platinum, nickel, or tungsten oxide for the hydrogenation function. The hydrogenation reactions occur because hydrogen is generated as a by-product in the course of catalytic reforming. The three types of catalytic cracking processes are fluid catalytic cracking, moving-bed catalytic cracking, and Thermofor catalytic cracking. The catalytic

cracking process is very flexible, and operating parameters can be adjusted to meet changing product demand. In addition to cracking, catalytic activities include dehydrogenation, hydrogenation, and isomerization in the presence of catalysts such as a crystalline aluminosilicates (zeolites) or molecular sieves. The literature on catalytic cracking of vegetable oils can be grouped into four main catalyst types including: (1) molecular sieve catalysts, (2) activated alumina catalysts, (3) transition metal catalysts and (4) sodium carbonate [112].

QUALITY ISSUES OF BIOFUEL

Vegetable oils currently used for biodiesel are mainly C_{16} and C_{18}. The most important properties of biofuel, cetane number (ignition quality), cold-flow properties, oxidative stability, and iodine value, are determined by the structure of fatty esters, which are part of it [5, 113]. In turn, properties of fatty esters are determined by the characteristics of fatty acids; i.e., carbon chain length and degree of unsaturation, and the alcohol content [113]. Most microalgal oils differ from plant oils because they are rich in polyunsaturated fatty acids with four or more double bonds [40]. This feature limits the algal species that can be used. Chemical formula of biodiesel is C_{14}–C_{24} methyl esters with boiling point of >475°K, flash point of 420–450°K and light to dark yellow. Microalgal oils are mostly composed of four unsaturated fatty acids, namely palmitolleic (16 : 1), oleic (18 : 1), linoleic (18 : 2) and linolenic acid (18 : 3). Saturated fatty acids such as palmitic (16 : 0) and stearic (18 : 0) also present with a small proportion [114]. These components can polymerize into waxy solids, causing filter clogging and injector fouling. A high level of long chained fatty acid esters also increases the viscosity of the biodiesel, leading to more stress on the diesel injection pump and incomplete fuel combustion, as the droplets formed in the cylinder tend to be larger. The proportion of convertable oil in the algae lipid fraction is another, often overlooked problem specific to algae biodiesel. Due to the high proportion of isoprenoids, glycolipids, phospholipids and aromatics in the algae lipid fraction only a small percentage of the extracted lipid fraction might be mono-, di-, and triglycerides suitable for transesterification. Numerous authors report that the fatty acid composition (chain length, saturation) does not only vary significantly between different algae species and genera, but also that the fatty acid composition of algae is affected by environmental factors such as illumination, temperature, nutrient and CO_2 availability, etc. For example, microalgal hydrocarbon content has been shown to be affected by nutrient availability, increasing under nutrient-limited conditions (particularly nitrogen) [28].

Cetane number. Cetane number is an important parameter in evaluating the quality of biodiesel fuel. It is established that the FAME composition of the methyl esters used has a predominant effect on the cetane number (CN) of the biodiesel. From the results obtained, it is evident that CN is affected by the % composition of the FAME in the fuel. A higher cetane number gives better starting properties and a shorter ignition delay (the interval between injection and ignition), which produces smoother combustion and a quieter engine. FAME from vegetable oils are mostly unsaturated. CN is affected by the % composition of FAME, as CN values of the saturated FAME are above 60, while those of unsaturated FAME are below 60 [115].

Cloud point (CP). CP the temperature at which a sample of fuel just shows a cloud or haze of methyl or ethyl ester crystals when it is cooled under standard test conditions.

Cold filter plug point (CFPP). CFPP the temperature at which fuel crystals cause a fuel filter to plug. This test is considered a better indicator than cloud point of low temperature operability.

Pour point (PP). PP the lowest temperature at which a fuel will just flow when tested under standard conditions.

Total acid number. Total acid number titrations are performed for both the feedstock before biodiesel production and after for the determination of total acid number. It is necessary to determine the amount of catalyst needed for transesterification to initially pretreat the feedstock to first accomplish acid-catalyzed esterification before conducting the much faster base-catalyzed transesterification procedure.

Iodine values. Iodine values are useful for determination of the overall degree of saturation of the oil, which is important for viscosity, cloud point, and reactivity characteristics. At lower temperatures the oil becomes solid when saturated, but remains liquid with higher degrees of unsaturation. This is important for biodiesel characteristics where ideally the fuel will remain more liquid at lower temperatures, but remains somewhat stable from oxidation or hydrogenation reactions. Iodine is introduced and reacts with the double bonds within the fatty acid structure. The amount of iodine absorbed in grams per 100 ml of oil determines the iodine value. High degrees of unsaturation may result in irreversible polymerization to plastic-like substances. Iodine values greater than 50 may result in decreased engine life, but give better viscosity characteristics in cooler conditions.

Free and total glycerin. In some standard tests one of the more important quality parameters is the glycerin in the free form and the bonded mono-, di-, or triglycerol form, indicating of an incomplete transesterification process or incomplete washing of the final product. Presence of glycerin in the final fuel may result in the fouling of pumps and filters or separation during storage of the fuel. Free and total fatty acids and fatty acid esters may also be determined. HPLC

methods without the need for derivatization could be employed.

Viscosity. It is a measure of resistance to flow of a liquid due to internal friction of one part of a fluid moving over another, affects the atomization of a fuel upon injection into the combustion chamber and thereby, ultimately, the formation of engine deposits. The higher the viscosity, the greater the tendency of the fuel to cause such problems. The viscosity of transesterified oil, i.e., biodiesel, is about an order of magnitude lower than that of the parent oil [14].

ECONOMICAL OVERVIEW OF ALGAL BIOFUEL

The commercial viability of algae-based biofuels production is ultimately going to depend on economics. The major cost components for algae production is harvesting which include: the cost of drying algae, infrastructure and capital expense of equipments and maintenence, chemicals, electricity and manpower for all the operation. The production cost of algal oil depends on many factors, such as yield of biomass from the culture system, oil content, scale of production systems, and cost of recovering oil from algal biomass. Whether algal oil can be an economic source for biofuel in the future is still highly dependent on the petroleum oil price. Chisti [5] used the following equation to estimate the cost of algal oil where it can be a competitive substitute for petroleum diesel:

$$C_{\text{algal oil}} = 25.9 \times 10^{-3} C_{\text{petroleum}},$$

where: $C_{\text{algal oil}}$ is the price of microalgal oil in dollars per gallon and $C_{\text{petroleum}}$ is the price of crude oil in dollars per barrel. This equation assumes that algal oil has roughly 80% of the caloric energy value of crude petroleum. For example, with petroleum priced at $100/barrel, algal oil should cost no more than $2.59/gallon in order to be competitive with petroleum diesel. Results from algal biofuels modeling and analysis effort indicate a clear set of economic-driven research and development priorities, which can be summarized as follows.

1. Re-focus research and development activities towards minimizing operations and maintenance costs for algae production systems.

2. Emphasize co-product capture and marketability to maximize revenue generation.

3. Aggressively develop technologies and processes that significantly improve total algae yields, without dramatically increasing costs.

4. Reduce total capital costs, through advanced technology, of algae production and harvesting [116].

The economic model may include more than 50 independent variables supported by detailed engineering specifications, commodity market data, and vendor quotes for equipment costs. The model is based on a generic baseline algae growth system and is not specific to any particular technology. It is recognized that the analysis results could vary depending on the growth architecture selected and assumptions for algae productivity. Operations and maintenance costs include all expenses required to operate the algal biofuels system on an annual basis such as utilities (electricity, water, etc.), CO_2, maintenance of the algae growth system (generally N−P−K), CO_2 distribution, water replenishment due to evaporative losses and labor, and nutrients have the greatest influence on operations costs. Utility costs accounted for more than 1/3 of total operations and maintenance expenses. However, when considering the amount of energy required to transport, handle, and process extremely large volumes of water and biomass material, along with considerable evaporative water losses, it becomes apparent why utilities are a significant cost driver. So, the priorities suggested include:

— algal biofuels growth, harvesting (includes oil extraction), system architectures, and processes should be developed and matured in a way that minimizes the amount of energy (electricity, etc.) and water required for nominal operations;

— technologies should be developed and policies implemented that reduce/eliminate the cost of CO_2 for algal biofuel systems.

— algal biofuel technologies should be designed in such a way that maximizes lifetime/longevity and minimizes annual maintenance requirements.

In co-product capture and marketability triacylglycerols for biofuel production represent a relatively small portion of algae-related revenue opportunities. 50%−80% of the material produced in an algal biofuels system will be something other than oils either meals/solids or nutraceuticals. While nutraceutical content in the baseline algae strain is very small, current market values for these products are extremely high and can have a dramatic impact on overall project economics, although the risk of market saturation and depreciating product values exists when considering large-scale algal biofuels production. It is also worth noting that not all algae strains contain nutraceuticals and may not have the revenue opportunities. Nevertheless, harvesting and oil extraction technologies need to focus on highly efficient separation and capture of all valuable algae materials, while minimizing energy and capital costs. Co-product markets must be rigorously analyzed on a regional, national, and international basis to assess the feasibility of realizing revenue opportunities for meals/solids and nutraceuticals. Develop technologies is straight forward and requires no detailed explanation. If the same unit area can produce 2−3 times the algae, assuming that then total project economics improve. Capital costs for an algal biofuels production system are a major commercial viability concern. Estimates for algae system capital costs vary widely, with ranges of 10 to $100 per acre installed. The algae growth system, water manage-

ment/harvesting/extraction, and CO_2 delivery infrastructure have the greatest capital cost impact [116].

Economics of biodiesel production. Biodiesel is growing into one of the most essential 'near-market' biofuels since all industrial vehicles are diesel-based. "In the past decade, the biodiesel industry has seen massive growth globally, more than doubling in production every 2 years" [53]. "Markets for low-carbon energy products are likely to be worth at least $500 billion per year by 2050, and perhaps much more" [117]. Open algae cultures are used commercially in the US, Japan, Australia, China, India, Israel and elsewhere. Moreover, Aquaflow Bionomic in New Zealand recently announced the first ever commercial production of biodiesel from sewage pond microalgae [118]. Recovery of oil from microalgal biomass and conversion of oil to biodiesel are not affected by whether the biomass is produced in raceways or photobioreactors. Hence, the cost of producing the biomass is the only relevant factor for a comparative assessment of photobioreactors and raceways for producing microalgal biodiesel. It is estimated that the cost of producing a kg of microalgal biomass is 2.95 and 3.80$ for photobioreactors and raceways, respectively. These estimates assume that carbon dioxide is available at no cost [55]. If the annual biomass production capacity is increased to 10.000 t, the cost of production per kg reduces to roughly 0.47 and 0.60$ for photobioreactors and raceways, respectively, because of economy of scale. Assuming that the biomass contains 30% oil by weight, the cost of biomass for providing a liter of oil would be something like 1.40 and 1.81$ for photobioreactors and raceways, respectively. Oil recovered from the lower-cost biomass produced in photobioreactors is estimated to cost $2.80/l. This assumes that the recovery process contributes 50% to the cost of the final recovered oil. If the price of crude oil rises to $80/barrel, then microalgal oil costing $0.55/l is likely to economically substitute for crude petroleum [5].

Economic viability. The economics of microalgae systems are highly sensitive to the assumptions made about costs and revenues, with the difference between the best and worst case assumptions being over € 600/t of algal biomass. It should also be noted that even with the most favourable assumptions about algae production costs (€ 210/t) and revenues for biofuels (€ 120/t algae) and greenhouse gas (GHG) abatement (€ 50/t algae), the process would still not be economically feasible. Thus, fuel-only algal systems are not plausible, at least not in the foreseeable future and additional revenues are required, either from wastewater treatment or higher value co-products. However, the above suggests that to expand the potential of algal production systems in addition to wastewater treatment and associated fertilizer recovery and production, it is important to identify and generate high volume/high value coproducts from microalgae biomass that could provide significant revenue (>€ 100/t algae). High value ani-

mal feeds (e.g. high in pigments or omega-3 fatty acids) are plausible, as are industrial biopolymers (polysaccharides). A 50% increase of the current achievable annual productivity to 100 t biomass/ha is a key assumption and a pre-requisite for the economic viability of microalgae-based processes for GHG abatement [5, 118, 119]. If existing algae projects can achieve biodiesel production price targets of less than $1 per gallon, the United States may realize its goal of replacing up to 20% of transport fuels by 2020 by using environmentally and economically sustainable fuels from algae production [119]. The combination of the closed photobioreactor and open pond combines the benefits of the two and has been demonstrated to be effective at a 2-ha scale [120].

Enhancement of economic feasibility of biofuels from microalgae:

— biorefinery: the high-value coproduct strategy;

— design of advanced photobioreactors;

— selection of cost-effective technologies for biomass harvesting and drying.

CONCLUSION AND PERSPECTIVES

Increasing energy demand as well as policy commitments towards global environmental change make action in terms of the provision of clean sustainable energy stringent. Algae have the great potentiality to provide valuable biofuels for heat generation, electricity supply and the transport sector. Yield and cost analyses show that the cultivation of algal biomass solely for the production of biofuels is not cost competitive compared to other biomass sources by almost two orders of magnitude, while the energy balance appears to be poor. As it is difficult to identify breakthrough opportunities for significant yield increases and costs savings, algal biofuels are not likely to be competitive in the foreseeable future, also because competing alternative technologies are making significant (and faster) progress. Current high value products from algae or waste-water treatment would not support sufficient quantities to underpin large-scale development of algae for biofuels production or CO_2-mitigation. Therefore, the current large investments in the production of algal biofuels are highly premature, and divert funds from more beneficial and urgently needed technologies. It goes without saying that microalgae can be put to beneficial uses such as the production of chemicals, feed, food additives, and wastewater treatment.

REFERENCES

1. Hirsch, R.L., Bezdek, R., and Wendling, R. Peaking of World Oil Production, Impacts, Mitigation and Risk Management. National Energy Technology Laboratory, 2005.

2. Nicols, T., How the Energy Industry Works. An Insiders Guide, 2009, Silverstone Communications Ltd, pp. 142.

3. Ryan, C., Cultivation Clean Energy: The Promise of Algae Biofuels. Ed. A. Hartley, Terrapin, Bright Green, 2009, pp. 9–62.

4. Feinberg, D.A., Fuel Options from Microalgae with Representative Chemical Composition. Solar Energy Research Institute. SERI/TR-231-2427, FTP No. 386; 1984, pp. 12–31.

5. Chisti, Y., *Biotechnol. Adv.*, 2007, vol. 25, no. 3, pp. 294–306.

6. Rittmann, B.E., *Biotech Bioeng.*, 2008, vol. 100, no. 2, pp. 203–213. doi:10.1002/bit.21875.

7. *International Energy Outlook.* Energy Information Administration, Official Energy Statistics from the U.S. Government, 2008 WDC. www.eia.doe.gov/oiaf/ieo/index.html.

8. Demirbas, M., *Energy Edu. Sci Technol.*, 2000, vol. 5, pp. 21–45.

9. Thurmond, W., Algae 2020: Biofuels Markets, Business Models, Strategies, Players and Commercialization Outlook from 2012–2020. Emerging Market Online Releases, 2009. www.emerging-markets.com/.../Algae2020Next Generation Biofuels Study Emerging Markets Online.

10. Deng, X., Li, Y., and Fei, X., *Afr. J. Microbiol. Res.*, 2009, vol. 3, no. 13, pp. 1008–1014.

11. Ng, J.H., Ng, H.K., and Gan, S., Recent Trends in Policies, Socioeconomy and Future Directions of the Biodiesel Industry. Clean Techn. Environ. Policy 2009; DOI 10.1007/s10098-009-0235-2.

12. Bungay, H.R., *Trends Biotechnol.*, 2004, vol. 22, pp. 67–71.

13. Hu, Q., Sommerfeld, M., Jarvis, E., Ghirardi, M., Posewitz, M., Seibert, M., and Darzins, A., *Plant J.*, 2008, vol. 54, pp. 621–639.

14. Drapcho, C.M., Phu Nhuan, N., and Walker, T.H., Biofuels Engineering Process Technology. The McGraw-Hill Companies, Inc; 2008, pp. 69–344.

15. Morowvat, M.H., Rasoul-Amini, S., and Ghasemi, Y., *Bioresource Technol.* 2010, vol. 101, pp. 2059–2062.

16. Rasoul-Amini, S., Montazeri-Najafabady, N., Mobasher, M.A., Hoseini-Alhashemi, S., and Ghasemi, Y., *Appl. Energy.* 2011, vol. 88, no. 10, pp. 3307–3312.

17. Vasudevan, P.T., *J. Int. Microbiol. Biotechnol.*, 2008, vol. 35, pp. 421–430.

18. Becker, E.W., Baddiley, J., Higgins, I.J. and Potter, W.G., Microalgae: Biotechnology and Microbiology. Cambridge, NY:Cambridge University Press, 1994, pp. 178.

19. Verma, N.M., Mehrotra, S., Shukla, A. and Nath Mishra, B., *Afr. J. Biotechnol.*, 2010, vol. 9, no. 10, pp. 1402–1411.

20. Abou-Shanab, R.A.I., Jeon, B., Song, H., Kim, Y., and Hwan, J.H., Algae-Biofuel: Potential Use as Sustainable Alternative Green Energy**.** The Online Journal on Power and Energy Engineering (OJPEE)**.** Reference Number: W09-00021(1); 2009, pp. 4–7.

21. Rodolfi, L., Chini Zittelli, G., Bassi, N., Padovani, G., Biondi, N., Bonini, G. and Tredici, M.R., *Biotechnol. Bioeng.*, 2009, vol. 102, no. 1, pp.100–112.

22. Chojnacka, K. and Noworyta, A., *Enzyme Microb. Technol.*, 2004, vol. 34, pp. 461–465.

23. Mata, T.M., Martins, A.A., and Caetano, N.S., *Renew Sustain. Energy Rev.*, 2009, vol. 43, no. 14, pp. 217–232.

24. Wang, B., Li, Y., Wu, N., and Lan, C.Q., *Appl. Microbiol. Biotechnol.*, 2008, vol. 79, pp. 707–718.

25. Chaumont, D., *J. Appl. Phycol.*, 1993, vol. 5, pp. 593–604.

26. Grobbelaar, J.U., *S. Afr. J. Bot.*, 2007, vol. 73, no. 2, pp. 289–290.

27. Sheehan, J.T., Dunahay, J., Benemann, J.R., and Roessler, P.G. Look Back at the U.S. Department of Energy's Aquatic Species Program: Biodiesel from Algae: Close-Out Report 1998; pp. 34–302. http://govdocs.aquake.org/cgi/reprint/2004/915/9150010.pdf.

28. Borowitzka, M., *J. Biotechnol.*, 1999, vol. 70, pp. 313–321.

29. van Beilen, J.B., *Biofuels, Bioprod. Bioref.*, 2010, vol. 4, pp. 41–52.

30. Alabi, A.O., Tampier, M., and Bibeau, E., Microalgae Technologies and Processes for Biofuels/Bioenergy Production in British Columbia: Current Technology, Suitability and Barriers to Implementation. The British Columbia Innovation Council, Seed Science Ltd., 2009.

31. Richmond A., Handbook of Microalgal Culture: Biotechnology and Applied Phycology. Blackwell: Science Ltd, 2004.

32. Lee, Y.K., *J. Appl. Phycol.*, 2001, vol. 13, pp. 307–315.

33. Amin, S., *Energy Conversion Management.*, 2009, vol. 50, pp. 1834–1840.

34. Wijffels, R.H., *Trends Biotechnol*, 2008, vol. 26, pp. 26–31.

35. Travieso, L., Hall, D.O., Rao, K.K., Benitez, F., Sanchez, E., and Borja, R., *Int. Biodeterior. Biodegradation.*, 2001, vol. 47, pp. 151–155.

36. Camacho Rubio, F., Camacho, F.G., Sevilla, J.M.F., Chisti, Y., and Molina Grima, E., *Biotechnol. Bioeng.*, 2003, vol. 81, pp. 473–559.

37. Ugwu, C.U., Ogbonna, J.C., and Tanaka, H., *Proc. Biochem.*, 2005, vol. 40, pp. 340–341.

38. Eriksen, N.T., *Biotechnol. Lett.*, 2008, vol. 30, pp. 1525–1536.

39. Vunjak-Novakovic, G., Kim, Y., Wu, X., Berzin, I., and Merchuk, J.C., *Ind. Eng. Chem. Res.*, 2005, vol. 44, pp. 6154–6163.

40. Chini Zittelli, G., Rodolfi, L., Biondi, N., and Tredici, M.R., *Aquaculture.*, 2006, vol. 261, pp. 932–943.

41. Xu, L., Weathers, P.J., Xiong, X.R., and Liu, C.Z., *Eng. Life Sci.*, 2009, vol. 9, no. 3, pp. 178–189.

42. Miron, A.S., Gomez, A.C., Camacho, F.G., Monila Grima, E., and Chisti, Y., *J. Biotechnol.*, 1999, vol. 70, pp. 249–270.

43. Hu, Q., Guterman, H., and Richmond, A., *Biotechnol. Bioeng.*, 1996, vol. 51, pp. 51–60.

44. Hu Q., Kurano N., Kawachi, M., Iwasaki, I., and Miyachi, S., *Appl. Microbiol. Biotechnol.*, 1998, vol. 49, pp. 655–662.

45. Zijffers, J.W.F., Janssen, M., Tramper, J., and Wijffels, R.H., *Mar. Biotechnol.*, 2008, vol. 10, pp. 404–415.

46. Mallick, N., *Biometals.*, 2002, vol. 15, pp. 377–390.

47. Bailliez, C., Largeau, C., and Casadevall, E., *Appl. Microbiol. Biotechnol.*, 1985, vol. 23, pp. 99–105.

48. Thakur, A. and Kumar, H.D., *Acta Biotechnol.*, 2004, vol. 19, pp. 37–44.

49. Gonzalez, L.E. and Bashan, Y., *Appl. Environ. Microbiol.*, 2000, vol. 66, pp. 1527–1531.

50. Abdel Hameed, M.S. and Hammouda Ebrahim, O.L.A., *Int. J. Agric. Biol.*, 2007, vol. 9, no. 1, pp. 184–191.

51. Huntley, M. and Redalje, D., CO_2 Mitigation and Renewable Oil from Photosynthetic Microbes: A New Appraisal Report, University of Hawaii, University of Mississippi. Mitigation and Adaption Strategies for Global Change 2006. US.

52. Williams, J.A., Keys to Bioreactor Selection. CEP Magazine 2002, pp. 34–41.

53. Schenk, P.M., *Bioenergy Res. J.*, 2008, vol. 1, pp. 20–43.

54. Food and Agriculture Organization of the United Nations (FAO). Algae-based Biofuel: A Review of Challenges and Opportunities for Developing Countries. Rome, Italy, 2009. www.fao.org/bioenergy/aquaticbiofuels.

55. Molina Grima, E., Belarbi, E.H., Fernandez, F.G.A., Medina, A.R., and Chisti, Y., *Biotechnol. Adv.*, 2003, vol. 20, no. 7–8, pp. 491–515.

56. Benemann, J.R. and Oswald, W.J., Systems and Economic Analysis of Microalgae Ponds for Conversion of CO_2 to biomass. The Smithsonian/NASA Astrophysics Data System. Grant No. DE-FG22-93PC93204, 1996, pp. 21–191.

57. Tilton, R.C., Murphy, J., and Dixon, J.K., *Water Res.*, 1972, vol. 6, pp. 155–164.

58. Poelman, E., De Pauw, N., and Jeurissen, B., *Resour. Conserv. Recycl.*, 1997, vol. 19, no. 1, pp. 1–10.

59. Alfafara, C.G., Nakano, K., Nomura, N., Igarashi, T., and Matsumura, M., *J. Chem. Technol. Biotechnol.*, 2002, vol. 77, no. 8, pp. 871–876.

60. Fischer, C.R., Klein-Marcuschamer, D., and Stephanopoulos, G., *Metab. Eng.*, 2008, vol. 10, pp. 295–304.

61. Hillen, L.W., Pollard, G., Wake, L.V., and White, N., *Biotechnol. Bioeng.*, 1982, vol. 24, no. 1, pp. 193–205.

62. Ranga Rao, A. and Ravishankar, G.A., *J. Microbiol. Biotechnol.*, 2007, vol. 17, no. 3, pp. 414–419.

63. Mousdale, D.M., Biofuels: Biotechnology, Chemistry, and Sustainable Development. Taylor & Francis Group, CRC press, 2008.

64. Neenan, B., Feinberg, D., Hill, A., McIntosh, R., and Terry, K., Fuels from Microalgae: Technology Status, Potential, and Research Requirements, Colorado: Solar Energy Research Institute, 1986, SERIISP-231-2550 DE86OlO739UC Category, 61 c.

65. Huber, G.W., Iborra, S., and Corma, A., *Chem Rev.*, 2006, vol. 106, no. 9, pp. 4044–4098.

66. Sims, B., Biodiesel: a Global Perspective. Biodiesel Magazine, 2007. http://www.biodieselmagazine.com/article.jsp?article_id=1961.

67. Hamelinck, C.N., Van Hooijdonk, G., and Faaij, A.P.C., *Biomass Bioenerg.*, 2005, vol. 28, no. 4, pp. 384–410.

68. Cheryl, B., Algae Becoming the New Biofuel of Choice. Duelign Fuels, 2008, ⟨http:// duelingfuels.com/biofuels/non-food-biofuels/algae-biofuel.php⟩.

69. Kapdan, I.K. and Kargi, F., *Enzyme Microb. Technol.*, 2006, vol. 38, pp. 569–582.

70. Das, D. and Veziroglu, T.N., *Int. J. Hydrogen Energy.*, 2001, vol. 26, pp. 13–28.

71. Ghirardi, M.L., Zhang, J.P., and Lee, J.W., *Trends Biotechnol.*, 2000, vol. 18, pp. 506–511.

72. Fedorov, A.S., Tsygankov, A.A., Rao, K.K., and Hall, D.O., *Biotechnol. Lett.*, 1998, vol. 20, pp. 1007.

73. Weissman, J.C. and Benemann, J.R., *Appl. Environ. Microbiol.*, 1977, vol. 33, pp. 123–126.

74. Guan, Y.F., Deng, M.C., Yu, X.J., and Zhang, W., *Biochem. Eng. J.*, 2004, vol. 19, pp. 69–73.

75. Melis, A. and Happe, T., *Plant Physiol.*, 2001, vol. 127, pp. 740–748.

76. Miura, Y., *Proc. Biochem.*, 1995, vol. 30, pp. 1–7.

77. Banerjee, M., Kumar, A., and Kumar, H.D., *Int. J. Hydrogen Energy.*, 1989, vol. 12, pp 871–879.

78. Pinto, F.A.L., Troshina, O., and Lindblad, P., *Int. J. Hydrogen Energy.*, 2002, vol. 27, pp. 1209.

79. Brennan, L. and Owende, P., *Renew. Sustain. Energy Rev.*, 2010, vol. 14, pp 557–577.

80. Bilitewski, B., Härdtle, G., and Marek, C., *Waste Management*, Berlin: Springer, 1997.

81. Yena, H.W., *Bioresource Technol.*, 2007, vol. 98, no. 1, pp. 130–134.

82. Mozaffarian, M., Zwart, R.W.R., Boerrigter, H., Deurwaarder, E.P., and Kersten, S.R.A., Green Gas as Synthetic Natural Gas.-A Renewable Fuel with Conventional Quality, Contribution to the "Science in Thermal and Chemical Biomass Conversion, " Conf. Victoria, Canada, 2004.

83. Semelsberger, T.A., Borup, R.L., and Greene, H.L., *J. Power Sources*, 2006, vol. 156, no. 2, pp. 497–511.

84. Demirbas, M., *World Biofuel Scenario*. Handbook of Plant Based Biofuels, Boca Raton, London, New York: CRC Press Taylor & Francis Group, 2009, pp. 13–27.

85. Peña, N., Biofuels for Transportation: a Climate Perspective. Pew Center on Global Climate Change, 2008.

86. Ge, Q., Huang, Y., Qiu, F., and Li, S., *Appl. Catal. A.*, 1998, vol. 167, no. 1, pp. 23–30.

87. Fukuda, H., Kondo, A., and Noda, H., *J. Biosci. Bioeng.*, 2001, vol. 9, pp. 405–16.

88. Su, E.Z., Zhang, M.J., Zhang, J.G., Gao, J.F., and Wei D.Z., *Biochem. Eng. J.*, 2007, vol. 36, pp. 167–173.

89. Xu, Y., Du, W., and Liu, D., *J. Mol. Catal. B: Enzym.*, 2005, vol. 32, pp. 241–245.

90. Kumar Modi, M., Reddy, J.R.C., Rao, B.V.S.K., and Prasad, R.B.N., *Bioresource Technol.*, 2007, vol. 98, pp. 1260–1264.

91. Li, L., Liu, D., Wang, L., and Li, Z., *J. Mol. Catal. B: Enzym*,. 2006, vol. 43, pp. 58−62.

92. Nielsen, P.M., Enzymatic Biodiesel Workshop at the 6th Euro Fed Lipid Congress in Athens 2009, pp. 59−60.

93. Nagle, N. and Lemke, P., *Appl. Biochem. Biotechnol.*, 1990, vol. 24/25, pp. 355−361.

94. Miao, X. and Wu, Q., *Bioresource Technol.*, 2006, vol. 97, pp. 841−846.

95. Ehimen, E.A., Sun, Z.F., and Carrington, C.G., *Fuel.*, 2010, vol. 89, pp. 677−684.

96. Sialve, B., Bernet, N., and Bernard, O., *Biotechnol. Adv.*, 2009, vol. 27, no. 4, pp. 409−416.

97. Lepage, G. and Roy, C.C. *J. Lipid Res*. 1984, vol. 25, pp. 1391−1396.

98. Rodriguez-Ruiz, J., Belarbi, E.H., Sanchez, J.L.G., and Alonso, D.L. 1998. *Biotechnol. Tech*. vol. 12, pp. 689−691.

99. Carvalho A.P. and Malcata F.X. *J. Agric. Food Chem.*, 2005, vol. 53, № 13. pp. 5049−5059.

100. Rösch, C., Skarka, J. and Patyk, A., Microalgae Opportunities and Challenges of an Innovative Energy Source. 17th European Biomass Conference and Exhibition, 29 June−3 July 2009, Hamburg, Germany.

101. Feng, W., van der Kooi, H.J., and de Swaan Arons, J., *Chem. Eng. J.*, 2004, vol. 98, pp. 105−113.

102. Hallgren, A., Andersson, L., and Bjerle, I., *Adv. Thermochem. Biomass Convers.*, Ed. Rev. Pap. Int. Conf., 3rd 1994, pp. 338−349.

103. Yang, Y., Xiang, H., Zhang, R., Zhong, B., and Li, Y., *Catal. Today.*, 2005, vol. 106, no. 1−4, pp. 170−175.

104. McKendry, P., *Bioresource Technol.*, 2002, vol. 83, pp. 47−54.

105. Chiaramonti, D., Oasmaa, A., and Solantausta, Y., *Renew Sustain. Energy Rev.*, 2007, vol. 11, pp. 1056−1086.

106. Miao, X. and Wu, Q., *J. Biotechnol.*, 2004, vol. 110, pp. 85−93.

107. Miao, X., Wu, Q. and Yang, C., *J. Anal. Appl. Pyrol.*, 2004, vol. 71, pp. 855−863.

108. Peng, W., Wu, Q., Tu, P., and Zhao, N., *Bioresource Technol.*, 2001, vol. 80, pp. 1−7.

109. Spolaore, P., Joannis-Cassan, C., Duran, E., and Isambert, A., *J. Biosci. Bioeng.*, 2006, vol. 101, pp. 87−96.

110. Bridgwater, A.V., *App. Catal. A Gen.*, 1994, vol. 116, no. 1−2, pp. 5−47.

111. Ozbay, N., Putun, A.E., Uzun, B.B., and Putun, E., *Renew. Energy.*, 2001, vol. 24, pp. 615−625.

112. Maher, K.D. and Bressler, D.C., *Bioresource Technol.*, 2007, vol. 98, no. 12, pp. 2351−2368.

113. Knothe, G., *Fuel Process Technol.*, 2005, vol. 86, no. 10, pp. 1059−1070.

114. Meng, X., Yang, J., Xu, X., Zhang, L., Nie, Q., and Xian, M., *Renew. Energy.*, 2009, vol. 34, pp. 1−5.

115. Bamgboye, A.I. and Hansen, A.C., *Int. Agrophysics.*, 2008, vol. 22, pp. 21−29.

116. Brown, P., Algal Biofuels Research, Development, and Commercialization Priorities: A Commercial Economics Perspective 2009. www.diversified-energy.com.

117. Hankamer, B., *Physiol. Plant.*, 2007, vol. 131, pp. 10−21.

118. Chisti, Y., *Environ. Eng. Manag. J.*, 2006, vol. 5, pp. 261−274.

119. Kanes, S., The Choice of Next-Generation Biofuels (Algae Excerpt). Equity Research Industry Report. Scotia Capital, 2009.

120. Li, Y., Horsman, M., Wu, N., and Lan, C.Q., *Biotechnol. Prog.*, 2008, vol. 24, pp. 815−820.

ФЕРМЕНТАТИВНЫЙ СИНТЕЗ ЭЛЕКТРОПРОВОДЯЩИХ БИОКОМПОЗИТОВ НА ОСНОВЕ ДНК И ОПТИЧЕСКИ АКТИВНОГО ПОЛИАНИЛИНА

© 2012 г.   Ю. С. Зейфман*, И. О. Майборода*, Ю. В. Грищенко*, О. В. Морозова**,
И. С. Васильева**, Г. П. Шумакович**, А. И. Ярополов**

*НИЦ "Курчатовский институт", Москва, 123182
**Институт биохимии им. А.Н. Баха РАН, Москва,119071
e-mail: yaropolov@inbi.ras.ru

Методом окислительной полимеризации анилина с использованием двух различных биокатализаторов: пероксидазы из корней хрена и биомиметика — микропероксидазы-11 синтезированы электропроводящие интерполимерные комплексы полианилина на матрице ДНК. Исследованы спектральные характеристики и морфология полученных биокомпозитов. Показано различие стереоспецифичности получаемых образцов интерполимерных комплексов в зависимости от используемого биокатализатора. Полученные результаты свидетельствуют о важной роли биокатализатора в формировании направления закручивания спирали электропроводящего полимера на матрице ДНК, т.е. оптическая активность получаемых образцов полимеров, по-видимому, связана со свойствами биокатализатора.

Молекулы ДНК являются уникальными строительными блоками для создания биосовместимых наноматериалов и молекулярных электрических схем благодаря их самоорганизации, а также возможности получать различные наноструктуры высокой сложности. В последние годы было получено большое количество подобных наноструктур из молекул ДНК, например различные двумерные ансамбли [1, 2], геометрические объекты (кубы [3], октаэдры [4]) и др. Исследования также показали отсутствие существенной собственной проводимости ДНК [5, 6], что обусловливает необходимость разработки композитов на основе нуклеиновых кислот и электропроводящих материалов для создания электронных структур на их основе. Ранее была показана возможность использования ДНК в качестве матрицы для синтеза металлических нанопроводов [7], полупроводниковых наночастиц [8] и электропроводящих полимеров [9—11]. В частности, использование электропроводящих полимеров при конъюгации с ДНК может стать основой для разработки биокомпозитных материалов и создания молекулярных устройств, контролирующих влияние внешних факторов на биологические системы, например высвобождение лекарственных препаратов, конструирование нервных имплантатов и искусственных мышц [12], а также имплантируемых источников электропитания (суперконденсаторов) [13].

Полианилин (**ПАНИ**) является одним из наиболее важных электропроводящих полимеров в силу своей высокой химической стабильности, простоты получения, относительно высокой электропроводности и способности изменять физико-химические свойства при различных физических воздействиях (pH, электрическое напряжение). Классический химический метод синтеза электропроводящего ПАНИ, в котором окислителем реакции полимеризации мономера выступает персульфат аммония, требует эквимолярного количества окислителя и проведения реакции в сильно кислых средах при температуре, близкой к 0°C [14]. Использование ферментов при синтезе ПАНИ позволяет проводить процесс в экологически чистых и мягких условиях и получать полимер, не загрязненный продуктами разложения окислителя. В работах [9, 15, 16] была продемонстрирована возможность использования лакказы (КФ 1.10.3.2) и пероксидазы из корней хрена (**ПХ**, КФ 1.11.1.7) для синтеза электропроводящего ПАНИ. Кроме того, было показано, что в зависимости от используемых ферментов может быть получен электропроводящий полимер с различной оптической активностью [17, 18]. Однако при использовании ПХ в качестве биокатализатора полимеризации анилина и различных оптических изомеров сульфокамфорной кислоты в качестве допантов, оптическая активность ферментативно синтезированного ПАНИ была одинаковой [17]. При использовании другого фермента — грибной лакказы, катализирующего, как и ПХ, реакцию ферментативной полимеризации анилина, оптическая активность синтезированного ПАНИ раз-
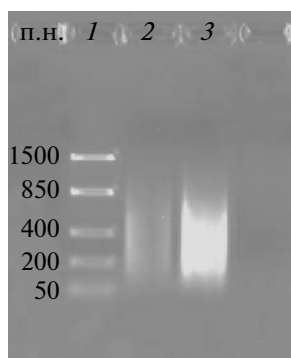
Рис. 1. Результаты электрофореза препарата ДНК в 1%-ном геле агарозы. *1* — маркеры, *2* и *3* — ДНК в количестве 150 нг и 1.5 мкг соответственно.

личалась в зависимости от хиральности используемой сульфокамфорной кислоты [18]. Следует отметить, что ввиду отсутствия асимметричных атомов в основной цепи ПАНИ его оптическая активность обусловлена спиралевидной конформацией полимера, которая достигается путем использования в синтезе хиральных допантов.

Цель работы — подбор условий и проведение синтеза электропроводящего ПАНИ на матрице короткоцепочечной ДНК с использованием в качестве катализаторов реакции окислительной полимеризации анилина двух биокатализаторов: пероксидазы из корней хрена и ранее не используемого для синтеза электропроводящих полимеров биомиметика — микропероксидазы-11, а также исследование физико-химических характеристик полученных интерполимерных комплексов.

МЕТОДИКА

Ферментативный синтез интерполимерного комплекса ПАНИ/ДНК проводили при 25°C с использованием ПХ и при 4°C с использованием микропероксидазы-11 (**МП**). Раствор ДНК с концентрацией 0.5 мг/мл в 10 мМ Na-цитратном буфере с pH 4.3, содержащий 1.55 мМ анилина (соотношение фосфатных групп ДНК и анилина равно 1 : 1), инкубировали при перемешивании в течение 30 мин при комнатной температуре для установления электростатического равновесия между отрицательно заряженными фосфатными группами ДНК и протонированными аминогруппами молекул анилина. После инкубации в реакционную среду добавляли соответствующий фермент с конечными концентрациями в реакционной смеси 85 мкг/мл для ПХ и 110 мкг/мл для МП соответственно. Удельные активности используемых биокатализаторов, измеренные по окислению АБТС в 0.1 М Na-цитратном буфере, pH 4.5, составляли 8.3 и 0.1 мкмоль/с · мг для ПХ и МП соответственно. Реакцию полимеризации мономера инициировали добавлением пероксида во-

дорода. Последний добавляли 4 порциями в течение 30 мин до конечной концентрации 1.55 мМ. Исходную концентрацию раствора пероксида водорода определяли перед проведением эксперимента по поглощению при длине волны 230 нм (молярный коэффициент экстинкции 72.7 M^{-1} $см^{-1}$). Реакцию полимеризации анилина на матрице ДНК проводили в течение 4 ч при использовании ПХ и 24 ч при использовании МП. Для удаления непрореагировавшего мономера полученные биокомпозиты диализовали против 2000-кратного избытка деионизованной воды, подкисленной соляной кислотой до pH 4.3, в течение 16 ч при 4°C. До проведения измерений полученные образцы хранили при 4°C.

Дедопированные образцы ПАНИ/ДНК получали добавлением ~1 мкл 0.1 М раствора NaOH к 100 мкл образца биокомпозита. Редопирование проводили добавлением ~1 мкл 1 М раствора соляной кислоты.

Спектрофотометрические измерения проводили на спектрофотометре Evolution 60 "Thermo Scientific" (США).

Измерения спектров кругового дихроизма (**КД**) проводила на КД-спектрометре Chirascan "Applied Photophysics" (Англия).

FTIR (Fourier transform infrared spectroscopy) — исследование биокомпозитов проводили по стандартной методике с использованием таблеток KBr на спектрофотометре IRPrestige-21 "Shimadzu" (Япония).

Морфологию синтезированных комплексов ПАНИ/ДНК изучали методом атомно-силовой микроскопии (**АСМ**) с использованием микроскопа NTEGRA "NT-MDT" (Россия) в полуконтактном режиме.

В работе использовали следующие реактивы: ДНК("Деринат") — "Техномедсервис ЗАО ФП" (Россия); маркеры для ДНК-электрофореза 50—1500 п.н. SM1108 "Fermentas" (Литва); лимонная кислота, пероксидаза из корней хрена — RZ 2.5—4.0, микропероксидаза-11 — "Sigma-Aldrich" (США); H_2O_2, NaOH, HCl — реактивы марки о.с.ч (Россия). Перед проведением синтеза ПАНИ анилин ("Химмед", Россия) очищали вакуумной дистилляцией. Все растворы готовили с использованием воды, очищенной на установке Milli-Q "Millipore" (США).

РЕЗУЛЬТАТЫ И ИХ ОБСУЖДЕНИЕ

Синтез электропроводящих биокомпозитов ПАНИ/ДНК. Для синтеза интерполимерного комплекса использовали коммерчески доступный препарат дезоксирибонуклеата натрия ("Деринат"), содержащий молекулы ДНК от 50 до 900 пар нуклеотидов (рис. 1). В результате проведения реакции полимеризации анилина на матрице ДНК
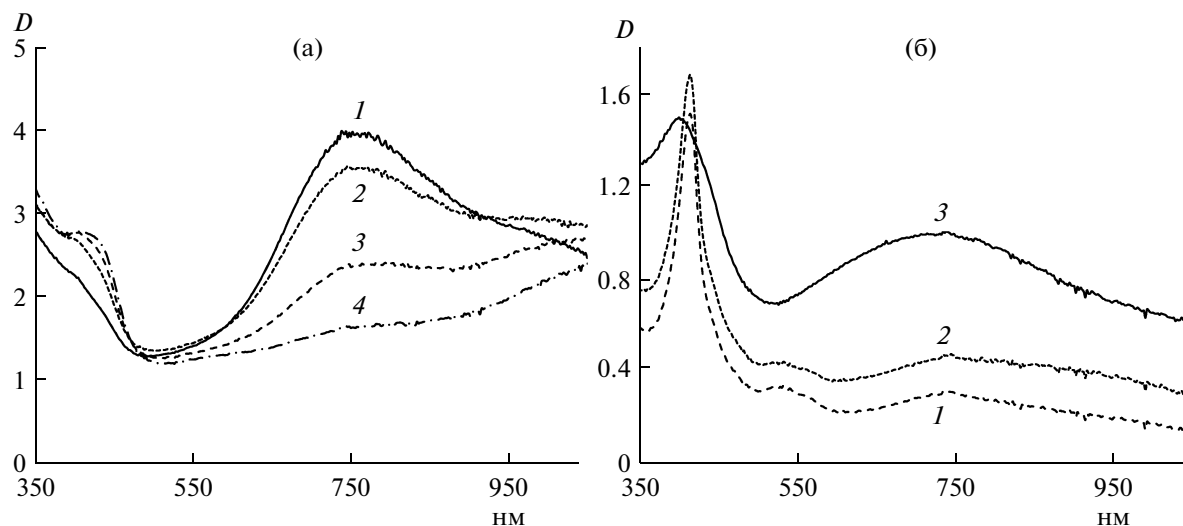
Рис. 2. Изменение электронных спектров комплекса ПАНИ/ДНК от времени синтеза: а — синтез с использованием ПХ (*1* — 5, *2* — 15, *3* — 60, *4* — 240 мин), б — синтез с использованием МП (*1* — 30 мин, *2* — 120 мин, *3* — 24 ч).

с использованием обоих биокатализаторов были получены водные дисперсии интерполимерных комплексов ПАНИ/ДНК зеленого цвета. УФ-видимые спектры, записанные для этих водных дисперсий, демонстрировали наличие пиков поглощения в областях 420—750 нм, соответствующих электропроводящему ПАНИ [9], в составе обоих биокомпозитов (рис. 2). В контрольном эксперименте при том же самом значении рН реакционной среды (рН 4.3) в отсутствии ДНК при полимеризации анилина происходило образование коричневого водонерастворимого осадка разветвленного полимера. Это свидетельствовало о влиянии матрицы ДНК на образование электропроводящего полимера. На рис. 2а представлено изменение спектров поглощения комплекса ПАНИ/ДНК при различных временах синтеза с использованием ПХ (образец ПАНИ/ДНК/ПХ). Пик поглощения в области 750 нм, присутствовавший на ранних стадиях протекания реакции, и отсутствие максимума поглощения в области 420 нм свидетельствовали об образовании перниграни-лина, согласно [9]. В процессе протекания реакции поглощение при этой длине волны уменьшалось, в то время как пик поглощения при 420 нм увеличивался, что может указывать на протонирование основной цепи ПАНИ и образование электропроводящего ПАНИ с более упорядоченной структурой. Увеличение времени синтеза также приводило к появлению широкой полосы поглощения в диапазоне длин волн 700—1100 нм, что может свидетельствовать об увеличении длины цепи π-сопряжения, т.е. длины растущих полимерных молекул. В спектрах поглощения ПАНИ/ДНК, синтезированного с использованием МП (образец ПАНИ/ДНК/МП) также происходило увеличение пика на 420 нм в процессе протекания

реакции (рис. 2б), однако вследствие существенно более низкой удельной активности МП время проведения реакции составляло сутки, а не несколько часов, как в случае с ПХ.

Для обоих полученных образцов интерполимерных комплексов ПАНИ/ДНК были записаны УФ-видимые спектры в дедопированном (неэлектропроводящем) состоянии (рис. 3). Форма спектров для системы ДНК/ПАНИ/ПХ (рис. 3а) как в допированном, так и в дедопированном состоянии хорошо согласуется с ранее полученными литературными данными [9] с использованием высокомолекулярной ДНК. Близким является и спектр для дедопированного комплекса ПАНИ/ДНК, полученного с использованием МП (рис. 3б). При переводе интерполимерных комплексов ПАНИ/ДНК в щелочную среду в обоих случаях исчезал пик поглощения при 420 нм и появлялся интенсивный пик с максимумом в области 550 нм, соответствующий поглощению хиноидного кольца, что свидетельствует о переходе ПАНИ в основную форму. Также полностью исчезала широкая полоса поглощения в области выше 700 нм. При этом дедопирование интерполимерных комплексов было обратимым процессом, о чем свидетельствовало возвращение к исходному виду спектров при доведении рН образцов снова до низких значений (рис. 3, кривые *3*).

Исследование комплексов ПАНИ/ДНК методом FTIR-спектроскопии. На рис. 4 (кривые *1*, *2*) представлены FTIR-спектры образцов интерполимерных комплексов ПАНИ/ДНК, синтезированных с использованием ПХ и МП. Спектры обоих образцов были достаточно близки и имели характерные для полимера, синтезированного традиционным химическим методом с использованием низкомолекулярных допантов, колеба-
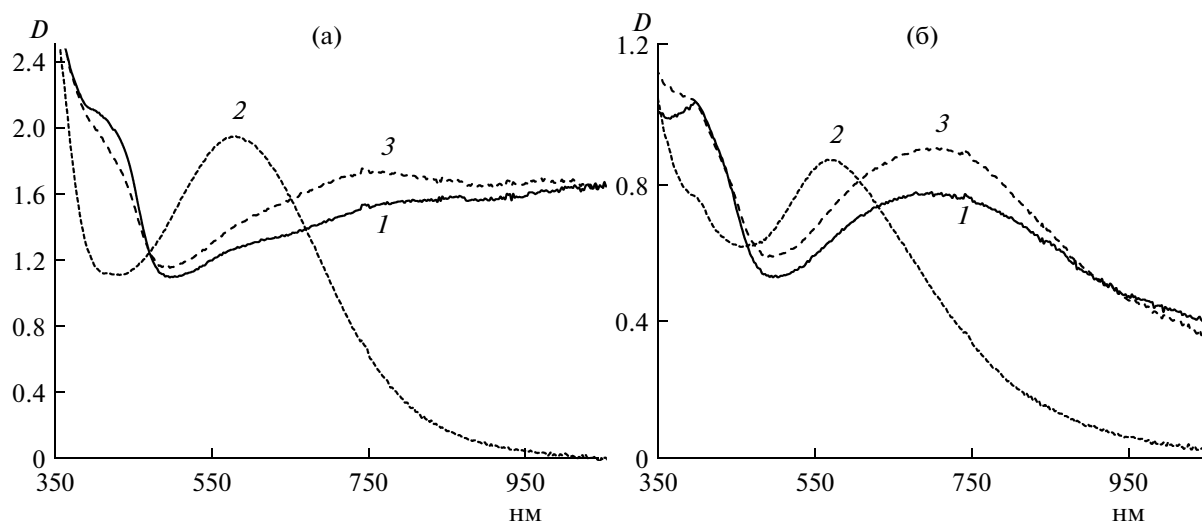
Рис. 3. Электронные спектры комплексов ПАНИ/ДНК, полученных с использованием ПХ (а) и МП (б). *1* – допированная форма, *2* – дедопированная форма, *3* – редопированный ПАНИ.
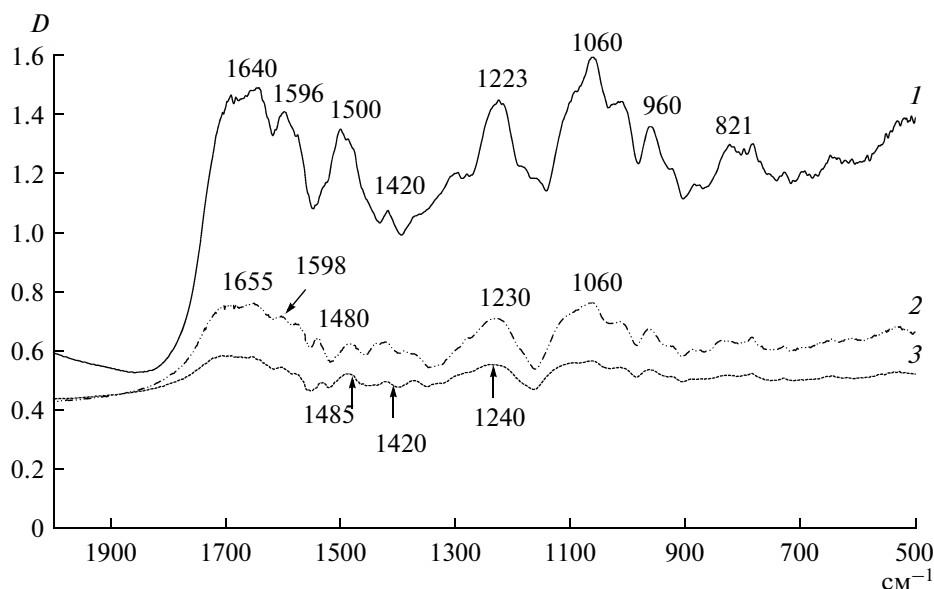

Рис. 4. FTIR-спектры комплексов ПАНИ/ДНК, синтезированных с участием ПХ (*1*), МП (*2*) и контрольного образца – матрицы ДНК (*3*).

тельные полосы, FTIR-спектры ПАНИ, синтезированного с использованием обоих биокатализаторов, имели характерные для электропроводящего ПАНИ волновые числа в областях 1480–1500 см$^{-1}$ и 1590–1600 см$^{-1}$, отвечающие за поглощение, соответственно, хинондииминных и фенилендиаминных групп в повторяющихся звеньях электропроводящего полимера [19]. Для сравнения на рис. 4 (кривая *3*) приведен FTIR-спектр используемой в настоящем исследовании матрицы – ДНК.

Изучение морфологии полученных комплексов методом атомно-силовой микроскопии (АСМ). Морфология и структура синтезированных с ис-

пользованием двух биокатализаторов комплексов ПАНИ/ДНК была изучена АСМ. На полученных АСМ-изображениях видно (рис. 5), что ПАНИ синтезировался преимущественно вдоль нитей ДНК, поскольку на изображениях отсутствовали объекты иной морфологии, отличные от контрольных нитей ДНК. Также наблюдалось увеличение высоты объектов образцов ПАНИ/ДНК по сравнению с контрольным образцом исходной ДНК, что может свидетельствовать о покрытии молекул ДНК ПАНИ.

Спектры КД синтезированных комплексов ПАНИ/ДНК. Спектры КД позволяют получить информацию о вторичной структуре полимера, синтезированного на матрице ДНК. Как уже от-
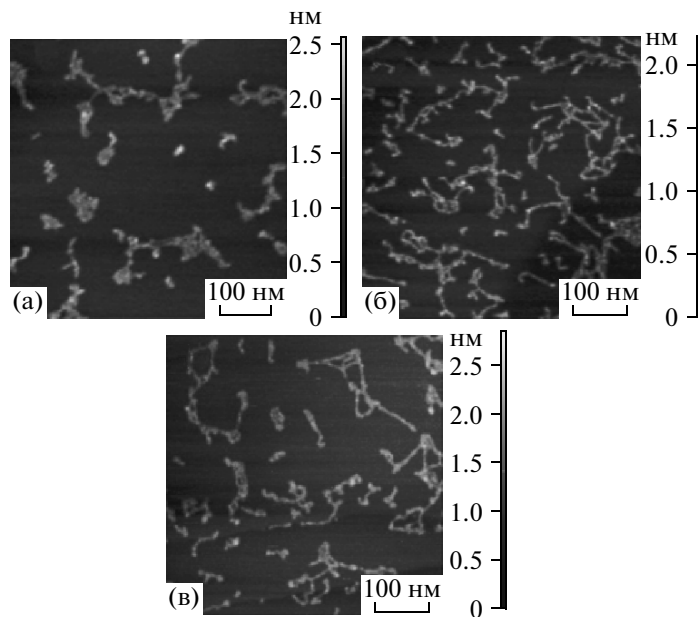
Рис. 5. АСМ-изображения образцов ДНК (а), ПАНИ/ДНК (б), синтезированных с использованием ПХ, и ПАНИ/ДНК (в), синтезированного с использованием МП.
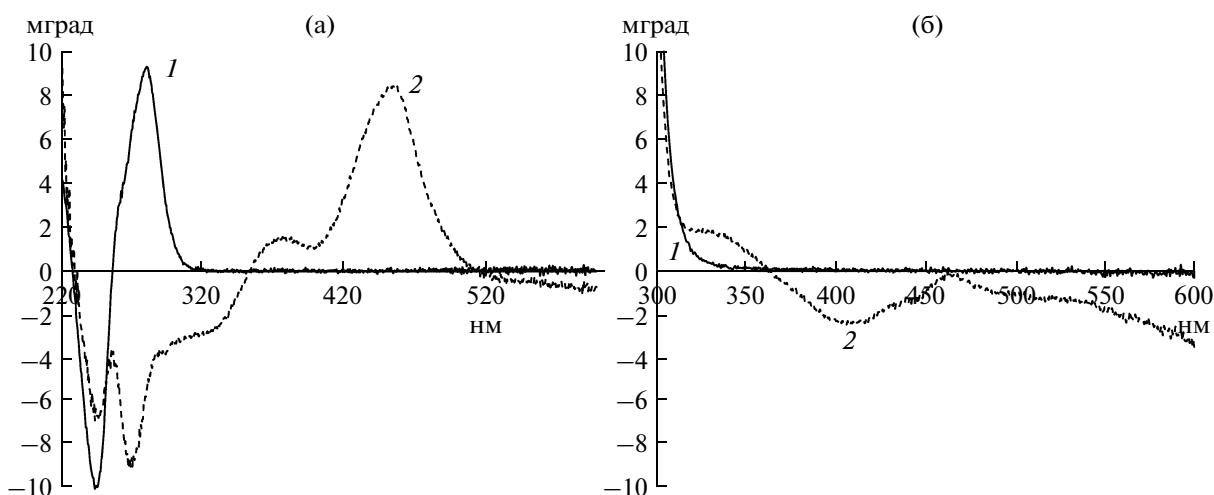

Рис. 6. Спектры КД интерполимерных комплексов ПАНИ/ДНК, синтезированных с использованием ПХ (а) и МП (б). *1* – ДНК, *2* – ПАНИ/ДНК.

мечалось ранее, ПАНИ не содержит асимметричных атомов углерода в своей структуре и его оптическая активность связана со спиралевидной конформацией за счет оптической активности матрицы ДНК. Хиральный ПАНИ ранее был получен с использованием ПХ на различных как хиральных (ДНК), так и ахиральных (полиакриловая кислота) матрицах. В последнем случае (использование оптически неактивной матрицы) хиральный электропроводящий полимер получали за счет добавления низкомолекулярных хиральных допантов, например энантиомеров суль-

фокамфорной кислоты. Следует отметить, что при использовании ПХ в синтезе хирального ПАНИ оптическая активность полимера не зависела от оптической активности низкомолекулярного энантиомера, выбранного в качестве допанта [17]. По мнению авторов, оптическая активность ПАНИ определялась только внутренними свойствами фермента.

КД-спектры образцов ПАНИ/ДНК, полученных в настоящей работе с использованием ПХ, согласуются с данными литературы [9, 17]. На спектре (рис. 6а) присутствовали два широких

пика в области 370 и 450 нм с положительной оптической активностью, которые соответствовали электропроводящему ПАНИ и отсутствовали в контрольных спектрах исходной ДНК. На КД-спектре дедопированного полимера эти пики также отсутствовали (данные не приведены). Спектры кругового дихроизма образцов ПАНИ/ДНК, полученных с использованием МП, представлены на рис. 6б. Использование МП в качестве катализатора ферментативного синтеза полимера на матрице ДНК позволило получить ПАНИ с противоположной оптической активностью по сравнению с образцом ДНК/ПАНИ/ПХ. На КД-спектре интерполимерного комплекса, синтезированного с участием МП, появлялся соответствующий отрицательной поляризации света пик в области 420 нм, а также отрицательная полоса поглощения в области выше 460 нм. Различия в стереоспецифичности получаемых биокомпозитов свидетельствуют об основополагающей роли биокатализатора в создании направления закручивания спирали электропроводящего полимера на матрице ДНК, т.е. оптическая активность получаемых образцов полимеров, по-видимому, связана с внутренними свойствами и строением фермента.

Полученные результаты могут являться основой для создания имплантируемых суперконденсаторов в качестве резервного источника электроэнергии для стимулирования сердечной мышцы.

СПИСОК ЛИТЕРАТУРЫ

1. *Winfree E., Liu F.R., Wenzler L.A., Seeman N.C.* // Nature. 1998. V. 394. P. 539−544.

2. *Yan H., Park S.H., Finkelstein G., Reif J.H., LaBean T.H.* // Science. 2003. V. 301. P. 1882−1884.

3. *Chen J.H., Seeman N.C.* // Nature. 1991. V. 350. P. 631−633.

4. *Zhang Y.W., Seeman N.C.* // J. Am. Chem. Soc. 1999. V. 116. P. 1661−1669.

5. *de Pablo P.J., Moreno-Herrero F., Colchero J., Gómez Herrero J., Herrero P., Baró A.M., Ordejón P., Soler J.M., Artacho E.* // Phys. Rev. Lett. 2000. V. 85. № 23. P. 4992−4995.

6. *Legrand O., Côte D., Bockelmann U.* // Phys. Rev. E. Stat. Nonlin. Soft. Matter. Phys. 2006. V. 73. № 3. Pt 1:031925.

7. *Braun E., Eichen Y., Sivan U., Ben-Yoseph G.* // Nature. 1998. V. 391. P. 775−778.

8. *Coffer J.L., Bigham S.R., Li X., Pinizzotto R.F., Rho Y.G., Pirtle R.M., Pirtle L.M.* // Appl. Phys. Lett. 1996. V. 69. P. 3851−3853.

9. *Nagarajan R., Liu W., Kumar J., Tripathy S.K.* // Macromolecules. 2001. V. 34. P. 3921−3927.

10. *Moon H.K., Kim H.J., Kim N.H., Roh Y.* // J. Nanosci. Nanotechnol. 2010. V. 10. № 5. P. 3180−3184.

11. *Ner Y., Invernale M.A., Grote J.G., Stuart J.A., Gregory A.S.* // Synthetic. Metals. 2010. V. 160. P. 351−353.

12. *Wallace G., Spinks G.* // Soft. Matter. 2007. V. 3. P. 665−671.

13. *Tang H., Chen L., Xing C., Guo Y.-G., Wang S.* // Macromol. Rapid. Commun. 2010. V. 31. P. 1892−1896.

14. *Huang W.S., Humphrey B.D., MacDiarmid A.G.* // J. Chem. Soc. Faraday Trans. 1986. V. 82. № 80. P. 2385−2400.

15. *Karamyshev A.V., Shleev S.V., Koroleva O.V., Yaropolov A.I., Sakharov I.Yu.* // Enz. Microb. Technol. 2003. V. 33. № 5. P. 556−564.

16. *Nickels P., Dittmer W.U., Beyer S., Kotthaus J.P., Simmel F.C.* // Nanotechnology. 2004. V. 15. P. 1524−1529.

17. *Thiagarajan M., Samuelson L.A., Kumar J., Cholli A.L.* // J. Am. Chem. Soc. 2003. V. 125. P. 11502−11503.

18. *Vasil'eva I.S., Morozova O.V., Shumakovich G.P., Shleev S.V., Sakharov I.Yu., Yaropolov A.I.* // Synthetic. Metals. 2007. V. 157. P. 684−689.

19. *Louarn G., Lapkowski M., Quillard S., Pron A., Buisson J.P., Letrant S.* // J. Phys. Chem. 1996. V. 100. P. 6998−7006.

Enzymatic Synthesis of Electroconductive Biocomposites Based on DNA and Optically Active Polyaniline

Yu. S. Zeifman[a], I. O. Maiboroda[a], Yu. V. Grishchenko[a], O. V. Morozova[b], I. S. Vasil'eva[b], G. P. Shumakovich[b], and A. I. Yaropolov[b]

[a] *National Research Centre Kurchatov Institute, Moscow, 123182 Russia*

[b] *Bach Institute of Biochemistry, Russian Academy of Sciences, Moscow, 119071 Russia*

e-mail: yaropolov@inbi.ras.ru

Abstract—Electroconductive interpolymer polyaniline complexes are synthesized on the DNA matrix, using the method of oxidative polymerization of aniline with two different biocatalyzers: horseradish root peroxidase and micropiroxidase-11 biomimetic. The spectral characteristics and morphology of the acquired biocomposites have been studied. The stereospecificity of the acquired samples of interpolymer complexes is shown, depending on the biocatalyzers used. The results acquired indicate the important role of a biocatalyzer in the formation of the twist direction of an electroconductive polymer spiral on the DNA matrix; i.e., the optical activity of the polymer samples acquired is apparently associated with the biocatalyzer properties.

ENZYMATIC MODIFICATION OF CHITOSAN WITH QUERCETIN AND ITS APPLICATION AS ANTIOXIDANT EDIBLE FILMS

© 2012   E. Torres*, V. Marín*, J. Aburto**, H. I. Beltrán***, K. Shirai****,
S. Villanueva*****, G. Sandoval*****

Center of Chemistry-ICUAP, University of Puebla, Edificio 103G. Puebla 72570 México
**Mexican Institute of Petroleum, Eje Central Lázaro Cárdenas Norte 152, Col. San Bartolo Atepehuacan,
México, D. F., 07730*
*** Metropolitan Autonomous University-Cuajimalpa, Artificios 40-sexto piso, Col. Hidalgo, México, D. F., 01120.*
**** Metropolitan Autonomous University-Iztapalapa, Av San Rafael Atlixco No.186, Col.Vicentina Mexico DF 09340*
***** Center of Investigation and Technological Assistance and design of Jalisco. Guadalajara, Jalisco. Mexico 44270*
e-mail: eduardo.torres@correo.buap.mx
Received August 15, 2011

Quercetin, rutin, naringin, hesperidin and chrysin were tested as substrates for cloroperoxidase to produce reactive quinones to graft onto chitosan. Quercetin and rutin quinones were successfully chemically attached to low molecular weight chitosan. The quercetin-modified chitosan showed an enhancement of plastic, antioxidant and antimicrobial properties as well as of thermal degradability. Finally, chitosan-quercetin films visibly decreased enzymatic oxidation when applied to *Opuntia ficus indica* cladodes.

Chitosan, poly((1 → 4)-2-amino-2-deoxy-β-D-glucose), is a product of the deacetylation of chitin, which is ranked, by prevalence, as the second polysaccharide in nature, just after cellulose. Chitosan has received increased attention for its commercial applications in the biomedical, food and chemical industries due to its biodegradability, biocompatibility and biological activities such as antimicrobial, antitumor, antioxidant and hypocholesterolemic functions. Chitosan contains a large number of hydroxyl and amino groups, which are two functional and strategic groups in organic synthesis; these groups provide several possibilities for derivatization or grafting. Modification with several reactive groups has produced chitosans with improved properties such as increased hydrophobicity, higher solubility in both water and organic media and improved antimicrobial properties [1–3] or with new properties, such as photosensitizing activity [4]. Enzymatic modification of chitosan has already been reported in the literature [5–8]. By using oxidative enzymes, chitosan has been grafted with phenol derivatives to confer higher hydrophobicity and viscosity [5, 9] or new functionalities, such as the ability to adsorb cationic dyes [7].

These experimental contributions make evident the importance and the potential of the functionalization of chitosan with specific molecules to provide biopolymers with improved properties [10]. Our first improvement of chitosan macromolecules is centered on the inclusion of natural flavonoids with known biological and chemical potential [11, 12] in their polymeric backbones. Therefore, in this report, we carried out the synthesis of chitosan-flavonoid conjugates by

enzymatic treatment with chloroperoxidase (CPO, EC 1.11.1.10). Flavonoids are found in fruits, vegetables and a variety of other dietary sources with anticancer, antiviral, antimutagenic and lipid peroxidation inhibitory activities. Here, by oxidizing flavonoids with CPO in the presence of chitosan, we expect to produce adducts through the reaction of the catechol (in its *ortho*-quinonic form) moiety of flavonoids and the amino groups of the chitosan. With this modification, some properties of chitosan were improved. The modified polymer was used to diminish browning on *Opuntia ficus indica* cladodes, applying the chitosan-quercetin bioconjugates as an edible film.

MATERIALS AND METHODS

CPO from the marine fungus *Caldaromyces fumago* was a gift from Dr. M. A. Pickard from the University of Alberta, Canada. The enzyme has a specific activity of 22.000 U min⁻¹ for the halogenation of monochlorodimedone. Quercetin, rutin, hesperidin, chrysin and naringin, chitosans of low molecular weight 75–85% deacetylated with 20–200 cP of viscosity, hydrogen peroxide, buffer salts and acids, and 2,2-diphenyl-1-picrylhydrazyl (DPPH) radicals were purchased from the Sigma-Aldrich Chemical Company (USA). HPLC organic solvents, isopropanol and acetonitrile, were purchased from J.T. Baker (USA).

Flavonoid oxidation by CPO. The enzymatic oxidation of flavonoids was carried out in a reaction mixture containing 20% isopropanol and 80% acetate buffer (60 mM, pH 3.0), 3.3 mM flavonoid, 100 pM CPO, 1.0 mM H₂O₂ and 20 mM KCl. The temperature was

kept constant at 25°C under stirring. The reaction progress was monitored by the decrease in absorbance in the range of 200−600 nm. All assays were performed 3 times to ensure repeatability.

Enzymatic grafting of quercetin to chitosan. A total of 2.0 g of chitosan was added after 5 min to 250 ml of the reaction mixture described in the previous section. Chitosan was dissolved by the addition of acetic acid to reach a concentration of 1% w/v. After 12 h of stirring at room temperature, the pH was raised by adding 1.0 M NaOH to precipitate the modified chitosan. This solid was washed several times with 50% isopropanol solution to remove the non-reacted oxidized product until the elution did not show any oxidized quercetin or rutin, as measured by the UV-VIS spectra between 200−600 nm. Finally, the modified chitosan was dried under a vacuum in a phosphorus pentoxide atmosphere.

Calorimetric studies. Thermograms were obtained in a differential scanning calorimeter (DSC) Shimadzu DSC60 (Japan). In a typical determination, chitosan or its derivative (~15 mg) was placed in an aluminum cell and the temperature ramp was raised up from 25 to 400°C at 10°C/min with a nitrogen flux of 20 ml/min. The enthalpy of thermal decomposition for every sample was calculated using the software TA-60WS.

Antioxidant activity. The antioxidant activity of neat and modified chitosan was determined using the DPPH (diphenylpicrylhydrazyl) and the ABTS (2,2'-azino-bis(3-ethylbenzothiazoline-6-sulphonic acid) method. For the former, 40 μM of DPPH radical were placed in a cuvette containing different concentrations of chitosan, 50% methanol and 1% acetic acid, in a total volume of 4 ml. The change in absorbance was measured at 515 nm after a 1-h incubation at room temperature.

The antioxidant capacity measured as the ABTS free radical-scavenging activity was determined according to the method described previously [13]. Chitosan samples previously dissolved in 1% acetic acid and properly diluted were added to the $ABTS^{\cdot+}$ solution, and the decrease of absorbance was measured at 734 nm after 15 min in the dark. A previous time scan was performed to check the stability of the $ABTS^{\cdot+}$ solution.

For both methods the antioxidant capacity was calculated according to the formula:

$$\text{Antioxidant capacity} = (A_0 - A_1)/A_0 \times 100\%,$$

where A_0 is the absorbance of the sample measured at time 0 and A_1 is that measured at 1 h of incubation.

Antimicrobial activity. To determine the antimicrobial activity of neat and modified chitosans seven pathogen microorganisms were selected and their growth in the presence and absence of the biopolymers was measured. The microorganisms assayed were: *Pseudomonas aeruginosa* PAO1T, *Staphylococcus aureus* ATTC 29789T, *Raoultella* (*Klebsiella*) *planticola* ATCC 33531T, *Ustilago maydis* 521 T, *Candida albicans* ATCC 10231T, *Pantoea ananatis* LMG 2665T and *Escherichia coli* 62348-69. The microorganisms were grown in TESMA and Luria-Bertani (LB) broth for 24 h at 30°C and 150 rpm.

To quantify the microbial populations, the preinoculum of each strain was performed in liquid medium TESMA (g/l):yeast extract − 2.7, glucose − 2.7, mannitol 1.8, K_2HPO_4 − 4.8, KH_2PO_4 − 0.65, agar − 16.0, and bromothymol blue − 50 (mg/l) one day before. Then the cells were washed with 10 mM $MgSO_4 \cdot 7H_2O$, followed by the population adjustment to an optical density of 0.05 at 450 nm. Four assays were tested: 1) inoculation of strains in the presence of neat chitosan at 2.5 mg/ml; 2) inoculation of strains in the presence of modified chitosan at 2.5 mg/ml, 3) inoculation of strains in the presence of acetic acid (0.25%), 4) inoculation of strains in culture broth as control. The type strains were inoculated in test tubes with 4 ml LB or TESMA broth and incubated at 30°C/150 rpm for 21 h. Finally, the account of microbial populations was done with serial dilutions using the "drop-plate" method [14, 15].

Preparation and application of antioxidant edible films on *Opuntia ficus indica* stems. Fresh cactus (*Opuntia ficus*) were purchased at the local market of Guadalajara Jalisco, México. The whole paddles were washed with water and dried on paper towels, and then the spines were removed manually using a kitchen knife. Five different batches of 11 paddles each (970 g per batch) were prepared for the assays. The samples were submerged for 5 min in 1.0% acetic acid containing no chitosan (batch 1), quercetin-modified chitosan at 0.3% (batch 2) and neat chitosan at 0.3% (batch 3). Two additional controls were carried out containing traditional antioxidants such as EDTA (0.08%) plus citric (0.5%) and ascorbic (1.5%) acid (batch 4) and citric (0.5%) and ascorbic (1.5%) acid (batch 5).

All of the batches were placed on open trays and kept at 23° ± 1°C relative humidity 48%. After treatment, the cactus batches were placed in a mesh to remove the excess water and were allowed to drain for 2 h; after that time, the cactus batches were placed on sheets of absorbent paper for half an hour, and, finally, put on trays for observation. Changes in the color of the cactus were followed by daily measurements of lightness (L), green-red dye (a) and yellow-blue dye (b) using a Hunter Lab (USA) colorimeter.

RESULTS AND DISCUSSION

Enzymatic oxidation of flavonoids. Quercetin and rutin were easily oxidized by CPO to produce a brown product, characteristic of *o*-quinones, which are generated by peroxidases and polyphenol oxidases [16]. Hesperidin and naringine were also oxidized according to UV-Vis spectra. Chrysin was not a substrate for
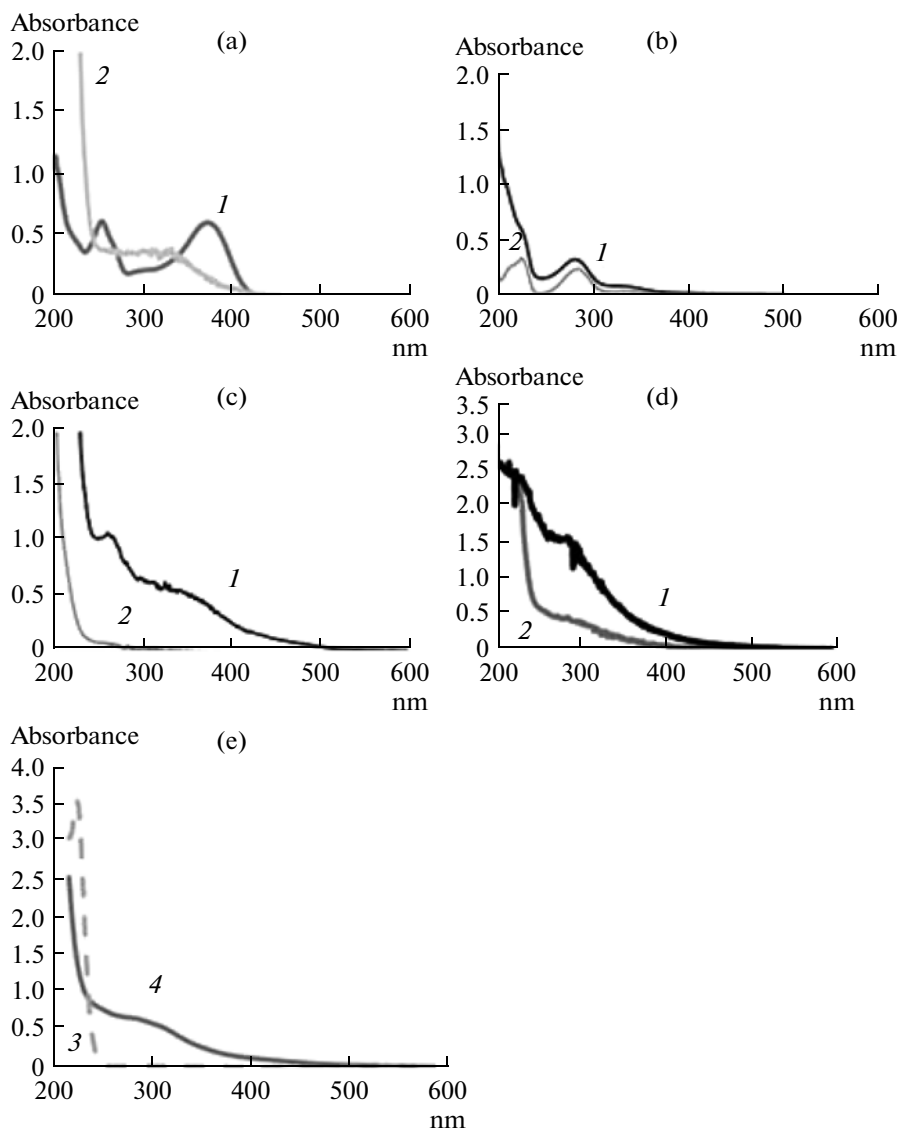
Fig. 1. Electronic absorption spectra of native (*1*) and oxidized (*2*) flavonoids (a–d) and native (*3*) and modified (*4*) chitosan by 1.0 mM H$_2$O$_2$ and 100 pM CPO (e). a – quercetin; b – naringin; c – rutin; d – hesperidin, e – chitosans.

CPO (data not shown). Fig. 1 displays the electronic absorption spectra of the assayed flavonoids before and after 1 min of the enzymatic action. As can be seen, the two bands at 250 and 350 nm of quercetin, hesperidin and rutin decreased significantly after enzymatic modification, and a new band appeared around 300 nm for quercetin.

Characterization of modified chitosan. It is well known that *o*-quinones produced from the oxidation of phenols can undergo subsequent non-enzymatic reactions [17] such as electrophilic attacks to nucleophilic moieties, i.e., amino groups from chitosan (Fig. 2). From all assayed flavonoids, only oxidized products from quercetin were able to be attached to chitosan.

Fig. 1 shows the absorption spectra of neat and quercetin-modified chitosan in a 1% acetic acid solu-

tion after being modified, washed and dried. As shown, the appearance of a band around 300 nm indicates the presence of the quercetin moiety in the structure of chitosan. As a control, we carried out the whole process in the absence of the enzyme and in the presence of all other components. As can be inferred from the figure, the control sample did not show any absorption band, meaning that there are not physical interactions between the two components. Additional spectroscopic evidences (FTIR and RMN) indicated that the chitosan was successfully modified with quercetin (data not shown). Among the most attractive properties of renewable polymers are their degradability, and antioxidant activity, which are especially important for the food industry to produce packaging or coatings to maintain important properties in food such as texture, taste and mouth feel [18, 19]. Therefore, we
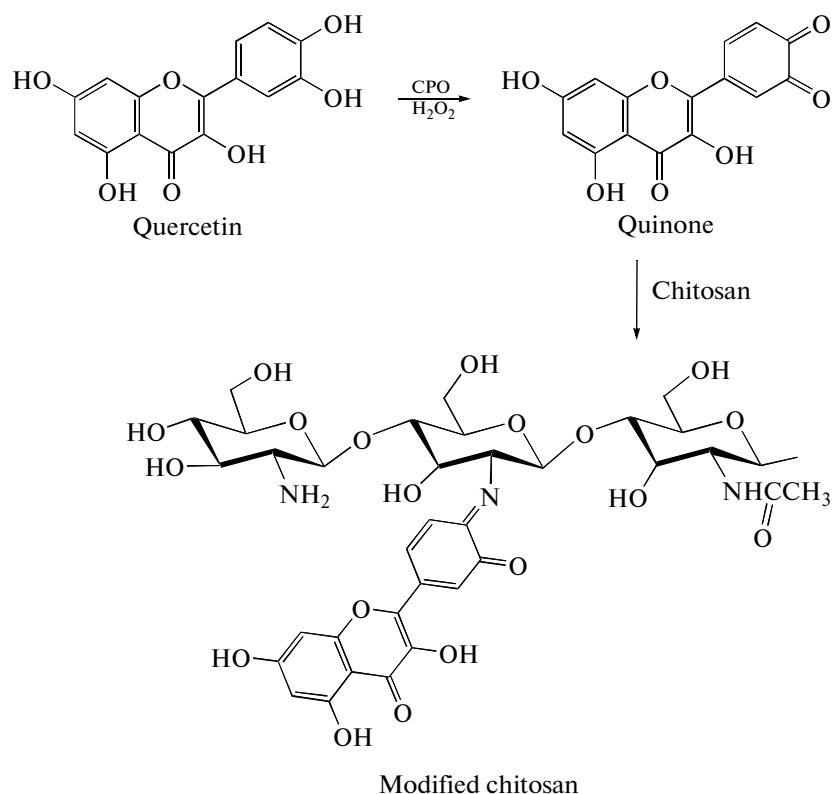
Fig. 2. Chloroperoxidase-catalyzed oxidation of quercetin, and the subsequent nucleoplilic modification of chitosan.
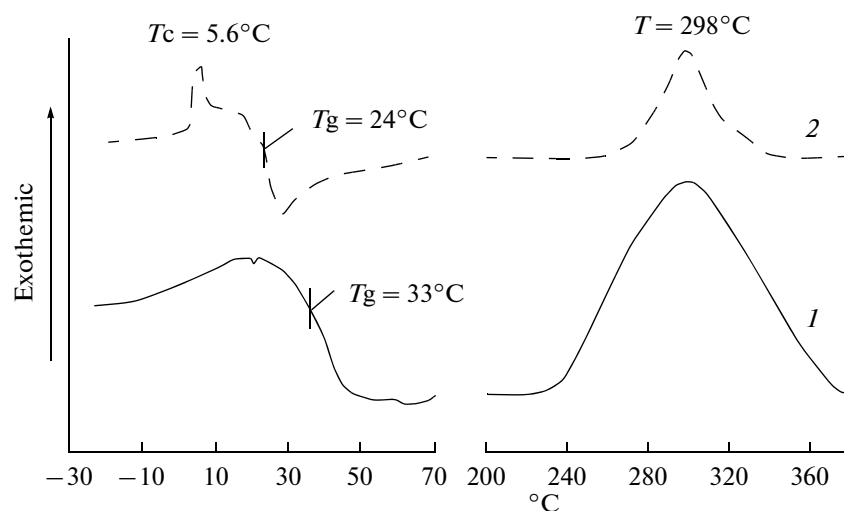
Fig. 3. Thermograms of unmodified chitosan (*1*) and modified chitosan (*2*).

conducted several experimental assays to quantify the changes in these properties as a first approximation for developing a food package or coating based on quercetin-modified chitosan.

Chitosan degradability. Differential scanning calorimetry (DSC) was employed to study the polymer degradability and also to check on any variation in struc-

tural properties of chitosan after modification with quercetin. The thermal curves of chitosan and quercetin-modified chitosan are depicted in Fig. 3. As can be seen in the DSC curve, neat chitosan showed a typical broad exothermic peak (T_{onset} 239.14°C, T_{peak} 298.71°C, T_{endset} 367.44°C) that can be attributed to the degradation of the saccharide structure of the mol-

Fig. 4. Antioxidant activity of unmodified (*1*) and modified (*2*) chitosan, measured as the reduction of the (a) ABTS and (b) DPPH radicals. The 100% activity corresponds to the complete reduction of 7.0 mM ABTS radical or 6.5 mM DPPH radical.
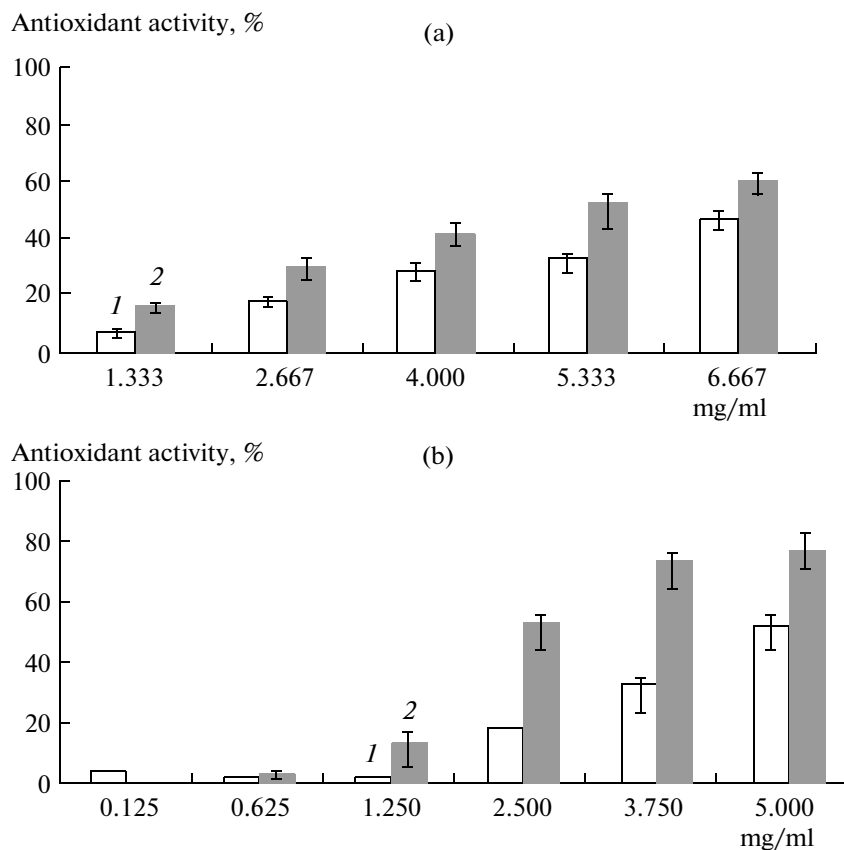
ecule, including the dehydration of saccharide rings and the decomposition of the acetylated and deacetylated units of chitosan [20, 21]. Modified chitosan displayed the same exothermic peak (T_{peak} 297.82°C) but less wide (T_{onset} 273.05°C, T_{endset} 319.22°C). The associated heats were 212.82 J/g and 33.62 J/g, respectively. This result could suggest that the chitosan modified with quercetin is even more degradable compared to the unmodified counterpart, because 6 times less heat is necessary to degrade the modified biopolymer. The lower thermal stability could be due to a new arrangement of the modified chitosan, whereby the quercetin molecules are inserted between chitosan macromolecules, which weakens the interconnection between polysaccharide chains [20]. As a result, the chitosan part of the modified biopolymer is more susceptible to thermal degradation.

In addition, some changes were observed at lower temperatures. Neat chitosan displayed an endothermic signal, Tg, at 33°C, associated with the transition from a crystalline to an amorphous state (Fig. 3). Meanwhile, modified chitosan showed a Tg at a lower value, 24°C, and also showed an exothermic signal at 5.6°C, attributed to the crystallization of polymer fragments. The change in the Tg value indicates a transition from a crystalline to an amorphous state for the

modified polymer at room temperature; however, the neat chitosan needs more heat to undertake the same transition. This relationship may indicate an increase in plasticity for the quercetin-chitosan polymer compared to the unmodified polymer.

Antioxidant activity. Recently, the antioxidant activity of chitosan and its derivatives has attracted attention. The effects are similar to those of phenolic antioxidants [22]. Here, the measure of antioxidant activity may help us to understand the functional properties of the polymers. The antioxidant activity of the modified chitosan was enhanced throughout the experimental range when compared to the neat chitosan. Indeed, for the ABTS method, at a concentration of 1.3 of mg/ml of both polymers, showed 6.6% of the antioxidant capacity for neat chitosan and 17% of the antioxidant activity for modified chitosan a value 1.5 times higher for the modified biopolymer (Fig. 3a). At a concentration of 6.7 mg/l, 47% (3.3 mM) of the ABTS radical was reduced for the neat chitosan (Fig. 4a) and 62% (4.2 mM) of the ABTS radical was reduced for the modified chitosan. We then evaluated the percent reduction of the DPPH radical as a measure of the antioxidant activity of the polymers (Fig. 4b). A reduction of 50% of the DPPH radical was reached at 5 mg/ml for the neat chitosan,
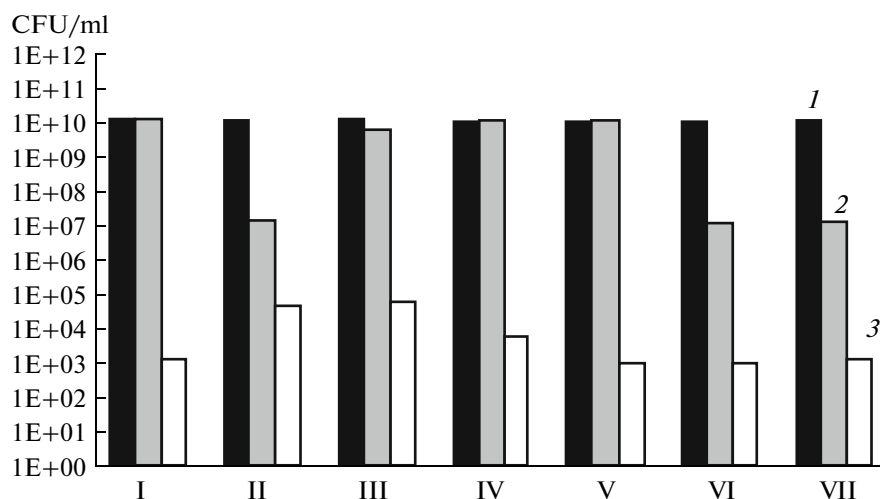
Fig. 5. Antimicrobial activity of control (*1*), unmodified (*2*) and modified chitosan (*3*) after 21 h growing at 30°C/150 rpm against seven different microorganism. Strains: I − *Candida albicans* ATCC 10231T; II − *Escherichia coli* 62348-69; III − *Raoultella planticola* ATCC 33531T; IV − *Pantoea ananatis* LMG 2665T; V − *Pseudomonas aeruginosa* PAO1T; VI − *Staphylococcus aureus* ATTC 29789T; VII − *Ustilago maydis* 521 T.

and at 2.5 mg/ml for the modified polymer. The maximal reductions of the DPPH radical were 32 μM (80%) and 20 μM (50%) for the modified and neat chitosan, respectively. A greater difference in antioxidant activity between the biopolymers was found at a concentration of 2.5 mg/ml, where the modified polymer showed a 50% antioxidant activity and the neat chitosan showed only a 17% antioxidant activity, an increment of about three times for the modified chitosan.

The increased antioxidant potential showed by the modified biopolymer could be explained in terms of some structural aspects provided for the oxidized quercetin moiety: a carbonyl function on the C-ring conjugated to two hydroxyl groups on C3 (C-ring) and C5 (A ring), and a double bond between C2 and C3. The hydroxyl groups may be dehydrogenized, deprotonated or oxidized. These structural features of quercetin have been reported as determinants for its free radical scavenging and/or its antioxidant activity [23, 24].

Antimicrobial activity. Chitosan has a natural antimicrobial activity well reported in the literature for a wide spectrum of microorganisms [25]. Although the mechanism of action is not yet fully elucidated and being highly dependent on the type of microorganism, the ability to kill bacteria has been correlated to its capacity to disrupt the outer and inner membrane mediated by its positive-charged amino group at C2 position, whereas it is related to direct interaction of the biopolymer with negatively charged fungal cells [25]. Immobilization of an antimicrobial agent like quercetin on chitosan must, in principle, change this capacity. To analyze this point, the effect of the chitosans on the growth of seven pathogen microorganisms was determined (Fig. 5). As it can be observed, control assays reached a cell population of 10 × 10^10 CFU/ml, and

the growth was not affected by the presence of 0.25% of acetic acid. Neat chitosan inhibited the growth of three microorganisms, *Escherichia coli*, *Ustilago maydis* and *Staphylococcus aureus* up to three orders of magnitude. On the other side, quercetin-modified chitosan was able to inhibit all microorganisms up to seven orders of magnitude, showing a higher and also a broader spectrum of antimicrobial activity than the neat chitosan. As mentioned before, the mechanism by which chitosan act is not completely elucidated, varying with the degree of acetylation, molecular weight (MW), distribution of the pendant acetyl groups as well as its conformational structure [26, 27]. For modified chitosan, the presence phenolic hydroxyl groups of quercetin could explain the better antimicrobial activity [28]. Since the antimicrobial capacity of chitosan oligomers [26] is higher we foresee that decreasing the molecular weight of chitosan, the modified biopolymer could show even higher antimicrobial activity. In addition, an increment in the deacetylation degree of chitosan up to 90−95% may enhance its antimicrobial activity. These determinations are currently carried out in our laboratory.

Inhibition of enzymatic browning of *Opuntia ficus indica* stems. *Opuntia ficus indica* has important nutritional and medical applications [29]. During storage of its stems, dark spots appear and the original bright green color turns into olive to brown shades; this browning is one of the main postharvest issues [30, 31]. According to our results, quercetin-modified chitosan is a better antioxidant, and in addition, we determine that it is still able to form films. Therefore, this bioconjugate could be used as an antioxidant edible film on fruits and vegetables. To test this property, stems of *Opuntia ficus indica* were coated with chitosan-quercetin, native chitosan and EDTA-ascorbic acid-citric

Color parameters of *Opuntia ficus* indica stems coated with edible films at day 0 and after 5 days of storage at 23°C

Batch**	a^*		L^*		b^*	
	0	5	0	5	0	5
1 — no treatment	-9 ± 1	-7 ± 1	58 ± 4	39 ± 4	36 ± 4	25 ± 4
2 — chitosan-quercetin	-11 ± 1	-9 ± 1	61 ± 4	45 ± 4	37 ± 4	28 ± 4
3 — neat chitosan,	-10 ± 1	-7 ± 1	58 ± 4	39 ± 4	33 ± 4	26 ± 4
4 — EDTA-ascorbic and citric acid	-9 ± 1	-7 ± 1	55 ± 4	34 ± 4	33 ± 4	25 ± 4
5 — ascorbic and citric acid	-10 ± 1	-8 ± 1	53 ± 4	39 ± 4	32 ± 4	23 ± 4

** The samples were submerged during 5 min in 1% acetic acid and placed in a mesh to remove the excess of water and letting it drain for 2 h; after that time, were placed on sheets of absorbent paper for half an hour to finally put them in trays for observation.

acid and ascorbic-citric acid. Also, a negative control without treatment was performed. The protective effect of the different coatings was measured by color conservation during controlled storage at ambient temperature (23°C).

Results of the color variation of the stems treated with different coatings are presented in the table. Statistical analysis showed that there was a significant effect between the different coatings on all of the color parameters (L^*, a^* and b^*). L^* measures the luminosity, ranging from black ($L^* = 0$) to white ($L^* = 100$). Values of a^* can be positive (red) or negative (green), while positive values of b^* are yellow and negative values of b^* are blue [32].

As can be observed in the table, a^* values of fresh stems are neatly negative, meaning that they have a green color. After five days of storage, the a^* values increase for all coatings, indicating a fading of the green color. It can be seen, however, that the paddles coated with chitosan-quercetin films showed the most negative a^* values after storage, indicating that they retain most of the green color compared to the stems treated with other antioxidants. The native chitosan treatment showed also a protective effect (although less than the quercetin doped chitosan), while the traditional antioxidant coatings and the stems without treatment showed a greater loss of green color (a^* values less negative).

High L^* values at day 0 reflect a luminous color and, after five days of storage, the luminosity of the stems decreased. Again, the stems coated with chitosan-quercetin films retained more luminosity compared to the stems coated with other treatments and the non-treated stems. Similarly, b^* values after storage were greater for the cladodes protected by chitosan-quercetin films, indicating a better retention of the yellow tone.

Therefore, it can be stated that enzymatic modification of chitosan has conferred to the biopolymer improved biological properties.

* * *

We demonstrate here the feasibility of covalent enzymatic chitosan modification with a representative flavonoid, quercetin. The quercetin-modified chitosan showed an enhancement of the antioxidant and antimicrobial properties and retained thermal degradability. Moreover, the quercetin moiety conferred a lower temperature of the crystalline-amorphous transition, i.e., an enhanced plasticity. In addition, the antioxidant activity of modified chitosan was improved by quercetin attachment. Finally, color conservation was improved during storage of *Opuntia ficus indica* stems coated with chitosan-quercetin films.

ACKNOWLEDGMENTS

REFERENCES

1. Kim, C.H., Choi, J.W., Chun, H.J., and Choi, K.S., *Polym. Bull.*, 1997, vol. 38, no. 4, pp. 387−393.
2. Jang, M.-K. and Nah, J-W. *Bull. Korean Chem. Soc.*, 2003, vol. 24, no. 9, pp. 1303−1307.
3. Tangpasuthadol, V., Pongchaisirikul, N., and Hoven, V.P., *Carbohydr. Res.*, 2003; vol. 338, no. 9, pp. 937−942.
4. Nowakowska, M., Lukasz, M., and Szczubialka, K., *Biomacromolecules*, 2008. vol. 9, no. 6, pp. 1631−1636.
5. Chen, T., Kumar, G., Harris, M.T., Smith, P.J., and Payne, G.F. *Biotechnol. Bioeng.*, 2000, vol. 70, no. 5, pp. 564−573.
6. Vachoud, L., Chen, T., Payne, G.F., and Vazquez-Duhalt, R., *Enzyme Microb. Technol.*, 2001, vol. 29, no. 6−7, pp. 380−385.
7. Chao, A.-C., Shyu, S.-S., Lin, Y.-C., and Mi, F.-L., *Bioresour. Technol.*, 2004, vol. 91, no. 2, pp. 157−162.
8. Kaneko, Y., Matsuda, S.-I., and Kadokawa, *J. Biomacromolecules*, 2007, vol. 8, no. 12, pp. 3959−3964.
9. Wu, L.Q., Embree, H.D., Balgley, B.M., Smith, P.J., and Payne, G.F., *Environ. Sci. Technol.*, 2002, vol. 36, no. 15, pp. 3446−3454.

10. Nyanhongo, G.S., Prasetyo, E.N., Kudanga, T., and Guebitz, G. Grafting of Functional Molecules: Insights into Peroxidase-Derived Materials. *Biocatalysis Based on Heme Peroxidases,* Ed E.Torres & M. Ayala, Berlin, Heidelberg: Springer, 2010, pp. 155−177.

11. Kadereit, D. and Waldmann, H., *Chem. Rev.,* 2001, vol. 101, no. 11, pp. 3367−3396.

12. Levitzki, A*., Acc. Chem. Res.*, 2003, vol. 36, no. 6, pp. 462−469.

13. Stratil, P., Klejdus, B., and Kuban, V., *J. Agric. Food Chem.*, 2006; vol. 54, no. 3, pp. 607−616.

14. Hoben, H.J. and Somasegaran, P., *Appl. Environ. Microbiol.*, 1982, vol. 44, no. 5, pp. 1246−1247.

15. Herigstad, B., Hamilton, M., and Heersink, J., *J Microbiol Methods*, 2001, vol. 44, no. 2, pp. 121−129.

16. Pourcel, L., Routaboul, J.-M., Cheynier, V., Lepiniec, L., and Debeaujon, I., *Trends Plant Sci*, 2007; vol. 12, no. 1, pp. 29−36.

17. Torres, E., Bustos-Jaimes, I., and Le Borgne, S., *Appl. Catal. B*, 2003; vol. 46, no. 1, pp. 1−15.

18. No, HK, Meyers, S.P., Prinyawiwatkul, W., and Xu, Z., *J. Food Sci*, 2007, vol. 72, no. 5, pp R87−R100.

19. Hansen, N.M.L. and Plackett, D., *Biomacromolecules*, 2008, vol. 9, no. 6, pp. 1493−1505.

20. Pawlak, A. and Mucha, M., *Thermochim Acta*, 2003, vol. 396, no. 1−2, pp. 153−166.

21. Paulino, A.T., Simionato, J.I., Garcia, J.C., and Nozaki, J., *Carbohydr Polym*, 2006, vol. 64, no. 1, pp. 98−103.

22. Je, J.-Y., Park, P.-J., and Kim, S.-K., *Food Chem Toxicol*, 2004, vol. 42, no. 3, pp. 381−387.

23. Ji, H.-F., Tang, G.-Y., and Zhang, H.-Y., *QSAR Comb. Sci.*, 2005, vol. 24, no. 7, pp. 826−830.

24. Fiorucci, S., Golebiowski, J., Cabrol-Bass, D., and Antonczak, S., *J. Agric Food Chem*, 2007, vol. 55, no. 3, pp. 903−911.

25. Pacheco, N., Larralde-Corona, C.P., Sepulveda, J., Trombotto, S., Domard, A., and Shirai, K., *Int. J. Biol. Macromol.*, 2008, vol. 43, no. 1, pp. 20−26.

26. No, H.K., Young Park, N., Ho Lee, S., and Meyers, S.P., *Int. J. Food Microbiol.*, 2002, vol. 74, no. 1−2, pp. 65−72.

27. Fernandez-Saiz, P., Ocio, M.J., and Lagaron, J.M., *Biopolymers*, 2006, vol. 83, no. 6, pp. 577−583.

28. Nonaka, T., Uemura, Y., Ohse, K., Jyono, K., and Kurihara, S., *J. Appl. Polym. Sci.*, 1997, vol. 66, no. 8, pp. 1621−1630.

29. Feugang, J.M., Konarski, P., Zou, D., Stintzing, F.C., and Zou, C., *Front Biosci.*, 2006, vol. 11, no. 1, pp. 2574−2589.

30. Cantwell, M., Rodrìguez-Felix, A., and Robles-Contreras, F., *Scientia Horticulturae*, 1992, vol. 50, no. 1−2, pp. 1−9.

31. Nerd, A., Dumoutier, M., and Mizrahi, Y., *Postharvest Biology and Technology*, 1997, vol. 10, no. 2, pp. 135−143.

32. McGuire, G.R., *HortScience*, 1992, vol. 27, no. 12, pp. 1254−1255.

ENZYMATIC SYNTHESIS OF L-TRYPTOPHAN FROM D,L-2-AMINO-Δ2-THIAZOLINE-4-CARBOXYLIC ACID AND INDOLE BY *Pseudomonas* sp. TS1138 L-2-AMINO-Δ2-THIAZOLINE-4-CARBOXYLIC ACID HYDROLASE, *S*-CARBAMYL- L-CYSTEINE AMIDOHYDROLASE, AND *Escherichia coli* L-TRYPTOPHANASE

© 2012 J. Du*, J. J. Duan*, Q. Zhang*, J. Hou*, F. Bai*, N. Chen**, G. Bai*

* *College of Pharmacy and Tianjin Key Laboratory of Molecular Drug Research, Nankai University, 300071 Tianjin, China*
e-mail: qizhang@nankai.edu.cn
** *College of Bioengineering, Tianjin University of Science and Technology, Tianjin, 300457, China*
e-mail: ningch@tust.edu.cn
Received September 27, 2011

L-Tryptophan (L-Trp) is an essential amino acid. It is widely used in medical, health and food products, so a low-cost supply is needed. There are 4 methods for L-Trp production: chemical synthesis, extraction, enzymatic synthesis, and fermentation. In this study, we produced a recombinant bacterial strain pET-tnaA of *Escherichia coli* which has the L-tryptophanase gene. Using the pET-tnaA *E. coli* and the strain TS1138 of *Pseudomonas* sp., a one-pot enzymatic synthesis of L-Trp was developed. *Pseudomonas* sp. TS1138 was added to a solution of D,L-2-amino-Δ2-thiazoline-4-carboxylic acid (DL-ATC) to convert it to L-cysteine (L-Cys). After concentration, *E. coli* BL21 (DE 3) cells including plasmid pET-tnaA, indole, and pyridoxal 5'-phosphate were added. At the optimum conditions, the conversion rates of DL-ATC and L-Cys were 95.4% and 92.1%, respectively. After purifying using macroporous resin S8 and NKA-II, 10.32 g of L-Trp of 98.3% purity was obtained. This study established methods for one-pot enzymatic synthesis and separation of L-Trp. This method of producing L-Trp is more environmentally sound than methods using chemical synthesis, and it lays the foundations for industrial production of L-Trp from DL-ATC and indole.

L-Tryptophan (L-Trp) is an essential amino acid and a low-cost supply is needed [1]. L-Trp is used in feed additives, therapeutic products, health foods, sleeping pills, etc. Furthermore, the possibility of using L-Trp to treat schizophrenia and alcoholism is being investigated [2].

There are 2 primary approaches for industrial production of L-Trp: chemical synthesis and microbial methods; the latter includes enzymatic synthesis and fermentation [2]. Chemical synthesis can produce only the mixture of D, L-forms of amino acids, and an additional optical resolution step is necessary to obtain the biologically active L-isomers. Because of the high production costs associated with this resolution step, only a few amino acids are manufactured by chemical synthesis [3]. Although recent progress in chemical synthesis has made it possible to use chiral catalysts to produce L-isomers directly from prochiral precursors [4], the technology for this asymmetric synthesis is not yet commercially viable [3]. The chiral reagents used in the resolution make chemical synthesis less environmentally friendly than microbial methods, and the costs are higher, too. The fermentation methods used are precursor-conversion fermentation and direct fermentation. These generally suffer from low productivity and feedback inhibition, and the strains used are not readily available. It is therefore important to obtain high-yielding strains by mutation [2]. For example, a regulatory mutant of *Corynebacterium glutamicum* has been reported to produce L-Trp directly from sugars. The productivity was 12.8 g/l [5]. Although the method has the advantage of using cheap starting materials, the productivity will still have to be improved. Application of biotechnology should improve fermentation methods, and greatly decrease the production costs of many amino acids [2]. Compared with precursor and fermentation methods, enzymatic methods use cheap, readily available starting materials, and relatively small amounts of by-products are formed [6]. Genetic engineering could be used to produce recombinant strains containing the appropriate enzymes, thereby increasing the amounts of products synthesized from the substrate. In the various methods proposed, a biocatalyst, in the form of an isolated enzyme or whole cells, has been used either in free or immobilized form. Deeley et al. [7] reported the nucleotide sequence of tryptophanase from *E. coli* K-12. Matsui et al. [8] constructed one Trp-producing recombinant strain of *Brevibacterium lactofermentum* using the engineered trp-operons, the yield was 7.5 g/l.
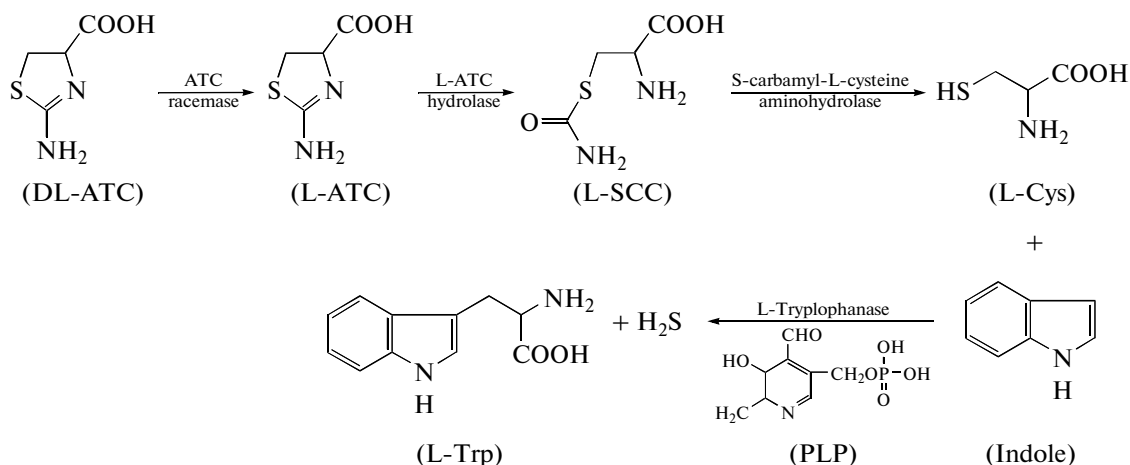
Fig. 1. The principle of enzymatic synthesis of L-Trp with DL-ATC and indole as substrates.

Tryptophanase (EC 4.1.99.1) is a bacterial pyridoxal-5'-phosphate (PLP)-dependent enzyme. It catalyzes α,β-elimination and β-substitution reactions of L-Trp and of some other natural and synthetic amino acids. It is of particular interest because of its possible use for the synthesis of L-Trp and physiologically active analogs of L-Trp [9]. It has been reported [10] that tryptophanase can be used to produce L-Trp with L-Ser, L-Cys and *S*-methyl-L-cysteine as substrates if indole is present in the catalytic system. Shimada et al. [11] reported that L-Trp can be produced from D-Ser, with tryptophanase as the substrate, in the presence of diammonium hydrogen phosphate.

It is known that bacteria convert D,L-2-amino-Δ2-thiazoline-4-carboxylic (DL-ATC) to L-Cys via 2 pathways: the *N*-carbamyl-L-cysteine pathway [12, 13], and the *S*-carbamyl-L-cysteine (L-SCC) pathway [14]. In our previous work, the L-SCC pathway was confirmed in *Pseudomonas* sp. TS1138 [15]. It was found that the *tsB* gene encoded an L-2-amino-Δ2-thiazoline-4-carboxylic hydrolase (L-ATC), which catalyzed the conversion of L-ATC to L-SCC, while the *tsC* gene encoded an L-SCC amidohydrolase, which made L-SCC converting to L-Cys catalytically [16].

In this study, we report the first one-pot enzymatic synthesis of L-Trp, using DL-ATC and indole as substrates (Fig. 1). The *Pseudomonas* sp. TS1138 strain, which produces ATC racemase, L-ATC hydrolase, and L-SCC amidohydrolase, was used to convert DL-ATC to L-Cys. The products of the three genes were involved in the conversion process. Then we constructed a high-level expression system for tryptophanase in *E. coli*, which could be applied to L-Trp synthesis from indole and L-Cys. The chemical substrates DL-ATC and indole were used instead of the L-Ser, L-Cys, or *S*-methyl-L-cysteine used in previously re-

ported studies. The L-Ser precursor was more expensive, and the L-Cys source was less environmentally friendly, which was usually obtained mainly by hydrolysis of hair. We developed a method of L-Trp production using D,L-ATC and indole as the substrates and an L-Trp separation method. This is an important green method of L-Trp production, and it lays the foundations for industrial production of L-Trp from D, L-ATC and indole.

MATERIALS AND METHODS

Materials. *Pseudomonas* sp. TS1138 was isolated from industrial wastewater and stored in our laboratory. *E. coli* JM109 (*recA*1 *supE*44 *endA*1 *hsdR*17 *gyrA*96 *relA*1 *thiA*(*lac-proAB*) F' [*traD*36 *proAB*⁺ *lacIq lacZ*Δ*M*15]) and BL21(D3) were purchased from Stratagene (La Jolla, USA) and stored in our laboratory. pET-21a (+) vector was purchased from Novagen (Madison, WI, USA). DL-ATC was obtained from the Tianjin Chemical Reagent Co. (Tianjin, China). The polymerase chain reaction (PCR) fragment recovery kit, pMD 18-T vector, restriction endonucleases, and T4 DNA ligase were purchased from TaKaRa (Dalian, China). Pyridoxal 5'-phosphate, L-Cys, and L-Trp were purchased from Sangon Biotech Co., Ltd. (Shanghai, China). Other chemicals used in this study were of analytical grade and commercially available.

Detection and analysis of samples. DL-ATC, L-Cys, L-Trp, and products were identified using a precolumn derivatization method. 100 µl of 10 mM Na₂CO₃ solution (pH 9.0) or 25 mM amino acid, or product sample was placed in separate 2 ml plastic tube. 200 µl of a 1% acetone solution of 18 mM 1-fluoro-2,4-dinitrophenyl-5-L-alanine amide (FDAA) was added to each tube. The molar ratio of FDAA to amino acid was

1.4 : 1. The solutions were mixed and heated on a hot plate at 40°C for 1 h with frequent mixing. After cooling to room temperature, 20 μl of 2 N HCl was added to the reaction mixture. After mixing, 20 μl samples were removed and injected for HPLC. The chromatographic conditions were: a C18 column (Phenomenex Luna 5μ, 100A, 250 × 4.6 mm; Phenomenex Inc., Torrance, CA, USA), with A-phase water containing 0.1% trifluoroacetic acid (TFA), and B-phase acetonitrile (containing 0.1% TFA) as the mobile phase; gradient elution: 0.0 min, 55% A-phase. The process performed for 11.0 min to 47% A-phase at room temperature, detection wavelength 340 nm and flow rate 1 ml/min.

Because of the presence of an indole ring, L-Trp had a maximum absorption at 225 nm, and could be analyzed by HPLC with a UV detector. The chromatographic conditions were: C18 column (Phenomenex Luna 5μ, 100A, 250 × 4.6 mm; Phenomenex Inc., Torrance, CA, USA); mobile phase: methanol/1 mM potassium dihydrogen phosphate (30 : 70); room temperature, detection wavelength 225 nm and flow rate 1 ml/min.

Cloning and expression of *E. coli* tryptophanase. The *E. coli* tryptophanase gene was amplified using a pair of primers: tnaA1 (5'-CCG GAA TTC ATG GAA AAC TTT AAA CAT CTC C-3') and tnaA2 (5'-CCC AAG CTT TTA AAC TTC TTT CAG TTT TGC GG-3'). Chromosomal DNA of *E. coli* JM109 was used as the template. The PCR conditions were as follows: 95°C, 5 min; 94°C, 1 min; 56°C, 1 min; 72°C, 1 min 20 s, 30 cycles; 72°C, 10 min. The amplified fragments were purified and cloned into the *Eco*R I and *Hin*d III sites of pET21a(+). The resulting plasmids were designated as pET-tnaA and transformed into *E. coli* BL21(DE3) cells, named pET-tnaA. The cells were grown at 37°C in Luria broth (LB) medium containing 100 mg/ml of ampicillin to an OD_{600} of 0.6, and then protein production was induced with 1 mM of isopropyl-β-D-thiogalactopyranoside (IPTG) at 30°C for 4 h. The BL21/pET-tnaA *E. coli* cells were collected by centrifugation at 5.000 *g* for 10 min at 4°C, and then washed twice with TE buffer (20 mM Tris-HCl, 1 mM EDTA, pH 8.0). The washed cells were resuspended in 2 ml of TE buffer containing 10% glucose and then lyzed by sonication on ice (400 W, 3 s with 3 s breaks for 5 min). The cell wall debris was removed by centrifugation at 12000 *g* for 10 min. The supernatants were used for the enzymatic activity analysis. Proteins in the supernatant were analyzed by SDS-PAGE, and the gel was stained with coomassie brilliant blue. Standard protein markers (TaKaRa, Dalian, China) were applied for molecular weight determination.

Enzyme assay. The assay of tryptophanase activity was carried out by the Ujimaru method [17] with little modification. An assay reaction mixture (0.3 ml) containing 20 μl 0.2 mg/ml pyridoxal 5'-phosphate, 10 μl 5 mM reduced glutathione, and 270 μl of tryptophanase solution was prepared, and then mixed with 1 ml of toluene. After incubation at 37°C for 5 min, 100 μl of L-Trp (5.0 mg/ml) were added; the mixture was then incubated for 10 min at 37°C. The reaction was stopped by addition of 3 ml of 0.1 M *p*-dimethylaminobenzaldehyde solution (*p*-dimethylaminobenzaldehyde was dissolved in the mixture solution of ethanol–sulfuric acid 948 : 52). After 30 min, the OD_{570} was measured using a BIO-RAD680 Microplat Reader (Bio-Rad, USA). One unit of tryptophanase activity was defined as that amount which formed 1 pmol of indole per min under the assay conditions.

Preparation of zymogen cells. *Pseudomonas* sp. TS1138 was cultured at 30°C in ATC medium (%): DL-ATC − 0.2, glucose − 2.0, yeast extract − 0.5, NaCl − 0.15, K_2HPO_4 − 0.3, $(NH_2)_2CO_3$ − 0.2, $MgSO_4 \cdot 7H_2O - 0.05$, $FeSO_4 \cdot 7H_2O - 0.001$, pH 7.4) for 14 h, and then washed twice with PBS buffer (20 mM NaH_2PO_4/Na_2HPO_4, 150 mM NaCl, pH 7.4) to obtain zymogen cells, which contained ATC hydrolase and *S*-carbamyl-L-cysteine amidohydrolase. *E. coli* BL21/pET-tnaA was grown at 37°C in an LB medium; 100 μg/ml of ampicillin were used as the selection marker. After being induced as described above, the cells were collected and washed twice with PBS. The zymogen cells contained tryptophanase.

Conversion conditions and analysis of DL-ATC. The optimal conditions for conversion of DL-ATC to L-Cys were determined, namely: temperature, pH, reaction time and concentration of cells, substrate and hydroxylamine. The DL-ATC and L-Cys were detected by the precolumn derivatization/HPLC method described above.

Optimization of L-Trp production. The concentration of BL21/pET-tnaA *E. coli* cells was optimized from 1.0 to 50 g/l and 20 g/l of *E.coli* was chosen for the L-Trp production experiments. On that basis, the conditions for conversion of L-Cys to L-Trp were determined, namely: temperature, pH, reaction time, concentration of PLP and substrate. The L-Cys and L-Trp were detected by the precolumn derivatization/HPLC method described above.

One-pot preparation. L-Trp was produced by a one-pot method, using the optimized conditions. 2.1 l of reaction solution were prepared, and DL-ATC was converted to L-Cys using the *Pseudomonas* sp. TS1138 enzyme system. The reaction solution was then concentrated to 1.0 l using membrane filtration system (LNG-AF-101, Shanghai, China). The *Pseudomonas* sp. TS1138 cells were removed, and the recombinant pET-tanA strain of *E.coli* was added to catalyze the conversion of L-Cys to L-Trp.
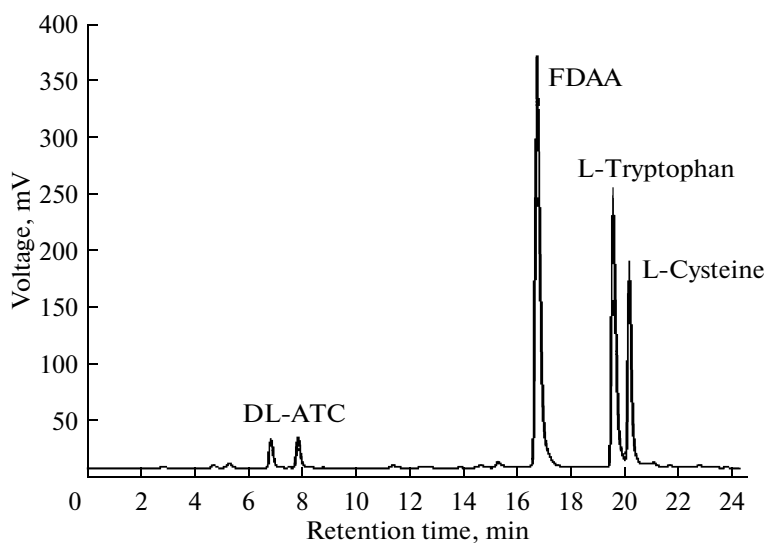
Fig. 2. Test HPLC analysis of the amino acids studied.

Separation of L-Trp. After the conversion, 9 types of macroporous resin, namely AB-8, ADS-17, ADS-21, ADS-F8, D3520, NKA-II, NKA-9, S8, and X-5, were screened for use in purifying L-Trp. The adsorption rates of DL-ATC, L-Cys, indole, and L-Trp were measured. S8 was chosen for removal of indole, and NKA-II was chosen for isolation of L-Trp. The pH of 500 ml of the conversion solution was adjusted to 5.0 using HCl. Then it was added to the column (60 cm × 5 cm) containing macroporous S8 resin, the outflow liquid was collected and added to the column (60 cm × 5 cm) of macroporous NKA-II resin. After careful washing, 50% ethanol was used to elute the

Fig. 3. SDS-PAGE analysis of the expression level of tryptophanase of *E.coli*.

1 − protein standards; *2* − crude cell extracts of *E. coli* BL21 (DE3) harboring pET-21a (+); *3* − crude cell extracts of *E. coli* BL21 (DE3) harboring pET-tnaA.

column and the fractions were detected using an HPLC/UV detector. The products were collected, concentrated, identified, and quantified using the precolumn derivatization/HPLC method described above.

RESULTS AND DISSUSSION

HPLC analysis of amino acids. Amino acids and DL-ATC contain amino groups, therefore an FDAA precolumn derivatization method can be used for analysis of amino acids and DL-ATC. The test results are shown in Fig. 2. It was possible to detect and separate FDAA, DL-ATC, L-Trp, and L-Cys under the same conditions; the results show that this was a suitable method. To purify and directly detect L-Trp, a UV detector was used because L-Trp contains one indole ring, which could be detected at 225 nm. We have therefore also established a detection method for L-Trp. The precolumn derivatization/HPLC method was used to detect DL-ATC, L-Cys, and L-Trp. The UV/HPLC method was used to monitor L-Trp in the separation process and was found to be an effective method.

Tryptophanase cloning and expression. The PCR was used to clone an L-tryptophanase gene, *tnaA*; this gene had a high sequence homology (99.9%); it was the same size (1416 bp) and had the same protein sequence as the gene from *E. coli* K12. After expression, the lysate of *E. coli* was analyzed by SDS-PAGE. The *E. coli* strain with pET-21a (+) was used as negative controls. The recombinant plasmids, pET-tnaA, were expressed in *E. coli* BL21 (DE3). As shown in Fig. 3, compared with *E. coli* BL21 (DE3) with pET-21a (+) (lane2), the lysate of *E. coli* harboring pET-tnaA (lane3) showed one additional protein band with a
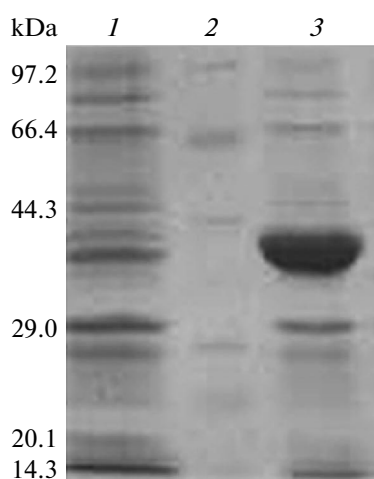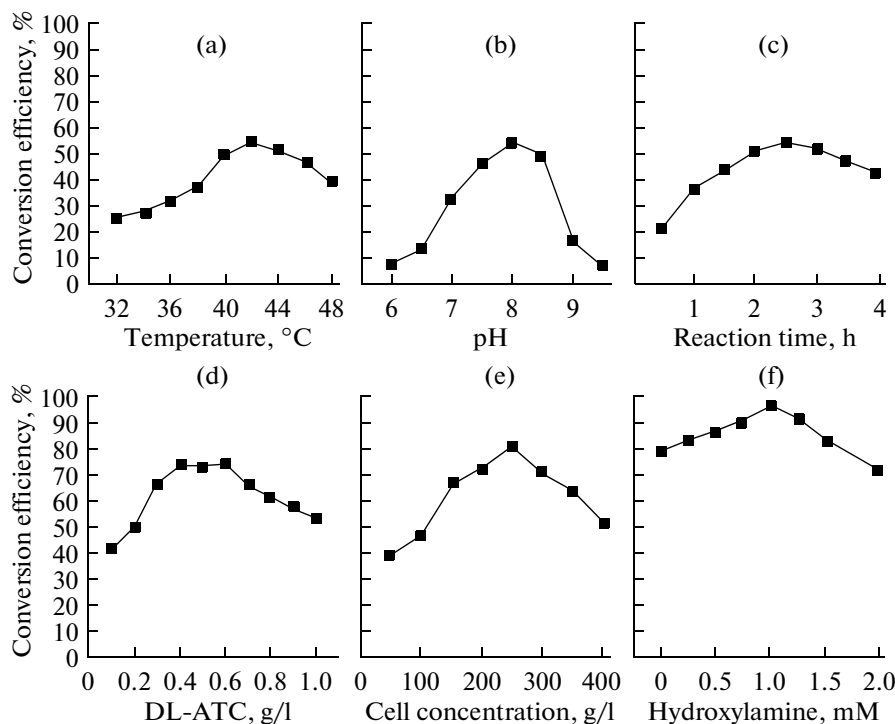
Fig. 4. Optimization of conversion conditions from ATC to L-Cys.
a − conversion temperature; b − conversion pH; c − reaction time; d − concentration of DL-ATC; e − zymogens cell concentration; f − concentration of hydroxylamine inhibitor.

molecular weight of about 39 kDa, which coincided with the expected molecular weight of the gene product of *tnaA*. This observation suggested that *tnaA* might encode the functional protein. After enzyme assay, and the tryptophanase activity from recombinant *E. coli* strain was 3912.6 U/g.

Optimization of conversion of ATC to L-Cys. To improve the ATC conversion rate, temperature, pH, reaction time, concentration of substrate, cells and hydroxylamine were investigated. As Fig. 4 shows, the optimum conditions were 45°C, pH 8.0, 2.5 h, 6 g/l DL-ATC, 20 g/l of bacterial wet weight, and 1 mM hydroxylamine. At the optimum conditions, the conversion rate of ATC was 95.6%. ATC racemase was an important enzyme in this process, and it could effectively improve the conversion rate by transforming D-ATC

to L-ATC. *Pseudomonas* sp. TS1138 contained this enzyme and could meet the allosteric requirements of DL-ATC. Because L-cysteine desulfhydryl enzyme could hydrolyze and reduce L-Cys, it was very important to inhibit this enzyme activity. Hydroxylamine was used as inhibitor for that. However, because this compound could partially inhibit the activity of enzymes in the reaction system involved in L-Cys synthesis, it was important to determine the optimum hydroxylamine concentration; the best concentration was found to be 1 mM.

Optimization of conversion of L-Cys to L-Trp. To improve the conversion rate of ATC, the temperature, pH, reaction time, concentration of coenzyme and substrates were investigated. As Fig. 5 shows, the corresponding optimum conditions were 45°C, pH 8.0,

Conversion rate analysis of DL-ATC and L-Cys

No.	Conversion rate of DL-ATC, %	Conversion rate of L-Cys, %	Production of L-Trp, g	Production of purified L-Trp, g	Yield of L-Trp, %
1	94.3	90.1	14.96	10.31	68.9
2	96.7	92.9	15.82	10.09	63.8
3	95.2	93.3	15.64	10.54	67.4
Mean	95.4 ± 1.21	92.1 ± 1.74	15.47 ± 0.45	10.32 ± 0.23	66.7 ± 0.03
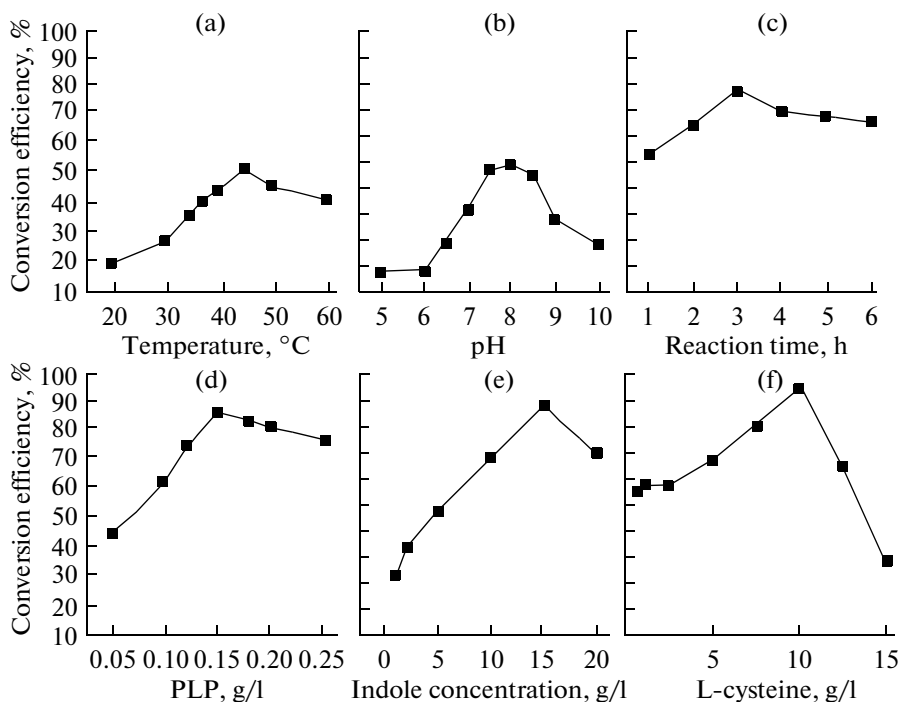
Fig. 5. Optimization of conversion conditions from L-Cys to L-Trp.
a − conversion temperature; b − conversion pH; c − reaction time; d − concentration of PLP coenzyme; e − concentration of indole; f − concentration of L-Cys.
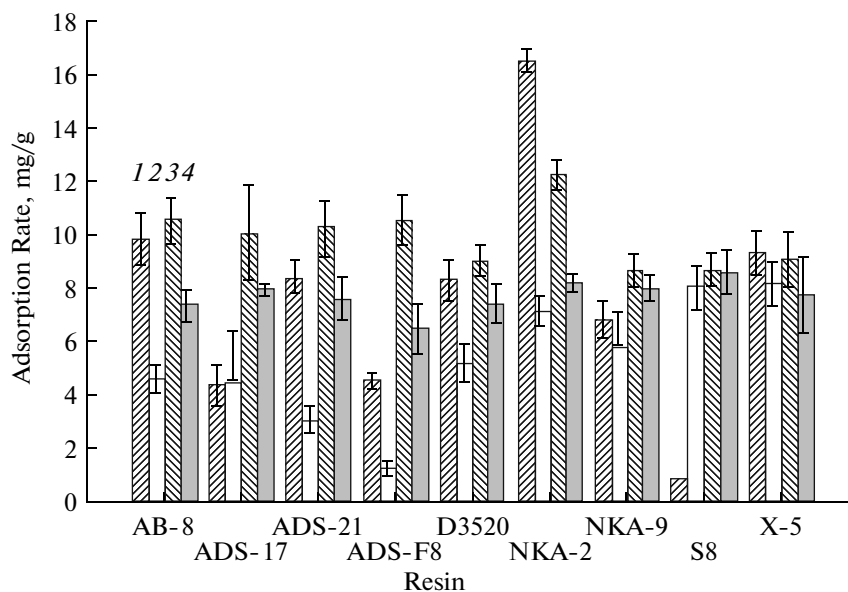
Fig. 6. Adsorption capacity of macroporous resins for L-Trp (*1*), DL-ATC (*2*), L-Cys (*3*) and indole (*4*).

2.5 h, 0.15 g/l of PLP, 15 g/l of indole, and 10 g/l of L-Cys. At the optimum conditions, the L-Cys conversion rate was 92.7%. L-Trp could be effectively produced from indole and L-Ser or L-Cys using L-tryptophanase. The coenzyme PLP was essential in this process, and sufficient coenzyme was needed to improve the combined PLP/L-tryptophanase activity.

L-Trp production and separation. Enzymatic synthesis of L-Trp, using DL-ATC and indole as substrates, was performed using the *E. coli* with a high L-tryptophanase expression level and the *Pseudomonas* sp. TS1138 cells. After catalytic conversion of DL-ATC to L-Cys by *Pseudomonas* sp TS1138 and concentration of the reaction solution, *E. coli* pET-

Fig. 7. Purification and identification of L-Trp. a − L-Trp eluting curve from NKA-II resin column; b − HPLC identification of L-Trp.

tnaA was used to convert L-Cys to L-Trp. Under the optimum conditions described above, the conversion reaction was performed 3 times in one pot. The results are shown in Table; the mean conversion rates of DL-ATC and L-Cys were 95.4% and 92.1%, respectively. Quantitative analysis by HPLC, showed that the mean production of L-Cys and L-Trp produced was 9.96 g and 15.47 g, respectively. The results were almost identical with the optimization results.

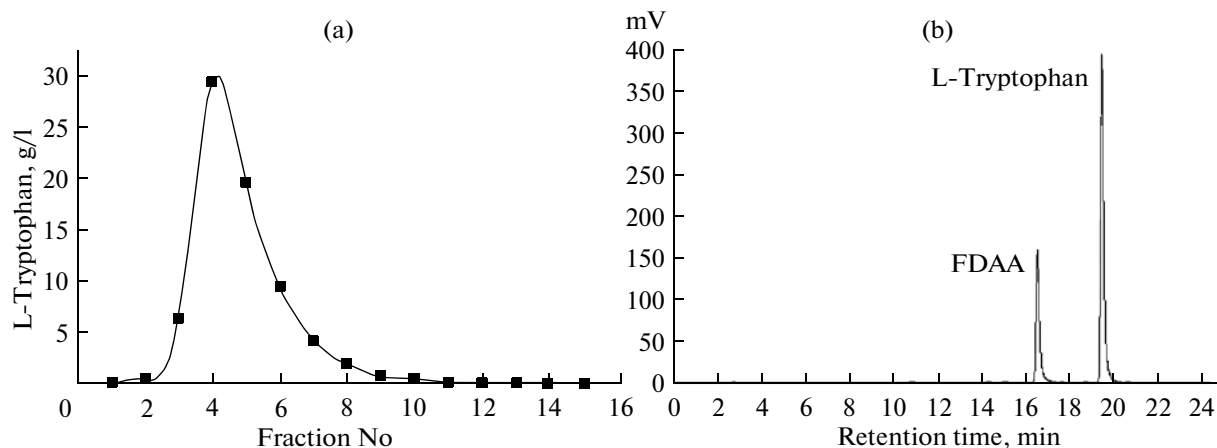To remove residual DL-ATC, L-Cys, and indole from the reaction solution, 9 types of macroporous resins, namely AB-8, ADS-17, ADS-21, ADS-F8, D3520, NKA-II, NKA-9, S8, and X-5, were analyzed. The S8 resin could effectively adsorb indole, DL-ATC and L-Cys, and it was used to remove them. NKA-II resin at pH 5 was used to adsorb L-Trp (Fig. 6). After eluting with 50% ethanol and vacuum concentration drying, 10.32 g of L-Trp were obtained; the yield was 66.7% (Table). Every fraction was detected by HPLC/UV detector and converted to concentration of L-Trp. Then the eluting curve was drafted and shown as Fig. 7a. HPLC analysis using L-Trp as the standard (purity: ~ 100%) was performed. In L-Trp production experiments the ratio of area under the peak was defined as the degree of purification. The result revealed that the purity of product was 98.3% (Fig. 7b).

In this study, we established a process for producing L-Trp from DL-ATC via 2 steps involving different enzymatic reactions. First, the enzymatic synthesis of L-Cys from DL-ATC was achieved using the *Pseudomonas* sp. TS1138 strain. The product solution was mixed with indole and used as the substrate for the synthesis of L-Trp using the *E. coli* pET-tnaA cells. The procedure was a one-pot method. DL-ATC is a relatively cheap compound, so if this method could be successfully applied to industrial production, the enzymatic route for synthesis of L-Trp would have more commercial value, and would result in significant economic benefits.

In the enzymatic synthesis of L-Trp, its separation and purification are the main difficulties. In this study, to overcome them, 9 types of resin were investigated. The results showed that indole, DL-ATC and L-Cys could be strongly adsorbed by most of the resins, and that S8 did not absorb L-Trp. However, we found that NKA-II macroporous resin had different adsorption capacities for them at pH 5.0, and it could be used in the separation of L-Trp. L-Trp was isolated by screening with S8 and NKA-II macroporous resins. The product purity was 98.3%, which verified the feasibility of the separation, and showed that it provided a good basis for enzymatic production of L-Trp.

ACKNOWLEDGMENTS

REFERENCES

1. Kawasaki, K., Yokota, A., and Tomita, F., *Biosci. Biotechnol. Biochem.*, 1995, vol. 59, no. 10, pp. 1938−1943.
2. Maiti, T.K. and Chatterjee, S.P., *Hindustan Antibiot. Bull.*, 1991, vol. 33, no. 1−4, pp. 26−61.
3. Ikeda, M., *Adv. Biochem. Eng. Biotechnol.*, 2003, vol. 79, pp. 1−35.
4. Calmes, M. and Daunis, J. *Amino Acids*, 1999, vol. 16, no. 3−4, 215−250.
5. Hagino, H. and Nakayama, K., *Agric. Biol. Chem.*, 1975, vol. 39, no. 2, pp. 343−349.

6. Zeman, R., Plachý, J., Bulantová, H., Sikyta, B., Pavlasová, E., and Stejskalová, E., *Folia Microbiol (Praha)*, 1990, vol. 35, no. 3, pp. 200−204.

7. Deeley, M.C. and Yanofsky, C.J., *Bacteriol.*, 1981, vol. 147, no. 3, pp. 787−796.

8. Matsui, K., Ishida, M., Tsuchiya, M., and Sano, K., *Agric. Biol. Chem.*, 1988, vol. 52, no. 7, pp. 1863−1865.

9. Zakomirdina, L.N., Kulikova, V.V., Gogoleva, O.I., Dementieva, I.S., Faleev, N.G., and Demidkina, T.V., *Biochemistry (Moscow)*, 2002, vol. 67, no. 10, pp. 1189−1196.

10. Mateus, D.M.R., Alves, S.S., and Fonseca M.M.R.D., *J. Biosci. Bioeng.*, 2004, vol. 97, no. 5, pp. 289−293.

11. Shimada, A., Ozaki, H., Saito, T., and Noriko, F., *Int. J. Mol. Sci.*, 2009, vol. 10, no. 6, pp. 2578−2590.

12. Tamura, Y., Nishino, M., Ohmachi, T., and Asada, Y., *Biosci. Biotechnol. Biochem.*, 1998, vol. 62, no. 11, pp. 2226−2229.

13. Tamura, Y., Ohmachi, T., and Asada, Y., *J. Gen. Appl. Microbiol.*, 2001, vol. 47, no. 4, pp. 193−200.

14. Ryu, O.H. and Shin, C.S., *J. Microbiol. Biotechnol.*, 1991, vol. 1, no. 1, pp. 50−53.

15. Jin, Y.J., Yang, W.B., Liu, Z., Bai, G., and Yu, Y.S., *Wei Sheng Wu Xue Tong Bao (China),* 2004, vol. 31, no. 6, pp. 68−72.

16. Yu, Y.S, Liu, Z., Liu, C.Q., Li, Y., Jin, Y.J, Yang, W.B., and Bai, G., *Biosci. Biotechnol. Biochem.*, 2006, vol. 70, no. 9, pp. 2262−2267.

17. Ujimaru, T., Kakimoto, T., and Chibata, I., *Appl. Environ. Microbiol.*, 1983, vol. 46, no. 1, pp. 1−5.

PROLINE DEHYDROGENASE FROM *Pseudomonas fluorescence*: GENE CLONING, PURIFICATION, CHARACTERIZATION AND HOMOLOGY MODELING

© 2012   H. Shahbaz Mohammadi, E. Omidinia

Biochemistry Dept., Pasteur Institute of Iran, Tehran, Iran 13164
e-mail: skandar@pasteur.ac.ir
Received August 5, 2011

The gene encoding proline dehydrogenase (ProDH) from *Pseudomonas fluorescence* was isolated using PCR amplification and cloned into pET23a expression vector. The expression of the recombinant target enzyme was induced by addition of IPTG. The produced His-fusion enzyme was purified and its kinetic properties were studied. The 3D structure modeling was also performed to identify key amino acids involved in FAD-binding and catalysis. The PCR product contained a 1033 bp open reading frame encoding 345 amino acid residue polypeptide chain. SDS-PAGE analysis revealed a MW of 40 kDa, whereas the native enzyme exhibited a MW of 40 kDa suggesting a monomeric protein. The K_m and V_{max} values of the *P. fluorescence* ProDH were estimated to be 35 mM and 116 µmol/min, respectively. ProDH activity was stable at alkaline pH and the highest activity was observed at 30°C and pH 8.5. The modeling analysis of the three dimensional structure elucidated that Lys-173 and Asp-202, which were oriented near the hydroxyl group of the substrate, were essential residues for the ProDH activity. This study, to our knowledge, is the first data on the cloning and biochemical and structural properties of *P. fluorescence* ProDH.

The amino acid L-proline is metabolized to glutamic acid in a two-step oxidation reaction. In the most bacteria, both enzymatic steps for proline utilization are catalyzed by a multifunctional encoded by the *putA* gene [1]. Multifunctional proline utilizing A flavoprotein (PutA) contains proline dehydrogenase (ProDH; L-proline: FAD oxidoreductase; EC 1.5.99.8) and Δ^1-pyrroline-5-carboxylate dehydrogenase (P5CDH; P5C: NAD$^+$ oxidoreductase, EC 1.5.1.12) domains. ProDH is an important flavoenzyme in the first step of proline metabolism and catalyzes the conversion of proline to Δ^1-pyrroline-5-carboxylate (P5C) in the presence of FAD as a cofactor. In the second step of proline degradation, P5C is hydrolyzed to glutamate-γ-semialdehyde (GSA), which is then oxidized to glutamate by P5CDH in a reaction requiring NAD$^+$ cofactor (Fig. 1) [2]. In addition to this enzymatic role, PutA polypeptide has also DNA-binding activity and participates in the transcriptional control of *put* genes. In the absence of proline, PutA accumulates in the cytoplasm and represses transcription of the *put* regulon by binding to the control intergenic region between *putP* and *putA* genes. The *putP* gene encodes the PutP Na$^+$-proline transporter. In the absence of proline, PutA associates with the membrane and performs its enzymatic functions [3, 4]. The presence of PutA protein has been reported in different bacteria such as *Escherichia coli* [4], *Pseudomonas aeruginosa* [5], *P. putida* [6], *Salmonella typhimurium*

[7] and *Bradyhizobium japonicum* [8]. In the current paper, we report the gene cloning, and characterization of ProDH domain from *P. fluorescence*. To best of our knowledge, there has been no report on the ProDH from *P. fluorescence*. This enzyme is functionality similar to the human version, so its results can help us to gain more information about the structure and function of human enzyme. ProDH has recently received much attention in cancer researches because it plays a role in apoptosis by creating the superoxide [4]. According to these facts, studying the bacterial enzymes involved in proline metabolism could provide valuable information for understanding the human ProDH. Moreover, this enzyme exhibits a high potential for application in biosensors.

MATERIALS AND METHODS

Chemicals and enzymes. All chemicals and buffers were obtained from Sigma-Aldrich (St. Louis, USA) and Merck (Germany). Restriction endonucleases, DNA modifying enzymes and molecular mass markers for electrophoresis were purchased from Fermentas (Germany).

Bacterial strains and plasmids. The *Pseudomonas fluorescence* pf-5 wild-type strain (ATCC BAA-477) was used for this research. *E. coli* strains DH5α and BL-21 plysS (DE3) were kindly provided from the National Stratagene (LaJolla, CA, USA). The expression
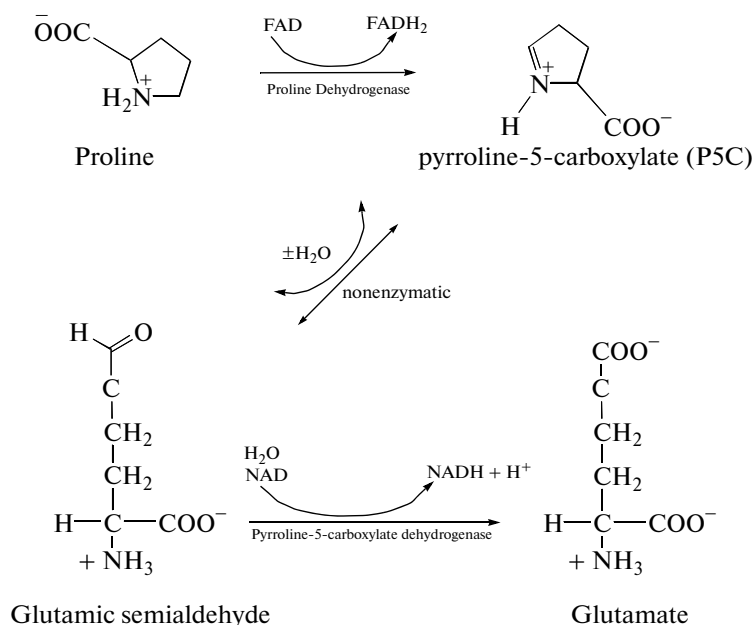
Fig. 1. Chemical reactions catalyzed by the bi-functional PutA flavoenzyme in metabolism of proline to glutamate.

vector of pET-23a was obtained from the National Recombinant Gene Bank of Pasteur Institute of Iran.

General molecular biology techniques. Isolation of genomic DNA and plasmid purification was performed as described by Sambrook and Russell [9]. DNA digestions with restriction enzymes, ligations, and transformations were performed by standard procedures [9]. Sequencing was performed by the commercial services of MacroGen Co. ltd. (Seoul, Korea) with the appropriate sequencing primers.

PCR amplification and construction of expression plasmid for ProDH domain gene. PCR primers were designed based on the available nucleotide sequence of PutA of the *P. fluorescence* genome using DNASIS MAX software (DNASIS version 2.9, Hitachi Software Engineering Co., Ltd., Japan). A 1035-kb DNA fragment containing the truncated ProDH domain was amplified by PCR from the genomic DNA of *P. fluorescence* with specific primers PDHPF5Fw (5'-TAT*CATATG*CTGACCTCCTCCCTG-3') and PDHPF5Rev (5'-AGGATCCATGTCGGCGATACG-3'), which contained the restriction sites for *Nde*I and *Bam*HI, respectively. PCR amplification was performed in a 50 µl reaction mixture containing 20 pmol of each primer, 1x PCR buffer, 0.2 mM of each dNTP, 1.5 mM MgCl$_2$, 0.3 mg template DNA and 2.5 units of *pfu* DNA polymerase under amplification condition: preincubation at 95°C for 1 min and then 30 cycles of 95°C for 1 min, 60°C for 1 min and 72°C for 2 min. The product of the PCR reaction was cut with *Nde*I and *Bam*HI, gel purified and then ligated into the pET23a (+) expression vector carrying a C-terminal

His$_6$-taq previously digested with the same restriction enzymes. The resulting construct bearing the ProDH gene was named pET23aPDHPF5 (Fig. 2) and transformed into the *E. coli* BL-21 (DE3) plysS. The correctness of the cloned gene was confirmed by nucleotide sequencing and no mutation was revealed [9].

Expression, solublization, refolding and reconstitution of recombinant enzyme. *E. coli* BL21 (DE3) plysS cells bearing pET23aPDHPF5 construct were cultivated overnight in Luria-Bertani (LB) medium containing 100 mg/ml of ampicillin at 37°C and 150 rpm. 100 ml preculture broth was transferred into 1 l of LB medium in culture flasks and incubated at the same conditions. When cell density reached an OD$_{600}$ of 0.6–0.8, ProDH enzyme was expressed by the addition of 0.5 mM of sterile isopropyl-β-D-thiogalactopyranoside (IPTG). After 6 h induction at 23°C, cells were harvested, washed twice with 0.9% NaCl solution and stored at −20°C for further uses. Bacterial pellet were suspended in the lysis buffer (50 mM Tris-HCl, 50 mM NaCl, 10 mM EDTA, pH 8.0), mechanically disrupted by sonication in pulse sequence of 15 s on and 10 s off and clarified by centrifugation at 5000 g for 1 h. The precipitate (inclusion bodies) containing recombinant ProDH enzyme was washed twice with the wash buffer (50 mM Tris-HCl, 50 mM NaCl, 10 mM EDTA, pH 8.0, 1% Triton X-100). The washed pellet was resuspended in 50 mM Tris-HCl (pH 8.0) contaning 100 mM NaCl, 10 mM EDTA, 10% glycerol and 0.1 mM DTT (buffer A) supplemented 8.0 M urea and incubated at 4°C with continuous stirring for 24 h to solubilize the inclusion bodies. Any insoluble material
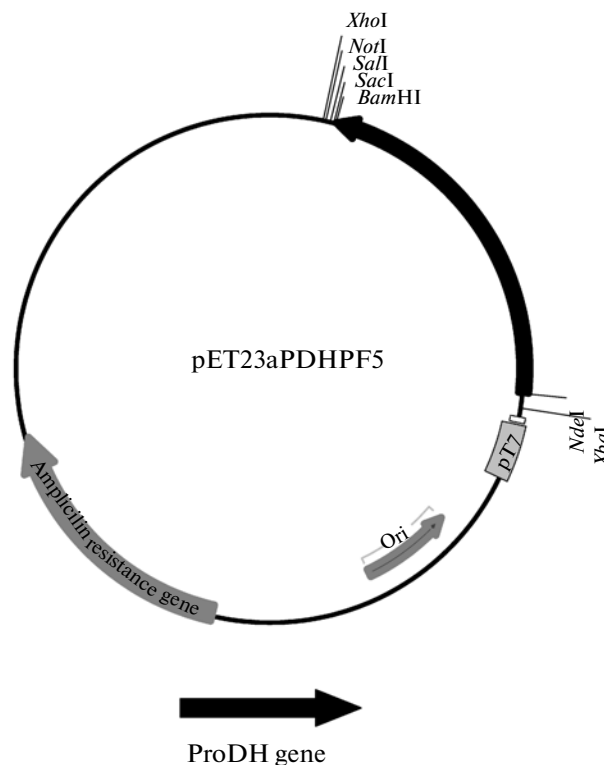
Fig. 2. Construction of PDHPF5 expression plasmid pET23aPDHPF5. The PCR fragment corresponding to *pdh* gene digested with *Nde*I nad *Bam*HI and ligated with the vector pET23a previously digested with *Nde*I and *Bam*HI.

was removed by centrifugation at 5000 g at 4°C for 1 h. Refolding was performed by stepwise dialysis against descending concentrations of urea. The unfolded recombinant ProDH was first dialyzed against buffer A supplemented with 4.0, 2 M and then without urea. The buffer was changed every 24 h. For reconstitution, the renatured enzyme was dialyzed overnight at 4°C in buffer A containing 0.15 mM FAD. The dialysate was centrifuged at 5000 g at 4°C for 1 h. The supernatant solution containing renatured proteins was used for further purification [9].

Enzyme activity assay. ProDH activity was measured using the proline: 2-(p-iodophenyl)-3-(p-nitrophenyl)-5-phenyltetrazolium chloride (INT) oxidoreductase assay which was performed by INT as a terminal electron acceptor and phenazine methosulfate (PMS) as a mediator electron carrier [10]. The standard reaction mixture was composed of 100 mM Tris-HCl (pH 8.5) containing 10 mM $MgCl_2$, 10% glycerol, 200 mM L-proline, 0.2 mM FAD, 0.45 mM INT, 0.08 mM PMS and the enzyme in a total volume of 1 ml. The increase in absorbance at 490 nm was estimated and corrected for blank values lacking proline. Also, all values were corrected for the low rate of enzyme-independent proline oxidation observed in assay mixtures containing all components except enzyme.

One unit (U) of ProDH activity was defined as the quantity of enzyme, which transfers electrons from 1 μmol of proline to INT per minute at 25°C [11]. All assay experiments were done in triplicate and the average results were used for data analysis.

Protein determination. Protein concentrations were measured by the method of Bradford using bovine serum albumin as a standard [12].

Purity analysis. The ProDH purification was analyzed by SDS-PAGE [9]. This procedure was performed using discontinuous gels (10 × 10 cm) with a 12% separating gel and a 6% stacking gel. The protein samples were boiled for 5 min in 10 mM Tris-HCl buffer (pH 7.0) containing 1% SDS, 80 mM 2-mercatoethonal and 15% glycerol. Electrophoresis was run at 30 V and 10 mA for 5 h. Protein bands were visualized by staining with 0.025 Coomassie brilliant blue R-250 in the mixture of 50% methanol and 10% acetate. Apoferritin (443 kDa), myosine (200 kDa), β-galactosidase (175 kDa), lactate dehydrogenase (142 kDa), fructose-6-phosphate (88 kDa), bovin serum albumin (66 kDa) and ovalalbumin (45 kDa) were used as molecular markers.

Kinetic analysis. Initial reaction rates of the ProDH were measured with various concentrations of proline. The Michalis-Menten parameter (K_m) was deter-
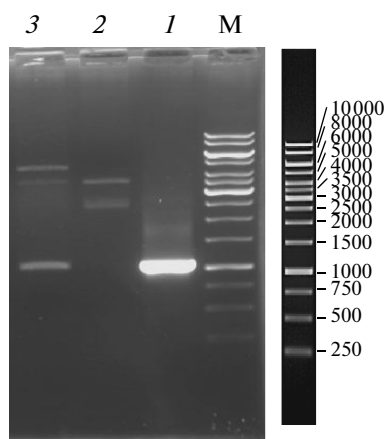
Fig. 3. Analysis of the PCR-amplified ORF of ProDH and confirmation of the cloning of the ProDH gene specific fragment (1035 bp) from *P. fluorescence* in the pET23a. M — 1-kb ladder; *1* — PCR-amplified sample; *2* — isolated plasmid; *3* — *Nde*I and *Bam*HI-digested clones (the presence of the 1035 bp fragment is present).

mined from Lineweaver-Burk plots of the data obtained form initial rates using UV probe software.

Sequence alignment and homology modeling. BLAST through NCBI was used to identify homologous structures of ProDH, with default settings against the database of protein sequences in the protein data bank (PDB). The crystal structure of PutA from *E. coli*

Substrate specificity for the ProDH reaction of *P. fluorescence*

Amino acid	Concentration, mM	Relative activity, % *
L-Proline	200	100
D-Proline	200	0
L-Hydroxyproline	200	100
L-Tryptophan	10	0
L-Arginine	10	62
L-Serine	10	55
L-Glutamate	10	0
L-Histidine	10	72
L-Threonine	10	66
L-Valine	10	33
L-Leucine	10	42
L-Alanine	10	48
Glycine	10	52
Aspartate	10	0

* Each value represents the average of three experiments.

K12 with bound FAD (PDB code: 1k87) was selected as a template for homology modeling. The quality of the 1k87 hit was indicated by a score of 82 bits, an E-value of 7e-14 and 88% identity. Multiple sequence alignment was performed with Clustal W program. Alignments were checked for deletions and insertions in structurally conserved regions and finally fine-tuned manually modified before 3D modeling. The three-dimensional model of ProDH protein was constructed using the homology modeling program Modeler version 9v4 (default parameters), based upon the crystal structure of *E. coli* K12 ProDH. Furthermore, FAD was docked into the protein model. The geometry of loop regions was corrected using MODELER/ Refine Loop command. The minimized model was then analyzed further and validated using Ramachandran plots obtained from the PROCHECK server [13]. Visual analysis and manipulation of the model were done with PyMOL program, which was also used for illustrations.

RESULTS AND DISCUSSION

Cloning and sequencing of ProDH gene from *P. fluorescence*. After PCR amplification, a 1035-bp DNA fragment containing ProDH gene domain was obtained (Fig. 3), which was gel purified and cloned into pET-23a in the frame with 6x-His tag. The corresponding plasmid was designated pET23PDHPF5, and transformed in the *E. coli* strain BL21 (DE3) pLysS. Among 40 transformants of *E. coli* strain, 20 colonies were selected for plasmid isolation. All the clones exhibited an insert of 1035-bp along with a 3666-bp vector band after digestion with *Nde*I and *Bam*HI (Fig. 3). The restriction pattern confirmed the cloning of ProDH gene (Fig. 2). The nucleotide sequence of the insert DNA of pET23PDHPF5 was determined by the dideoxynucleotide chain termination method [9] using M13 forward and M13 reverse primers. The 1107-bp open reading frame (ORF) of the ProDH gene had a coding capacity of 325 amino acids (Fig. 4). This suggested that the ProDH would be synthesized as 40 kDa enzyme.

Expression and purification of recombinant enzyme. ProDH was purified to homogeneity by affinity chromatography from the recombinant *E. coli* strain BL21 (DE3) pLysS carrying pET23PDHPF5 with an overall yield of 72% and a purification factor of 11. The purified enzyme gave a single band with a molecular mass of 40 kDa on SDS-PAGE (Fig. 5). The molecular mass of the isolated enzyme was found to be about 40 kDa by gel filtration. This result indicated that the target enzyme consists of one subunit. The observed band matched with the expected molecular weight for recombinant ProDH.

```
                                                                          60
  1 ATGCTGACCTCCTCCCTGAGCCGCATCATCGGCAAGAGCGGCGAGCCGATGATCCGCAAG    60
    M  L  T  S  S  L  S  R  I  I  G  K  S  G  E  P  M  I  R  K
                                                                         120
 61 GGCGTGGACATGGCCATGCGCTTGATGGGCGAACAGTTCGTCACCGGCGAAACCATCGCC   120
    G  V  D  M  A  M  R  L  M  G  E  Q  F  V  T  G  E  T  I  A
                                                                         180
121 GAAGCCCTGGCCAACGCCAGCAAGTTCGAAGCCAAGGGCTTCCGCTATTCCTACGACATG   180
    E  A  L  A  N  A  S  K  F  E  A  K  G  F  R  Y  S  Y  D  M
                                                                         240
181 CTCGGCGAAGCCGCACTGACCGAGCACGACGCACAGAAGTACCTCGCGTCCTACGAGCAG   240
    L  G  E  A  A  L  T  E  H  D  A  Q  K  Y  L  A  S  Y  E  Q
                                                                         300
241 GCCATCCACTCCATCGGCAAGGCCTCCCACGGTCGCGGCATCTATGAAGGCCCGGGCATC   300
    A  I  H  S  I  G  K  A  S  H  G  R  G  I  Y  E  G  P  G  I
                                                                         360
301 TCCATCAAGCTCTCGGCCCTGCACCCGCGCTACAGCCGCGCCCAGTACGAGCGCGTGATG   360
    S  I  K  L  S  A  L  H  P  R  Y  S  R  A  Q  Y  E  R  V  M
                                                                         420
361 GAAGAGCTGTACCCGCGCCTGCTGTCCCTTACCCTGCTGGCCAAGCAGTACGACATCGGC   420
    E  E  L  Y  P  R  L  L  S  L  T  L  L  A  K  Q  Y  D  I  G
                                                                         480
421 CTGAACATCGACGCCGAGGAAGCCGACCGCCTGGAGCTGTCCCTGGACCTGCTGGAGCGC   480
    L  N  I  D  A  E  E  A  D  R  L  E  L  S  L  D  L  L  E  R
                                                                         540
481 CTGTGCTTCGAGCCGCAACTGACCGGCTGGAACGGTATCGGCTTCGTGATCCAGGCCTAC   540
    L  C  F  E  P  Q  L  T  G  W  N  G  I  G  F  V  I  Q  A  Y
                                                                         600
541 CAGAAGCGCTGCCCGTACGTGATCGACTATGTCATCGATCTGGCCCGTCGCAGCCGTCAC   600
    Q  K  R  C  P  Y  V  I  D  Y  V  I  D  L  A  R  R  S  R  H
                                                                         660
601 CGCCTGATGATCCGCCTGGTGAAAGGCGCCTACTGGGACAGCGAGATCAAGCGCGCCCAG   660
    R  L  M  I  R  L  V  K  G  A  Y  W  D  S  E  I  K  R  A  Q
                                                                         720
661 GTCGAAGGCCTGGAAGGCTATCCGGTCTACACCCGCAAGGTGTACACCGACGTTTCCTAC   720
    V  E  G  L  E  G  Y  P  V  Y  T  R  K  V  Y  T  D  V  S  Y
                                                                         780
721 ATCGCCTGCGCACGCAAGCTGCTGTCGGTGCCGGAAGTCATCTACCCGCAGTTCGCCACC   780
    I  A  C  A  R  K  L  L  S  V  P  E  V  I  Y  P  Q  F  A  T
                                                                         840
781 CACAACGCCCACACTTTGTCGGCGATCTACCACATTGCCGGTCAGAACTATTACCCCGGC   840
    H  N  A  H  T  L  S  A  I  Y  H  I  A  G  Q  N  Y  Y  P  G
                                                                         900
841 CAGTACGAGTTCCAGTGCCTGCACGGCATGGGCGAACCGCTGTACGAGCAAGTGGTGGGC   900
    Q  Y  E  F  Q  C  L  H  G  M  G  E  P  L  Y  E  Q  V  V  G
                                                                         960
901 AAGGTTGCCGAGGGCAAGCTGAACCGTCCATGCCGCGTCTATGCACCGGTGGGCACCCAC   960
    K  V  A  E  G  K  L  N  R  P  C  R  V  Y  A  P  V  G  T  H
                                                                        1.020
961 GAAACCCTGCTGGCCTACCTGGTACGCCGGCTGCTGGAAAACGGCGCCAACACCTCGTTC 1.020
    E  T  L  L  A  Y  L  V  R  R  L  L  E  N  G  A  N  T  S  F
                                                                        1.080
1.021 GTCAACCGTATCGCCGACATGGATCCGAATTCGAGCTCCGTCGACAAGCTTGCGGCCGCA 1.080
      V  N  R  I  A  D  M  D  P  N  S  S  V  D  K  L  A  A  A
                                                                        1.140
1.081 CTCGAGCACCACCACCACCACCACTGA.................................. 1.107
      L  E  H  H  H  H  H  H   *
```

Fig. 4. Nucleotide sequence of the *Nde*I and *Bam*HI fragment subcloned from PDH in pET23a. The predicted amino acid sequence is in the single-letter code. The underline sequence represents the His-tag region. The numbers on the left are nucleotide accounts.

Kinetic parameters, substrate specificity and effect of temperature and pH. Initial velocity experiments were done by varying the concentration of L-Pro. The K_m and V_{max} values of *P. fluorescence* ProDH were calculated to be 35 mM and 116 µmol/min, respectively. The K_m value is lower than that reported for other bacterial ProDH enzymes. For example, K_m value of pro-

line for the PutA enzymes in *P. aeruginosa* [5] and *S. typhimurium* [7] has been reported 45 mM and 43 mM, respectively. As it has been noted in the literature, high K_m value of ProDHs for proline is one of the common features of proline metabolizing enzymes in bacteria [11, 14]. Therefore, the higher affinity of *P. fluorescence* ProDH toward proline made this en-
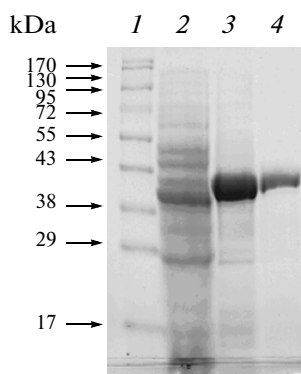
Fig. 5. SDS-PAGE of the purified ProDH. Protein samples of various stages of the purification process. *1* — molecular weight markers; *2* — supernatant of the cell lysate; *3* — pellet of the cell lysate; *4* — purified enzyme.

Fig. 6. Influence of temperature (a) and pH (b) on the activity of ProDH from *P. fluorescence*.

zyme very attractive for use in biosensors and protein engineering studies. The ability of ProDH to catalyze the dehydrogenation of various amino acids was examined. L-Pro (100%) was the most preferred substrate for the ProDH reaction (Table). The enzyme also showed weak activities towards L-Val, L-Leu and L-Ala. The following amino acids were inert for the ProDH reaction: D-Pro, Asp, L-Glu, and L-Trp. Moreover, chelating agents such as EDTA did not inhibit the enzyme. Similar results have been observed for the *P. aeruginosa* [5] and *S. typhimurium* [7] ProDHs. The ProDH reaction exhibited its maximal activity at temperature range of 25 to 30°C, and its highest activity was achieved at 30°C (Fig. 6a). As can be seen (Fig. 6a), a sharp decrease was observed above 30°C and enzyme activity was completely inactivated at 70°C. From this feature, it was concluded that like many other ProDHs [5, 7], the *P. fluorescence* ProDH was a form of mesophilic enzymes. Similar results have been reported for ProDHs isolated from *P. aeruginosa* [5] and *P. putida* [6]. The effect of various pH values on the enzymatic reaction of ProDH were evaluated in the pH range from 3.0 to 12.0 at 30°C. ProDH had a good activity in the range of pH 7.0–9.0 with optimal pH at 8.5 (Fig. 6b). Similar results have been reported for other bacterial ProDHs [14].

Amino acid sequence alignment and homology modeling of 3D structure. The search for the closet paralog led to the structure of ProDH from *E. coli* K12. Based on this evidence, *E. coli* K12 ProDH was taken as a template for ProDH of *P. fluorescence* pf-5. The amino acid sequence of *E. coli* K12 ProDH displayed 88% identity when aligned with that of 3D structure (Fig. 7). We constructed the three dimensional structure of the *P. fluorescence* ProDH based on its similarity to the structure of the previously crystallized ProDH from *E. coli* K12. The 100 models were evaluated and the
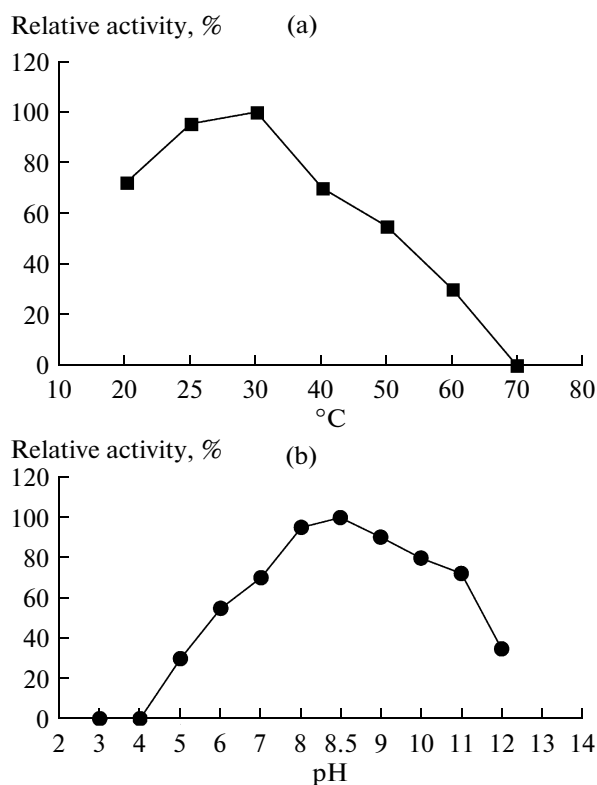
one with the lowest DOPE score was chosen for further analysis. The Ramachandran plot for local backbone conformation of each residue in the final model was produced by PROCHECK. In the *P. fluorescence* ProDH model, φ and Ψ dihedral angles of 100% of residues were located within the allowed regions (94.7% most favored). This result expressed the strong confidence in the homology model. Moreover, we used the three dimensional homology modeling to identify key amino acids involved in FAD-binding and catalysis. The 3D structure of ProDH from *P. fluorescence* is presented at Fig. 8. As seen in the 3D structure of ProDH of *P. fluorescence* presented in Fig. 8, Lys-173 and Asp-202, which were oriented near the hydroxyl group of the substrate in the model were essential for the ProDH activity. The model provided considerable information on substrate and FAD interactions with the active site of the *P. fluorescence* ProDH.

We isolated the gene encoding of the ProDH enzyme from *P. fluorescence*, expressed it in *E. coli* BL-21 (DE3) plysS with a C-terminal His-tag, and examined the biochemical characteristics of recombinant enzyme. The target enzyme is a good candidate for specific determination of proline amino acid in biosensors. Modeling studies also provided valuable information about the active site of the *P. fluorescence* ProDH.

	10	20	30	40	50	60
Pseudomonas fluorescens Pf-5	LTSSLSRIIG	KSGEPMIRKG	VDMAMRLMGE	QFVTGETIAE	ALANASKFEA	KGFRYSYDML
Escherichia coli K-12	LSRSLNRIIG	KSGEPLIRKG	VDMAMRLMGE	QFVTGETIAE	ALANARKLEE	KGFRYSYDML

	70	80	90	100	110	120
Pseudomonas fluorescens Pf-5	GEAALTEHDA	QKYLASYEQA	IHSIGKASHG	RGIYEGPGIS	IKLSALHPRY	SRAQYERVME
Escherichia coli K-12	GEAALTAADA	QAYMVSYQQA	IHAIGKASNG	RGIYEGPGIS	IKLSALHPRY	SRAQYDRVME

	130	140	150	160	170	180
Pseudomonas fluorescens Pf-5	ELYPRLLSLT	LLAKQYDIGL	NIDAEEADRL	ELSLDLLERL	CFEPQLTGWN	GIGFVIQAYQ
Escherichia coli K-12	ELYPRLKSLT	LLARQYDIGI	NIDAEESDRL	EISLDLLEKL	CFEPELAGWN	GIGFVIQAYQ

	190	200	210	220	230	240
Pseudomonas fluorescens Pf-5	KRCPYVIDYV	IDLARRSRHR	LMIRLVKGAY	WDSEIKRAQV	EGLEGYPVYT	RKVYTDVSYI
Escherichia coli K-12	KRCPLVIDYL	IDLATRSRRR	LMIRLVKGAY	WDSEIKRAQM	DGLEGYPVYT	RKVYTDVSYL

	250	260	270	280	290	300
Pseudomonas fluorescens Pf-5	ACARKLLSVP	EVIYPQFATH	NAHTLSAIYH	IAGQNYYPGQ	YEFQCLHGMG	EPLYEQVVGK
Escherichia coli K-12	ACAKKLLAVP	NLIYPQFATH	NAHTLAAIYQ	LAGQNYYPGQ	YEFQCLHGMG	EPLYEQVTGK

	310	320	330	340	350	360
Pseudomonas fluorescens Pf-5	VAEGKLNRPC	RVYAPVGTHE	TLLAYLVRRL	LENGANTSFV	NRIAD.....	....
Escherichia coli K-12	VADGKLNRPC	RIYAPVGTHE	TLLAYLVRRL	LENGANTSFV	NRIAD.....	....

Fig. 7. Sequence alignment of *P. fluorescence* ProDH sequence with *E. coli* using DNASIS MAX software. Identical residues are highlighted in grey.
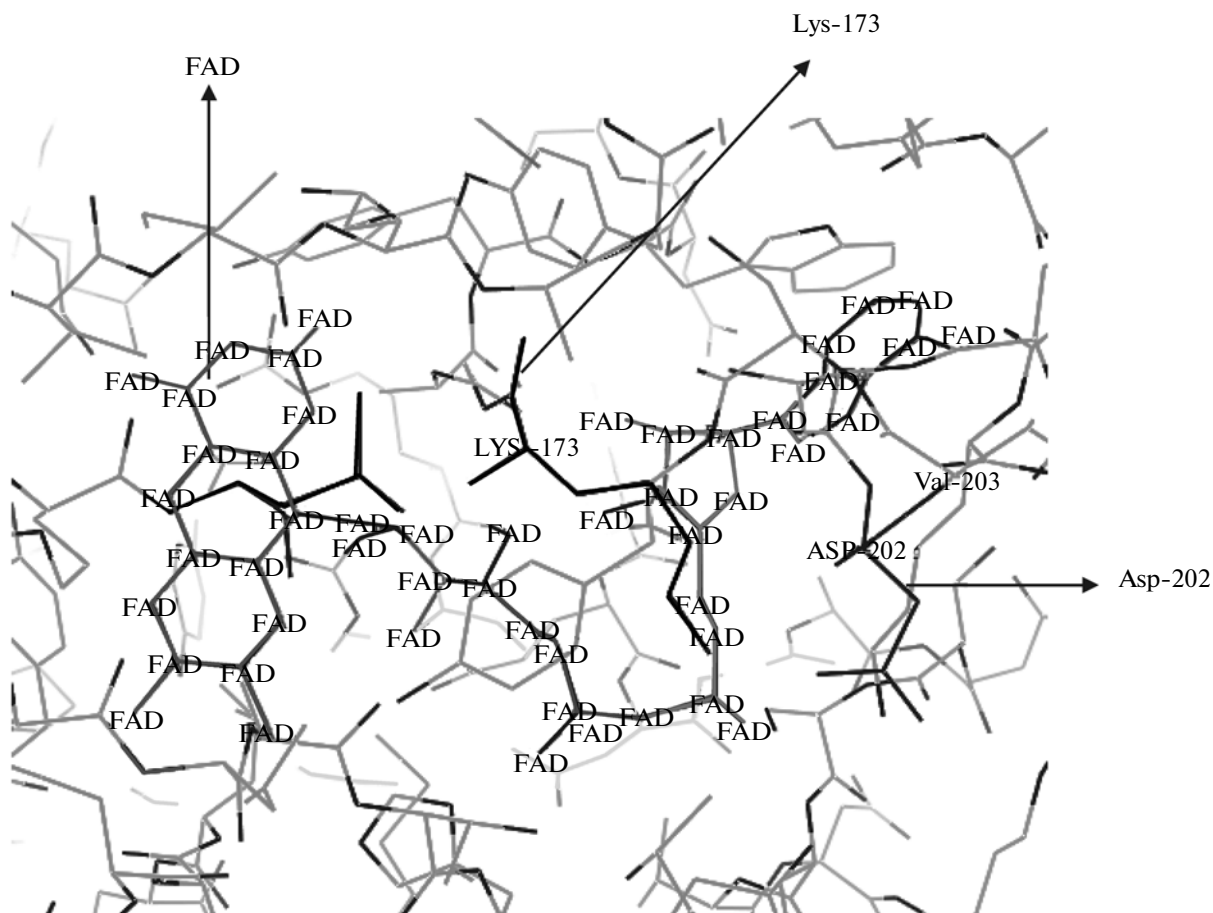

Fig. 8. Modeling of ProDH from *P. fluorescence* based on homology modeling. Stick model showing the conserved residues interacting with FAD. The figure was created with Pymol.

REFERENCES

1. Lee, Y.H., Nadaraia, S., Gu, D., Becker, D.F., and Tanner, J.J., *Nat. Struct. Biol.*, 2003, vol. 10, no. 2, pp. 109−114.

2. Muro-Pastor, A.M. and Maloy, S., *J. Biol. Chem.,* 1995, vol. 270, no. 17, pp. 9819−9827.

3. White, T.A., Krishnan, N., Becker, D.F., and Tanner, J.J. *J. Biol. Chem.,* 2007, vol. 282, no. 19, pp. 14316−14327.

4. Baban, B.A., Vinod, M.P., Tanner, J.J., and Becker, D.F., *Biochim. Biophys. Acta,* 2004, vol. 1701, no. 1−2, pp. 49−59.

5. Meile, L. and Leisinger, T., *Eur. J. Biochem.,* 1982, vol. 129, no. 1, pp. 67−75.

6. Vilchez, S., Molina, L., Ramos, C., and Ramos, J., *J. Bacteriol.,* 2000, vol. 182, no. 1, pp. 91−99.

7. *Menzel, R.* and Roth, J., *J. Biol. Chem.*, 1981, vol. 256, no. 18, pp. 9762−9766.

8. Straub, P.F., Reynolids, P.H.S., Althomsons, S., Mett, V., Zhu, Y., Shearer, G., and Kohl, D.H., *Appl. Environ. Microbiol.,* 1996, vol. 62, no. 1, pp. 221−229.

9. Sambrook, J., Fritsch, E.F., and Maniatis, T., Molecular Cloning: A laboratory manual. 2nd ed., Cold Spring Harbor, New York: Cold Spring Harbor Laboratory press, 1994, pp. 1847−1857.

10. Shahbaz Mohammadia, H., Omidinia, E., Sahebghadam Lotfi, A., and Saghiri, R., *Iranian Biomed. J.*, 2007, vol. 11, no. 2, pp. 131−135.

11. Becker, D.F. and Thomas, E.A., *Biochemistry*, vol. 40, no. 15, pp. 4714−4722.

12. Bradford, M.M., *Anal. Biochem.*, 1976, vol. 72, pp. 248−254.

13. Laskowski, R., Macarthur, M., Moss, D., and Thornton, J.G., *J. Appl. Crys.*, 1993, vol. 26, pp. 283−291.

14. Satomura T., Kawakami R., Sakuraba H., and Ohshima, T., *J. Biol. Chem.*, 2002, vol. 277, no. 15, pp. 12861−12867.

15. Lee, G.H., Park, N.Y., Lee, M.H., and Choi, S.H., *J. Bacteriol.*, 2003, vol. 185, no. 13, pp. 3842−3852.

ISOLATION AND CHARACTERIZATION OF FEATHER DEGRADING ENZYMES FROM *Bacillus megaterium* SN1 ISOLATED FROM GHAZIPUR POULTRY WASTE SITE

© 2012 S. Agrahari, N. Wadhwa

Department of Biotechnology, Jaypee Institute of Information Technology University, Uttar Pradesh, India
e-mail: neeraj.wadhwa@jiit.ac.in

The SN1 strain of *Bacillus megaterium*, isolated from soil of Ghazipur poultry waste site (India) produced extracellular caseinolytic and keratinolytic enzymes in basal media at 30°C, 160 rpm in the presence of 10% feather. Feathers were completely degraded after 72 h of incubation. The caesinolytic enzyme was separated from the basal media following ammonium sulphate precipitation and ion exchange chromatography. We report 29.3-fold purification of protease after Q Sepharose chromatography. The molecular weight of this enzyme was estimated to be 30 kDa as shown by SDS-PAGE and zymography studies. Protease activity increased by 2-fold in presence of 10 mM Mn^{2+} whereas Ba^{2+} and Hg^{2+} inhibited it. Ratio of milk clotting activity to caseinolytic was found to be 520.8 activity for the 30–60% ammonium sulphate fraction in presence of Mn^{2+} ion suggesting potential application in dairy industry. Keratinase was purified to 655.64 fold with specific activity of 544.7 U/mg protein and 12.4% recovery. We adopted the strategy of isolating the keratinolytic and caesinolytic producing microorganism by its selective growing in enriched media and found that feather protein can be metabolized for production of animal feed protein concentrates.

Milk-clotting enzymes, isolated from microbial sources *Endothia parasitica, Bacillus cereus*, *Mucor pusillus lindt* and *Mucor miehei* are used and reported in production of cheese, cottage cheese, sour cream and Emmentaler cheese. The major application of proteases in the dairy industry is in the manufacture of cheese. The milk-coagulating enzymes fall into three main categories, - animal rennets, microbial milk coagulants, and genetically engineered chymosin. In food industry, rennet prepared from the abomasum (fourth stomach from unweaned calves) is used in the production of cheese. Its supply has become less available and expensive. The shortage of calf's rennet has also highly increased due to religious restriction and ethnic regulations against the use of animal secretion in food.

Most commercial proteases (mainly neutral and alkaline) are produced by organisms belonging to the genus *Bacillus*. Bacterial neutral proteases are active in a narrow pH range (pH 5.0 to 8.0) and have relatively low thermotolerance. Due to their intermediate rate of reaction, neutral proteases generate less bitterness in hydrolyzed food proteins than the animal proteinases and hence they are valuable for use in the food industry. A world shortage of calf rennet due to the increased demand for cheese production has intensified the search for alternative microbial milk coagulants too. The keratinases (EC 3.4.99.11) belong to the group of hydrolases that are important for hydrolyzing feather, hair, wool, collagen and casein. They are large serine or metalloproteases capable of degrading the structure forming keratinous proteins. Keratin chain is very tightly packed in the α-helix (α-Keratin) and β-sheets (β-keratin) into super-coiled polypeptide chain [1] and produces mechanical stability resistant to common proteolytic enzymes such as pepsin, trypsin and papain. Keratinolytic enzymes are known to have important use in biotechnological processes involving keratin-containing waste from poultry and leather industries, through the development of non-polluting processes [2, 3]. After hydrolysis, the feather can be converted to feed stuffs, fertilizers, glues and films [4].

The aim of the study is to isolate and to characterize extracellular proteases and keratinases by *Bacillus megaterium* SN1 that can degrade the poultry waste feather and clot milk thus having potential application in bioremediation of feather waste and dairy industry.

MATERIALS AND METHODS

Selection of protease-producing strains on the skim milk agar. Soil isolates showing maximum protease activity were plated on the skim milk agar (10% skim milk powder, 0.1% peptone, 0.5% NaCl and 2% agar). Plates were incubated at 37°C for 24 h and the colonies that showed clear zone were selected and subcultured in the LB broth. The bacterial isolate was further incubated in cultivation media checked for protease activity.

Morphological studies of isolated bacterial strains. Bacterial strain of *Bacillus megaterium* was identified, maintained and kept as glycerol stock. Bacterial iden-

tification was conducted by morphological, cultural and biochemical tests. Results were compared with Bergey's Manual [5] and Genus Bacillus: Agriculture Handbook [6]. The strain was also identified by chromogenic method on the bacillus differential agar M1651 from Himedia (India), recommended for rapid identification of *Bacillus* species from a mixed culture [7].

Production of enzyme in cultivation media. Seed culture of *B. megaterium* were prepared in 500 ml Erlenmeyer conical flask containing 100 ml of feather meal medium that composed of (g/l): $NH_4Cl - 0.5$; $NaCl - 0.5$; $K_2HPO_4 - 0.3$; $KH_2PO_4 - 0.4$; $MgCl_2 \cdot 6H_2O - 0.1$; yeast extract $- 0.1$ and 10% washed feather, pH 7.5. Cultivation was performed at 30°C at 160 rpm for 72 h and the fresh overnight culture was inoculated in cultivation media. Pigeon feathers (10%), hair (10%) or nail (10%) were also used instead of chicken feathers (10%) to compare the growth of *B. megaterium* as well as enzyme production after 7 days. Biomass of bacteria was monitored by taking absorbance at 600 nm on spectrophotometer.

Purification of enzyme. Feather meal media with pigeon feather as substrate was selected for keratinase and protease production, the broth was harvested in 72 h of the growth for the enzyme assay. Isolated *B. megaterium* SN1 was allowed to grow in 500 ml conical flask containing 100 ml of the culture medium at 30°C at 160 rpm for 72 h and fresh culture was inoculated in cultivation media. Cells were harvested by centrifugation (10.000 g, 4°C, 10 min). The 30−60% ammonium sulfate precipitate was obtained from the cell free crude culture broth. The resulting precipitate was collected by centrifugation (10.000 g, 4°C, 30 min) and dissolved in a minimal volume of 10 mM Tris−HCl buffer (pH 8.0) and dialyzed against the same buffer overnight. Then dialysate was loaded on 10 ml Q Sepharose. The 2−4 mM NaCl eluate was collected and protein, protease and keratinase activity were detected in it. All the fractions with high enzyme activity were separately pooled, dialyzed, concentrated by lyophilization and used for further studies.

Determination of keratinase activity. The keratinase activity was assayed by the modified method of Cheng et al. [8] by using keratin as a substrate. The reaction mixture contained 200 µl of enzyme preparation and 800 µl of 20 µg/ml keratin in 10 mM Tris−HCl buffer, pH 8.0. The reaction mixture was incubated at 45°C for 20 min and the reaction was terminated by adding 1 ml of 10% chilled trichloroacetic acid. The mixture was centrifuged at 10.000 g for 5 min and the absorbance of the supernatant fluid was determined at 440 nm. All assays were done in triplicate. One unit (U) of enzyme activity was the amount of enzyme that caused a change of 0.01 of absorbance unit at 440 nm in 20 min at 45°C.

Determination of protease activity. Protease activity was assayed in the various fractions by a modified

method of Tsuchida et al. [9] by using casein as substrate. 100 µl of the enzyme solution was added to 900 µl of substrate solution (2 mg/ml casein in 10 mM Tris−HCl buffer, pH 8.0).The mixture was incubated at 50°C for 20 min. Reaction was stopped by the addition of an equal volume of 10% chilled trichloroacetic acid and then the reaction mixture was allowed to stand in ice for 15 min to precipitate the insoluble proteins. The supernatant was separated by centrifugation at 10.000 g for 10 min at 4°C; the acid soluble product in the supernatant was neutralized with 5 ml of 0.5 M Na_2CO_3 solution. The color developed after adding 0.5 ml of 3 fold diluted Folin−Ciocalteau reagent was measured at 660 nm. All assays were done in triplicate. One protease unit was defined as the amount of enzyme that releases 1 µmol of tyrosine per ml per minute. The specific activity was expressed in the units of enzyme activity per mg of protein.

Determination of milk-clotting activity. It was determined according to the method of Arima [10], which is based on the visual evaluation of the appearance of the first clotting flakes, and expressed in terms of Soxhlet units (SU). One SU is defined as the amount of enzyme which clots 1 ml of a solution containing 0.1 g of the skim milk powder in 40 min at 35°C. In brief, 0.5 ml of tested materials was added to a test-tube containing 5 ml of the reconstituted skim milk solution (10 g of dry skim milk in 100 ml of 10 mM $CaCl_2$ and 10 mM $MnSO_4$) preincubated at 35°C for 5 min. The mixture was mixed well and the clotting time T (s) (the time period starting from the addition of test material to the first appearance of clots of milk solution) was recorded and the clotting activity was calculated using the following formula:

$$SU = 2400 \times 5 \times D/T \times 0.5; \text{ where } T - \text{clotting time}$$
$$\text{(s) and } D - \text{dilution of the test material.}$$

Protein concentration. Protein concentration of all the crude and dialyzed fractions of 0−30% and 30−60% ammonium sulphate was determined by the method of Bradford with bovine serum albumin as a standard [11].

Polyacrylamide gel electrophoresis and zymography. SDS-PAGE was performed on a slab gel containing 10% (w/v) polyacrylamide by silver staining according to the method of Switzer et al. [12]. Casein zymography was performed in polyacrylamide slab gels containing SDS and casein (0.12% w/v) as co-polymerized substrate, as described by Choi et al. [13]. After electrophoresis, the gel was incubated for 30 min at room temperature on a gel rocker in 50 mM Tris-HCl (pH 7.4), which contained 2.5% Triton X-100 to remove SDS. Then it was incubated in a zymogram reaction buffer (30 mM Tris-HCl with 200 mM NaCl and 10 mM $CaCl_2$, pH 7.4) at 37°C for 12 h on rocker. The gel was stained with 0.5% Coomassie brilliant blue for 30 min. The activity band was observed as a clear colorless area depleted of casein in the gel against the

blue background when destained in 10% methanol and 5% acetic acid for a limited period of time.

Effect of pH, temperature and various metal ions on enzyme activity. Effect of pH on the purified enzyme activity was measured at various pH ranges (3.0–12.0). The pH was adjusted using the following buffers – 50 mM acetate (pH 2.0–4.0), 50 mM phosphate (pH 5.0–7.0), 50 mM Tris-HCl (pH 8.0) and 50 mM glycine-NaOH (pH 9.0–12.0).

The activity of the enzyme was determined by incubating the reaction mixture at different temperatures ranging from 20, 30, 40, 50, 60, 70 and 80°C.

The effects of 10 mM metal ions (Ca^{2+}, Mg^{2+}, Fe^{2+}, Mn^{2+}, Zn^{2+}, Hg^{2+}, and Cu^{2+}) on enzyme activity were investigated by adding them to the reaction mixture.

RESULTS AND DISCUSSION

Isolation and identification of protease-producing bacterial strains. Screening of microorganisms that produced protease and keratinase was done on cultures isolated from soil of Ghazipur poultry waste site. Organic waste such as feathers and other poultry waste are essentially composed of proteins. Biodegradation of such samples is generally caused due to the microbial population present at this site. Protease and keratinase producing strains were selected on skim milk agar as described in Methods. Among the cultures tested, the laboratory isolate SN1 showed zone of clearance on these media. The purity of the isolated bacteria was ascertained through repeated streaking (data not shown). Using morphological and biochemical characteristics based on Bergey's Manual the bacterial isolate SN1 was identified as *B. megaterium* SN1.

Protease and keratinase production and effects of different nutrient sources. The growth of isolated colony was detected and protease as well as keratinase activity was measured for 7 days after regular intervals (Figs. 1 and 2). Various substrates like chicken feather, pigeon feather, hair and nail were evaluated for the production of enzymes (Fig. 3). Isolated strain of *B. megaterium* SN1 grown in four nutrient sources produced protease and keratinase. The maximum yield of protease and keratinase was seen in basal media supplemented with pigeon feather. Also complete degradation of the pigeon feather and chicken feather was detected (Figs. 3 and 4).

Purification of protease and keratinase. The extracellular protease and keratinase produced by *B. megaterium* SN1 were purified by 30–60% ammonium sulphate precipitation of culture broth followed by strong anion exchange chromatography on Q Sepharose. The bound protease was eluted with 0.2 and 0.4 M NaCl in 10 mM Tris–HCl buffer pH, 8.0. The fractions showing the presence of protease or caseinolytic activity was pooled (Fig. 5). We report 29.3-fold purification of protease with activity 296.0 U/mg of protein. The re-
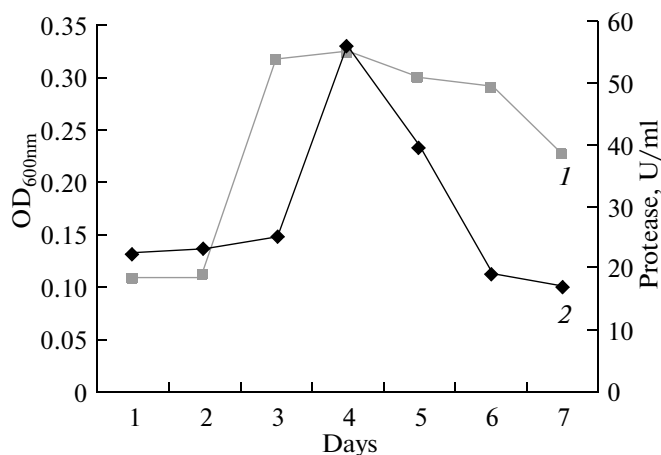

Fig. 1. Growth curve (*1*) and determination of protease activity (*2*) of the SN1 isolate of *B. megaterium*.
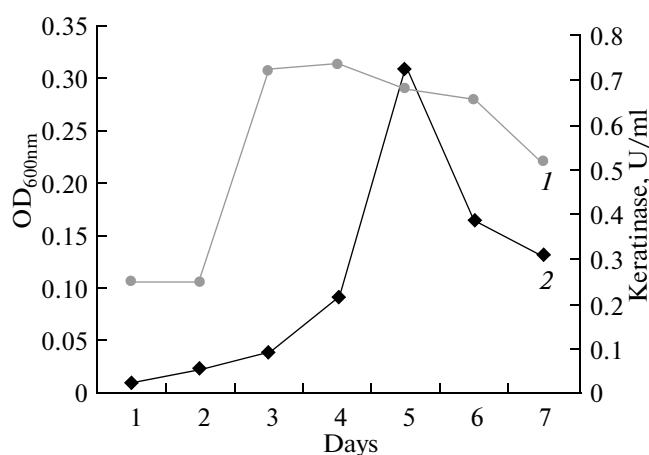

Fig. 2. Growth curve (*1*) and determination of keratinase activity (*2*) of the SN1 isolate of *B. megaterium*.
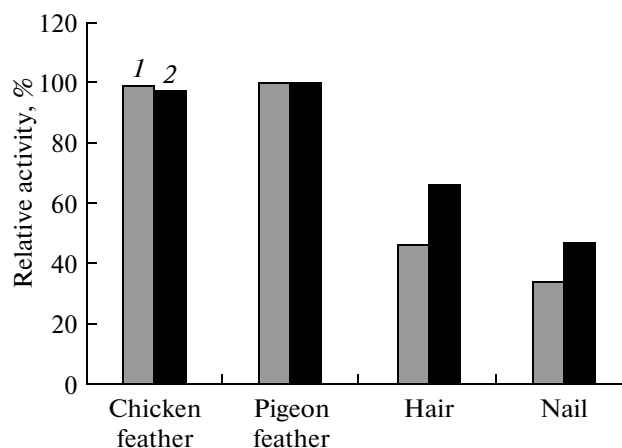

Fig. 3. The relative activity of proteases (*1*) and keratinases (*2*) of *B. megaterium* SN1 in the presence of different proteinaceous substrates.
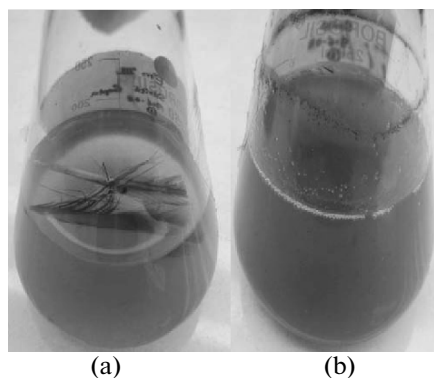
Fig. 4. Degradation of pigeon feathers by the *B. megaterium* SN1 isolated from soil of Ghazipur poultry dumping site (India) in submerged cultivation at 30°C. a — feathers were incubated in the growth medium without the bacterial strain for 72 h of incubation. b — degraded feather after 72 h of incubation with the isolated bacterial strain.

sults of purification of protease from *B. megaterium* SN1 are summarized in Table 1. Keratinase was 655.6-fold purified with specific activity of 544.7 U/mg of protein and 12.4% recovery (Table 2). This keratinolytic-active fraction was further separated on SDS–PAGE for molecular weight determination and zymography studies.

Many authors have suggested various strategies in purification of keratinases. Correa et al. [14] reported that the amazonian bacterium *Bacillus* sp. P7 produced extracellular keratinase that was partially purified by 60% ammonium sulphate precipitation, gel filtration Sephadex G-200, and ion-exchange chromatography on SP Sepharose, DEAE Sepharose FF, resulting in a purification factor of 29.8-fold and a yield of 27%. Zhang et al. [15] studied a new alkaline keratinase extracted from *Bacillus* sp. 50-3 by ammo-

nium sulfate precipitation and DEAE Sephadex-A50 column and 17.7-fold purification with a yield of 46.5%.

The results in Table 3 summarize that the isolated bacterial culture and their ammonium sulphate fractions showed the presence of caesinolytic activity and milk clotting activity. The effect of calcium and magnesium metal ions on the production of milk-clotting enzymes was also studied. Milk clotting activity was detected in crude and ammonium sulphate fraction of *B. megaterium* SN1. The caesinolytic activity was 0.192 at OD_{660} and ratio of milk clotting activity to caseinolytic activity of the 30–60% ammonium sulphate fraction was found to be 520.8 with 100 SU/ml in the presence of Mn^{2+} suggesting potential application in dairy industry. The thermostability and wide pH range shown for the caesinolytic activity are promising for that.

Microorganisms like *Bacillus subtilis, Bacillus licheniformis and Enterococcus faecalis*, produce milk-clotting enzyme which may be potential rennet substitute [16–18]. 685.7 SU/ml of milk-clotting activity (MCA) is reported from *B. subtilis* (natto) enzyme and according to the authors it was found comparable with those of Pfizer microbial rennin and Mucor rennin [19]. Solid-state fermentation resulted in 1.080 and 952.3 U/gds (per g of dried substrate) of milk-clotting protease using soybean meal and rice bran [20]. The protease from *B. licheniformis* had the ability to produce milk curds and exhibited typical milk-clotting kinetics [21]. *B. subtilis* B1, in the presence of optimized medium showed an increase from 782 SU/ml to 1129.05 ± 74.55 SU/ml when wheat bran was used [22]. However, there are no reports on MCE-producing bacteria using feather as substrate.
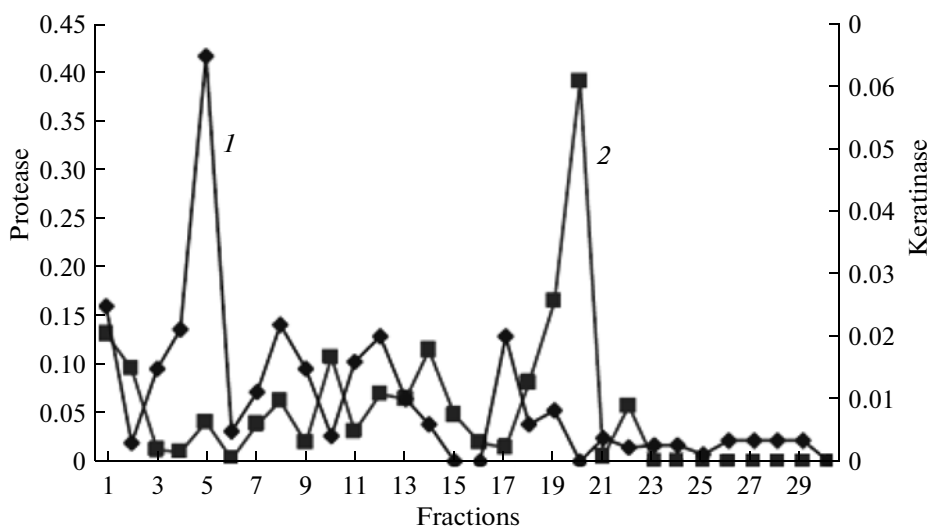

Fig. 5. Activity profile of protease (*1*) and keratinase (*2*) isolated from *B. megaterium* SN1 by Q sepharose ion exchange chromatography.

Table 1. Purification steps of protease from *B. megaterium* SN1

Purification step	Specific activity, U/mg	Purification, fold	Recovery, %
Crude enzyme	10.11	1.0	100
0−30% $(NH_4)_2SO_4$ ppt, dialyzed	3.57	0.35	12.83
30−60% $(NH_4)_2SO_4$ ppt, dialyzed	6.06	0.60	41.46
Q Sepharose	295.98	29.28	1.02

Table 2. Purification steps of keratinase from *B. megaterium* SN1

Purification step	Specific activity, U/mg	Purification, fold	Recovery, %
Crude enzyme	0.84	1	100
0−30% $(NH_4)_2SO_4$ ppt, dialyzed	0.58	0.69	25.09
30−60% $(NH_4)_2SO_4$ ppt, dialyzed	0.49	0.59	40.78
Q Sepharose	544.69	655.64	12.74

SDS-PAGE and zymogram analysis. The Q sepharose fraction was analysed on SDS PAGE (10%) and showed the presence of single band indicating a homogeneous preparation. The enzyme has a molecular weight of 30 kDa. Zymogram activity staining also revealed one clear zone of proteolytic activity against the blue background for purified sample at corresponding positions in SDS-PAGE (Fig. 6, lane 5).

pH optimum, temperature optimum and effect of metal ions. Activity of the enzyme was determined at different pH ranging from 2.0−11.0. The maximum pH recorded was 3.0 for protease and keratinase activity (Fig. 7a). Maximum activity in the acidic range suggests a positive biotechnological potential in the food and detergent industry thus the feather protein can be metabolized and utilized as animal feed protein [23−25]. Additionally, the relative enzyme activity was higher than 40% even at neutral and some alkaline conditions, indicating the potential versatility of such enzyme preparations for diverse applications. Several authors have reported that microbial keratinases typically have optimum pH in more alkaline range [25−29].

The optimum temperature recorded was at 60°C for protease and 70°C for keratinase (Fig. 7b). The protease and keratinase activity was found to be stable in the temperature range from 40°C to 80°C and 50°C to 70°C respectively.

Mn^{2+}, Co^{2+} (10 mM) strongly activated protease activity of *B. megaterium* SN1 by 2.1-fold, 1.3-fold respectively, whereas Mn^{2+}, Co^{2+} and Mg^{2+} strongly activated keratinase activity by 1.2-, 1.1- and 1.1-fold respectively (Fig. 7c). Maybe they act as salt or ion bridges that stabilize the enzyme in its active conformation and might protect the enzyme against thermal denaturation [28, 30]. While Hg^{2+} and Ba^{2+} strongly inhibited protease activity, and Hg^{2+} and Fe^{2+} strongly inhibited keratinase activity. Hg^{2+} is recognized as an oxidant agent of thiol groups, and the enzyme inhibition by this ion could suggest the presence of important −SH groups (such as free cysteine) at or near the active site [26, 31]. However, Hg^{2+} might also react with tryptophan residues and carboxyl groups in amino acids of the enzyme [32].

Table 3. Milk clotting and caseinolytic activities, ratio of milk clotting units to caseinolytic activity of *B. megaterium* SN1

Fractions of purified culture broth of *B. megaterium* SN1	Milk clotting activity, SU/ml*		Caseinolytic activity, OD_{660}	Ratio, Units/OD_{660}	
	$CaCl_2$	$MnSO_4$		$CaCl_2$	$MnSO_4$
Crude enzyme	1.43	2.5	0.250	5.72	10.00
0−30% $(NH_4)_2SO_4$ ppt, dialyzed	10.00	12.5	0.115	86.96	108.69
30−60% $(NH_4)_2SO_4$ ppt, dialyzed	50.00	100	0.192	260.4	520.84

*0.5 ml of tested materials was added to a test-tube containing 5 ml of reconstituted skim milk solution (10 g of dry skim milk/100 ml, 10 mM $CaCl_2$ and 10 mM $MnSO_4$) preincubated at 35°C for 5 min[10].
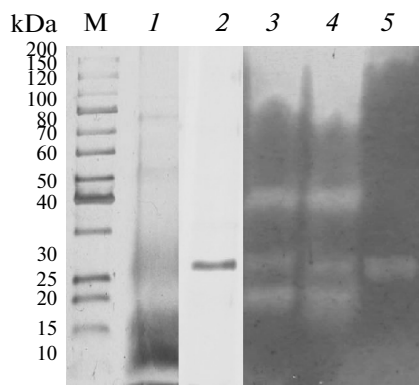
Fig. 6. Silver staining of protease of on 10% SDS PAGE. M − molecular weight markers; *1* − crude enzyme; *2* − 30−60% ammonium suphate fraction; zymogram lanes: *3* − crude enzyme; *1* and *4* − 30−60% ammonium sulphate fraction; *5* − 25 Q sepharose purified fraction.

B. megaterium SN1 was shown to extensively degrade both pigeon and chicken feathers during submerged cultivations, whereas human hair and nail was not degraded. We developed a two step methodology to purify protease by ammonium sulphate precipitation followed by Q Sepharose ion exchange chromatography from this bacterium. The purified enzyme was thermostable at 60°C, pH 3.0 and had a molecular weight of 30 kDa as shown by casein zymography. Ratio of milk clotting activity to caseinolytic activity of the 30−60% ammonium sulphate fraction was found to be 520.84 with 100 SU/ml in presence of Mn^{2+} ion (Table 3). We report isolation of acidic casenolytic protease that showed milk clotting activity, thus it can have high potential in industrial applications as dairy industry in cheese making. The crude extracellular fraction showing the presence of keratinase and protease activities could also degrade feathers completely within 72 h. Keratinase activity was detected at 25 Q Sepharose step of purification showing 655.6-fold purification with specific activity of 544.7 U/mg of protein.

Thus, it could be concluded that both caesinolytic protease and keratinase are produced extracellularly by *B. megaterium* SN1 in feather meal media. They possess moderate acidic stability and are thermostable, which might be desirable features for the efficient control of enzyme reactivity in the processes involving protein hydrolysis. These activities were separated by strong anionic exchanger Q Sepharose.

Food industry needs for acidic proteases active at high temperatures. Keratinase is a useful enzyme for promoting the hydrolysis of feather keratin and improving the digestibility of feather meal and protease is useful in milk industry. The protein hydrolysates resulting from the microbial conversion of feather keratin can be utilized as an ingredient in animal feed or as an organic fertilizer and the milk clotting function of
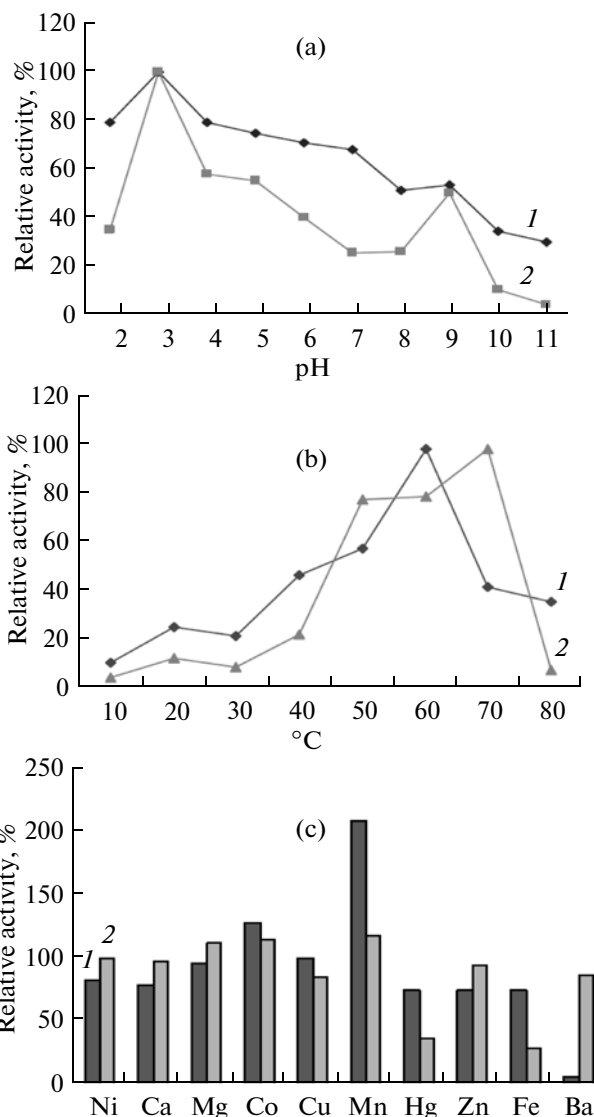

Fig. 7. Effect of pH (a), temperature (b) and of metal ions (c) on caseinolytic (*1*) and keratinolytic (*2*) activities from *B. megaterium* SN1. The maximum of enzyme activity obtained at pH 3.0, temperature 60°C and 70°C for protease and keratinase respectively and without metal ions was considered as 100%.

protease can be utilized by the dairy industry in cheese making.

ACKNOWLEDGMENTS

REFERENCES

1. Parry, D.A.D. and North, A.C.T.J., *Struct. Biol.*, 1998, vol. 122, no. 1−2, pp. 67−75.
2. Shih, J.C.H, *Poultry Sci.*, 1993, vol. 72, pp. 1617−1620.

3. Onifade, A.A., Al-Sane, N.A., Al-Musallan, A.A., and Al-Zarban, S., *Bioresour. Technol.*, 1998, vol. 66, no. 1, pp. 1−11.

4. Papadopoulos, M.C., El Boushy, A.R., Roodbeen, A.E., and Ketelaars, E.H., *Animal Feed Sci. Technol.*, 1986, vol. 14, pp. 279−290.

5. Buchanan, R.E. and Gibbons, N.E., Bergey's Manual of Determinative Bacteriology, 8th Ed., Baltimore: The Williams and Wilkins Co, 1974.

6. Gordon, G., Ruth, E., William, C., Haynes, H., and Pang, C., The Genus Bacillus: *Agriculture Handbook* No. 427. Washington, D.C: ARS-USDA, 1973.

7. Agrahari, S. and Wadhwa, N., *Internat. J. Poultry Sci.*, 2010, vol. 9, no. 5, pp. 482−489.

8. Cheng, S.W., Hu, H.M., Shen, S.W., Takagi, H., Asano, M., and Tsai, Y.C., *Biosci. Biotechnol. Biochem*, 1995, vol. 59, no. 12, pp. 2239−2243.

9. Tsuchida, O., Yamagota, Y., Ishizuka, J., Arai, J., Yamada, J., Takeuchi, M., and Ichishima, E., *Current Microbiol*, 1986, vol. 14, no. 1 pp. 7−12.

10. Arima, K., Yu, J., and Iwasaki, S., *Methods in Enzymology*, 1970, vol. 19, pp. 446−459.

11. Bradford, M.M., *Anal. Biochem.*, 1976, vol. 72, no. 1−2, pp. 248−254.

12. Switzer, R.C., Merril, C.R., and Shifrin, S.A., *Anal. Biochem.,* 1979, vol. 98, no. 1, pp. 231−237.

13. Choi, N.S., Yoon, K.S., Lee, J.Y., Han, K.Y., and Kim, S.H., *J. Biochem. Mol. Biol.,* 2001, vol. 34, pp. 531−536.

14. Correa A.P.F., Daroit D.J., and Brandelli A., *Int. Biodeterioration Biodegradation,* 2010, vol. 64, no. 1, pp. 1−6.

15. Zhang, B., Jiang, D.D., Zhou, W.W., Hao, H.K., and Niu, T.G., *World J. Microbiol. Biotechnol.*, 2009, vol. 25, no. 4, pp. 583−590.

16. Sato, S., Hiroharu, T., Takeo, K., and Kotoyoshi, N., *Food Sci. Technol. Res.,* 2004, vol. 10, no. 1, pp. 44−50.

17. Ageitos, J.M., Vallejo, J.A., Sestelo, A.B.F., Pozaand, M., and Villa, T.G., *J. Appl. Microbiol.*, 2007, vol. 103, no. 6, pp. 2205−2213.

18. Dutt, K., Meghwanshi, G.K., Gupta, P., and Saxena, R.K., *Lett. Appl. Microbiol.*, 2008, vol. 46, no. 6, pp. 513−518.

19. Shieh, C.J., Thi, L.A. P., and Shih, I.L., *Biochem. Engineering J.,* 2009, vol. 43, no. 1, pp. 85−91.

20. Dutt, K., Gupta, P., Saran, S, Misra, S., and Saxena, R.K., *Appl. Biochem. Biotechnol.*, 2009, vol. 158, no. 3, pp. 761−772.

21. Ageitos, J.M., Vallejo, J.A., Sestelo, A.B., Poza, M., and Villa, T.G., *J. Appl. Microbiol.*, 2007, vol. 103, no. 6, pp. 2205−2213.

22. Ding, Z., Liu, S., Gu, Z., Zhang, L., Zhang, K., and Shi, G., *African J. Biotechnol.*, vol. 10, no. 46, pp. 9370−9378.

23. Agrahari, S. and Wadhwa, N., *J. Pharmacy Res.*, 2010, vol. 4, no. 3, pp. 929−932.

24. Lee, C.G., Ferket, P.R., and Shih, J.C.H., *FASEB J.*, 1991, vol. 59, pp. 1312.

25. Gupta, R. and Ramnani, P., *Appl. Microbiol. Biotechnol.* 2006, vol. 70, no. 1, pp. 21−33.

26. Thys, R.C.S. and Brandelli, A., *J. Appl. Microbiol.*, 2006, vol. 101, no. 6, pp. 1259−1268.

27. Suh, H.J. and Lee, H.K., *J. Protein Chem.*, 2001, vol. 20, no. 2, pp. 165−169.

28. Balaji, S., Kumar, M.S., Karthikeyan, R., Kumar, R., Kirubanandan, S., Sridhar, R., and Sehgal, P.K., *World J. Microbiol. Biotechnol.*, 2008, vol. 24, no. 11, pp. 2741−2745.

29. Letourneau, F., Soussotte, V., Bressollier, P., Branland, P., and Verneuil, B., *Letters Appl. Microbiol.,* 1998, vol. 26, no. 1, pp. 77−80.

30. Sareen, R. and Mishra, P., *Appl. Microbiol. Biotechnol.*, 2008, vol. 79, no. 3, pp. 399−405.

31. Daroit, D.J., Simonetti, A., Hertz, P.F., and Brandelli, A., *J. Microbiol. Biotechnol.*, 2008, vol. 18, no. 5, pp. 933−941.

32. Lusterio, D.D., Suizo, F.G., Labunos, N.M., Valledor, M.N., Ueda, S., Kawai, S., Koike, K., Shikata, S., Yoshimatsu, T., and Ito, S., *Biosci., Biotechnol. Biochem.,* 1992, vol. 56, pp. 1671−1672.

EFFECT OF PARTIAL PRESSURE OF CO$_2$ ON THE PRODUCTION OF THERMOSTABLE α-AMYLASE AND NEUTRAL PROTEASE BY *Bacillus caldolyticus*

© 2012   J. Bader*, L. Skelac**, S. Wewetzer**, M. Senz*, M. K. Popović**, R. Bajpai***

Technische Universität Berlin, Fakultät III, Biotechnologie, Department of Applied and Molecular Microbiology, Berlin 13353, Germany

**Beuth Hochschule für Technik Berlin, University of Applied Sciences, Department of Biotechnology, Berlin 13347, Germany*

***University of Louisiana at Lafayette, Chemical Engineering Department, Lafayette LA 70504, USA*

e-mail: popovic@beuth-hochschule.de

Received June 20, 2011

Controlling the concentration of dissolved oxygen is a standard feature in aerobic fermentation processes but the measurement of dissolved CO$_2$ concentrations is often neglected in spite of its influence on the cellular metabolism. In this work room air and room air supplemented with 5% and 10% carbon dioxide were used for aeration during the cultivation of the thermophilic microorganism *Bacillus caldolyticus* (DSM 405) on starch to produce α-amylase (E.C. 3.2.1.1) and neutral protease (E.C. 3.4.24.27/28). The increased CO$_2$ concentrations resulted in a 22% raise in activity of secreted α-amylase and a 43% raise in protease activity when compared with aeration with un-supplemented room air. There was no effect on the final biomass concentration. Furthermore, the lag-phase of fermentation was reduced by 30%, further increasing the productivity of α-amylase production. Determinations of dissolved CO$_2$ in the culture broth were conducted both in situ with a probe as well as using exhaust gas analysis and both the methods of quantification showed good qualitative congruence.

Amylases and proteases are widely used industrial enzymes. They are used in washing powders and detergents as well as in food, textile, and paper production. The estimated world market for these enzymes is projected to be $1.8 billion for amylases and $3.6 billion for proteases [1, 2] in 2011. Many applications of the enzymes involve operations at high temperature. The thermostable proteases and α-amylases are presently produced from *Bacillus licheniformis* or *Bacillus stearothermophilus*. We have focused our studies on the less examined thermophilic microorganism *Bacillus caldolyticus* DSM 405 to establish the conditions for optimal production of the enzymes, α-amylase and protease [3].

Carbon dioxide is produced in nearly all industrial fermentation processes. In common aerobic fermentation processes involving gas sparging, most carbon dioxide is fast stripped out of the medium by the sparged gases. In anaerobic processes, however, considerable accumulation of carbon dioxide (total concentration up to several g l^{-1}) may occur and may result in growth inhibition [4]. In several cases, however, CO$_2$-enhanced growth of several microorganisms has also been reported [5–8]. As far as α-amylase production is concerned, a stimulating effect of increased CO$_2$ level on α-amylase production by *Bacillus subtilis* was found by 2 groups of authors [9, 10]. In both the cases, biomass production recorded a decrease simul-

taneously. Narahara et al. [11] also reported an increase in α-amylase and protease activities during fermentation of *Aspergillus oryzae* when partial pressure of CO$_2$ was increased from 0.02 to 0.05 atm. Mudgett and Bajracharya [12] also found that high CO$_2$ pressure had a distinct influence on cell growth and α-amylase synthesis during solid state fermentation of *Aspergillus oryzae* in the rice Koji process. But there are no reports of the effect of carbon dioxide on *Bacillus caldolyticus*.

The aim of this paper was to study the influence of carbon dioxide on growth of the *Bacillus caldolyticus* DSM405 cells and on production of α-amylase and protease by this thermophilic microorganism. Furthermore, the comparative measurements of dissolved CO$_2$ concentrations in the cultivation medium were carried out using exhaust gas analyzer and fluorescence-based CO$_2$ probe.

MATERIALS AND METHODS

Strain and medium. The thermophilic bacterium *B. caldolyticus* DSM 405 used in this study was obtained from the German Collection of Microorganisms and Cell Cultures, Braunschweig, Germany [13]. The growth and production medium contained (g l^{-1}): peptone from casein — 2.0, KH$_2$PO$_4$ — 0.05, CaCl$_2$ · 2H$_2$O — 0.1, Zulkowsky (soluble) starch — 1.0 and (mg

l^{-1}): MgSO$_4 \cdot$ 7H$_2$O $-$ 250.0, MnCl$_2 \cdot$ 4H$_2$O $-$ 1.57 and FeSO$_4 \cdot$ 7H$_2$O $-$ 30.0.

Culture conditions and operating parameters. Inocula were prepared by preculturing 100 ml of growth medium in 500-ml shake flasks for 8 h at 70°C and 150 rpm. Exponential phase preculture was used for inoculation of the bioreactor to achieve OD$_{600}$ of 0.08 in the fermenter at the beginning of cultivation.

Cultivation of bacterial cells for enzyme production was carried out in a lab-scale stirred tank bioreactor (Biostat E, Sartorius Stedim Systems GmbH, Germany) equipped with a dissolved O$_2$ (DO) probe, a dissolved CO$_2$ probe, and controllers for pH, temperature, agitation, and foam. Total broth volume in the reactor was 3.3 l. pH was controlled at 7.0 $\pm$ 0.1 using 20% (w/v) KOH or 1.0 M HCl solution. Polypropyleneglycol P2000 was used to control foam. Temperature in the bioreactor was controlled at 70°C. Flow rate of inlet air was fixed at 1 vvm (volume of air per volume of fermentation broth and minute) and the concentration of dissolved oxygen in the medium was kept above 50% saturation by gradually increasing the speed of agitation.

Experiments were conducted with room air and with room air supplemented with CO$_2$ to 5 and 10% (v/v) for aeration. At least 3 experimental runs were made with each inlet concentration of CO$_2$. The concentrations of cells, starch, α-amylase, and protease were monitored in each experiment.

Analytical procedures. α-amylase activity was determined by a modified method developed by Manning and Campbell [13]. A mixture of 40 μl of culture supernatant, 40 μl of 1% starch solution, and 40 μl of 1.0 M sodium acetate buffer (pH 5.4) was incubated at 70°C for 10 min. Subsequently 1 ml of cold water and 30 μl of iodine solution (30 g l^{-1}) were added to the incubated mixture on ice, and absorbance (OD$_{620nm}$) was measured. As a reference, 40 μl fresh medium was used instead of 40 μl of supernatant. The enzymatic activity was calculated using equation (1).

$$A = \frac{\Delta E_{620\,nm} \cdot VF \cdot V_T \cdot 1000}{t_{Ink} \cdot V_R \cdot m \cdot MW}, \qquad (1)$$

where A is the enzymatic activity (U l^{-1}), $E = E_{reference} - E_{sample}$ is the difference between absorbances (AU) in the reference and the sample at 620 nm, VF is the dilution factor for the sample ($-$), V_T is the total volume (ml), V_R is the reaction volume (ml), t_{Ink} is time of incubation (10 min), m is the slope of calibration curve (4.7646 ml mg^{-1}), and MW is the molecular weight of anhydroglucose (162 g mol^{-1}).

Activity of neutral protease was determined by a modified method developed by Strydom et al. [14]. 200 μl of the sample was mixed with 200 μl of 2% azocaseine solution dissolved in 50.0 mM Tris-HCl buffer (pH 7.0) containing 5.0 mM CaCl$_2$ and incubated for

30 min at 70°C. 400 μl of 1.5 M HClO$_4$ was added and the mixture was cooled on ice for 30 min to complete precipitation. After centrifugation at 8.000 g, 400 μl of the supernatant was mixed with 400 μl 1.0 M NaOH, and optical density (OD$_{440}$) was measured. One unit of the enzyme was defined as 1 mmol of azocasein cleaved per minute; the calculation of enzymatic activity was conducted using equation 2.

$$A = \frac{\Delta E_{440\,nm}}{\varepsilon d} \cdot \frac{V_T}{V_R} \cdot \frac{1000 \cdot VF}{t_{Ink}}, \qquad (2)$$

where ε is the extinction coefficient of azocasein (38 AU l mol^{-1} cm^{-1}) and d is the thickness of cuvette (1 cm).

Cell density was monitored as OD$_{600}$ with Philips PU 8625 UV/VIS spectrophotometer (Philips GmbH, Germany). OD was converted into cell dry weight (DW) by using equation 3.

$$DW = OD_{600} \cdot 0.33, \qquad (3)$$

where DW is cell dry weight (g l^{-1}) and OD$_{600}$ is optical density of broth at 600 nm.

Starch concentration in cell-free broth was analyzed by adding 750 μl DI water and 15 μl 4% iodine solution in water to 250 μl sample supernatant and measuring OD$_{620}$ using a UV/VIS-Photometer. Starch concentration (g l^{-1}) was calculated using a calibration curve prepared from solutions of known concentrations of starch (equation 4).

$$c_{St} = \frac{E_{620} - 0.053}{0.9965}, \qquad (4)$$

where c_{St} is the concentration of starch (g l^{-1}).

Glucose concentration was quantified with a glucose-kit (Roche Diagnostik, Germany: Kit-No. 10716251035). Acetate concentration was determined in the supernatant using the acetate-kit (Roche Diagnostik, Germany: Kit-No.: 10148261035). Cooled and dried exhaust air was analyzed with a multi-component gas analyzer (Sidor, Sick Maihack GmbH, Germany).

The concentration of dissolved carbon dioxide in medium was calculated from the exhaust air composition and dissolved oxygen probe reading using the procedure of Royce and Thornhill [15] (equation 5).

$$c_L^{CO_2} = \frac{(P - p_w)\, x_g^{CO_2 out}}{H^{CO_2}} + \\ + \frac{1}{0.89}\left(\frac{(P - p_w)\, x_g^{CO_2 out}}{H^{O_2}} - c_L^{O_2}\right), \qquad (5)$$

where c_L is the concentration of dissolved gas component in fermentation medium (mol m^{-3}), P is the overhead pressure (Pa), p_W is the partial pressure of water in the bioreactor overhead space (Pa), x_g is mole frac-
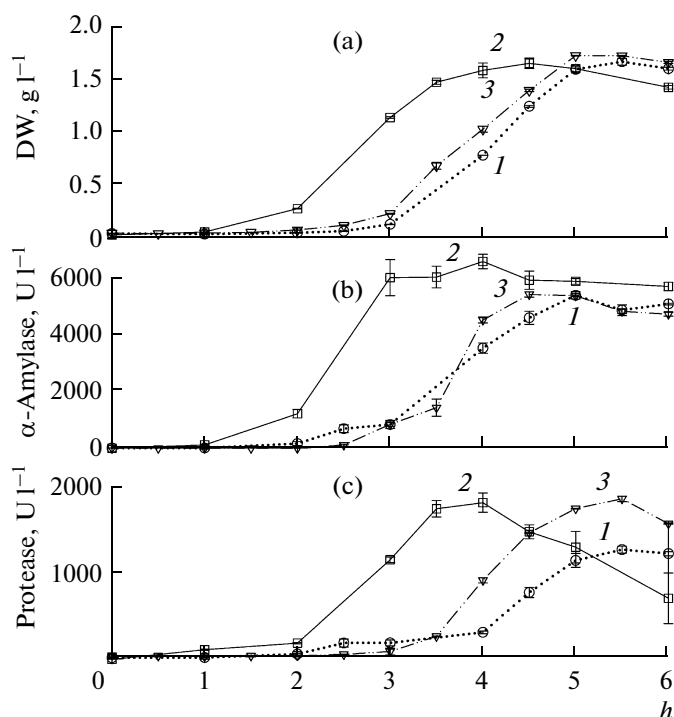
Fig. 1. Dry weight (DW, a), α-amylase (b) and protease (c) activities during the fermentations of *B. caldolyticus* aerated with room air (*1*); air supplemented with 5% CO_2 (*2*) and air supplemented with 10% CO_2 (*3*).

tion of the component in gas phase (−), *H* is Henry′s law constant for the gas (Pa m³ mol⁻¹).

The Henry′s law constants for 70°C were calculated using equations (6) and (7) [16, 17].

$$H^{CO_2} = e^{\left(11.25 - \frac{395.9}{T - 175.9}\right)} \text{ and } \quad (6)$$

$$H^{O_2} = e^{\left(12.74 - \frac{133.4}{T - 206.7}\right)} \quad (7)$$

Here, *T* is temperature of medium (K).

The concentration of oxygen in medium ($c_L^{O_2}$) was calculated from the response of dissolved oxygen probe using the following equations:

$$c_L^{O_2} = \frac{c_{O_2}^* \cdot p_{O_2}}{100}. \quad (8)$$

Here $c_{O_2}^*$ is the solubility of oxygen in medium at 70°C (mol m⁻³), p_{O_2} is the dissolved oxygen probe signal (%).

$$c_{O_2}^* = \frac{(P - p_W) x_{O_2}}{H^{O_2}}, \quad (9)$$

where x_{O_2} is mole fraction of oxygen in inlet gas which was also used to calibrate the DO probe response to 100%.

In situ measurement of dissolved CO_2 was also done with a fluorescence-based YSI 8500 CO_2 Monitor (YSI Inc., USA).

RESULTS AND DISCUSSION

When room air (without CO_2 supplementation) was used to aerate the batch fermentation broth, the onsets of logarithmic growth phase and α-amylase formation were observed after approximately 2 h of inoculation. In the subsequent 3−4 h, cell dry weight concentration peaked at 1.7 g l⁻¹, and α-amylase and protease activities rose up to 5432 U l⁻¹ and 1296 U l⁻¹ respectively (Fig. 1). When the volume fraction of CO_2 in the inlet-air was increased to 5%, the lag-phase reduced considerably. In this case the final cell dry weight concentration was not affected by CO_2 fraction in air but the concentrations of α-amylase and protease increased to 6634 U l⁻¹ and 1853 U l⁻¹, respectively, by 4.5 h. This amounted to 22% increase in amylase activity and 43% increase in protease activity over the highest levels achieved with room air only. When the inlet-air CO_2 fraction was increased further to 10%, however, the maximum amylase levels decreased (Fig. 1) even though the maximum protease activity increased slightly again to 1899 U l⁻¹. In all the cases, the activities of both the enzymes recorded some drop beyond the maximum, suggesting that harvesting needs to be done at the right time to prevent losses (Fig. 1). It is noticeable that the activity of protease has the potential for more significant drop than the activity of α-amylase. Similar effect of CO_2 on the duration of lag phase has been reported by Gaffney [16], who explained the effect by the improved synthesis of oxaloacetate in the tricarboxylic acid (TCA) cycle. Gandhi and Kjaergaard [9] also revealed similar effect of carbon dioxide on amylase production by *B. subtilis*. These authors observed the highest amylase production at 6% CO_2 volume fraction in the sparged air and hypothesized that CO_2 influence is exerted possibly through reduced rate of metabolism of glucose. To emphasize the effect of CO_2 fraction in air on product formation by *Bacillus caldolyticus*, the maximum values of cell dry weight concentration and activity of enzymes at different CO_2 fractions in air are listed in Fig. 2.

A link between dissolved CO_2 concentration and enhanced secretion of enzymes, especially that of protease, was also observed by Stretton and Goodman [17], who suggested that high CO_2 concentrations affect production of enzymes involved in improving growth conditions and in secretion of toxic components that suppress competing microorganisms. It is also possible that increased CO_2 concentration alters intracellular pH in cells even though the fermentation was conducted under controlled pH conditions. Another explanation for the increased concentrations of
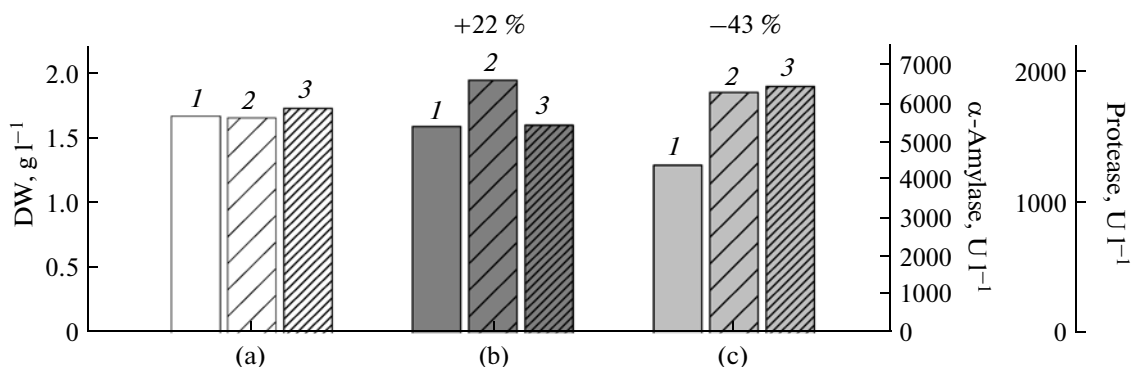
Fig. 2. Comparison of biomass concentration (DW) (a) and the maximum activities of α-amylase (b) and protease (c) enzymes during the fermentation of *B. caldolyticus* aerated with room air (*1*); air supplemented with 5% CO_2 (*2*) and air supplemented with 10% CO_2 (*3*).

the secreted enzymes might be a regulatory influence of CO_2 on transcriptional level, as reported for *B. anthracis* by Drysdale et al. in 2005 [18].

The concentrations of glucose, starch, and acetate in broth at different CO_2 fractions in air are presented in Fig. 3. Note that starch was consumed the fastest when inlet air contained 5% CO_2. Starch hydrolysis leads to formation of polysaccharides and ultimately to glucose which is metabolized by the cells. As expected, a higher rate of starch hydrolysis was accompanied with a higher level of glucose in the broth. In general, the concentration of glucose above a threshold triggers overflow metabolism and results in production of acetate, a growth inhibitory chemical [3]. Concentration profiles of acetate in the different experiments are shown in Fig. 3. It is interesting to note that although starch was hydrolyzed very fast in the fermentation with 5% CO_2, less acetate accumulated in the broth than in the fermentations with 0 and 10% CO_2 in aeration air. This suggests that glucose metabolism is influenced by carbon dioxide in a manner such that glucose is consumed by the cells without entering the carbon overflow pathway, indicating a more effective utilization of the carbon source. A possible explanation may be the enhanced activity of phosphoenole pyruvate carboxylase and pyruvate carboxylase under elevated concentration of CO_2 [19]. Both enzymes catalyze formation of oxaloacetate from their substrates and oxalocetate enters the TCA. Hence less pyruvate is available to enter the enzymatic pathway leading to acetate formation. On the other hand, the activities of α-amylase and protease increased much faster in the experiments with 5% of CO_2 than with other concentrations (Fig. 1).

In all our experiments, a dry weight concentration of 1.7 g l^{-1} was achieved (Fig. 2). This observation, that the different CO_2 fractions in the aeration air did not influence the maximal biomass concentration in the experiments, are in disagreement with the results presented by Gandhi and Kjaergaard [9] who reported a

growth inhibiting effect of CO_2 even with much smaller increases of CO_2 in inlet air. On the other hand, our observations of increased amylase and protease activities with increased CO_2 level in feed air are in agreement with the observations of Gandhi and Kjaergaard [9]. The extent of positive effect of CO_2 in the aeration air depends, however, on the specific enzyme system.

Measurement of dissolved CO_2 in fermentation broth. The observed influence of CO_2 on the secretion
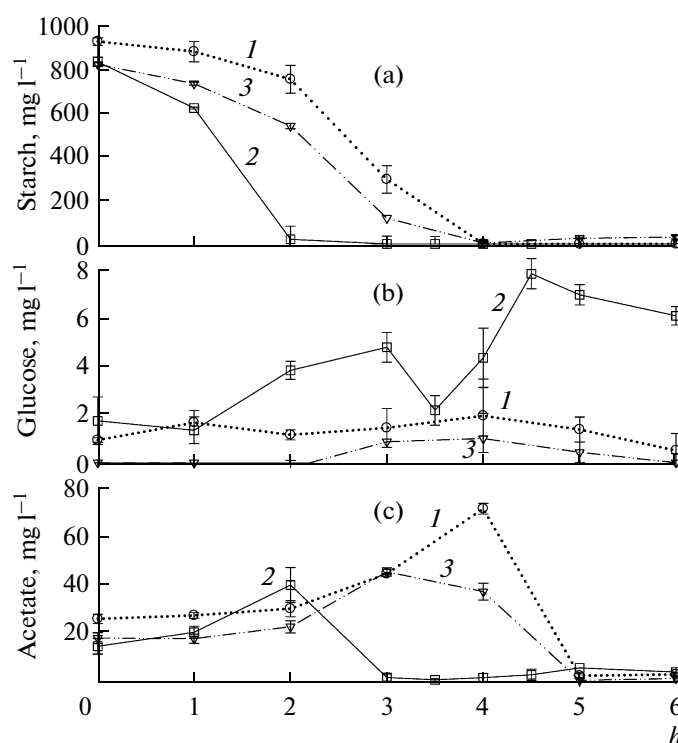

Fig. 3. Starch (a), glucose (b) and acetate (c) concentrations during the fermentation of *B. caldolyticus* aerated with room air (*1*); air supplemented with 5% CO_2 (*2*) and air supplemented with 10% CO_2 (*3*).
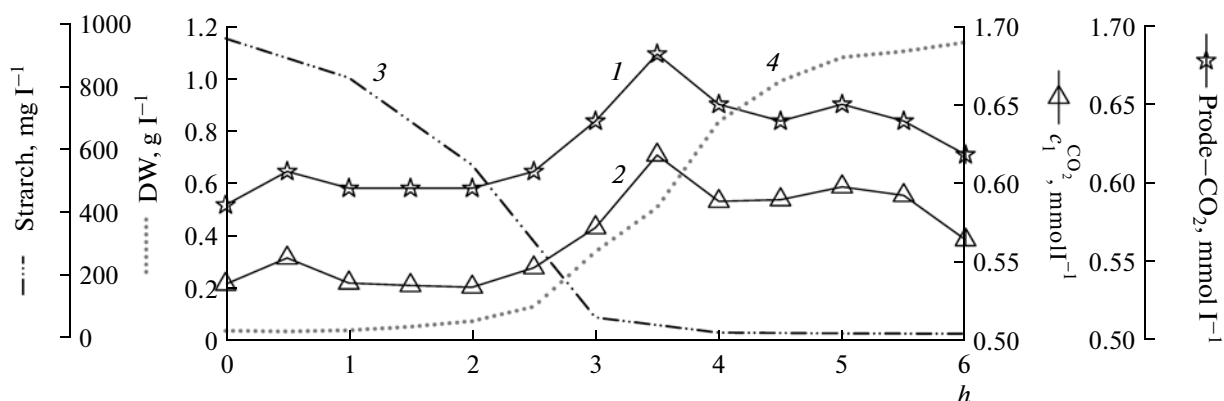
Fig. 4. Comparison between the CO_2 concentration measured directly with the in situ CO_2 probe (*1*) and the concentration calculated using data from the exhaust gas measurement (*2*); starch concentration (*3*) and growth of the culture as dry weight (*4*).

of amylase and protease (both hydrolases) indicates the importance of a fast and reliable CO_2 measurement in the bioreactor at 70°C. Two methods for estimation of dissolved CO_2 concentrations during thermophilic production of amylase and protease by *B. caldolyticus* were utilized and compared in this work. The first one involved an in situ measurement by CO_2 probe that offers potential for direct real time measurements of non-ionic forms of CO_2 in culture broth. The second method involved analysis of exit gas composition. This method, however, requires removal of water vapors from gas phase before exhaust gas analyses. The composition of dissolved CO_2 was then determined using equations (5 to 9) suggested by Royce and Thornhill in 1991 [15].

The measured and the calculated concentrations of dissolved CO_2 during an experiment with room air containing 5% CO_2 are presented in Fig. 4. Note the congruence between the two methods of measurement of dissolved CO_2. Still, the dissolved CO_2 values obtained from the probe signal are considerably higher than those predicted from exhaust gas composition. This observation is in qualitative agreement with those of Dahod [20] who also reported that probe-measured dissolved CO_2 concentrations in high cell density fermentation were higher than the values calculated using exhaust gas analyses. Dahod [20] found that the measured concentrations of CO_2 were 90% higher than those calculated using the exhaust gas analysis by the procedure suggested by Royce and Thornhill [15]. These differences could be a result of the factor of 0.89 attributed to the ratio of $k_L a$ for CO_2 mass transfer and $k_L a$ for O_2 mass transfer in equations (1 to 5). Another potential explanation can be the effect of medium constituents on Henry law constants (equations 6 and 7).

In our knowledge, the application of a fluorescence based CO_2 probe at high temperatures has been not published before. It is often suggested the fluores-

cence-based in-situ CO_2 probes have low temperature tolerance. The observations of this work that the measurements by the in situ fluorescence-based probe and the calculations based on exhaust gas analyses are congruent, however, suggest that the probe is a reliable and cost efficient method of monitoring the dissolved carbon dioxide concentration even under temperature as high as 70°C.

A positive influence of carbon dioxide was observed on the formation of α-amylase and neutral protease during batch fermentations of *B. caldolyticus*. Increasing the fraction of carbon dioxide in inlet air from 0.038% to 5% (v/v) resulted in a 22% increase of α-amylase activity in culture broth, although no change in the biomass production was revealed. When the content of CO_2 was increased further to 10% (v/v), the cell growth remained unchanged but the enhancement in amylase production was lost. On the other hand, protease activity continued to increase as the CO_2 fraction was increased. A major positive effect observed during the fermentations with 5% CO_2 was reduction of lag-phase by more than 1 h resulting in even higher enzyme productivity. Further investigations are necessary to explain the observed positive influence of CO_2 on metabolic level. In addition, a fluorescence-based in situ probe was found to stably measure dissolved CO_2 concentration even at 70°C. To our knowledge, such application of fluorescence based probes for the reliable in situ measurement of dissolved carbon dioxide at a fermentation temperature of 70°C has been reported here for the first time.

REFERENCES

1. Sivaramakrishnan, S., Gangadharam, D., Nampoothiri, K.M., Soccol, C.R., and Pandey, A., *Food Technol. Biotechnol.,* 2006, vol. 44, no. 2, pp. 173−184.

2. Shivanand, P. and Jayaraman, G., *Proc. Biochem.*, 2009, vol. 44, pp. 1088−1094.

3. Schwab, K., Bader, J., Brokamp, C., Popović, M.K., Bajpai, R., and Berovic, M., *New Biotech.*, 2009, vol. 26, no. 1−2, pp. 68−74.

4. Jones, R.P. and Greenfield, P.F., *Enzyme Microb. Technol.,* 1982, vol. 4, pp. 210−223.

5. Bäumchen, C., Knoll, A., Husemann, B., Seletzky, J., Maier, B., Dietrich, C., Amoabediny, G., and Büchs, J., *J. Biotechnol.,* 2007, vol. 128, pp. 868−874.

6. Luca, S.F. and Brückner, H., *Branntweinwirtschaft*, 1994, vol. 2, pp. 174−181.

7. Nishikido, T., Izui, K., Iwatani, A., Katsuki, H., and Tanaka, S., *J. Biochem.*, 1968, vol. 63, no. 4, pp. 532−541.

8. McLean, D.J.and Purdie, E.F., *J. Bacteriol.*, 1955, vol. 69, no. 2, pp. 204−209.

9. Gandhi, A.P. and Kjaergaard, L., *Biotechnol. Bioeng.*, 1975, vol. 17, pp. 1109−1118.

10. Zajic, J.E., Volesky, B., and Wellman A., *Can. J. Microbiol.*, 1969, vol. 15, no. 10, pp. 1231−1236.

11. Narahara, H., Koyama, Y., Yoshida, T., Pichangkura, S., Ueda, R., and Taguchi, H., *J. Ferment. Technol.*, 1982, vol. 60, no. 4, pp. 311−319.

12. Mudgett, R.E. and Bajracharya, R., *J. Food Biochem.*, 1980, vol. 3, no. 2−3, pp. 135−150.

13. Manning, G.B. and Campbell, L.L., *J. Biol. Chem.*, 1961, vol. 236, no. 11, pp. 2952−2957.

14. Strydom, E., Mackie, R.I., and Woods, D.R., *Appl. Microbiol. Biotechnol.*, 1986, vol. 24, no. 3, pp. 214−217.

15. Royce, P.N.C. and Thornhill, N.F., *AIChE Journal,* 1991, vol. 37, no. 11, pp. 1680−1686.

16. Gaffney, P.E., *Appl. Microbiol.*, 1965, vol. 13, no. 4, pp. 507−510.

17. Stretton, S. and Goodman, A.E., *Antonie van Leeuwenhoek.* 1998, vol. 73, no. 1, pp. 79−85.

18. Drysdale, M., Bourgogne, A., and Koehler, T.M., *J. Bacteriol.*, 2005, vol. 187, no. 15, pp. 5108−5114.

19. Kaszab, I., Hogye, I., Komocsi, S., and Szilagyi, J., *Process Biochem.*, 1981, vol. 16, no. 2, pp. 38−49.

20. Dahod, S.K., *Biotechnol. Prog.*, 1993, vol. 9, no. 6, pp. 655−660.

RHAMNOLIPID PRODUCTION BY *Pseudomonas aeruginosa* ENGINEERED WITH THE *Vitreoscilla* HEMOGLOBIN GENE

© 2012   H. Kahraman, S. O. Erenler

Department of Biology, Faculty of Art and Science, Inonu University, Malatya 44280, Turkey
e-mail: huseyin.kahraman@inonu.edu.tr, sebnem.erenler@inonu.edu.tr

The potential of *Pseudomonas aeruginosa* expressing the *Vitreoscilla* hemoglobin gene (*vgb*) for rhamnolipid production was studied. *P. aeruginosa* (NRRL B-771) and its transposon mediated *vgb* transferred recombinant strain, PaJC, were used in the research. The optimization of rhamnolipid production was carried out in the different conditions of cultivation (agitation rate, the composition of culture medium and temperature) in a time-course manner. The nutrient source, especially the carbon type, had a dramatic effect on rhamnolipid production. The PaJC strain and the wild type cells of *P. aeruginosa* started producing biosurfactant at the stationary phase and its concentration reached maximum at 24 h (838 mg/l^{-1}) and at 72 h (751 mg l^{-1}) of the incubation respectively. Rhamnolipid production was optimal in batch cultures when the temperature and agitation rate were controlled at 30°C and 100 rpm. It reached 8373 mg l^{-1} when the PaJC cells were grown in 1.0% glucose supplemented minimal media. Genetic engineering of biosurfactant producing strains with *vgb* may be an effective method to increase its production.

Microbial surfactants have many advantages over the chemical analogs. Lower toxicity for organisms and environment, biodegradability, high selectivity and specific activity at extreme conditions are just a few to mention [1–2]. Further, the ability of microorganisms to synthesize these compounds from renewable feedstock makes biosurfactants economically comparable to chemical synthesis. Biosurfactants are of increasing industrial interest because of their broad range of potential applications, including emulsification, wetting, phase separation, and viscosity reduction. They belong to a group of secondary metabolites with surface active properties and are synthesized by a great variety of microorganisms. These metabolites are complex amphiphilic molecules whose hydrophobic and polar domains depend on the carbon substrate and the type of microorganism used [3]. A large variety of microbial surface active compounds are produced by bacteria, yeasts, and fungi [4, 5]. Rhamnolipids are the most effective among them today [6]. Many potential applications of these compounds have been described. They have been shown to exhibit antimicrobial activity against competing microorganisms, to be ejective in biological control of zoosporic phytopathogens, and to facilitate the removal of heavy metals from soil [7]. The type and proportion of the rhamnolipids produced depends on the bacterial strain, the carbon source used and the culture conditions. The genus *Pseudomonas* is capable of using different substrates, such as glycerol, mannitol, fructose and glucose, to produce rhamnolipid type biosurfactants [8–10]. *Pseudomonas aeruginosa* is an environmental bacterium that can be isolated from many different habitats, including water, soil, and plants, where it survives due

to its extraordinary metabolic abilities. This bacterium was shown by Jarvis and Johnson [11] to produce the biosurfactant rhamnolipids, which are amphiphilic molecules composed of a hydrophobic fatty acid moiety and a hydrophilic portion composed of one or two rhamnose molecules [12, 13]. Rhamnolipids from *P. aeruginosa* have been studied extensively. They produce two types of rhamnolipids containing two rhamnoses attached to β-hydroxydecanoic acids or one rhamnose connected to the identical fatty acid from glucose and hydrocarbon substrates. Mono- and di-rhamnolipids have quite different physicochemical properties [3, 7, 14]. Rhamnolipids from *P. aeruginosa* are glycolipid biosurfactants produced during growth phase especially in stationary phase of growth on hydrocarbons or carbohydrates as the sole carbon source [15, 16]. It was shown that their production is under quorum sensing control [17] and depends on several environmental and nutritional factors, including nitrogen and iron limitation, pH, and temperature [18]. The stimulating effect of rhamnolipid was attributed to enhanced transport of substrate to the bacteria and its inhibitory effect induced flocculation of the cells. It is known that the stimulation of many *P. aeruginosa* strains is more pronounced for rhamnolipid than for other surfactants [19].

Vitreoscilla hemoglobin (VHb) is the first well characterized prokaryotic hemoglobin. The role of VHb in bacteria is to raise the effective dissolved oxygen tension within the cells and to scavenge and release oxygen to terminal oxidases during oxygen-limited growth conditions. Bacteria engineered with the *vgb* gene had 2.0- to 10-fold higher oxygen uptake rates than the *vgb*$^{-}$ counterparts [20]. It has been demon-

strated that expression of bacterial hemoglobin VHb in heterologous bacterial hosts engineered by *vgb* gene often results in enhancement of cell density, oxidative metabolism, protein and antibiotic production, and bioremediation, especially under oxygen limiting conditions [21].

The aim of the study was to optimize the production of rhamnolipid by *P. aeruginosa* and its *vgb* transferred recombinant strain, PaJC in different conditions of cultivation including various carbon sources, agitation rate and temperature.

MATERIALS AND METHODS

Chemicals. L-(+)-rhamnose monohydrate was purchased from MP Chemicals (USA). Phenol, H_2SO_4 and $NaHCO_3$ were obtained from Carlo Erba Chemicals (Italy). Ethyl acetate was purchased from Riedelde Haen Chemicals (Germany). All other chemicals used were of analytical grade.

Bacterial strains. *P. aeruginosa* (NRRL B-771) and its transposon mediated *vgb* transferred recombinant strain, PaJC [22] were used in the study (PaJC strain was obtained from Illinois Institute of Technology (USA) Benjamin C. Stark, Ph.D. Professor of Biology).

Cultivation of bacteria for rhamnolipid production. For rhamnolipid production the bacteria were cultivated in LB medium (g l^{-1}): peptone − 10.0; NaCl − 10.0 and yeast extract − 5.0; or in mineral salts medium (MM) (g l^{-1}): KH_2PO_4 − 0.7; Na_2HPO_4 − 0.9; $CaCl_2$ − 0.1; $FeSO_4$ − 0.001; $NaNO_3$ − 2.0; and $MgSO_4 \cdot 7H_2O$ − 0.4 [7], both at pH 7.0. MM was supplied with selected carbon sources (glucose, sucrose and glycerol). Autoclaved separately, carbon sources were added to MM at a final concentration of 1.0%. The effect of carbon sources on rhamnolipid production was also determined in LB with 1.0% glucose (LBG). 250 µl of overnight cultures grown in 20 ml LB or carbon supplemented MM in 125 ml Erlenmeyer flasks was inoculated into 50 ml of the medium in 150 ml volume flasks. Shake-flasks were incubated at 30 or 37°C in a 100 or 200 rpm in a gyratory water-bath, drawing the samples at certain intervals 12, 24, 48, and 72 h.

Rhamnolipid extraction and assay. At selected intervals, 3 ml culture was withdrawn and centrifuged at 10 000 *g* for 10 min at 4°C. The supernatant was pipetted into a new set of 10 ml plastic tubes. The pH of supernatant was adjusted to 2.0 with 1 M HCl. After adding an equal volume of ethyl acetate, the mixture was briefly vortexed and left at room temperature for 20 min. The aqueous phase (i.e., the lower phase) was discarded by dipping a pipette through the organic phase (i.e., the upper phase). The solvent organic phase was evaporated in about 4−5 h at 55°C. The dry material was dissolved in 1 ml 0.1 M $NaHCO_3$, pH 8.6 [23].

The rhamnolipid level of cell-free cultures was determined using the phenol sulfuric acid method [24].

250 µl of mixture containing $NaHCO_3$ was pipetted into 5 ml glass tubes and after adding 250 µl of 5.0% phenol and a brief vortexing, 1.25 ml of concentrated H_2SO_4 was added, gently vortexed and left at room temperature for 20 min for color development. The color intensity of each sample was read at 480 nm against a blank (i.e., the sample missing the rhamnolipid material) and the rhamnolipid level in each sample was determined from a standard curve utilizing rhamnose.

Each value is the average of at least 3 independent experiments. For clarity, no error bars are given on the figures, but they are mostly less than 10% of the respective data point.

Rhamnolipid content was calculated by multiplying the rhamnose concentration by a factor of 3. This factor was calculated experimentally using rhamnose calibration curve, representing rhamnolipid/rhamnose correlation [25].

RESULTS AND DISCUSSION

Rhamnolipid production in various media with glucose as a carbon source − effect of temperature and agitation. As the agitation rate and temperature are two leading factors and crucial for the cell growth and rhamnolipid formation, *P. aeruginosa* and its *vgb* bearing strain (PaJC) were cultivated in shake flasks under different agitation rates (100 and 200 rpm) and temperature (30 and 37°C). The cell density in MM was significantly lower than in complex LB medium (data not shown). For the cultures grown in LB at 37°C, the agitation rates had no significant effect on rhamnolipid production (Fig. 1b), while at 30° C there was nearly 2-fold rhamnolipid increase at higher agitation rate (200 rpm) (Fig. 1a). Rhamnolipid levels (drawn as the average from the values at all incubation time points, i.e., 12, 24, 48, and 72 h) of *P. aeruginosa* and PaJC in both media, however, showed a similar trend (Figs. 1c and 2a). At 37°C and 100 rpm agitation, the average level of rhamnolipid in LBG (LB + 1% glucose) cultures were 973 (±27) and 982 (±16) mg l^{-1} for *P. aeruginosa* and PaJC, respectively. These values were 1061 (±20) and 1065 (±51) mg l^{-1} in that respect at 200 rpm agitation (Fig. 1d). The average level of rhamnolipid in MM plus 1% glucose cultures grown at 37°C was 1012 (±40) and 1060 (±34) mg l^{-1} at 100 rpm, 980 (±14) and 969 (±32) mg l^{-1} at 200 rpm agitation for *P. aeruginosa* and PaJC, respectively (Fig. 2b). The temperature effect on rhamnolipid accumulation was even more pronounced in LBG. Both strains had a substantial increase in rhamnolipid at 30°C. Compared with cultures at 37°C (Fig. 1d), there was up to 7-fold rhamnolipid increase at 30°C (Fig. 1c). Being a product of secondary metabolism, rhamnolipid production in both media started after stationary phase and generally leveled up at 48 h. In LBG cultures at 30°C under 100 rpm agitation, the average rhamnolip-
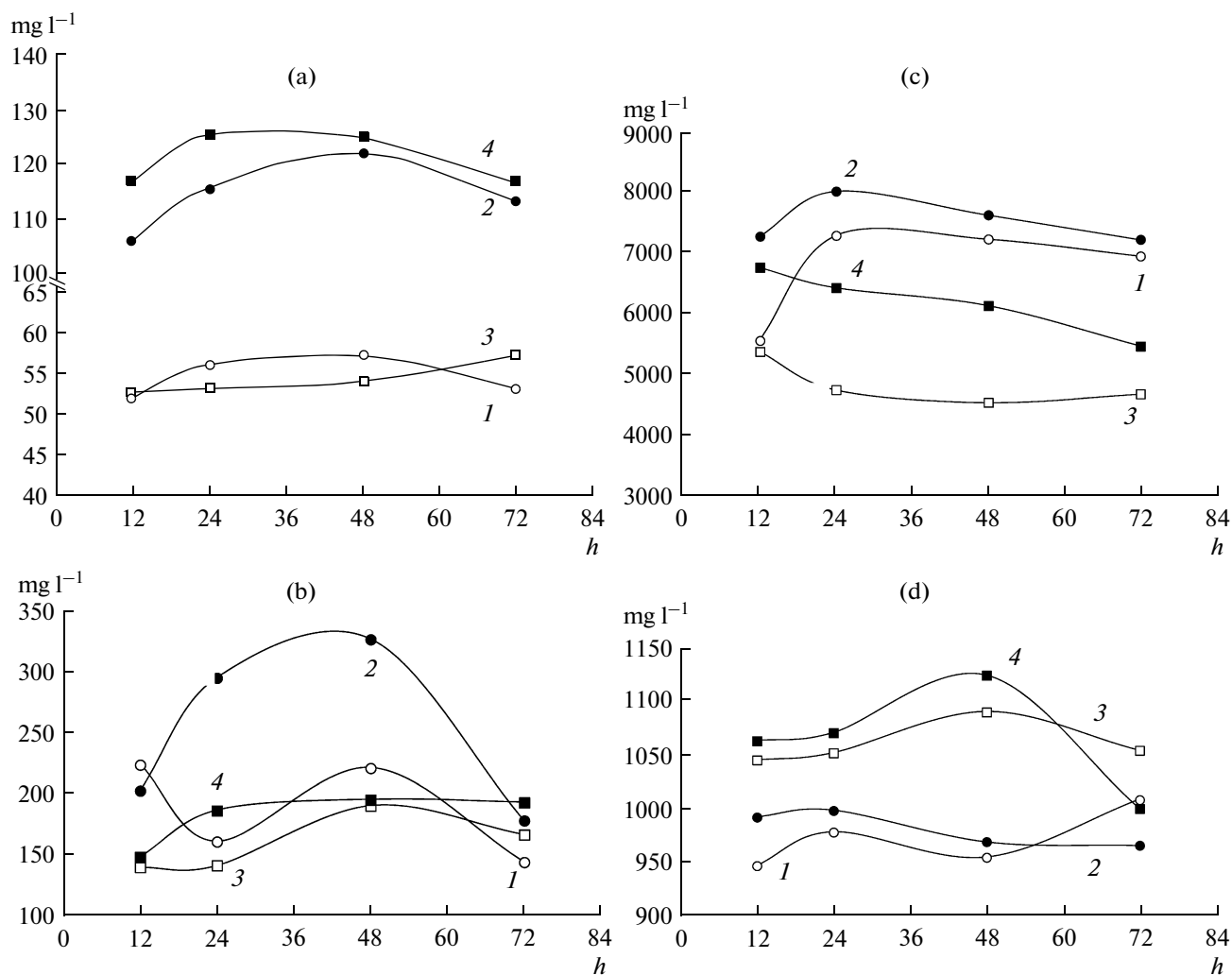
Fig. 1. Rhamnolipid levels of *P. aeruginosa* and its *vgb* recombinant strain, PaJC, under different agitation conditions at 30 (a, c) and 37°C (b, d), grown in LB (a, b) and LB supplemented 1% glucose (c, d) culture medium. *1* — *P. aeruginosa,* 100 rpm; *2* — PaJC, 100 rpm; *3* — *P. aeruginosa*, 200 rpm, *4* — PaJC, 200 rpm.

id values were 6765 (±811) and 7543 (±367) mg l⁻¹ for *P. aeruginosa* and PaJC, respectively. These values were 4847 (±370) and 6207 (±551) mg l⁻¹ during cultivation at 200 rpm. In MM plus 1% glucose medium at 30°C (Fig. 2a), *P. aeruginosa* showed a rhamnolipid level of 6918 (±643) and PaJC 7593 (±857) mg l⁻¹ under 100 rpm, while these values were 3884 (±714) and 5827 (±781) mg l⁻¹ for *P. aeruginosa* and PaJC, respectively, under 200 rpm.

Effect of other carbon sources on rhamnolipid production. Two carbon sources other than glucose (glycerol and sucrose) were also investigated for their effectiveness on rhamnolipid production. *P. aeruginosa* and PaJC in glycerol supplemented (1%) MM medium (Fig. 2c) showed an average 9.2 and 9.3-fold lower rhamnoipid values, respectively, than their counterparts in glucose supplemented medium (Fig. 2a) under similar physical conditions (i.e., 30°C and 100 rpm). At the same temperature but 200 rpm agitation, they were 3.8

and 4.0 fold in that respect. Under both agitation rates (100 and 200 rpm) the glycerol cultures grown at 37°C (Fig. 2d), however, showed similar level of rhamnolipid to the glucose cultures (Fig. 2b) under the same agitations.

Sucrose was a much better substrate for rhamnolipid production compared to glycerol. As it is apparent from Fig. 3a, the level of rhamnolipid in *P. aeruginosa* and PaJC cultures in sucrose supplemented MM medium (30°C and 100 rpm) was 5.3 and 3.5-fold higher than for the respective cultures in glycerol (Fig. 2c). At the same temperature but 200 rpm agitation, these values were 3.5 and 4.8-fold in favor of sucrose. These differences between glycerol and sucrose, however, were not observed at 37°C 100 rpm cultures, while *P. aeruginosa* and the PaJC cells showed 3.5 and 2.9-fold higher rhamnolipid levels than the corresponding cultures in glycerol at 200 rpm agitation (Figs. 3b and 2d).
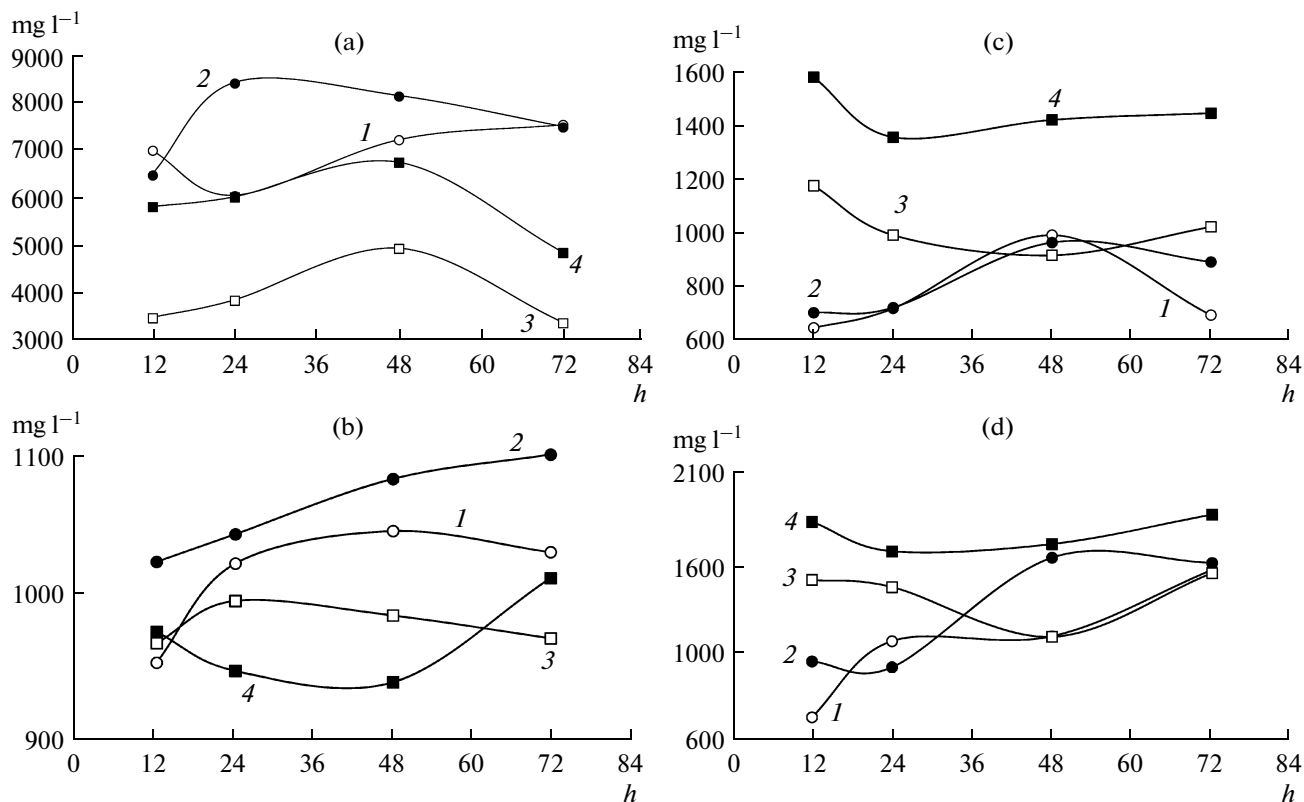
Fig. 2. Rhamnolipid levels of *P. aeruginosa* and its *vgb* recombinant strain, PaJC, under different agitation conditions at (a, c) 30°C and (b, d) 37°C, grown in MM supplemented 1% glucose (a, b) and 1% glycerol (c, d). *1* − *P. aeruginosa,* 100 rpm, *2* − PaJC, 100 rpm, *3* − *P. aeruginosa*, 200 rpm, *4* − PaJC, 200 rpm.

LB medium used since it is one of the most commonly adopted culture media for *P. aeruginosa* strains [23]. As it shown in Fig. 1c at 30°C and 100 rpm, PaJC started producing rhamnolipid at the stationary phase and the concentration of rhamnolipid reached its maximum 8373 mg l⁻¹, at the 24 h of the incubation. *P. aeruginosa*, started producing rhamnolipid at the stationary phase and the concentration of rhamnolipid reached maximum (7507 mg l⁻¹) at the 72 h of the incubation (Fig. 1c). Agitation rate affects the mass transfer efficiency of both oxygen and medium components and is considered crucial to the rhamnolipid formation of the strictly aerobic bacterium *P. aeruginosa* and its recombinant strain, especially when it was grown in a shake flask. *P. aeruginosa* has been used carbon sources such as fructose, lactic acid, glucose, mannitol, mannose and glycerol [9]. Under 37°C, the recombinant strain improved the maximum rhamnolipid level in the MM +1% sucrose, MM +1% glycerol, LB +1% glucose, respectively. At 30°C, the same advantages of the recombinant strain were rhamnolipid production in MM +1% glucose, MM +1% sucrose, and MM +1% glycerol, respectively. Therefore, it would be more economical to use 30°C in practical applications. Rhamnolipid production was optimal in batch cultures when the temperature and agitation rate were controlled at 30° C and 200 rpm, respective-

ly [23]. Increase in agitation rate from 100 to 200 rpm indicates that elevation of dissolved oxygen level seemed to have a positive effect on rhamnolipid production. Normal aeration, however, supported the higher surfactant production of both bacterial strains than limited aeration. This is consistent with the fact that rhamnolipid production was inefficient under oxygen-limiting conditions [6]. This further supports that MM gave the higher rhamnolipid production and the difference between *vgb*-bearing and untransformed strains was greater at normal than at limited aeration. In the case of PaJC, the positive effects (rhamnolipid production) are similar or greater at normal versus limited aeration. Most rhamnolipids were found to accumulate at the stationary stage of cell growth. Their accumulation in the supernatant started at the end of the logarithmic phase because rhamnolipids are secondary metabolites.

Rhamnolipid production by bacteria grown in the medium with glucose or sucrose is much higher than that with other substrates including glycerol. It differs from the results of Monteiro et al. [26] obtained 3.9 g l⁻¹ of a rhamnolipid type biosurfactant or Rashedi et al. [9] and Santa Anna et al. [8] shown the production 690 mg l⁻¹ and 2650 mg l⁻¹ rhamnolipid by *P. aeruginosa* grown in the medium containing 1.0% and 3.0%
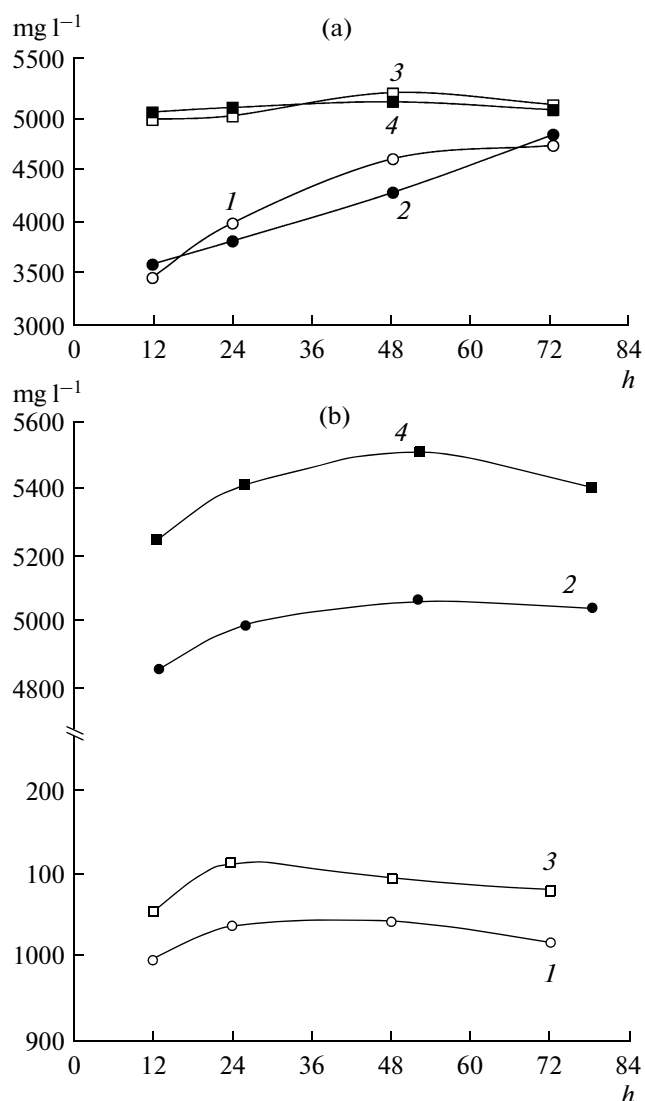
Fig. 3. Rhamnolipid levels of *P. aeruginosa* and its *vgb* recombinant strain, PaJC, under different agitation conditions at (a) 30°C and (b) 37°, grown in MM supplemented 1% sucrose. *1 – P. aeruginosa,* 100 rpm, *2 –* PaJC, 100 rpm, *3 – P. aeruginosa*, 200 rpm, *4 –* PaJC, 200 rpm.

glycerol as a carbon and energy source respectively. Besides that, Wei et al. worked with the strain *P. aeruginosa*, which produced ramnolipid (733 mg l^{-1}) when grown in LB media [23]. According to our results, *P. aeruginosa* produced rhamnolipid (326 mg l^{-1}) when grown in LB media. The poor performance of the rich media (LB) on rhamnolipid production may be attributed to their abundance in nitrogen sources, which are known to limit rhamnolipid production [27]. Thus, at 72 h of incubation, where the PaJC strain showed slightly better rhamnolipid production than *P. aeruginosa*. The results show that PaJC strain was able to produce rhamnolipid efficiently with in 1.0% glucose supplemented MM. When LB media was used the final pH reached values 9.0 (data not

shown). Our results are in agreement with those obtained by Gautam and Tyagi who shown that rhamnolipid production in *Pseudomonas* sp. was maximal at a pH range from 6 to 6.5 and decreased sharply above pH 7 [28].

The PaJC cells exhibit favorable properties including enhanced rhamnolipid productivity over the wild strain. In this work glucose and sucrose were the most effective carbon sources for rhamnolipid production. As a result, genetic engineering of rhamnolipid producing strains with *vgb* may be an effective method to.

REFERENCES

1. Maier, R.M., *Adv. Appl. Microbiol.*, 2003, vol. 52, pp. 101−121.
2. Rodrigues, L., Banat, I.M., Teixeira, J., and Oliveira, R., *J. Antimicrob. Chemother.*, 2006, vol. 57, no. 4, pp. 609−618.
3. Lang, S., *Curr. Opin. Colloid. Interface Sci.*, 2002, vol. 7, pp. 12−20.
4. Ochsner, U.A., Hembach, T., and Fiechter, A., *Adv. Biochem. Eng. Biotechnol.*, 1996, vol. 53, pp. 89−118.
5. Katemai, W., Maneerat, S., Kawai, F., Kanzaki, H., Nitoda, T., and H-Kittikun, A., *J. Gen. Appl. Microbiol.*, 2008, vol. 54, no. 1, pp. 79−82.
6. Chayabutra, C., Wu, J., and Ju, L., *Biotechnol. Bioeng.*, 2001, vol. 72, no. 1, pp. 25−33.
7. Deziel, E., Lepine, F., Dennie, D., Boismenu, D., Mamer, O. A., and Villemur, R., *Biochim. Biophys. Acta*, 1999, vol. 1440, no. 2−3, pp. 244−252.
8. Santa Anna, L.M., Sebastian, G.V., Menezes, E.P., Alves, T.L.M., Santos, A.S., Pereira Jr.N., and Freire, D.M.G., *Braz. J. Chem. Eng.*, 2002, vol. 19, no. 2, pp. 159−166.
9. Rashedi, H., Jamshidi, E., Mazaheri Assadi, M., and Bonakdarpour, B., *Int. J. Environ. Sci. Tech.*, 2005, vol. 2, no. 2, pp. 121−127.
10. Rashedi, H., Mazaheri Assadi, M., Jamshidi, E., and Bonakdarpour, B., *Int. J. Envior. Sci. Tech.*, 2006, vol. 3, no. 3, pp. 297−303.
11. Jarvis, F.G., and Johnson M.J., *J. Am. Chem. Soc.*, 1949, vol. 71, no. 12, pp. 4124−4126.
12. Gunther N.W., Nunez, A., Fett, W., and Solaiman, D.K.Y., *Appl. Environ. Microbiol.*, 2005, vol. 71, no. 5, pp. 2288−2293.
13. Soberón-Chávez, G., Lépine, F., and Déziel, E., *Appl. Microbiol. Biotechnol.*, 2005, vol. 68, no. 6, pp. 718−725.
14. Perfumo, A., Banat, I.M., Canganella, F., and Marchant, R., *Appl. Microbiol. Biotechnol.*, 2006, vol. 72, no. 1, pp. 132−138.
15. Ochsner, U.A., and Reiser, J., *Proc. Natl. Acad. Sci.*, 1995, vol. 92, no. 14, pp. 6424−6428.
16. Sullivan, E.R., *Curr. Opin. Biotechnol.*, 1998, vol. 9, pp. 263−269.
17. Caiazza, N.C., Shanks, R.M.Q., and O'Toole, G.A., *J. Bacteriol.*, 2005, vol. 187, no. 21, pp. 7351−7361.
18. Ochsner, U.A., Fiechter, A., and Reiser, J., *J. Biol. Chem.*, 1994, vol. 269, no. 31, pp. 19787−19795.

19. Noordman, W.H., Wachter, J.H.J., de Boer, G.J., and Janssen, D.B., *J. Biotechnol.*, 2002, vol. 94, no. 2, pp. 195−212.

20. Geckil, H. and Gencer, S., *Appl. Microbiol. Biotechnol.*, 2004, vol. 63, no. 6, pp. 691−697.

21. Dogan, I., Pagilla, K.R., Webster, D.A., and Stark, B.C., *J. Ind. Microbiol. Biotechnol.*, 2006, vol. 33, no. 8, pp. 693−700.

22. Chung, J.W., Webster, D.A., Pagilla, K.R., and Stark, B.C., *J. Ind. Microbiol. Biotechnol.*, 2001, vol. 27, no. 1, pp. 27−33.

23. Wei, Y., Chou, C., and Chang, J., *Biochem. Eng. J.*, 2005, vol. 27, no. 2, pp. 146−154.

24. Dubois, M., Gilles, K.A., Hamilton, J.K., Rebers, P.A., and Smith, F., *Anal. Chem.*, 1956, vol. 28, no. 3, pp. 350−356.

25. Abalos, A., Maximo, F., Manresal, M.A., and Bastida, J., *J. Chem. Technol. Biotechnol.*, 2002, vol. 77, no. 7, pp. 777−784.

26. Monteiro, S.A., Sassaki, G.L., de Souza, L.M., Meira, J.A., de Araujo, J.M., Mitchell, D.A., Ramos, L.P., and Krieger, N., *Chem. Phys. Lipids*, 2007, vol. 147, no. 1, pp. 1−13.

27. Lang, S. and Wullbrandt, D., *Appl. Microbiol. Biotechnol.*, 1999, vol. 51, no. 1, pp. 22−32.

28. Gautam, K.K. and Tyagi, V.K., *J. Oleo Sci.*, 2006, vol. 55, no. 4, pp. 155−166.

ПРОЛОНГИРОВАННОЕ КУЛЬТИВИРОВАНИЕ АНАЭРОБНОГО СООБЩЕСТВА БАКТЕРИЙ, ПРОДУЦИРУЮЩЕГО ВОДОРОД

© 2012 г.   Б. Ф. Белокопытов, Я. В. Рыжманова, К. С. Лауринавичюс, В. А. Щербакова

Институт биохимии и физиологии микроорганизмов им. Г.К. Скрябина РАН, Пущино, Московская обл., 142290
e-mail: shcherb@ibpm.pushchino.ru

Исследованы различные способы длительного поддержания процесса выделения водорода при выращивании анаэробного сообщества бактерий на крахмалсодержащей среде. При культивировании в режиме отъемно-доливной ферментации в течение 72 сут образовывалось от 0.10 до 0.23 л H_2/л среды/сут. Режим регулярных пересевов продолжался более 100 сут с образованием в среднем 0.81 л H_2/л среды/сут. Выявлены достоинства и недостатки различных способов микробиологического получения водорода в темновом процессе сбраживания крахмала. Из сформированного H_2-образующего сообщества микроорганизмов выделена анаэробная спорообразующая бактерия, штамм BF. Филогенетический анализ последовательности гена 16S рРНК нового штамма показал, что по своим генотипическим свойствам он относится к виду *Clostridium butyricum*.

Развитие современной энергетики предполагает активное внедрение различных, альтернативных ископаемым, экологически чистых источников энергии, одним из которых является водород. Получать водород можно химическими, физико-химическими, фотохимическими и микробиологическими методами. Микробиологический водород (биоводород) продуцируют анаэробные и факультативно-анаэробные бактерии при брожении (темновой процесс) в мезофильных и термофильных условиях, а также он образуется фотосинтезирующими бактериями (светозависимый процесс) [1, 2]. Основная часть проектов [3–5] по получению биоводорода, реализуемых в настоящее время, как в России, так и за рубежом, направлена на разработку систем, состоящих из биореактора для темнового образования водорода сообществами анаэробных бактерий и биореактора для светозависимого образования водорода фотосинтетиками. Важными условиями обеспечения рентабельности производственного процесса получения биоводорода, с одной стороны, является доступность и дешевизна сырья и его переработки, с другой стороны — возможность поддержания процесса достаточно длительное время на высоком уровне производительности. Как показали исследования последних лет, крахмалсодержащее сырье и отходы являются коммерчески привлекательным исходным субстратом для бактериального получения водорода [6–8], но с технологической точки зрения его использование анаэробными бактериями еще не достаточно изучено.

Цель работы — выбор способа проведения анаэробной ферментации крахмала для получения водорода сообществом анаэробных бактерий и таксономическое определение бактерий, играющих ключевую роль в исследуемом сообществе микроорганизмов.

МЕТОДИКА

Объект исследования. Исследовали анаэробное сообщество микроорганизмов ризосферы травяных растений, сформированное при культивировании на крахмалсодержащей среде в мезофильных условиях и представляющее смешанную культуру спорообразующих бактерий. Перед использованием в экспериментах микробное сообщество прошло длительную (более 10 пересевов) адаптацию к условиям культивирования.

Среды и условия культивирования. Ферментации анаэробного сообщества и выделение чистой культуры анаэробных бактерий проводили на среде KM следующего состава (г/л): крахмал — 20, K_2HPO_4 — 5.0, KH_2PO_4 — 5.0, NaCl — 0.9, $MgCl_2 \cdot 6H_2O$ — 0.2, $CaCl_2 \cdot 2H_2O$ — 0.1, $FeCl_2 \cdot 4H_2O$ — 0.15, $ZnCl_2$ — 0.01, L-серин — 1.0, L-цистеин · HCl — 0.5, раствор микроэлементов — 10 мл, раствор витаминов - 10 мл. Раствор микроэлементов содержал (мг/л): $FeSO_4 \cdot 7H_2O$ — 5.0, $MnCl_2 \cdot 4H_2O$ — 1.0, $CoCl_2 \cdot 6H_2O$ — 1.7, $CaCl_2 \cdot 2H_2O$ — 1.0, $ZnCl_2$ — 0.1, $CuCl_2$ — 0.1, H_2BO_3 — 0.1, Na_2MoO_4 — 0.1, NaCl — 10.0, Na_2SeO_3 — 0.17, $NiCl_2$ — 5.0, Na_2WO_4 — 1.0, нитрилотриуксусная кислота — 128.0. Раствор витаминов содержал (мг/л): биотин — 0.02, тиамин · HCl (B_1) — 0.05, п-аминобензойная кислота — 0.05, пиридоксин · HCl — 0.1, рибофлавин — 0.05, никотиновая кислота — 0.05, пантотеновая кисло-

та — 0.05, липоевая кислота — 0.05, фолиевая кислота — 0.02, цианокобаламин — 0.001.

Культивирование. Выращивание смешанной культуры бактерий осуществляли в медицинских флаконах на 500 мл и объемом среды 200 мл. Флаконы герметично закрывали специальными резиновыми пробками и алюминиевыми колпачками. Кислород из газовой фазы удалялся вакуумированием в течение 3 мин. Стерилизацию сред проводили автоклавированием в режиме 0.5 атм в течение 30 мин. Ферментацию осуществляли без перемешивания при 37°С. Посевной материал пастеризовали прогреванием культуры при 80°С в течение 10 мин и добавляли к среде в количестве 1—10%.

Для выделения чистой культуры водородобразующей бактерии использовали анаэробную технику Хангейта [9]. Получение чистой культуры вели повторными рассевами на среду КМ с добавлением 20 г/л агара ("Difco", США) на чашках Петри, помещенных в анаэростат ("Oxoid", Великобритания), с прогреванием и повторным выделением колоний.

Параметры роста. Рост определяли по оптической плотности культуральной жидкости на спектрофотометре "Spekol 201" ("ANALYTIK JENA AG", ГДР), длина оптического пути составляла 1 см, длина волны 600 нм. pH среды и культуральной жидкости определяли на ионометре Анион 4101 ("Инфраспак-Аналит", Россия), заданный диапазон pH 6.2—6.5 поддерживали добавлением 50%-ного раствора КОН.

Микроскопия. Морфологию культур изучали на препаратах типа раздавленная капля с глицериновой иммерсией в режиме фазового контраста при увеличении в 1000 раз. Препараты просматривались регулярно на оптическом микроскопе ("Carl Zeiss — Axiostar plus", Германия).

Аналитические методы. Объем образующегося газа определяли по количеству вытесненной им воды [10]. Концентрацию водорода в выходящем газе измеряли на газовом хроматографе ЛХМ80 ("МПО Манометр", Россия) с использованием катарометра и стеклянной колонки (1 м × 3 мм), заполненной молекулярными ситами, 30—40 меш. Температура колонки, инжектора и детектора составляла 40°С. В качестве газа-носителя использовали аргон, скорость потока 20 мл/мин. Пробу газа объемом 5 мл помещали в герметичный пенициллиновый флакон, заполненный водой, и хранили в перевернутом виде до определения.

Определение нуклеотидной последовательности гена 16S рРНК. Выделение ДНК из биомассы бактерий проводили по методике, описанной ранее [11]. Для амплификации фрагмента гена 16S рРНК использовали универсальные праймеры 27f (5'-AGAGTTTGATCCTGGCTCAG—3'), 1429R (5'-ACGG(Y)TACCTTGTTACGACTT—3') и 515—

533F (5'-GTGCCAGC(M)GCCGCGGTAA-3'). Полимеразную цепную реакцию (**ПЦР**) проводили на амплификаторе Терцик ("ДНК-Технология", Россия). Для получения ПЦР-фрагментов применяли следующий температурно-временной режим: начальная денатурация — 94°С, 3 мин; последующие 30 циклов — 94°С — 20 с, 55°С — 10 с, 72°С — 1 мин 30 с; конечная полимеризация — 72°С — 3 мин. Реакционная смесь (25 мкл) содержала: 1× буфер для Taq-полимеразы ("Fermentas", Литва), 10—50 нг ДНК-матрицы, по 50 мкмоль каждого дезоксирибонуклеотидтрифосфата (dNTP) ("Fermentas", Литва), по 10 пмоль соответствующих праймеров ("Синтол", Россия), 2.5 ммоль MgCl₂ и 1 ед. *Taq*-полимеразы ("Силекс", Россия). Выделение и очистку фрагментов из агарозного геля выполняли с использованием набора реактивов ("Силекс", Россия) согласно рекомендациям производителя. Секвенирование ДНК проводили в Межинститутском Центре коллективного пользования "Геном" Института молекулярной биологии РАН (http://www.genome-centre.narod.ru/) с помощью набора реактивов ABI PRISM® BigDye™ Terminator v.3.1 ("Applied Biosystems", США) и с последующим анализом продуктов реакции на автоматическом секвенаторе ДНК ABI PRISM 3730 ("Applied Biosystems", США) и прилагаемого к набору протокола.

Филогенетический анализ. Предварительный анализ полученной нуклеотидной последовательности фрагмента гена 16S рРНК проводили с помощью программного пакета BLAST (http://blast.ncbi.nlm.nih.gov/Blast.cgi). Редактирование и выравнивание последовательностей проводили с помощью пакета программ ClustalX [12]. Филогенетическое древо было построено на основании нуклеотидных последовательностей генов 16S рРНК штамма BF и родственных видов рода *Clostridium* с помощью алгоритма "ближайших соседей" ("neibour-joining"), реализованного в пакете программ MEGA 4 [13, 14].

РЕЗУЛЬТАТЫ И ИХ ОБСУЖДЕНИЕ

Наши эксперименты состояли из двух пролонгированных ферментаций, из которых первая представляла собой сопряженное отъемно-доливное (**ОД**) культивирование, а вторая ферментация осуществлялась путем регулярного пересева (**РП**) анаэробного сообщества на новую среду.

Сопряженная отъемно-доливная ферментация. Осуществлялась для более глубокой переработки субстрата и накопления большего количества конечных продуктов обмена, особенно ацетата и жирных кислот, которые могут быть субстратами для фотосинтезирующих бактерий. Этот вид ферментации проводили параллельно в двух флаконах (**флакон 1**, **флакон 2**) (рис. 1). При этом из
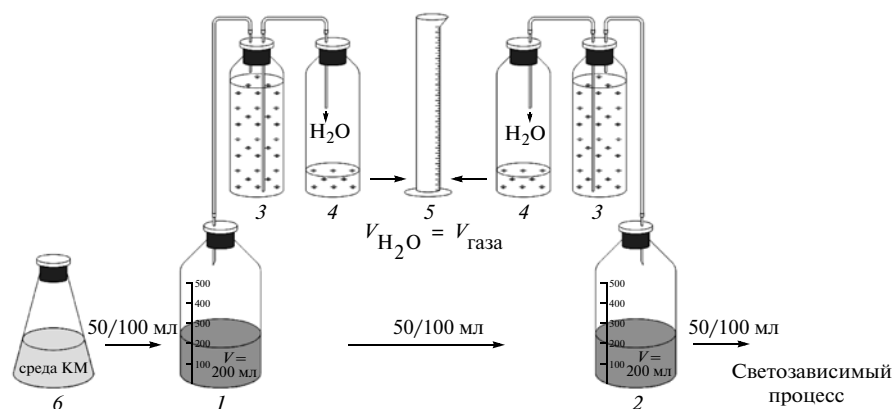
Рис. 1. Схема установки отъемно-доливного культивирования анаэробного крахмалферментирующего микробного сообщества. *1* – флакон 1; *2* – флакон 2; *3* – сосуд для сбора газовой фракции; *4* – сосуд для сбора вытесненной воды; *5* – цилиндр для измерения объема вытесненной воды; *6* – емкость со свежей средой КМ.

флакона 2 удаляли от 50 до 100 мл культуры, вместо них добавляли такое же количество культуры из флакона 1, а во флакон 1 добавляли компенсирующее количество свежей питательной среды.

Ферментация во флаконе 1. Продолжительность ферментации анаэробного, продуцирующего водород сообщества бактерий во флаконе 1 составила 72 сут, и ее можно разделить на 3 этапа.

Первый этап продолжался 7 сут, и сообщество анаэробных бактерий росло как периодическая культура. В течение этой ферментации в среднем выделилось биогаза (смесь H_2 и CO_2) 1.48 л/л среды, при этом концентрация водорода в выходящем газе варьировала от 16 до 34%, а общий объем выделенного водорода составил около 22% от объема выделенного газа.

Второй этап ферментации анаэробного сообщества протекал в режиме ОД культуры в течение 21 сут. Ежесуточно проводили отъем культуры из флакона 1 в количестве 50 мл, после чего добавляли в него новую питательную среду в том же объеме. Таким образом, объем анаэробной культуры во флаконе оставался постоянным (200 мл) в течение всего периода культивирования. За все время второго этапа из флакона 1 было изъято 1050 мл культуры, которая далее была использована в качестве посевного материала для флакона 2, и добавлено 1050 мл питательной среды, что соответствовало коэффициенту обновления культуры 5.2.

В течение второго этапа анаэробное сообщество флакона 1 продуцировало в среднем 99 мл газа в 1 сут. Концентрация водорода в выходящем газе варьировала от 13 до 29%, а среднесуточная концентрация водорода составила 19.5%. Таким образом, по образованию водорода относительные показатели на первом этапе культивирования сообщества были существенно лучше, чем на втором, где количество выделенного водорода со-

ставило 0.10 л/л среды/сут, что в 2 раза меньше, чем на первом этапе.

Третий этап процесса проходил также в режиме ОД ферментации, но объемы отлива и долива были увеличены и составили 100 мл каждый. Этот этап ферментации продолжался 44 сут, и коэффициент обновления культуры был равен 22. За все время третьего этапа из флакона культивирования выделилось 36.94 л биогаза на 1 л среды со среднесуточным объемом 0.23 л/л среды. Максимальная концентрация водорода в газовой фазе составляла 39% (54 сут), а минимальная концентрация была 12% (69 сут). Общий объем выделенного на этом этапе водорода составил 27.1% от общего выхода газа третьего этапа.

Максимальная оптическая плотность сообщества (D_{600}) составляла 1.30 на первом этапе, 1.81 — на втором и 1.92 — на третьем. На каждом из этапов ферментации во флаконе 1 происходило закисление среды культивирования. Первый этап характеризовался максимальным снижением pH среды до 5.0, во время второго этапа средний уровень pH составил 6.0, а третий этап сопровождался изменением pH от 4.5 до 6.7.

Сравнивая процессы продукции газа и водорода на втором и третьем этапах ферментации крахмала анаэробным сообществом бактерий можно отметить, что увеличение объема долива и отлива культуральной среды позволило в 1.7 раза увеличить среднесуточное выделение газа и в 1.9 раза образование водорода при сопоставимой концентрации водорода: 19.5 и 22% соответственно.

Как показывают данные, представленные в табл. 1, за весь 72-суточный период ферментации из флакона 1 было выделено около 53.92 л биогаза на 1 л среды. Содержание водорода составило 25.2% от объема выходящего газа.

Ферментация во флаконе 2. Параллельно ферментации во флаконе 1 проводили культивирова-

Таблица 1. Основные показатели ОД ферментации анаэробного сообщества бактерий на крахмалсодержащей среде

№ флакона	Этапы ферментации	Время, сут	Выход биогаза, л/л среды	Диапазон содержания H_2, %	Выход H_2, л/л среды	Выход H_2, л/л среды сут$^{-1}$	D_{600}*
1.	Первый	7	6.59	16—34	1.48	0.21	1.30
	Второй	21	10.39	13—29	2.12	0.10	1.81
	Третий	43	36.94	12—39	10.03	0.23	1.92
	Всего	72	53.92	12—39	13.63	0.19	1.92
2.	Первый	7	5.27	24—47	412	0.29	1.13
	Второй	48	5.57	4—32	109	0.01	1.59
	Третий	17	3.55	0.6—6.0	20	0.06	1.72
	Всего	72	14.39	0.6—47	541	0.04	1.72

* Приведены значения максимальной оптической плотности в процессе ферментации.

ние анаэробного гидрогеногенного сообщества бактерий во флаконе 2 в режиме ОД культуры, но в качестве доливной жидкости использовали отливную культуру флакона 1.

Культивирование на первом этапе продолжалось 7 сут в режиме периодической культуры. При этом было выделено 5.27 л биогаза/л среды, содержащего 2.06 л H_2/л среды, что составило 39% объема от всего выделенного на этом этапе газа.

Второй этап продолжался 48 сут и проходил в режиме ОД культуры. Объемы как доливной, так и отъемной культур составляли 50 мл. За время второго этапа ферментации имело место 12-кратное обновление объема культуры. На этом этапе ферментации из флакона 2 среднее суточное выделение газа составило 23 мл. Как количество газа в целом, так и образование водорода на втором этапе ферментации характеризовались своей неравномерностью. D_{600} культуры находилась в диапазоне от 0.92 до 1.63.

Третий этап ферментации анаэробного сообщества флакона 2 продолжался 17 сут с ежесуточной процедурой отъема культуры флакона 2 (100 мл) и долива культуры флакона 1 (100 мл). За 17 сут этого этапа ферментации коэффициент обновления составил 8.5. Общий объем выделенного биогаза на третьем этапе составил 3.55 л/л среды. ОД ферментация третьего этапа характеризовалась слабой продукцией водорода (0.6—6%); D_{600} в среднем составляла 1.60, то есть соответствовала плотности, свойственной стационарной фазе роста культуры. Третий этап характеризовался постоянным снижением pH, который достигал 6.0 (60 сут), а после нейтрализации щелочью максимально до значения в 6.45 (56 сут). За всю 72-суточную ферментацию сообщества, из флакона 2 было выделено 14.39 л биогаза на 1 л среды, в том числе 2.71 л H_2/л среды.

Ферментация во флаконе 2 показала, что отливная культура флакона 1 продолжает поддержи-

вать процесс ферментации. Однако по многим физиологическим показателям сообщество флакона 2 существенно уступало сообществу флакона 1. Так, во флаконе 2 газа было выделено в 3.75 раза меньше, чем в первом, а водорода в 5 раз меньше.

Микроскопирование препаратов ОД культуры, как во флаконе 1, так и во флаконе 2 выявило наличие палочковидных бактерий клостридиального типа. Наблюдались подвижные и неподвижные клетки, а также спорангии с терминально расположенными спорами, отдельные споры, зернистые и деформированные клетки.

Ферментация методом регулярных пересевов (РП). Результаты ОД культивирования анаэробного микробного сообщества показали, что даже половинное ежесуточное разбавление культуры свежей средой (третий этап флакона 1) не приводило к продукции достаточного количества водорода. В связи с этим нами был проведен эксперимент, в котором регулярно через 4—6 сут производили пересев сообщества в следующий 500 мл медицинский флакон, содержащий 200 мл питательной среды. Ферментация в данном режиме продолжалась 103 сут, и было произведено 22 цикла пересевов консорциума, в среднем через каждые 4.7 сут. Суммарный объем выделенного газа составил 31.5 л (157.27 л/л среды), и в среднем на один пересев приходилось 1.37 л газа. Колебания в объемах выделенного биогаза за каждый цикл пересева составляли от 1.46 до 8.30 л/л среды. Водород выделялся на всех этапах ферментации в разных количествах. Максимальная суточная концентрация водорода в выходящем газе достигала 64% (79 сут ферментации): в 4 случаях она превышала 60%, в 16 случаях была больше 50%. Предварительные опыты по обогащению выходящего газа водородом путем пропускания его через раствор щелочи (50%-ный раствор KOH) показали, что коэффициент обогащения был равен приблизительно 2. При концентрации водорода в вы-

Таблица 2. Основные показатели ферментации анаэробного сообщества бактерий на крахмалсодержащей среде методом последовательных пересевов

Номер пересева	Время, сут	Выход биогаза, л/л среды	Диапазон содержания H_2, %	Выход H_2, л/л среды	Выход H_2, л/л среды/сут	D_{600}*
0	6	5.52	19—51	2.61	0.44	1.67
1	2	1.46	27—38	0.50	0.25	1.72
2	6	4.11	10—42	1.54	0.27	1.76
3	6	7.10	44—57	3.85	0.64	1.74
4	4	6.65	43—57	3.65	0.91	1.78
5	4	6.64	43—57	3.68	0.92	1.73
6	6	8.06	43—53	4.14	0.69	1.80
7	4	8.19	49—57	4.39	1.10	1.69
8	4	6.17	52—59	3.45	0.86	1.74
9	4	5.53	53—62	2.95	0.74	1.71
10	4	6.17	52—61	3.28	0.82	1.76
11	5	8.34	44—57	4.52	0.91	1.83
12	4	7.29	47—55	3.83	0.96	1.64
13	4	6.42	47—52	3.20	0.80	1.79
14	6	8.61	49—56	4.35	0.72	1.75
15	4	7.00	50—57	3.86	0.97	1.66
16	4	7.86	53—62	4.67	1.16	1.58
17	4	7.28	53—64	4.49	1.12	1.75
18	4	7.65	46—59	4.12	1.03	1.62
19	5	7.05	48—58	3.97	0.79	1.73
20	4	8.30	48—56	4.40	1.10	1.73
21	4	8.16	30—55	4.19	1.05	1.71
22	5	7.76	45—56	4.17	0.83	1.74
Всего	103	157.27	10—64	83.78	0.81	1.83

* Приведены значения максимальной оптической плотности в процессе ферментации.

ходящем газе более 50% можно было получить обогащенный газ, содержащий до 100% водорода.

Оптическая плотность. В течение ферментаций в режиме РП наблюдалось закономерное изменение оптической плотности культуры в каждом промежутке времени между пересевами с максимумом к середине цикла. В начале каждого пересева D_{600} была, как правило, меньше 1, но уже на 1 сут культивирования сообщества оптическая плотность обычно превышала 1, и наибольшее ее значение составило 1.83.

pH среды культивирования. На протяжении всей ферментации имело место закисление среды культивирования, но оно носило циклический характер, соответствующий пересевам. Наибольшее закисление наблюдали обычно в 1 сут после пересева, но оно постепенно уменьшалось к 4 сут. Соответственно, уменьшался и расход щелочи для нейтрализации среды.

Морфология клеток анаэробного консорциума. Микроскопическая картина препаратов крахмалферментирующего сообщества при РП была весьма пестрой и во многом определялась фазой его роста. Обычно в начале каждого цикла пересева культуры наблюдались активные, в основном подвижные прямые палочки и пары клеток, тогда как в конце цикла клетки были неподвижными, наблюдались деформированные, зернистые формы, спорангии и отдельные споры. В целом, спорообразующие клетки составляли до 80% популяции клеток.

Характеристика культуры водородобразующих бактерий. Для получения чистой культуры крахмалферментирующих бактерий, исследуемое сообщество микроорганизмов после пастеризации было посеяно в десятикратных разведениях в жидкую и на твердую среду КМ. В результате последовательных пересевов был выделен штамм BF строго анаэробных палочек, образующих эндоспоры, окрашивающихся по Граму положи-
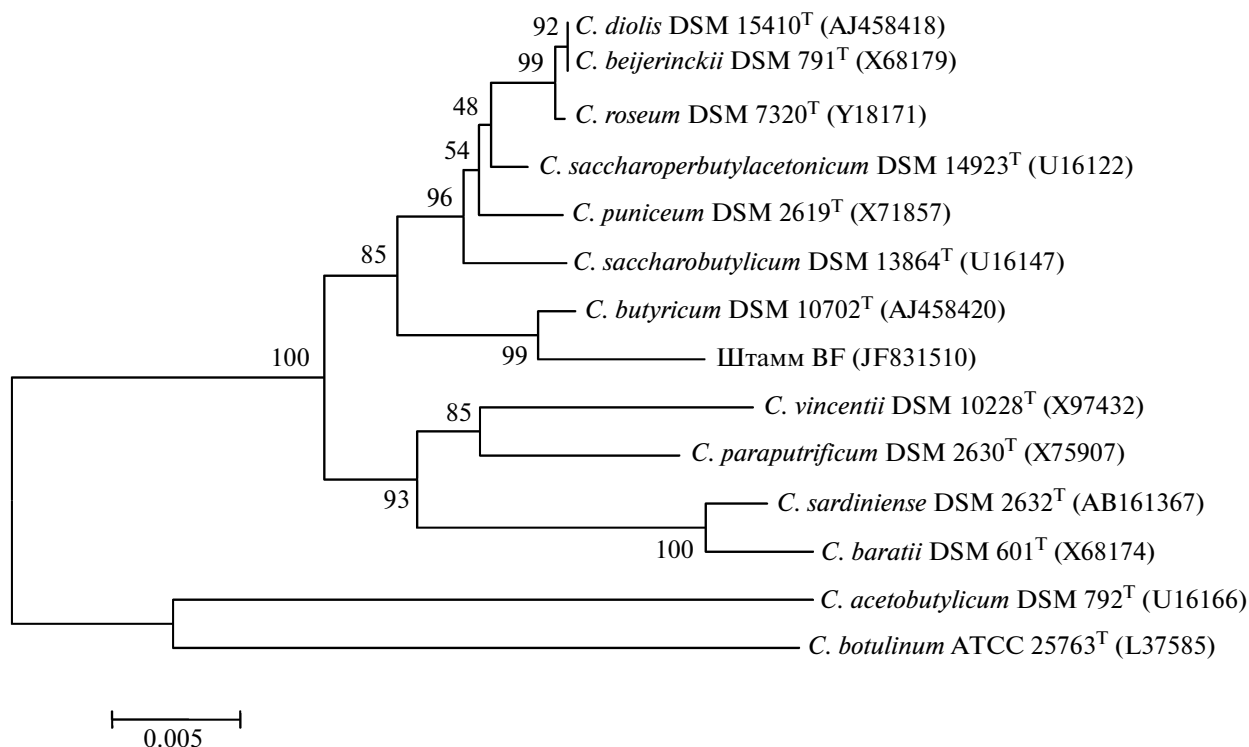
Рис. 2. Бескорневое филогенетическое древо представителей рода *Clostridium*, показывающее положение штамма BF. Цифрами показаны значения "bootstrap"-анализа. Для филогенетического анализа использованы типовые штаммы рода *Clostridium*. В скобках показаны номера последовательностей в GenBank.

тельно, и образующих H_2 на различных субстратах. Для этого штамма нами определена нуклеотидная последовательность гена 16S рРНК, которая составила 1438 нуклеотидов, последовательность была депонирована в GenBank под номером JF831510. Поиск в GenBank с помощью программы BLASTn показал близкое родство штамма BF к представителям кластера I рода *Clostridium*. Штамм BF имел достаточно высокий уровень сходства по 16S рРНК (99.1–99.7%) с некоторыми штаммами, отнесенными к виду *Clostridium butyricum,* выделенными из анаэробных осадков сточных вод, из содержимого желудка кенгуру, компоста коровьего навоза и озерных отложений [15, 16].

На филогенетическом древе (рис. 2) показано положение штамма BF в составе рода *Clostridium*. Штамм BF объединяется в единый кластер с типовым штаммом вида *C. butyricum* с уровнем сходства нуклеотидных последовательностей 99.3%. Род *Clostridium* объединяет грамположительные спорообразующие строго анаэробные бактерии, не способные к сульфатредукции, и является к настоящему времени одним из самых больших по количеству видов. Он включает порядка 180 видов, отличающихся разнообразием морфологии и метаболических особенностей [17]. На основании сравнения последовательностей генов 16S

рРНК штамм BF следует отнести к виду *C. butyricum*, который хорошо известен как вид, образующий H_2 и масляную кислоту [18]. Предварительные исследования показали, что новый штамм может образовывать от 0.25 до 0.50 л H_2 г$^{-1}$ субстрата на крахмале, муке, глицерине, лактозе и глюкозе в условиях периодического культивирования, что соответствует лучшим показателям
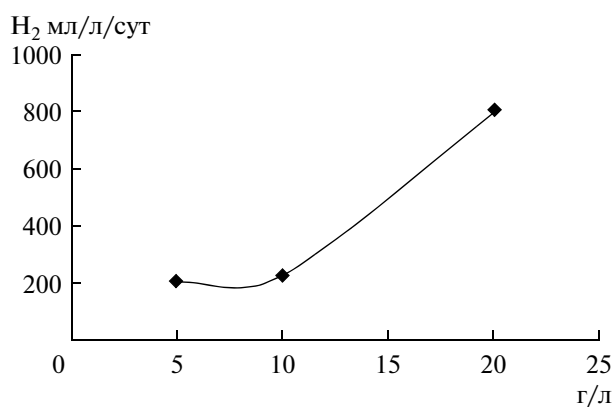

Рис. 3. Зависимость образования H_2 от содержания крахмала (г/л) в различных режимах культивирования: 5 и 10 — ОД ферментация; 20 — метод РП.

среди изученных штаммов мезофильных H_2-образующих бактерий рода *Clostridium*.

Для решения технологических задач крахмалолитическое гидрогеногенное анаэробное сообщество бактерий должено удовлетворять определенным требованиям: в нем должны отсутствовать метаногены, водородпотребляющие, сульфатвосстанавливающие и ацетогенные бактерии. Для исключения из исследуемого сообщества посторонней микрофлоры и активации споровых бактерий, в том числе и клостридий, посевной материал подвергали пастеризации [19]. Особенностью питательной среды, использованной в экспериментах, являлось преобладание в ее составе хлоридных солей над сульфатными с целью ограничения развития сульфатвосстанавливающих бактерий. Другим важным фактором стало введение в нее соли цинка для того, чтобы предотвратить развитие метаногенов — основных потребителей водорода в анаэробных сообществах микроорганизмов [20]. В качестве основных источников азота были использованы аминокислоты, которые, как показали предыдущие исследования, оказались лучшими стимуляторами продукции водорода клостридиальными культурами [19]. Кроме того, состав среды культивирования анаэробного консорциума, в основном, определялся совместимостью темнового процесса со светозависимым и обладал определенными селективными свойствами [4, 19].

Как показали проведенные исследования, культивирование анаэробного бактериального сообщества, как в режиме ОД культуры, так и в режиме РП обеспечивало пролонгирование продукции водорода примерно в 10—15 раз. Однако исследованные варианты ОД культуры не позволили получить достаточно высоких концентраций водорода в выходящем газе. Использование отъемной культуры анаэробного консорциума в качестве доливной жидкости приводило к дополнительной небольшой продукции водорода. Фактически, все изученные режимы культивирования различались по концентрации начального содержания крахмала на всех этапах ферментаций. Кривая на рис. 3 демонстрирует зависимость суточного выделения H_2 от содержания крахмала при различных режимах культивирования. Таким образом, полученные экспериментальные данные показывают, что использование метода регулярных пересевов позволяет поддерживать необходимое содержание крахмала в среде для наиболее эффективного образования водорода. Исследованное анаэробное сообщество содержало, в основном, споровые крахмалферментирующие бактерии по филогенетическим свойствам представляющие собой вид *C. butyricum*.

СПИСОК ЛИТЕРАТУРЫ

1. *Цыганков А.А.* // Рос. хим. журн. 2006. Т. 50. № 6. 26—33.

2. *Levin D.B., Pitt L., Love M.* // Int. J. Hydrogen Energy. 2004. V. 29. № 2. 173—185.

3. *Claassen P.A.M., De Vrije T.* // Int. J. Hydrogen Energy. 2006. V. 31. № 11. P. 1416—1423.

4. *Laurinavichene T.V., Belokopytov B.F., Laurinavichius K.S., Tekucheva D.N., Seibert M., Tsygankov A.A.* // Int. J. Hydrogen Energy. 2010. V. 35. № 16. P. 8536—8543.

5. *Нетрусов А.И., Карякин А.А., Тепляков В.В., Шалыгин М.Г., Воронин О.Г., Абрамов С.М., Садрадинова Э.Р., Митрофанова Т.И., Шестаков А.И.* // Катализ в промышленности. 2010. № 5. С. 77—83.

6. *Zhang T., Liu H., Fang H.H.P.* // J. Environ. Management. 2003. V. 69. № 2. P. 149—156.

7. *Yokoi H., Maki R., Hirose J., Hayashi S.* // Biomass Bioeng. 2002. V. 22. № 5. P. 389—395.

8. *Liu G., Shen J.* // J. Biosci. Bioeng. 2004. V. 98. № 4. P. 251—256.

9. *Hungate R.E.* // Methods in Microbiology / Eds. J.B. Norris, D.W. Ribbons. N.Y: Academic Press, 1969. P. 117—132.

10. *Kosourov S.N., Tsygankov A.A., Seibert M., Ghirardi M.L.* // Biotechnol. Bioeng. 2002. V. 78. № 7. P. 731—740.

11. *Sambrook J., Fritsch E.F., Maniatis T.* // Molecular Cloning: A Laboratory Manual. N.Y.: Cold Spring Harbor Lab. Press, 1989. 1626 p.

12. *Thompson J.D., Higgins D.G., Gibson T.J.* // Nucleic Acids Research. 1994. V. 22. № 22. P. 4673—4680.

13. *Tamura K., Dudley J., Nei M., Kumar S.* // Mol. Biol. Evol. 2007. V. 24. № 8. P. 1596—1599.

14. *Saitou N., Nei M.* // Mol. Biol. Evol. 1987. V. 4. № 4. P. 406—425.

15. *Chong M-L., Rahim R.A., Shirai Y., Hassan M.A.* // Int. J. Hydrogen Energy. 2005. V. 30. № 10. P. 1063—1070.

16. *Chen W.M., Tseng Z.J., Lee K.S., Chang J.S.* // Int. J. Hydrogen Energy. 2009. V. 34. № 2. P. 764—771.

17. Bergey's Manual of Systematic. V. 3: The Firmicutes / Eds. P.D. Vos, G. Garrity, D. Jones, N.R. Krieg, W. Ludwig, F.A. Rainey, K.-H. Schleifer, W.B. Whitman. N.Y.: Springer, 2009. 1450 p.

18. *Cummins C.S., Johnson J.L.* // J. Gen. Microbiol. 1971. V. 67. № 1. P. 33—46.

19. *Belokopytov B.F., Laurinavichius K.S., Laurinavichene T.V., Ghirardi M.L., Seibert M., Tsygankov A.A.* // Int. J. Hydrogen Energy. 2009. V. 34. № 8. P. 3324—3332.

20. *Заварзин Г.А.* // Изв. АН СССР. Сер. биол. 1986. № 3. С. 341—360.

Prolonged Cultivation of an Anaerobic Bacterial Community Producing Hydrogen

B. F. Belokopytov, Ya. V. Ryzhmanova, K. S. Laurinavichyus, and V. A. Shcherbakova

*Scryabin Institute of Biochemistry and Physiology of Microorganisms, Russian Academy of Sciences,
Pushchino, Moscow oblast, 142290 Russia*
e-mail: shcherb@ibpm, pushchino.ru
Received June 15, 2011

Abstract—This paper studies various methods of long-term maintenance of the process of hydrogen evolution during the growth of an aerobic bacterial community on a starch-containing environment. When cultured in separable trip fermentation mode for 72 days, from 0.10 to 0.23 H_2/l of medium/day was formed. The regime of regular reseeding lasted more than 100 days, forming an average of 0.81 l H_2/l of medium/day. The advantages and disadvantages of different methods of microbial hydrogen production during a dark starch fermentation process are presented. From the obtained H_2 forming microbial communities, we isolated an anaerobic spore-forming bacterium (strain BF). Phylogenetic analysis of the 16S PNA gene sequence of the new strain showed that according to its genotype it belongs to the *Clostridium butyricum* species.

УДК 579.66/579.222

ВЛИЯНИЕ ЭКЗОГЕННЫХ ЖИРНЫХ КИСЛОТ НА РОСТ И ПРОДУКЦИЮ ЭКЗОПОЛИСАХАРИДА ОБЛИГАТНОЙ МЕТИЛОТРОФНОЙ БАКТЕРИИ *Methylophilus quaylei*

© 2012 г.   С. А. М. Отман, А. Б. Пшеничникова, В. И. Швец

Московская государственная академия тонкой химической технологии им. М.В. Ломоносова, Москва, 117571

e-mail: a_pshenichnikova@mail.ru

Обнаружен эффект ускорения роста и увеличения продукции экзополисахарида облигатной метилотрофной бактерии *Methylophilus quaylei* в присутствии жирных кислот C_{12}—C_{18}, добавленных в питательные среды. Наилучшим ростовым фактором оказался олеат натрия. На основании данных о составе фракции свободных жирных кислот в клетках, величин ζ-потенциала и анизотропии флуоресценции целых клеток высказано предположение о включении жирных кислот в состав наружной мембраны бактерии *M. quaylei*.

Жирные кислоты (**ЖК**) с длиной цепи от C_{14} до C_{20} представляют собой уникальные природные вещества, которые в виде производных липидов являются структурными компонентами клеточных мембран, выполняют энергетические и регуляторные функции. Кроме этого свободные жирные кислоты проявляют разнообразную биологическую активностью и прежде всего антимикробную (активны против вирусов, бактерий, грибов, водорослей, простейших) и цитотоксическую [1, 2]. Бактерицидное действие свободных ЖК наблюдали как по отношению к грамположительным бактериям родов: *Streptococcus* [3—5], *Staphylococcus* [6—9], *Bacillus* [9, 10], *Lactobacillus* [11], *Mycobacterium* [12, 13] и других [1, 14], так и грамотрицательным, родов: *Escherichia* [9, 15, 16], *Pseudomonas* [17], *Neisseria* [17], *Salmonella* [16, 17], *Helicobacter* [18, 19] и других [1, 14]. Как правило, грамположительные бактерии более чувствительны к ЖК, чем грамотрицательные, которые защищены липополисахаридом внешней мембраны [16]. Несмотря на свое бактерицидное действие, свободные ЖК были обнаружены в составе внеклеточных метаболитов бактерий *Pseudomonas carboxydoflava* [20], *Bacillus cereus* [21], *Methylococcus capsulatus* [22]. Добавленные экзогенно олеиновая или пальмитолеиновая кислоты в низких концентрациях (менее 4 мг/л) способствовали сокращению лаг-фазы и ускоряли рост метанотрофной бактерии *M. capsulatus*, а в более высоких концентрациях вызывали лизис культуры [22]. Авторы предположили, что ЖК выполняют регуляторную функцию по поддержанию жидкостности клеточных мембран.

Несмотря на большой научный интерес к биологическим функциям свободных ЖК, механизм их бактерицидной активности изучен недостаточно. Известно, что основной мишенью является клеточная мембрана и процессы в ней протекающие — функционирование электронтранспортной цепи, окислительное фосфорилирование, ферментативные процессы, транспорт питательных веществ, перекисное окисление липидов [2]. Свободные ЖК являются компонентами врожденного иммунитета и присутствуют на коже, в грудном молоке и кровотоке человека и животных [23], где выполняют защитные функции. Наиболее детально изучена активность ЖК, особенно олеиновой кислоты (**ОК**), по отношению к бактериям родов *Staphylococcus* и *Streptococcus* — наиболее распространенных возбудителей инфекций кожи и других органов человека [3—8]. В концентрациях, не вызывающих цитотоксического действия, ОК разрушает клеточные стенки и приводит к гибели популяции *Staphylococcus aureus* [7]. По мнению авторов [7, 8], в качестве антимикробных веществ ЖК являются альтернативой традиционным антибиотикам, применение которых часто приводит к формированию лекарственной устойчивости у патогенных бактерий. Использование ЖК предлагается авторами [7, 8] в качестве элемента новой антимикробной стратегии, основанной на свойствах врожденного неспецифического иммунитета. Показано, что бактерицидная активность ОК по отношению *S. aureus* возрастает в составе липосом [8].

В рассматриваемом контексте важно отметить, что экзогенно добавленные в среду для культивирования бактерий ЖК не всегда ингибируют их рост, при определенных концентрациях наблюдается и ускорение роста, повышение выживаемости некоторых бактерий в неблагоприятных условиях, например для лактобацилл, при дефиците биотина, или в условиях, моделирующих кислую среду желудка [1, 22, 24]. Важнейший представи-

тель биоценоза вина − молочнокислая бактерия *Oenococcus oeni* в присутствии экзогенной ОК обладала повышенной выживаемостью в присутствии этанола [25]. Более того, ЖК являются необходимыми ростовыми факторами для некоторых бактерий, относящихся к таким родам, как *Lactobacillus*, *Corynebacterium*, *Clostridium* [26, 27]. В присутствии экзогенной ОК повышалась продукция поли-3-гидроксибутирата грамотрицательными бактериями *Sphaerotilus natans* и *Pseudomonas* sp. [28].

Бактерицидный или ростостимулирующий эффект ЖК определяется их строением (особенно важно количество, а иногда и положение двойных связей), видом бактерии, концентрацией кислоты и условиями культивирования [1, 26]. Таким образом, при разработке бактерицидных препаратов на основе ЖК необходимо учитывать сложный механизм их биологического действия и состав биоценоза, подвергающегося обработке препаратом. Например, в составе биоценоза кожи здоровых людей, помимо хорошо известных бактерий, таких, как *Staphylococcus epidermidis*, *Propionibacterium acnes* и других, обнаружены облигатные метилотрофные бактерии *Methylophilus methylotrophus* [29]. Нами были исследованы внеклеточные нейтральные липиды другого представителя рода *Methylophilus* − облигатной метилотрофной бактерии *Methylophilus quaylei* и обнаружены свободные ЖК миристиновая, пальмитиновая и стеариновая, а в условиях осмотического стресса еще и пальмитолеиновая, олеиновая и линолевая [30]. Добавление в питательную среду свободных ЖК увеличивало выход биомассы и экзополисахарида, а также − выживаемость бактерий *M. quaylei* в условиях стресса. Следовательно, воздействие препаратов ЖК на биоценоз, например кожи, включающий организмы, по-разному с ними взаимодействующие, может привести к трудно прогнозируемым эффектам.

Цель работы − изучение механизма взаимодействия экзогенных ЖК с облигатными метилотрофными бактериями *M. quaylei*.

МЕТОДИКА

В работе использовали облигатные метилотрофные бактерии *Methylophilus quaylei*, штамм МТ (ВКМ B-2338[T]), выделенный нами из утилизирующей метанол смешанной культуры [31]. Для культивирования использовали минеральную среду, содержащую 1.0 об. % метанола [32]. Для получения плотных питательных сред добавляли 1.5% агара. Жирные кислоты добавляли в стерильную питательную среду в виде метанольных растворов асептически после пропускания через мембранные фильтры 0.22 мкм Millex® GS, ("Millipore", Ирландия).

Для приготовления питательных сред использовали реактивы Российского производства марки х.ч. Органические растворители предварительно перегоняли.

ЖК лауриновую, миристиновую, пальмитиновую, стеариновую (х.ч., "Реахим", Россия) предварительно перекристаллизовывали из метанола. Примеси насыщенных жирных кислот в коммерческой ОК (ч., "Химмед", Россия) удаляли при температуре −18°C осаждением из ацетона. ОК выделяли в виде комплекса с мочевиной, как описано [33]. Линолевую кислоту (99%-ная, фирмы "Aldrich", США) и олеат натрия ("Sigma", США) использовали без предварительной очистки.

Бактерии выращивали в колбах объемом 250 мл (100 мл среды) на шейкере ("Labline", США) при 100 об/мин и 28°C. В качестве инокулята использовали 28-часовую культуру в экспоненциальной фазе роста в количестве 2.5 об. %. Оптическую плотность измеряли на спектрофотометре ("Beckman DU-7", США), при $\lambda = 600$ нм, в кювете $l = 10$ мм. Концентрацию экзополисахарида (**ЭПС**) определяли фенольным методом [34].

Добавки вносили в начальный момент времени в виде метанольного раствора. Для определения скорости роста и построения кинетических кривых находили зависимость концентрации высушенной биомассы (**ВБ**) от времени. Концентрацию ВБ определяли по калибровочной зависимости $Y = 0.915X - 0.152$, где Y − концентрация биомассы, высушенной до постоянного веса, г/л, X − оптическая плотность при $\lambda = 600$ нм. Для получения биомассы культуральную жидкость центрифугировали (центрифуга ОПн-8УХЛ4.2, "Поликом", Россия) при 10000 g 20 мин.

Липиды экстрагировали по методу Блайя–Дайэра [35]. Экстракты фракционировали на колонке размером 0.8×24 см с 0.2−0.5 мм силикагелем 60 ("Merck", Германия). Элюцию проводили хлороформом, собирая фракцию свободных ЖК аналогично, описанному в работе [30].

Для выделения фосфолипидов из фракции суммарных липидов использовали низкотемпературное осаждение. Для этого к 1 мл раствора суммарных липидов в диэтиловом эфире (20−30 мг/мл) добавляли 5 мл ацетона и 0.1 мл 10%-ного водного раствора хлорида магния и выдерживали при −20°C [36]. Метиловые эфиры ЖК получали реакцией с ацетилхлоридом (6 об. %) в метаноле [37].

Жирнокислотный состав фракций свободных ЖК и фосфолипидов (**ФЛ**) определяли методом хромато-масс-спектрометрии. Хромато-массспектрометр включал ионную ловушку Finnigan MAT ITD-700 ("Finnigan", Великобритания) и газовый хроматограф Varian 3400 ("Varian", США), снабженный капиллярной колонкой "Hewlett-Packard HP-101" (США) длиной 25 м, внутренним диаметром 0.2 мкм и с толщиной слоя непо-
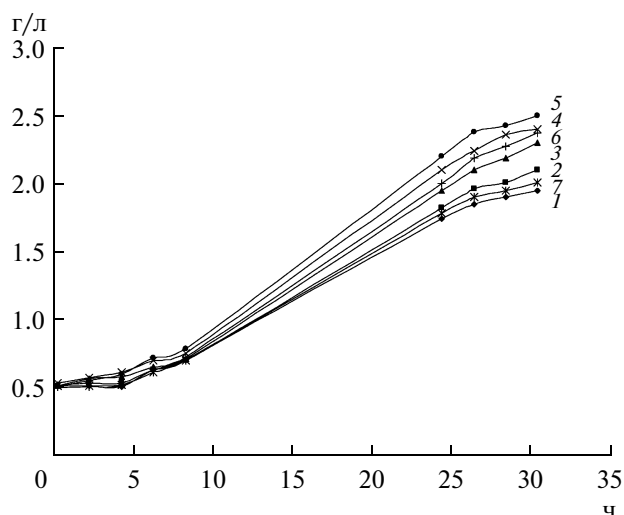
Рис. 1. Влияние длины цепи и степени ненасыщенности экзогенных ЖК на рост *M. quaylei*: *1* – $C_{12:0}$, *2* – $C_{14:0}$, *3* – $C_{16:0}$, *4* – $C_{18:0}$, *5* – $C_{18:1}$, *6* – $C_{18:2}$, *7* – без добавок. Концентрация ЖК 50 мкМ.

движной привитой фазы 0.2 мкм, температура инжектора 250°C, газ-носитель – гелий, 1 мл/мин. Программирование температуры термостата: 80°C – изотерма 1 мин, линейный рост 10°C/мин до 290°C; проба – 1 мкл хлороформа. Ионная ловушка Finnigan MAT ITD-700 была настроена на сканирование в области m/z от 41 до 400, частота сканирования 1 скан/с, задержка регистрации – 100 с, энергия ионизирующих электронов 70 эВ, температура интерфейса 220°C, порог регистрации пиков 1. Программное обеспечение ITDS ("Finnigan MAT"), версия 4.10. Файлы были конвертированы в формат программы HPChem, идентификация веществ проводилась с использованием базы данных Wiley 275.

Спектры ^{1}Н-ЯМР были получены на импульсном Фурье-спектрометре Bruker DPX-300 с рабочей частотой 300 МГц.

Измерение ζ-потенциала интактных клеток бактерий проводили на анализаторе частиц Delsa™ Nano Series Zeta Potential and Submicron Particle Size Analyzers ("Beckman Coulter, Inc.", США) методом электрофоретического рассеяния под углом 30° по изменению распределения частиц в электрическом поле. Бактерии культивировали 48 ч в стандартных условиях и в присутствии ОК (5.0×10^{-5} М), фиксировали раствором формальдегида, центрифугировали 10 мин при 10000 g и 4 раза промывали, а затем ресуспендировали в 0.1 М растворе KCl с добавлением КОН, рН 7.0 (15–22 мг ВБ/мл), содержащем 1.0% БСА.

Для измерения анизотропии флуоресценции бактерии культивировали 48 ч в стандартных условиях и в присутствии ОК (5.0×10^{-5} М), фик-

сировали раствором формальдегида, центрифугировали 10 мин при 10000 g и 4 раза промывали, а затем ресуспендировали в 2 мл 50 мМ раствора трис-HCl буфера, рН 7.5 (15–22 мг ВБ/мл), с добавлением 100 мкл раствора 0.1 мМ 1,3-дифенил-1,3,5-гексатриена (**ДФГ**) в тетрагидрофуране. Смесь инкубировали 1 ч при температуре 28°C, а затем в течение ночи при 4°C, затем клетки центрифугировали 15 мин при 10000 g. Супернатант удаляли, осадок ресуспендировали в 10 мл 50 мМ трис, рН 7.5. Оптическая плотность не превышала 0.1. Анизотропию флуоресценции меченных ДФГ клеток определяли на флуоресцентном спектрофотометре Varian Cary Eclipse ("Walnut Creek", CA, Австралия), используя длину волны излучения 350 нм с шириной щели 5 нм, длину волны испускания – 452 нм с шириной щели 10 нм.

ТСХ проводили в системе: петролейный эфир–диэтиловый эфир 9 : 1 об./об. на пластинках ПТСХ-АФ-А-УФ ("Sorbfil", Россия). Для проявления хроматограмм использовали фосфорномолибденовую кислоту и молибденовый синий [38, 39]. Для колоночной хроматографии использовали 0.2–0.5 мм силикагель 60 ("Merck", Германия).

РЕЗУЛЬТАТЫ И ИХ ОБСУЖДЕНИЕ

Бактерия *Methylophilus quaylei* не способна утилизировать в качестве источника углерода органические соединения за исключением метанола, т.е. является облигатным метилотрофом и поэтому удобной моделью для изучения влияния экзогенных мембраноактивных веществ.

Жирные кислоты C_{14}–C_{20} являются амфифильными веществами, в водной среде образуют мицеллы в концентрациях, достигающих значений критической концентрации мицеллообразования (**ККМ**) – 0.7–3.5 мМ [40]. Известно, что биологическое действие ЖК зависит от формы, в которой они присутствует в водной среде, – мономерной (молекулярной) или мицеллярной. Так, ОК активирует протеинкиназу C (КФ 2.7.11.13) только в мономерной форме [41]. В связи с этим в настоящей работе экзогенные ЖК включали в состав питательной среды в концентрациях как меньших, так и больших значений их ККМ в интервале от 10^{-6} до 10^{-3} М. Добавки ЖК вводили в питательную среду в виде растворов в метаноле. Кривые роста *M. quaylei* в присутствии экзогенно добавленных ЖК в концентрации 50 мкМ представлены на рис. 1. В присутствии ЖК C_{14}–C_{18} наблюдали ускорение роста и сокращение лаг-фазы, причем с увеличением длины цепи способность ЖК стимулировать рост увеличивалась. Наибольший эффект наблюдали в присутствии ОК. При этом наблюдалось наиболее сильное сокращение лаг-фазы.
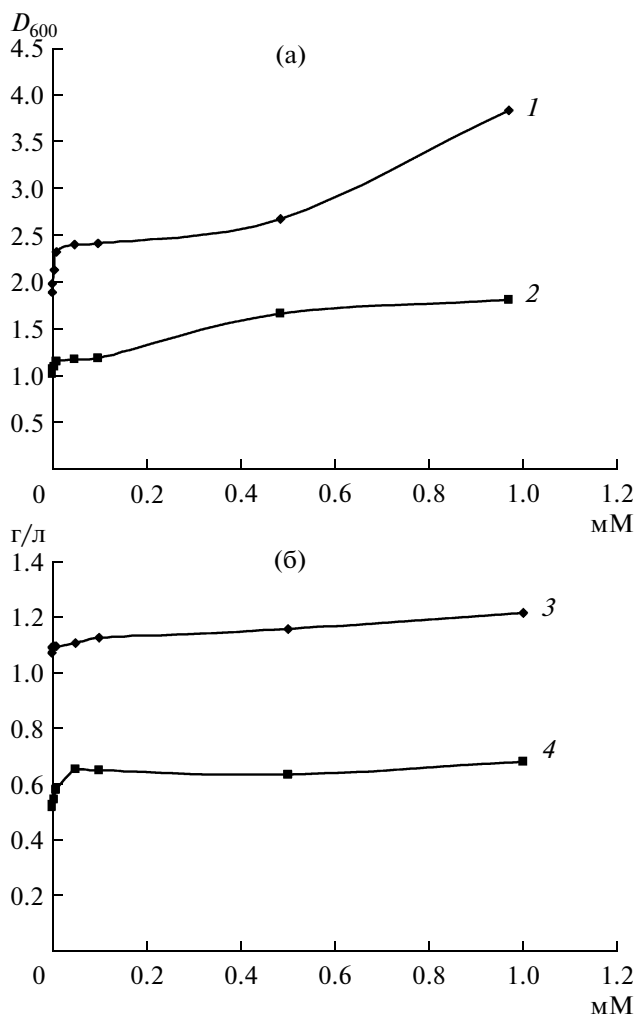
Рис. 2. Влияние экзогенного олеата натрия в культуральной жидкости на рост (а) и продукцию ЭПС (б) *M. quaylei*: D_{600} и концентрация ЭПС при 24 (*1*, *2*) и 48 (*3*, *4*) ч роста соответственно.

Рис. 3. Влияние концентрации олеата натрия на оптическую плотность питательной среды при $\lambda = 450$ нм (*1*) и $\lambda = 600$ нм (*2*).

Увеличение выхода биомассы в присутствии ОК к 30 ч роста достигало 25%, что позволило ее рассматривать в качестве ростового фактора. Однако для практического использования ОК, имеющая вязкую консистенцию, крайне неудобна, предпочтительнее олеат натрия, хорошо растворяющийся в воде и метаноле. Нами было изучено влияние концентрации олеата натрия на выход биомассы и экзополисахарида *M. quaylei* (рис. 2). Важно отметить, что олеат натрия дозозависимо ускорял выход биомассы и экзополисахарида, однако характер этих зависимостей довольно сложный. Сначала наблюдалось резкое ускорение роста, затем через плато — переход к более медленному росту. Те же закономерности наблюдались для зависимости выхода ЭПС от концентрации олеата натрия (рис. 2). Поскольку питательные среды с олеатом натрия в концентрации выше 0.1 мМ до добавления инокулята были мутными, было изу-
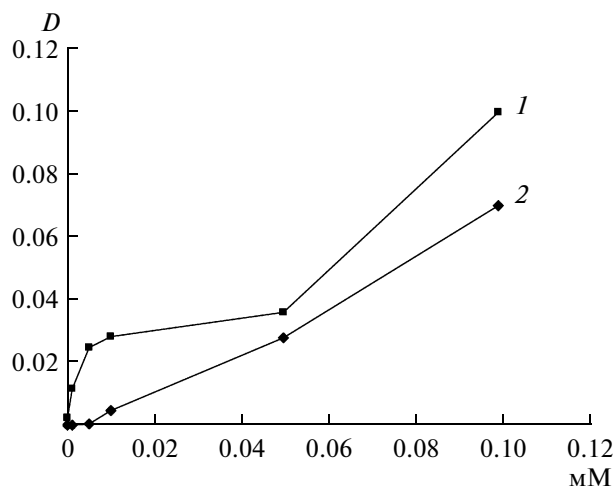
чено влияние концентрации олеата натрия на оптическую плотность питательных сред (рис. 3). Кривая *1* позволяет предположить наличие как минимум двух критических концентраций, соответствующих образованию различных мицеллярных структур. Но самое интересное — это повторение формы кривых, соответствующих изменению выхода биомассы и ЭПС от концентрации олеата натрия в среде (рис. 1). Чисто арифметический вклад мицелл олеата натрия в светорассеяние культуральной жидкости можно исключить ввиду низких значений оптической плотности при $\lambda = 600$ нм (рис. 3, кривая *2*). Возможно, различные мицеллярные структуры с разной эффективностью взаимодействуют с клетками бактерии. Однако этот вывод требует дополнительного подтверждения.

Взаимодействие ЖК с клетками бактерии *M. quaylei* может осуществляться на поверхности или в результате проникновения в наружную мембрану. Нами были выделены и фракционированы клеточные липиды из биомассы, полученной в присутствии ОК и стеариновой кислоты (СК) в концентрации 50 мкМ, а также изучен жирнокислотный состав фракций свободных ЖК и фосфолипидов методом хромато-масс-спектрометрии. При добавлении в питательную среду ОК и СК доля этих ЖК в составе фракций свободных ЖК существенно увеличивалась, тогда как состав фракций ФЛ изменялся незначительно (таблица).

При включении ЖК в состав наружной мембраны, вероятно, должно происходить уменьшение заряда поверхности при нейтральных значениях рН благодаря наличию карбоксильных групп. Действительно, величина ζ-потенциала бактерий, выращенных в стандартных условиях и в присутствии экзогенной ОК (5.0×10^{-5} М), со-

Влияние экзогенных ОК и СК на жирнокислотный состав фракций липидов *M. quaylei*

Добавка	Фракция	$C_{14:0}$	$C_{16:0}$	$C_{16:1}$	$C_{18:0}$	$C_{18:1}$
Без добавок	Свободные ЖК	2.0	42.3	45.1	7.4	3.2
	ФЛ	–	33.5	66.5	–	–
50 мкмоль/л ОК	Свободные ЖК	–	26.3	17.7	–	56.0
	ФЛ	–	46.8	53.2	–	–
50 мкмоль/л СК	Свободные ЖК	–	14.4	6.9	78.7	–
	ФЛ	–	40.8	40.8	18.4	–

ставила −40.77 и −43.06 мВ соответственно. Промывка клеток буфером, содержащим 1% БСА, связывающего не включившиеся в мембрану ЖК, привела лишь к незначительному снижению ζ-потенциала: −40.09 и −43.01 мВ соответственно. Была проведена оценка текучести мембран целых клеток *M. quaylei* по величинам анизотропии флуоресценции с использованием в качестве гидрофобного зонда ДФГ. Значения анизотропии клеток, выращенных в стандартных условиях и в присутствии ОК, составили 0.0111 и 0.0087 соответственно, что коррелирует с повышением текучести мембран в присутствии ОК.

Таким образом, эффект ускорения роста метилотрофной бактерии *M. quaylei* экзогенными ЖК достигался за счет включения их в состав наружной мембраны и изменения физико-химических свойств поверхности клетки, а также свойств липидного бислоя.

СПИСОК ЛИТЕРАТУРЫ

1. *Nieman C.* // Bacteriol. Rev. 1954. V. 18. P. 147−163.
2. *Desbois A.P., Smith V.J.* // Appl. Microbiol. Biotechnol. 2010. V. 85. № 6. P. 1629−1642.
3. *Norman P.W., Guy E.M.* // J. Bacteriology. 1966. V. 91. № 6. P. 2245−2250.
4. *Speert D.P., Wannamaker L.W., Gray E.D., Clawson C.C.* // Infect Immun. 1979. V. 26. № 3. P. 1202−1210.
5. *Carson D.D., Daneo-Moore L.* // J. Bacteriol. 1980. P. 1122−1126.
6. *Kenny J.G., Ward D., Josefsson E., Jonsson I.-M., Hinds J., Rees H.H., Lindsay J.A., Tarkowski A., Horsburgh M.J.* // PLoS One, 2009. V. 4. № 2. e4344.
7. *Chen C.-H., Wang Y., Nakatsujil T., Liu Y.-T., Zouboulis C.C., Gallol R.L., Zhang L., Hsieh M.-F., Huang C.-M.* // J. Microbiol. Biotechnol. 2011. V. 21. № 4. P. 391−399.
8. *Huang C.M., Chen C.H., Pornpattananangkul D., Zhang L., Chan M., Hsieh M.F., Zhang L.F.* // Biomaterials. 2011. V. 32. P. 214−221.
9. *Raychowdhury M.K., Goswami R.* // J. Appl. Microbiol. 1985. V. 59. № 2. P. 183−188.
10. *Sheu C.W., Freese E.* // J. Bacteriol. 1972. V. 111. № 2. P. 516−524.
11. *Jenkins J.K., Courtney P.D.* // Can. J. Microbiol. 2003. V. 49. P. 51−57.
12. *Saito H., Tomioka H., Yoneyama T.* // Antimicrobial Agents and Chemotherapy. 1984. V. 26. № 2. P. 164−169.
13. *Kondo E., Kanai K.* // Jpn. J. Med. Sci. Biol., 1977. V. 30. № 4. P. 171−178.
14. *Kabara J.J., Swieczkowski D.M., Conley A.J., Truant L.P.* // Antimicrobial Agents and Chemotherapy. 1972. V. 2. № 1. P. 23−28.
15. *Fay J.P., Farias R.N.* // J. Gen. Microbiol. 1975. V. 91. P. 233−240.
16. *Sheu C.W., Freese E.* // J. Bacteriology, 1973. V. 115. № 3. P. 869−875.
17. *Miller R.D., Brown K.E., Morse S.A.* // Infect. Immun. 1979. V. 17. № 2. P. 303−312.
18. *Khulusi S., Ahmed H.A., Patel P., Mendall M.A., Northfield T.C.* // J. Med. Microbiol. 1995. V. 42. P. 276−282.
19. *Petschow B.W., Batema R.P., Ford L.L.* // Antimicrobial Agents and Chemotherapy. 1996. V. 40. № 2. P. 302−306.
20. *Светличный В.А., Романова А.К., Эль-Регистан Г.И.* // Микробиология. 1986. Т. 55. № 1. С. 55−59.
21. *Светличный В.А., Эль-Регистан Г.И., Романова А.К., Дуда В.И.* // Микробиология. 1983. Т. 52. № 1. С. 33−38.
22. *Бабусенко Е.С., Эль-Регистан Г.И., Градова Н.Б., Козлова А.Н., Осипов Г.А.* // Успехи химии. 1991. Т. 60. № 11. С. 2362−2372.
23. *Nicolaides N.* // Science. 1974. V. 186 (4158). P. 19−26.
24. *Corcoran B.M., Stanton C., Fitzgerald G.F., Rossl R.P.* // Microbiology. 2007. V. 153. P. 291−299.
25. *Guerrini S., Bastianini A., Granchi L., Vincenzini M.* // Curr. Microbiol. 2002. V. 44. № 1. P. 5−9.
26. *Hassinen, J.B., Durbin, G.T., Bernhard, F.W.* // Arch. Biochem., 1950. V. 25. P. 91−96.
27. *Boughton B.W., Pollock M.R.* // Biochem. J. 1953. V. 53. P. 261−265.
28. *Lo K.W., Chua H., Lawford H., Lo W.H., Peter H.F.Y.* // Appl. Biochem. Biotechnol. 2005. V. 122. № 1−3. P. 575−580.
29. *Dekio I., Hayashi H., Sakamoto M., Kitahara M., Nishikawa T., Suematsu M., Benno Y.* // J. Med. Microbiol. 2005. V. 54. P. 1231−1238.
30. *Терехова Е.А., Степичева Н.А., Пшеничникова А.Б., Швец В.И.* // Прикл. биохимия и микробиология. 2010. Т. 46. № 2. С. 180−186.

31. *Doronina N., Ivanova E., Trotsenko Y., Pshenichnikova A., Kalinina E., Shvets V.* // Sistem. Appl. Microbiol. 2005. V. 28. P. 303−309.

32. *Нево А.Н.С., Пшеничникова А.Б., Складнев Д.А., Швец В.И.* // Микробиология. 2004. Т. 73. № 2. С. 1−5.

33. *Физер Л., Физер М.* // Реагенты для органического синтеза. М.:Мир, 1970. Т. II. С. 320.

34. *Dubois M., Gilles K.A., Hamilton J.K., Rebers P.A.* // Anal. Chem. 1983. V. 28. P. 350−356.

35. *Bligh E., Dyer W.A.* // Can. J. Biochem. 1959. № 8. P. 911−917.

36. *Кейтс М.* Техника липидологии. М.: Мир, 1975. 322 с.

37. *Christie W.W.* // Advances in Lipid Methodology / Ed. W.W. Christie. Dundee, England: Oily Press, 1993.V. 2. P. 69−111.

38. *Шталь Э.* // Хроматография в тонких слоях. М.: Мир, 1965. С. 151, 295, 482.

39. *Touchstone J.C., Balin A.K., Murawec T., Kasparow M.* // J. Chromatogr. Sci. 1970. V. 8. P. 443.

40. *Mukerjee P., Mysels K.J.* Critical Micelle Concentrations of Aqueous Surfactant Systems. National Standard Reference Data Series, National Bureau of Standards. Washington, D.C.: Government Printing Office, 1971. P. 136, 170.

41. *Murakami K., Chan S.Y., Routtenberg A.* // J. Biol. Chem. 1986. V. 261. № 33. P. 15424−15429.

Effect of Exogenous Fatty Acids on the Growth and Production of Exopolysaccharides of Obligately Methylotrophic Bacterium *Methylophilus quaylei*

S. A. M. Otman, A. B. Pshenichnikova, and V. I. Shvets

Lomonosov State Academy of Fine Chemical Technology, Moscow, 117571 Russia

e-mail: a_pshenichnikova@mail.ru

Abstract—Accelerating growth and increasing exopolysaccharide production in obligate methylotrophic bacterium *Methylophilus quaylei* were observed in the presence of C_{12}−C_{18} fatty acids added to the growth media. Sodium oleate was the best growth factor. Based on data on the composition of the free fatty acids fraction in the cells and the values of the ζ-potential and fluorescence anisotropy of whole cells, we suggested that fatty acids were incorporated in the outer membrane of *M. quaylei*.

ОТНОШЕНИЕ [13C]/[12C] КАК ПОКАЗАТЕЛЬ ДЛЯ ЭКСПРЕСС-ОЦЕНКИ УГЛЕВОДОРОДОКИСЛЯЮЩЕГО ПОТЕНЦИАЛА МИКРОБИОТЫ В ПОЧВЕ, ЗАГРЯЗНЕННОЙ СЫРОЙ НЕФТЬЮ

© 2012 г.   А. М. Зякун*,**, А. М. Боронин*,**, В. В. Кочетков*, Б. П. Баскунов*, К. С. Лауринавичюс*, В. Н. Захарченко*, В. П. Пешенко*, Т. О. Анохина*, Т. В. Сиунова*

*Институт биохимии и физиологии микроорганизмов им. Г.К. Скрябина РАН,
Пущино, Московская обл., 142290
**Пущинский государственный университет,
Пущино, Московская обл., 142290
e-mail: zyakun@ibpm.pushchino.ru
Поступила в редакцию 26.08.2011 г.

Исследован углеводородокисляющий потенциал почвенной микробиоты и интродуцированных в почву углеводородокисляющих микроорганизмов на основе количественных и изотопных характеристик углерода продуктов, образующихся при микробной деградации нефти. Из сравнения скоростей продукции CO_2 в нативной почве и почве, загрязненной сырой нефтью, обнаружено, что интенсивность микробной минерализации почвенного органического вещества (**ПОВ**) в присутствии нефти выше по сравнению с незагрязненной почвой, т.е., обнаруживается затравочное влияние (прайминг-эффект) углеводородов нефти. Показано, что количество углерода вновь синтезированных органических продуктов за счет потребленной нефти (биомасса клеток и экзометаболиты) значительно превосходит количество ПОВ, израсходованное на продукцию CO_2. Обнаружено, что в результате микробиологических процессов в почве, загрязненной нефтью, наблюдается мощный поток углекислоты, поступающей в атмосферу.

Главным фактором, способствующим снижению нефтяных загрязнений в почвах, является потребление и минерализация углеводородов почвенными микроорганизмами в качестве субстратов. К настоящему времени изучена роль микроорганизмов в биоремедиации загрязненных углеводородами почв, где ключевыми составляющими этого процесса являются биотрансформация, биодеструкция и биоминерализация антропогенных поллютантов.

В современной биотехнологии в случае углеводородного загрязнения почвы известны три типа биоремедиации: а) естественная убыль поллютанта в результате его потребления нативной почвенной микробиотой; б) биостимуляция микробных процессов в почве путем внесения дополнительных минеральных и органических добавок; в) внесение в загрязненные почвы специфических штаммов микроорганизмов, которые способны активно потреблять углеводородные поллютанты (биоаугментация) [1].

Самый простой метод биоремедиации заключается в использовании биодеградирующей активности природной микробиоты и предсказании возможного снижения загрязнения до безопасного уровня на основе наблюдений, подтверждающих необходимую интенсивность этих природных процессов.

При низких скоростях снижения нефтяных загрязнений в почвах проводят биостимуляцию углеводородокисляющей почвенной микробиоты, т.е., дополнительно вносят минеральные и органические вещества, необходимые для жизнедеятельности микроорганизмов, обеспечивают оптимальную влажность почвы и аэрацию. При крайне малом количестве углеводородокисляющих микроорганизмов или их отсутствии в загрязненных почвах проводят биоаугментацию почв, т.е. вносят специфические штаммы микроорганизмов, которые способны использовать в качестве субстрата углеводороды нефти и нефтепродукты.

Все эти факторы могут существенно влиять на физиолого-биохимические свойства почвенных популяций микроорганизмов, в частности на продукцию метаболической углекислоты, количественный и качественный состав почвенного органического вещества (**ПОВ**), а также на масштабы эмиссии CO_2 из почв в атмосферу. Адекватная оценка углеводородокисляющего потенциала микробиоты в почве предусматривает использование экспрессных, высоко специфических и высокоточных методов для анализа скоростей снижения углеводородных загрязнений, а также выявление как благоприятных, так и потенциально

опасных для окружающей среды факторов, которые сопровождают процесс биоремедиации.

Цель исследования — разработка технологии экспресс-оценки эффективности микробной деградации углеводородов в почве, изучение влияния сырой нефти на микробные процессы, определение метаболического потенциала нативных микроорганизмов и интродуцированных в почву лабораторных штаммов, обладающих повышенной способностью окислять углеводороды нефти, выявление факторов, способствующих эмиссии метаболической углекислоты в атмосферу в результате активации почвенной микробиоты.

МЕТОДИКА

Почва. Использовали образцы пахотной почвы из Краснодарского края после выращивания на них кукурузы (C$_4$-растение). Образцы почвы просеивали через сито с ячейками около 2 мм, удаляли растительные остатки, затем увлажняли до 60% максимальной влагоемкости. Исходное содержание органического вещества в почве составляло около 4.9% веса сухой почвы (**СП**), что соответствовало 19.6 г C/кг СП. Образцы почвы в количестве 100 г по сухой массе помещали в 750 мл стеклянные сосуды, которые герметично закрывали пластмассовыми крышками и предварительно перед внесением нефти выдерживали в течение 3 сут при 22°C. Для фиксации метаболической углекислоты, образующейся при микробной минерализации ПОВ и нефти, над поверхностью почвы располагали стеклянные чашки (10 мл), содержащие от 2 до 3 мл раствора 1M NaOH. Количество CO$_2$, зафиксированное в водном растворе NaOH, после добавления BaCl$_2$ осаждали в виде BaCO$_3$. Продукцию CO$_2$ в ходе экспериментов в каждом из сосудов определяли по количеству 0.1 M HCl водного раствора, расходуемого на титрование остаточной щелочи в чашках. Карбонат бария промывали водой, осаждали, высушивали и взвешивали полученные осадки. Затем их использовали для количественной оценки продукции метаболической CO$_2$ и изотопного анализа углерода.

Нефть — экзогенный тест-субстрат. В модельных опытах внесенное количество сырой нефти в почву составляло 3.2% от веса СП, что соответствовало 27.43 г C нефти на кг СП. Так как в образце сухой почвы содержание ПОВ было около 19.6 г C/кг СП, то доля внесенного в почву углерода нефти превышала в 1.4 раза количество углерода ПОВ. Полагая, что основная часть сырой нефти при разливе ее на почве будет содержаться в верхнем 10 см слое, находим, что предполагаемая степень загрязненной почвы составит около 32 т сырой нефти из расчета на 1 га площади.

Микроорганизмы. Модельные опыты по определению микробной минерализации внесенной в почву нефти проводили в 12 стеклянных сосудах в 4 вариантах (2 контроля и 2 опыта, по 3 повторности в каждом опыте и контроле). В опыте 1 в сосуды с почвой и содержащейся в ней нативной микробиотой вносили сырую нефть, в опыте 2 — в такую же почву с нефтью дополнительно вносили лабораторный штамм *Pseudomonas aureofaciens* BS1393(pBS216) [2]. В контроле 1 использовали почву без добавления нефти, а в контроле 2 в такую же почву дополнительно вносили бактерии *P. aureofaciens* BS1393(pBS216). Указанный лабораторный штамм с плазмидой pBS216, контролирующей биодеградацию нафталина и салицилата, был способен утилизировать ароматические углеводороды нефти и обладал антагонистическим эффектом по отношению к широкому кругу фитопатогенных грибов. Способность штамма к синтезу антибиотиков феназинового ряда, окрашивающих его колонии в ярко-оранжевый цвет на агаризованной среде LB [3], позволила использовать эту особенность в качестве маркера при количественном учете указанных микроорганизмов в почве в присутствии аборигенной микрофлоры.

Интродуцируемый штамм бактерий предварительно выращивали в жидкой среде LB до стационарной фазы при 28°C в течение 18 ч и затем равномерно вносили в почву до концентрации 10^6 кл./г почвы. Усредненную (суммарную) почвенную пробу для анализа количества содержащихся в них бактериальных клеток отбирали в трех независимых точках. Навеску (1 г) усредненной почвенной пробы суспендировали в 10 мл 0.85% NaCl, осаждали почвенные частицы и из 1 мл надосадочной жидкости делали разведения (10×—10000×). Соответствующие разведения по 0.1 мл высевали на чашки Петри с LB средой. Затем проводили подсчет колониеобразующих единиц (**КОЕ**) на чашках и рассчитывали средние значения в контроле и опытах.

Микробная активность. В контролях и опытах оценку проводили по количеству продукции CO$_2$, образующейся в результате минерализации ПОВ и внесенной в почву нефти. В контроле 1 определяли микробную минерализацию ПОВ с участием аборигенных микроорганизмов, присутствующих в этом типе почв. В контроле 2 определяли микробную минерализацию ПОВ с участием аборигенных микроорганизмов и интродуцированного штамма BS1393(pBS216), количество которого составляло около 10^6 кл./г почвы. В опыте 1 определяли микробную минерализацию ПОВ и внесенной в почву нефти (около 3.2% от веса СП) с участием только аборигенных микроорганизмов. В опыте 2 определяли микробную минерализацию ПОВ и внесенной в почву нефти (3.2% от

веса СП) с участием как аборигенных, так и интродуцированных микроорганизмов.

Кинетика субстрат-индуцируемого дыхания (СИД). Микробный метаболизм тест-субстрата (сырая нефть) характеризовался несколькими стадиями по скорости образования CO_2: адаптация микробиоты к тест-субстрату (лаг-период), экспоненциальный рост скорости эмиссии CO_2, достижение максимума этой скорости и последующее постепенное ее снижение до постоянного значения.

Удельные скорости эмиссии метаболической CO_2 (μ) в опытах 1 и 2 после внесения сырой нефти в почву определялись из кинетических характеристик субстрат-индуцируемого дыхания ($CO_2(t)$), получаемых из соответствующего аппроксимирующего уравнения $CO_2(t)$ (1):

$$CO_2(t) = K + r_{эксп}(\mu t), \qquad (1)$$

где параметр K представляет начальную скорость эмиссии CO_2, отражающую катаболические процессы почвенной микробиоты, не сопровождающие рост клеток и не связанные с продукцией АТФ, r отражает начальную скорость образования CO_2 растущей части почвенной микробиоты, которая связана с увеличением количества микробных клеток и, соответственно, с генерацией АТФ, t — время наблюдения [4–6]. Продолжительность лаг-периода роста микробных клеток ($t_{лаг}$) определяли по интервалу между временем внесением субстрата в почву и моментом, когда увеличение скорости эмиссии CO_2, обусловленное экспоненциальным ростом микроорганизмов (т.е., количественное значение $r_{эксп}(\mu t)$ в выражении (1)), превышало скорость углекислотного дыхания, не связанную с продукцией АТФ. Согласно кинетической теории микробного роста [7, 8], лаг-период можно рассчитать, используя параметры кривой (1), представляющей микробную эмиссию CO_2, с использованием выражения (2):

$$t_{лаг} = \ln(K/r)/\mu, \qquad (2)$$

где $t_{лаг}$ — лаг-период образования CO_2 микробиотой в почве.

Анализ изотопного состава углерода. Отношения распространенности изотопов углерода $^{13}C/^{12}C$ в ПОВ, сырой нефти и метаболической CO_2 (в виде $BaCO_3$) были измерены с использованием изотопного масс-спектрометра Breath MAT ("Thermo Finnigan", Германия), соединенного с газовым хроматографом через специальное устройство ConFlow. Для изотопного анализа метаболической CO_2 использовали около 3–4 мг полученного $BaCO_3$ [M.M.197.34], который затем разлагали до CO_2 с помощью ортофосфорной кислоты в 10 мл контейнере в присутствии воздуха. В случае анализа изотопного состава углерода ПОВ и сырой нефти образцы сжигали до CO_2 в ампулах при температуре $560°C$ в присутствии оксида меди (CuO).

Отношения интенсивностей пиков в масс-спектре CO_2 с m/z 45 ($^{13}C^{16}O_2$) и 44 ($^{12}C^{16}O_2$) использовали для количественной характеристики содержания изотопов ^{13}C и ^{12}C в анализируемых образцах. Согласно общепринятому выражению (3), величина $\delta^{13}C$, определенная в относительных единицах в промилях (‰), характеризовала количество изотопа ^{13}C в анализируемых образцах:

$$\delta^{13}C = (R_{обр}/R_{ст} - 1) \times 1000‰, \qquad (3)$$

где $R_{обр} = ([^{13}C]/[^{12}C])_{обр}$ представляет отношения распространенностей изотопов $^{13}C/^{12}C$ в образце, а $R_{ст} = ([^{13}C]/[^{12}C])_{ст}$ — отношения этих изотопов в международном стандарте PDB (Pee Dee Belemnite). Из выражения (3) следует, что в случае положительного или отрицательного значения $\delta^{13}C$ в анализируемом образце содержится больше или меньше изотопа ^{13}C по сравнению со стандартом, а при $\delta^{13}C = 0$, анализируемый образец наследует изотопный состав углерода стандарта. Каждый образец CO_2 анализировали в трех повторах, стандартная ошибка была около $\pm 0.2‰$.

Изотопный баланс. Средневзвешенный изотопный состав углерода метаболической CO_2 ($\delta^{13}C_{ср}$), которую получали на отдельных временных i-интервалах, определяли используя выражение (4):

$$\delta^{13}C_{ср} = (\Sigma q_i \cdot \delta^{13}C_i)/\Sigma q_i ‰, \qquad (4)$$

где q_i и $\delta^{13}C_i$ — скорость микробного образования CO_2 и характеристика ее изотопного состава углерода на i-интервалах соответственно.

В качестве специфических количественных показателей микробного метаболизма в тестируемых почвах были использованы: а) изотопные характеристики углерода суммарной CO_2, образующейся при микробной минерализации ПОВ и нефти ($\delta^{13}C_{сум}$) (опыты 1 и 2), б) характеристика CO_2, наблюдаемой при минерализации только ПОВ ($\delta^{13}C_{ПОВ}$) (контроль 1 и 2), в) характеристика CO_2, продуцируемой при минерализации нефти, которая с точностью до изотопного эффекта, сопровождаемого окисление углеводородов (около $-(1-3)‰$ [9], наследует изотопный состав нефти ($\delta^{13}C_{нефть}$). С учетом сформулированных положений (а, б и в) и используя выражение (5), вычисляли долю CO_2, которая образовалась при минерализации ПОВ ($F_{ПОВ}$) и нефти ($F_{нефть} = 1 - F_{ПОВ}$) соответственно.

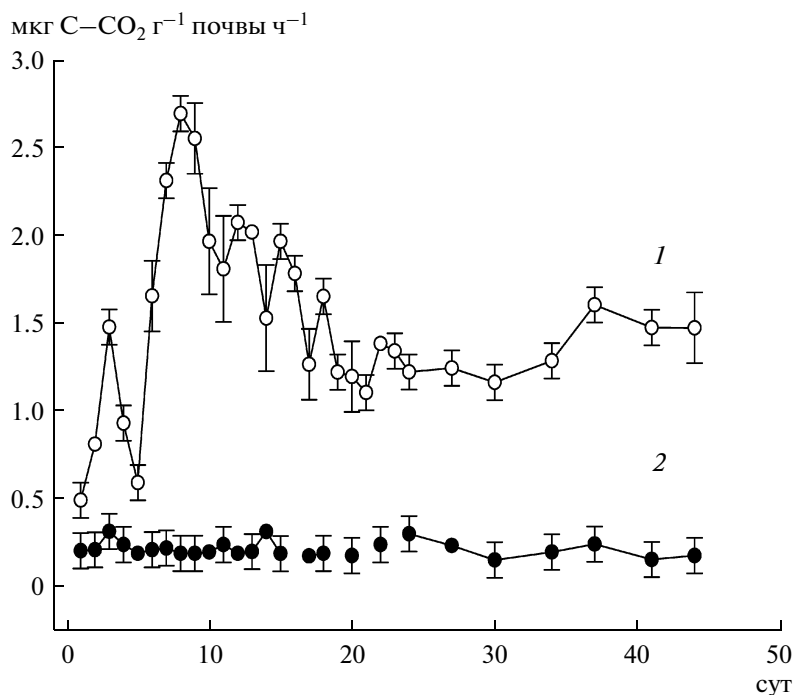$$F_{ПОВ} = (\delta^{13}C_{сум} - \delta^{13}C_{нефть})/(\delta^{13}C_{ПОВ} - \delta^{13}C_{нефть}). \ (5)$$

Рис. 1. Скорость эмиссии CO_2 (мкг С−CO_2 г$^{-1}$ СП) при микробной минерализации органических продуктов в экспериментах, моделирующих микробное потребление углеводородов нефти. Образование CO_2 почвенной микробиотой и интродуцированными бактериями *P. aureofaciens* BS1393(pBS216) после внесения 3.2% сырой нефти в почву (*1*) и то же без внесения сырой нефти в почву (*2*).

Затравочный (прайминг) эффект нефти. При внесении экзогенных органических продуктов в почву в ряде случаев наблюдаются активация или ингибирование микробной минерализации ПОВ по сравнению с существующими до этого процессами. В литературе это рассматривают как положительное или отрицательное затравочное влияние этих продуктов на микробную минерализацию ПОВ и представляют как прайминг-эффект (**ПЭ**) соответствующих продуктов [10, 11]. В нашем случае внесение углеводородов нефти в почву также может ускорять или замедлять скорость микробной минерализации нативного органического вещества, т.е. проявлять их ПЭ. Для оценки величины ПЭ количество CO_2, образующееся в результате минерализации ПОВ в присутствии нефти, сравнивали с количеством CO_2 при минерализации ПОВ в нативной почве. На основе изотопного баланса (выражение 5) рассчитывали долю CO_2 ($F_{ПОВ}$) в суммарном ее количестве, образующемся при микробной минерализации ПОВ и нефтепродуктов (опыты 1 и 2). Величину ПЭ нефти, как экзогенного субстрата, вычисляли путем сравнения количества CO_2 из ПОВ в опытах с количеством CO_2 в контроле, образовавшихся за соответствующие периоды наблюдения (выражение 6):

$$ПЭ = 100 \cdot (Q_{сум}F_{ПОВ} - Q_{ПОВ})/Q_{ПОВ}, \%, \qquad (6)$$

где $Q_{сум}$ − суммарное количество CO_2 при минерализации ПОВ и нефти (опыты 1 и 2), а $Q_{ПОВ}$ − количество CO_2 при минерализации только ПОВ (контроль).

РЕЗУЛЬТАТЫ И ИХ ОБСУЖДЕНИЕ

Эмиссия CO_2 из почвы. Активности микробной минерализации ПОВ и нефти в почве представлены суммарными скоростями эмиссии CO_2 из почвы в модельных экспериментах (рис. 1, *1* и рис. 2, *1*). В контролях 1 и 2 скорости минерализации ПОВ как почвенными микроорганизмами, так и смесью этих микроорганизмов с интродуцированным штаммом находились в диапазоне 0.2 ± 0.02 мкг С−CO_2 г$^{-1}$ СП ч$^{-1}$ и, практически, не изменялись в течение 47-суточного наблюдения (рис. 1, *2* и рис. 2, *2*). В почвах, в которые была внесена нефть (опыты 1 и 2), скорость минерализации суммарного органического вещества (ПОВ + нефть) существенно увеличивалась и на 7−9 сут после начала экспозиции достигала максимальной величины около 3.2 мкг С−CO_2 г$^{-1}$ СП ч$^{-1}$ (рис. 1, *1* и рис. 2, *1*). Следует отметить, что в случае интродукции в почву бактерий *P. aureofaciens* BS1393(pBS216) (опыт 2) увеличение скорости эмиссии CO_2 отмечено сразу после начала эксперимента, а в опыте 1 (только аборигенная почвенная микробиота)
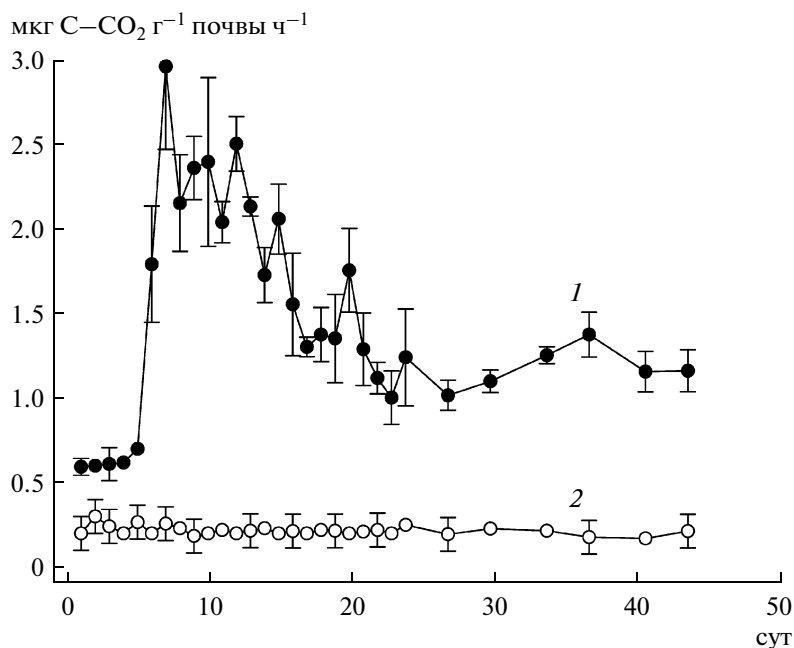
мкг C−CO$_2$ г$^{-1}$ почвы ч$^{-1}$

Рис. 2. Скорость эмиссии CO$_2$ (мкг C−CO$_2$ г$^{-1}$ СП) при микробной минерализации органических продуктов в экспериментах, моделирующих микробное потребление углеводородов нефти: *1* − образование CO$_2$ аборигенными почвенными микроорганизмами после внесения 3.2% сырой нефти в почву (опыт 1); *2* − то же без внесения сырой нефти (контроль 1).

продукция CO$_2$ практически не увеличивалась в течение 6 сут (лаг-период). Это наблюдение согласуется с результатами количественных измерений (число КОЕ), интродуцированных в почву бактерий *P. aureofaciens* BS1393(pBS216) с нефтью и без нефти в почве. Как видно из рис. 3, сразу после интродукции в почву штамма *P. aureofaciens* BS1393(pBS216) как в опыте 2 (почва с нефтью), так и в контроле 2 (почва без нефти) наблюда-
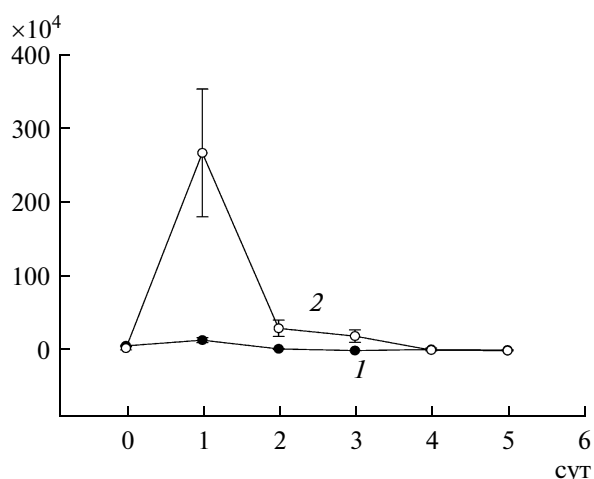
лось снижение количества клеток этого штамма до 10^4 кл./г почвы (стресс-эффект смены среды). Однако через 1 сут после начала эксперимента, число КОЕ интродуцированных бактерий в опыте 2 составило около 2.5 × 10^6 кл./г, что более чем в 17 раз превышало величину КОЕ этих же бактерий в контрольной почве, не содержащей нефть.

Убедительным подтверждением результатов, демонстрирующих рост бактерий *P. aureofaciens* BS1393(pBS216) в почве, содержащей углеводороды нефти, является изменение скорости эмиссии CO$_2$ в опыте 2 по сравнению с контролем (рис. 1). На кривой (рис. 1, *1*) отмечены два максимума скорости эмиссии CO$_2$: первый максимум наблюдается через 3 сут и второй − через 7 сут после внесения нефти. Предполагалось, что первый максимум обусловлен углеводородокисляющей активностью интродуцированных в почву бактерий *P. aureofaciens* BS1393(pBS216), а второй связан с проявлением углеводородокисляющей активности аборигенной (нативной) почвенной микробиоты. Подтверждением высказанного предположения явились результаты, полученные в опыте 1 (рис. 2), где в почву была внесена сырая нефть, а ее минерализация осуществлялась только нативной почвенной микробиотой. Как следует из рис. 2, *1*, максимум скорости эмиссии CO$_2$ в опыте 1 достигал через 7 сут после внесения нефти в почву и был близким по времени с появлением второго максимума эмиссии CO$_2$ в предыду-

×10^4

Рис. 3. Количество клеток (×10^4 КОЕ/г почвы) бактерий *P. aureofaciens* BS1393(pBS216) в процессе их роста: *1* − в образцах почвы без внесения сырой нефти (контроль 2); *2* − то же +3.2% сырой нефти (опыт 2).

Таблица 1. Кинетическая характеристика начальной скорости эмиссии микробной CO_2 в почвах, загрязненных сырой нефтью

Условия	K, мкг С—CO_2 г$^{-1}$СП ч$^{-1}$	r, мкг С—CO_2 г$^{-1}$СП ч$^{-1}$	μ, мкг С—CO_2 г$^{-1}$ СП ч$^{-1}$	$t_{\text{лаг}}$, сут
Опыт 1	0.61 ± 0.014	$(9 \pm 4) \times 10^{-6}$	1.78 ± 0.15	6.2 ± 0.7
Опыт 2	0.49 ± 0.024	$(7.4 \pm 3.6) \times 10^{-3}$	1.69 ± 0.15	2.4 ± 0.6

Примечание: Опыт 1 — нативная почвенная микробиота; опыт 2 — нативная почвенная микробиота + интродуцированные бактерии *P. aureofaciens* BS1393(pBS216).

щем опыте (рис. 1, *1*). Таким образом, анализ кинетики эмиссии CO_2 как в опыте 1, так и в опыте 2 показал, что спустя определенный период (около 6 сут) после внесения нефти в почву наблюдалось проявление активности аборигенных углеводородокисляющих микроорганизмов, которые широко распространены в почвенных и водных экосистемах [12—14].

Ранее на примере образцов почв, не загрязненных нефтью, которые различались географическим расположением на территории США, было показано, что внесение сырой нефти в такие почвы способствовало преимущественному росту микроорганизмов, имеющих сходство с *Rhodococcus erythropolis* [15]. В дополнение к этому на основе данных анализа гена 16S рРНК авторами работы [15] не было обнаружено микроорганизмов, относящихся к роду *Pseudomonas*, что рассматривается как свидетельство низкой конкурентной способности потребления углеводородов нефти указанными микроорганизмами по сравнению с другими углеводородокисляющими представителями, как например родококками и нокардиями. Следовательно, в нашем случае отмеченное снижение количества клеток *P. aureofaciens* BS1393(pBS216) в почве (рис. 3) и уменьшение скорости эмиссии CO_2 через 4—5 сут после внесения этих бактерий в почву, содержащую углеводороды нефти (опыт 2, рис. 1), можно рассматривать, как свидетельство низкой конкурентной способности интродуцированного штамма *P. aureofaciens* BS1393(pBS216) в сравнении с аборигенной углеводородокисляющей микробиотой относительно потребления субстрата (нефть).

Лаг-период микробной минерализации нефти. После внесения сырой нефти в почву удельные скорости эмиссии метаболической CO_2 (μ) в опытах 1 и 2 определяли из анализа начальных кинетических характеристик субстрат-индуцируемого дыхания, получаемых с помощью аппроксимирующего уравнения $CO_2(t)$ (1), а лаг-период ($t_{\text{лаг}}$) был рассчитан согласно выражению (2).

На начальных стадиях микробной минерализации нефти в опытах 1 и 2 были рассчитаны значения параметра K как показателя катаболического микробного метаболизма покоящихся клеток, указывающие на близкие скорости эмиссии

CO_2 в этих опытах (табл. 1). В то же время параметр r, свидетельствующий о наличии в почве растущих микроорганизмов, на три порядка был выше в опыте 2 с интродуцированными бактериями по сравнению с опытом 1, в почве которого находись аборигенные микроорганизмы. Параметр μ, отражающий удельные скорости эмиссии CO_2, в опытах 1 и 2 имел близкие значения в пределах ошибки измерения. Как и следовало ожидать, лаг-период потребления тест-субстрата и эмиссия CO_2 в опыте 2 с интродуцированными в почву бактериями *P. aureofaciens* BS1393(pBS216) составлял 2.4 ± 0.6 сут и был значительно меньше по сравнению с опытом 1, где в почве содержалась только нативная микробиота (лаг-период 6.2 ± 0.7 сут). По истечении 6-суточного периода скорость эмиссии метаболической углекислоты в результате деятельности почвенных микроорганизмов в опытах 1 и 2 начала резко возрастать (рис. 1, рис. 2). Таким образом, различие в скоростях эмиссии CO_2 на начальных стадиях экспериментов в этих опытах, очевидно, связано с наличием углеводородокисляющих бактерий *P. aureofaciens* BS1393(pBS216) и их ускоренным ростом в присутствии углеводородов нефти (опыт 2) (рис. 3).

После достижения максимальных скоростей эмиссии CO_2 в опытах 1 и 2 отмечено их постепенное снижение. Однако, начиная с 25 по 47 сут, скорости эмиссии CO_2 в опытах стабилизировались на уровне 1.25 ± 0.25 мкг С—CO_2 г$^{-1}$ СП ч$^{-1}$ (рис. 1, рис. 2), в то время как в контрольных экспериментах (контроли 1 и 2) скорости эмиссии CO_2 практически не изменялись и составляли 0.2 ± 0.02 мкг С—CO_2 г$^{-1}$ СП ч$^{-1}$. За 47-суточный период наблюдения общее количество CO_2 в контрольных измерениях (контроли 1 и 2) составляло 24.8 ± 0.2 мг С—CO_2 (табл. 2). Отсутствие значимой разницы в количествах CO_2 в контролях 1 и 2 рассматривалось, как свидетельство о незначительной дополнительной минерализации ПОВ за счет внесенной в почву культуры *P. aureofaciens* BS1393(pBS216). Количества метаболической CO_2 в опытах 1 и 2, почвы которых содержали нефть, в 6.8 раза превышали количества CO_2 в контролях 1 и 2 и составляли 167.0 мг С—CO_2 (опыт 1) и 174.0 мг С—CO_2, (опыт 2) соответственно (табл. 2). Как следует из полученных данных,

Таблица 2. Средние скорости эмиссии углекислоты (мкг $C-CO_2$ г$^{-1}$СП ч$^{-1}$) и общее количество $C-CO_2$ за время 47-суточного эксперимента (мг $C-CO_2$ на 100 г СП)

Условия	Скорость эмиссии CO_2, мкг $C-CO_2$ г$^{-1}$СП ч$^{-1}$	Общее количество CO_2, мг $C-CO_2$
Контроль 1	0.228 (0.013)*	25.72 (0.6)
Контроль 2	0.213 (0.0126)	24.03 (0.59)
Опыт 1	1.480 (0.122)	166.94 (5.7)
Опыт 2	1.546 (0.100)	174.4 (4.7)

*В скобках приведены стандартные ошибки трех параллельных определений.

дополнительное внесение углеводородокисляющего штамма *P. aureofaciens* BS1393(pBS216) в почву, содержащую нефть (опыт 2), способствовало увеличению количества метаболической CO_2 лишь в начальной стадии экспозиции и в незначительной степени (на 4%) отразилось на суммарной минерализации углеводородов нефти в сравнении с образованием CO_2 аборигенными почвенными микроорганизмами.

Анализ происхождения CO_2 с использованием $\delta^{13}C$. Общее количество CO_2, образующейся в опытах 1 и 2, обусловлено микробной минерализацией как ПОВ, так и углеводородов нефти. Для определения доли CO_2, образующейся при минерализации каждого из указанных субстратов, были проведены измерения изотопных характеристик ($\delta^{13}C$) субстратов (ПОВ и нефтепродукты) и образующейся при этом метаболической углекислоты. Известно, что в случае субстрат-индуцируемого дыхания для разделения потоков метаболической CO_2 используют изотопно-меченные по углероду ^{14}C или ^{13}C экзогенные субстраты, которые по этим показателям отличаются от углерода ПОВ. При определении вероятности включения ^{14}C-изотопа в метаболическую CO_2, несмотря на сравнительную простоту измерений, существуют известные сложности, связанные с рандомизацией субстрата в почве, и обусловленные этим сомнения в достоверности полученных результатов [16, 17]. Более удобным как в техническом решении, так и с точки зрения экологической безопасности оказалось использование субстратов, обогащенных стабильным изотопом ^{13}C. При значимом различии в естественных содержаниях ^{13}C-изотопа в субстрате (например, использование глюкозы как продукта C_4-растений) и ПОВ (почвы после длительного культивирования C_3-растений) была продемонстрирована возможность количественного определения скорости образования CO_2 при микробной минерализации этих продуктов в почве [18].

В наших экспериментах изотопный состав углерода ПОВ характеризовался величиной $\delta^{13}C$, равной $-23.01 \pm 0.2‰$, что рассматривалось как свидетельство вегетации C_4-растений на анализи-

руемой почве. Согласно предварительным измерениям, изотопный состав углерода используемой нефти из Краснодарских месторождений характеризовался величиной $\delta^{13}C$, равной $-28.4 \pm 0.2‰$, при этом легкая и тяжелая фракции нефти имели $\delta^{13}C$, равные $-28.9‰$ и $-27.2‰$ соответственно. Следует отметить, что характеристика изотопного состава углерода ($\delta^{13}C$) нефти, используемой в опытах, была близкой к образцам легкой нефти из месторождений Арабского региона, где величина $\delta^{13}C$ нефти составляла $-27.5 \pm 0.5‰$, алкановой фракции $-28 \pm 0.5‰$, а фракции, содержащей преимущественно ароматические углеводороды, соответственно $-26.5 \pm 1.5‰$ [19].

Принимая во внимание тот факт, что изотопный состав углерода углеводородов нефти существенно отличался от изотопной характеристики углерода ПОВ, появилась возможность использовать эти различия как специфические изотопные маркеры и оценить отдельно скорости микробной минерализации ПОВ и экзогенных углеводородов нефти.

На рис. 4 приведены значения $\delta^{13}C$ углерода CO_2, образующейся в опыте 1 (минерализация ПОВ и нефти только почвенной микробиотой) и в опыте 2 (минерализация ПОВ и нефти почвенной микробиотой и бактериями *P. aureofaciens* BS1393(pBS216)). В качестве контроля служила величина $\delta^{13}C-CO_2$ – характеристика изотопного состава углерода CO_2, образующейся при микробной минерализации ПОВ только почвенной микробиотой (контроль 1) и смесью почвенной микробиоты и интродуцированных бактерий *P. aureofaciens* BS1393(pBS216) (контроль 2). Величины $\delta^{13}C$ в случае CO_2, продуцируемой при микробной минерализации ПОВ (контроль 1 и 2), находились в пределах $-23.5 \pm 0.5‰$ в течение 47-суточного эксперимента и практически наследовали изотопный состав углерода ПОВ (рис. 4). Существенные изменения величины $\delta^{13}C-CO_2$ от -23.5 до $-28.5 \pm 0.5‰$ отмечены в опытах 1 и 2 в течение 7–9 сут после внесения нефти в почву. Принимая во внимание тот факт, что изотопные характеристики углерода алифатической фракции нефти характеризовались величиной $\delta^{13}C = -28.9‰$, то
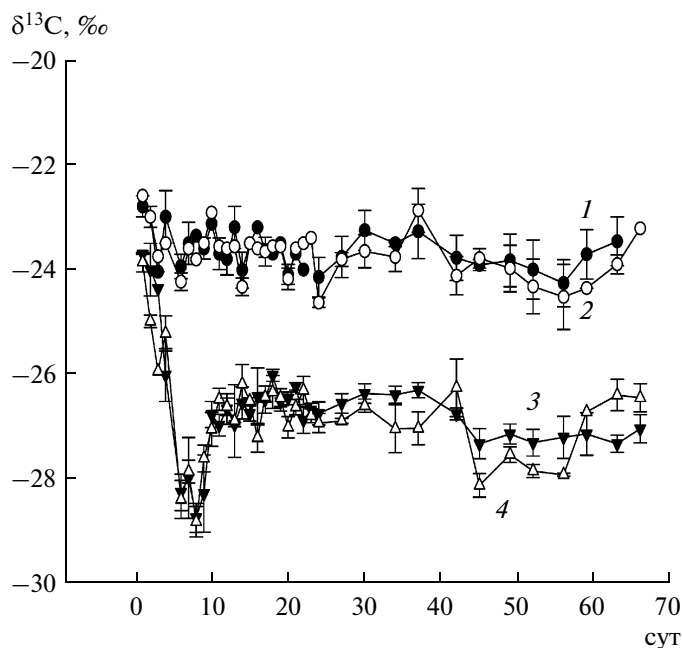
Рис. 4. Изотопная характеристика углерода (δ^{13}C (‰) CO$_2$, образующегося в модельных экспериментах при микробной минерализации ПОВ и углеводородов нефти, внесенных в почву: *1* – почвенная микрофлора без нефти (контроль 1); *2* – то же + бактерии *P. aureofaciens* BS1393(pBS216) (контроль 2); *3* – почвенная микрофлора + 3.2% сырой нефти (опыт 1); *4* – то же + + бактерии *P. aureofaciens* BS1393(pBS216) (опыт 2).

 нию с н-алканами углеводородных фракций, так и с увеличением окисления доли ПОВ. Независимо от этого, различие в величинах δ^{13}C, характеризующих изотопный состав углерода CO$_2$ в опытах и контроле в период от 10 до 47 сут, свидетельствует о продолжающейся микробной деградации углеводородов нефти и ПОВ в течение указанного периода.

Величину δ^{13}C, характеризующую изотопный состав углерода CO$_2$, которая образовалась в опытах в течение всего 47-суточного эксперимента, находили как средневзвешенное значение δ^{13}C согласно выражению (4). Полученное значение δ^{13}C(CO$_2$) для обоих опытов составляло около -26.6 ± 0.1‰.

При определении доли углерода CO$_2$, образующейся в результате минерализации ПОВ и углеводородов нефти на основе изотопного баланса (выражение 4), исходили из следующих допущений: а) изотопные характеристики углерода CO$_2$, образующейся при минерализации ПОВ, являются одинаковыми как в нативной почве, так и в почве, содержащей углеводороды нефти; б) средневзвешенные изотопные характеристики углерода CO$_2$, образующейся при минерализации углеводородов нефти, наследуют характеристики нефти с точностью до изотопного эффекта (не более 1–3‰).

С использованием выражения (5) была определена часть углерода ПОВ ($F_{ПОВ}$), которая минерализована микроорганизмами в опытах 1 и 2 за время 47-суточных экспериментов (табл. 3). Из суммарного количества метаболической углекислоты в опытах 1 и 2 обнаружено, что около 38% всей CO$_2$ образовалось в результате микробной минерализации ПОВ, а около 62% обусловлено минерализацией углеводородов внесенной нефти.

Затравочный (прайминг) эффект углеводородов нефти. Проблема затравочного влияния (ПЭ) легко метаболизируемых органических субстратов (свежие продукты растительного фотосинтеза, углеводы, аминокислоты, органические кислоты и др.) на минерализации ПОВ с участием почвенных микроорганизмов является предметом дис-

регистрируемые значения δ^{13}C–CO$_2$ в опытах 1 и 2 на начальной стадии минерализации нефти, достигающие -29‰, рассматривались, как свидетельство преимущественной микробной минерализации алифатических углеводородов. В последующий период после 10 и 47 сут наблюдения изотопные характеристики метаболической CO$_2$ стабилизировались на уровне δ^{13}C = -26.8 ± 0.5‰ и находились между изотопными характеристиками углерода ПОВ (δ^{13}C$_{ПОВ}$ = -23.01 ± 0.2‰) и нефти (δ^{13}C$_{нефть}$ = -28.4 ± 0.2‰). Наблюдаемое значение δ^{13}C = -26.8‰ в случае метаболической CO$_2$ может быть обусловлено как в результате окисления более тяжелых по сравне-

Таблица 3. Средневзвешенный изотопный состав углерода и доля CO$_2$, которая образовалась за счет минерализации ПОВ и затравочные эффекты в опытах 1 и 2 в течение 47-суточного эксперимента

Условия	*δ^{13}C$_{ср}$, ‰	**$F_{(ПОВ)}$, %	[CO$_2$](ПОВ), мг С–CO$_2$	ПЭ, %
Контроль 1	-23.70 (0.1)	100	25.72 (0.6)	0
Контроль 2	-23.77 (0.1)	100	24.03 (0.59)	0
Опыт 1	-26.59 (0.2)	38.5 (1.7)	64.3 (3)	150 (13)
Опыт 2	-26.63 (0.2)	38.2 (1.6)	66.6 (3)	177 (15)

*δ^{13}C$_{ср}$ – средневзвешенный изотопный состав углерода CO$_2$.

**F – доля метаболической CO$_2$, образующейся при микробной минерализации ПОВ, рассчитанная согласно (5).

Таблица 4. Балансовые расчеты минерализации ПОВ и сырой нефти микроорганизмами в почве за время 47-суточного эксперимента (мг $C-CO_2$ на 100 г СП)

Условия	Исходное $C_{орг}$, мг		Количество $C-CO_2$, мг		Минерализация нефти, %
	ПОВ	нефть	ПОВ	нефть	
Контроль 1	1960	0	25.72 (0.6)*	0	–
Контроль 2	1960	0	24.03 (0.6)	0	–
Опыт 1	1960	2743 (5)	64.3 (3)	103 (9)	3.8
Опыт 2	1960	2743 (5)	66.6 (3)	108 (8)	3.9

* В скобках приведены отклонения 3 параллельных определений.

куссий в ряде научных публикаций [11, 19—21]. Однако влияние экзогенных нефтепродуктов на степень минерализации ПОВ почвенными микроорганизмами, как затравочный (прайминг) эффект нефти, до настоящего времени не рассматривалось.

Для количественной оценки величины и направленности затравочного влияния углеводородов нефти на минерализацию ПОВ, как экзогенного субстрата (ПЭ нефти), нами было проведено сравнение скоростей эмиссии CO_2 при микробной минерализации ПОВ до и после внесения в почву этого субстрата. С учетом суммарных количественных и изотопных характеристик CO_2 в опытах 1 и 2, было рассчитано количество углекислоты, образовавшейся в результате минерализации ПОВ в присутствии углеводородов нефти (табл. 3). Как следует из табл. 3, количество CO_2, образовавшееся за счет потребления ПОВ, активируемое одновременной утилизацией нефтепродуктов, возросло в 1.5 раза по сравнению с процессами, наблюдаемыми в контрольных экспериментах. Таким образом, средняя величина дополнительной минерализации ПОВ (затравочный эффект), которая обусловлена микробным потреблением углеводородов нефти в течение 47-суточной экспозиции, достигла более 150% от нативной скорости минерализации ПОВ.

Микробное потребление нефти и трансформация ПОВ. Как следует из табл. 4, в опытах 1 и 2 в течение 47-суточной экспозиции около 4% нефти, внесенной в почву, было минерализовано до CO_2. Ранее [9] было показано, что при росте микробных клеток на углеводородах количества биомассы и CO_2 по углероду относились как 1 : 1. С учетом этого полагаем, что за 47 сут экспозиции количество углеводородов нефти, потребленных на биомассу клеток и образование органических экзометаболитов в почве, будет близким к количеству метаболической CO_2 и составит не менее 4% от внесенной нефти. В сумме микробное потребление нефти за указанный период на образование CO_2, биомассы клеток и экзометаболитов оценивается величиной, не менее 8% от внесен-

ной в почву нефти. Экстраполируя полученные данные на 7-месячный сезон, когда температурные условия в Краснодарском крае обеспечивают жизнедеятельность почвенной микробиоты, потребление углеводородов сырой нефти нативной почвенной микробиотой может достигать 36% от общего количества нефти в почве. Это означает, что в течение двух сезонов с положительными температурами углеводородокисляющий потенциал почвенной микробиоты может обеспечить снижение содержание сырой нефти в почве на 70% от ее количества, попавшего в почву. В нашем случае нефтяное загрязнение, составляющее около 32 т нефти на 1 га площади (или 3.2% от веса СП), снизится до уровня 9.6 т нефти на 1 га площади (или 0.96% от веса СП).

При положительной величине ПЭ нефти в почве происходит более интенсивная микробная деградация ПОВ по сравнению с процессами в нативной почве. С другой стороны, углеводороды нефти, потребленные микроорганизмами, расходуются как на образование CO_2, так и на синтез биомассы и органических экзометаболитов, которые затем включаются в ПОВ и трансформируют их структуру. Вновь синтезированные метаболиты и компоненты микробной биомассы могут быть использованы другими биологическими системами, не способными непосредственно утилизировать углеводороды нефти (растения, макро- и микроорганизмы). На основе количественных и изотопных данных, полученных в опытах, была проведена оценка степени замещения части ПОВ, минерализованного до CO_2, на вновь синтезированные продукты при микробном потреблении углеводородов нефти.

В табл. 5 приведены скорости микробной деградации ПОВ, т.е., убыль $C_{орг}$(ПОВ) и продукции биомассы клеток и органических экзометаболитов в модельных опытах при микробном потреблении нефти в качестве субстрата, т.е., увеличение $C_{орг}$ за счет трансформации нефти. Как в случае потребления нефти нативной почвенной микробиотой (опыт 1), так и смесью почвенной микробиоты и интродуцированных бак-

Таблица 5. Суммарная скорость образования метаболической CO_2 в почве, загрязненной нефтью, скорости убыли $C_{орг}$ при микробной минерализации ПОВ и увеличения $C_{орг}$ в почве за счет микробной минерализации углеводородов нефти

Условия	Суммарная скорость образования CO_2, мкг С г$^{-1}$ СП ч$^{-1}$	Скорость убыли $C_{орг}$ (ПОВ)*, мкг С г$^{-1}$ СП ч$^{-1}$	Скорость увеличения $C_{орг}$ (нефть)**, мкг С г$^{-1}$ СП ч$^{-1}$	γ***
Опыт 1	1.480 (0.122)	0.574 (0.046)	0.910 (0.076)	1.59 (0.13)
Опыт 2	1.546 (0.100)	0.591 (0.038)	0.955 (0.062)	1.62 (0.10)

* Убыль $C_{орг}$ (ПОВ) приравнена количеству CO_2, образовавшемуся при микробной минерализации ПОВ, и составляла 38% от суммарного количества CO_2;

** Скорость увеличения $C_{орг}$ (нефть) равнялась скорости эмиссии CO_2 при микробной минерализации нефти;

*** γ — скорость увеличения $C_{орг}$ (нефть)/скорость убыли $C_{орг}$ (ПОВ).

терий *P. aureofaciens* BS1393(pBS216) (опыт 2) количество углерода вновь синтезированных органических продуктов за счет потребленной нефти (биомасса клеток и экзометаболиты) почти в 1.6 раза превосходит количество углерода ПОВ, израсходованное на образование CO_2. Это означает, что микробная трансформация углеводородов нефти в продукты, доступные в качестве субстратов для других живых систем, может быть своеобразным источником органических удобрений. Кстати, при биоремедиации почв, загрязненных нефтепродуктами, отмечено стимулирование роста растений.

***

На основе количественных и изотопных характеристик продуктов, образующихся при микробной деградации углеводородов сырой нефти в почве, предложена модель оценки углеводородокисляющего метаболического потенциала почвенной микробиоты и интродуцированных в почву углеводородокисляющих микроорганизмов. На примере пахотных почв Краснодарского края показана возможность обнаружения почвенной микробиоты, которая при попадании в почву углеводородов нефти может переходить в активное состояние, используя их в качества субстрата. Скорость эмиссии метаболической CO_2 является основным показателем активности почвенной микробиоты. На основе изотопных характеристик углерода нефтепродуктов и почвенного органического вещества (ПОВ) установлено, что источниками углерода метаболической CO_2 являются углеводороды нефти и ПОВ. Из сравнения скоростей микробного образования CO_2 в нативной почве и почве, загрязненной нефтью, обнаружено, что интенсивность минерализации ПОВ в присутствии нефти выше по сравнению с незагрязненной почвой, т.е., обнаруживается затравочный (прайминг) эффект углеводородов нефти. Показано, что количество углерода вновь синтезированных органических продуктов за счет потребленной нефти (биомасса клеток и экзоме-

таболиты) значительно превосходит количество углерода ПОВ, израсходованное на образование CO_2. В проведенных опытах показано, что микробная деградация углеводородов нефти в почве до продуктов, доступных в качестве субстратов для других живых организмов, является своеобразным источником органических удобрений, которые могут стимулировать рост растений. Часть недеградируемых углеводородов нефти включается в пул биологически устойчивых органических почвенных продуктов. Наряду с этим обнаружено, что результатом микробиологических процессов в почве, загрязненной нефтью, является мощный поток углекислоты, поступающей в атмосферу.

СПИСОК ЛИТЕРАТУРЫ

1. *Kaplan C.W., Kitts C.I.* // Appl. Environ. Microbiol. 2004. V. 70. № 3. P. 1777—1786.

2. *Кочетков В.В., Балакшина В.В., Мордухова Е.А., Боронин А.М.* // Микробиология. 1997. Т. 66. № 2. С. 211—216.

3. *Сиунова Т.В., Кочетков В.В., Валидов Ш.З., Сузина Н.Е., Боронин А.М.* // Микробиология. 2002. Т. 71. № 6. С. 778—785.

4. *Panikov N.S., Sizova M.V.* // J. Microbiol. Methods. 1996. V. 24. № 3. P. 219—230.

5. *Stenström J., Stedberg B., Johanson M.* // Ambio. 1998. V. 27. № 1. P. 35—39.

6. *Blagodatsky S.A., Heinemeiyer O., Richter J.* // Biol. Fert. Soils. 2000. V. 32. № 1. P. 73—81.

7. *Panikov N.S.* Microbial Growth Kinetics. L. Glasgow: Chapman and Hall, 1995. 378 pp.

8. *Blagodatskaya E.V., Blagodatsky S.A., Anderson T.-H., Kuzyakov Y.* // Eur. J. Soil Sci. 2009. V. 60. № 2. P. 186—197.

9. *Зякун А.М., Кошелева И.А., Захарченко В.Н., Кудрявцева А.И., Пешенко В.П., Филонов А.Е., Боронин А.М.* // Микробиология. 2003. Т. 72. № 3. С. 592—596.

10. *Shen J., Bartha R.* // Appl. Environ. Microbiol. 1996. V. 62. № 4. P. 1428−1430.

11. *Kuzyakov Y., Friedel J.K., Stahr K.* // Soil Biol. Biochem. 2000. V. 32. № 11−12. P. 1485−1498.

12. *Belhaj A., Desnoues N., Elmerich C.* // Res. Microbiol. 2002. V. 153. № 6. P. 339−344.

13. *Bhattacharya D., Sarma P.M., Krishnan S., Mishra S., Lal B.* // Appl. Environ. Microbiol. 2003. V. 69. № 3. P 1435−1441.

14. *Röling W.M.M., Milner M.G., Jones D.M., Lee K., Duniel F., Swanneli R.J.P., Head I.M.* // Appl. Environ. Microbiol. 2004. V. 70. № 5. P. 2603−2613.

15. *Hamamura N., Olson S.H., Ward D. M., Inskeep W.P.* // Appl. Environ. Microbiol. 2006. V. 72. № 9. P. 6316−6324.

16. *Dalenberg J.W., Jager G.* // Soil Biol. Biochem. 1989. V. 21. № 3. P. 443−448.

17. *Harabi N.E.-D., Bartha R.* // Appl. Environ. Microbiol. 1993. V. 59. № 4. P. 1201−1205.

18. *Зякун А.М., Дилли О.* // Appl. Biochem. Microbiol. 2005. V. 41. № 5. P. 512−520.

19. *Mazeas L., Budzinski H., Raymond N.* // Org. Geochem. 2002. V. 33. № 11. P. 1259−1272.

20. *Hamer U., Marschner B.* // J. Plant Nutr. Soil Sci. 2002. V. 165. № 3. P. 261−268.

21. *Fontaine S., Bardoux G., Mariotti A.* // Ecol. Lett. 2004. V. 7. № 4. P. 314−320.

Ratio [13C]/[12C] as an Index for Express Estimation of Hydrocarbon-Oxidizing Potential of Microbiota in Soil Polluted with Crude Oil

A. M. Zyakun[a, b], A. M. Boronin[a, b], V. V. Kochetkov[a], B. P. Baskunov[a], K. S. Laurinavichus[a], V. N. Zakharchenko[a], V. P. Peshenko[a], T. O. Anokhina[a], and T. V. Siunova[a]

[a] *Skryabin Institute of Biochemistry and Physiology of Microorganisms, Russian Academy of Sciences, Pushchino, Moscow Region, 142290 Russia*

[b] *Pushchino State University, Pushchino, Moscow Region, 142290 Russia*

e-mail: zyakun@ibpm.pushchino.ru

Received August 26, 2011

Abstract—The hydrocarbon-oxidizing potential of soil microbiota and hydrocarbon-oxidizing microorganisms introduced into soil was studied based on the quantitative and isotopic characteristics of carbon in products formed in microbial degradation of oil hydrocarbons. Comparison of CO_2 production rates in native soil and that polluted with crude oil showed the intensity of microbial mineralization of soil organic matter (SOM) in the presence of oil hydrocarbons to be higher as compared with non-polluted soil, that is, revealed a priming effect of oil. The amount of carbon of newly synthesized organic products (cell biomass and exometabolites) due to consumed petroleum was shown to significantly exceed that of SOM consumed for production of CO_2. The result of microbial processes in oil-polluted soil was found to be a potent release of carbon dioxide to the atmosphere.

CONSTRUCTION OF THE INDUSTRIAL ETHANOL-PRODUCING STRAIN OF *Saccharomyces cerevisiae* ABLE TO FERMENT CELLOBIOSE AND MELIBIOSE

© 2012   L. Zhang, Z.-P. Guo, Z.-Y. Ding, Z.-X. Wang, G.-Y. Shi

The Key Laboratory of Industrial Biotechnology, Ministry of Education; Center for Bioresources & Bioenergy, School of Biotechnology, Jiangnan University, Wuxi 214122, P.R. China
e-mail: biomass_jnu@126.com

The gene *mel1*, encoding α-galactosidase in *Schizosaccharomyces pombe*, and the gene *bgl2*, encoding and β-glucosidase in *Trichoderma reesei*, were isolated and co-expressed in the industrial ethanol-producing strain of *Saccharomyces cerevisiae*. The resulting strains were able to grow on cellobiose and melibiose through simultaneous production of sufficient extracellular α-galactosidase and β-glucosidase activity. Under aerobic conditions, the growth rate of the recombinant strain GC1 co-expressing 2 genes could achieve $0.29\ OD_{600}\ h^{-1}$ and a biomass yield up to $7.8\ g\ l^{-1}$ dry cell weight on medium containing $10.0\ g\ l^{-1}$ cellobiose and $10.0\ g\ l^{-1}$ melibiose as sole carbohydrate source. Meanwhile, the new strain of *S. cerevisiae* CG1 demonstrated the ability to directly produce ethanol from microcrystalline cellulose during simultaneous saccharification and fermentation process. Approximately $36.5\ g\ l^{-1}$ ethanol was produced from 100 g of cellulose supplied with $5\ g\ l^{-1}$ melibiose within 60 h. The yield (g of ethanol produced/g of carbohydrate consumed) was 0.44 g/g, which corresponds to 88.0% of the theoretical yield.

Tremendous researches have been devoted to producing fuel ethanol from cellulosic raw materials, and cellulases are key factors in solving this problem. The two-step conversion of biomass to ethanol involves the enzymatic hydrolysis of cellulosic biomass to produce reducing sugars, and the conversion of the resulting sugars to ethanol. However, this is a very costly process due to the recalcitrance of cellulose, and therefore the low yield and high cost of the enzymatic hydrolysis process [1]. β-Glucosidases working synergistically with endoglucanases (EC 3.2.1.4) and exoglucanases (EC 3.2.1.91) on the degradation of cellulose [2] not only catalyze the final step in the degradation of cellulose, but also stimulate the extent of cellulose hydrolysis by relieving the cellobiose-mediated inhibition of exoglucanase and endoglucanase [3, 4].

Development of a yeast strain capable of producing ethanol by fermenting cellulosic substrates has received a great deal of interest over recent years. The advantages using this microorganism include: (i) high ethanol productivity and tolerance, (ii) large cells size, which simplify their separation from the culture broth and (iii) resistance to viral infection [5]. Although *Saccharomyces cerevisiae* is one of the most suitable microorganisms for practical purposes, it cannot degrade polysaccharides such as cellobiose. Since cellobiose (and longer chain cello-oligosaccharides) is the major soluble by-product of cellulose hydrolysis, its efficient utilization is of primary importance to cellulose bio-degradation process development. Enzymatic hydrolysis of cellobiose requires the action of β-glu-

cosidases. This heterogeneous group of enzymes displays broad substrate specificity towards cellobiose, cello-oligosaccharides and different aryl- and alkyl-β-D-glucosides. β-Glucosidases were found widely in animals, plants, fungi and bacteria [6]. Though many efforts have been done to express heterogenous gene of β-glucosides in yeast and bacteria to improve the ethanol productivity, the strains they used mostly are haploid auxotrophic strains and primarily for laboratory research [7–11]. In addition, melibiose, a disaccharide containing glucose and galactose linked through α-1,4 glycosidic bond, is one of the main non-reducing saccharides not effectively utilized during *S. cerevisiae*–mediated very high gravity ethanol fermentation from starchy materials such as wheat, corn, and cassava. Thus, it is necessary to enhance the ability of the yeast to ferment melibiose to improve the utilization rate of these materials and ethanol yield.

In this study, the gene *mel1*, encoding α-galactosidase in *Schizosaccharomyces pombe*, and the gene *bgl2*, encoding β-glucosidase in *Trichoderma reesei*, were isolated and separately expressed or co-expressed in the industrial ethanol-producing strain of *Saccharomyces cerevisiae*. The resulting strains were studied under anaerobic conditions and ethanol production from cellobiose and melibiose was achieved by expressing these genes.

MATERIALS AND METHODS

Yeast strains and media. *E. coli* JM109 {*recA*1 *supE*44 *endA*1 *hsdR*17 (r$_K^-$, m$_K^+$) *gyrA*96 *relA*1 *thi*-1 (*lac-proAB*) [F', *traD*36 *proAB*$^+$ *lacI^q lacZ*M15]} (Stratagene, USA) was used for plasmid transformation and propagation. *T. reesei* was grown in a medium containing (g/l): bean cake powder − 45.0, wheat bran − 10.0, corn meal − 20.0, KH$_2$PO$_4$ − 5.0, CaCl$_2$ − 3.0, NH$_4$Cl − 5.0.

The industrial yeast, *S. cerevisiae* CICIMY0086 (http://cicim-cu.sytu.edu.cn/, ethanol producing yeast used in industrial plants) was used for genetic manipulation. The yeasts including *S. pombe* were routinely grown in a medium composed of 1% yeast extract, 2% bactopepton, and 2% glucose (YEPD), solid media contained 2% agar. For selection of yeast transformants, geneticin (G418) was added with the final concentration 300 μg/ml. Incubation conditions were standardized on the rotary shaker with 150 rpm at 30°C.

Construction of the strains. The plasmid for expressing β-glucosidase was constructed. The total RNA of *T. reesei* was extracted using with a guanidine thiocyanate-phenyl-chloroform method [12]. Poly A$^+$ mRNA was isolated from the obtained total RNA of *T. reesei* using Oligoex Kit (Qiagen, Germany) according to the manufacturer's instructions. The gene *bgl2*, encoding β-glucosidase in *T. reesei*, was obtained by PCR amplification using Qiagen One Step RT-PCR kit from the poly A$^+$ mRNA with primers P1(5'-CCG-*GAATTC*ATGTTGCCCAAGGACTTTCAGTGGG-3') and P2(5'-CCC*TTCGAA*ATTTCCCCTTTGA AGA-AGCATCAGG-3') [13, 14] containing *Eco*RI and *Hin*dIII sit, respectively. A 1538-bp PCR fragment including the entire coding region for β-glucosidase was obtained. This *Eco*R I/*Hin*dIII digested fragment was inserted into the vector pYX212 (Ingenenius MBV-028-10) at the same sit, resulting plasmid pYX-*BGL*. Kanamycin resistance gene which confers resistance to geneticin in *S. cerevisiae* was isolated from the vector pPIC9K and was inserted into the downstream of the target gene in pYX-*BGL* resulting in the plasmid pYX-*BGL-Km*. The β-glucosidase expressing cassette including *TPI* (triosephosphate isomerase) promoter, and geneticin resistance gene was isolated from the plasmid pYX-*BGL-Km* with primers P3, 5'-AAC-TTAACTTCCGGCCACTTGAATGCTGGTAGAA-AGAGAAGTTCCTCTTCTGTTAACGGGAGCG-TAATGGTGATGGAA-3' and P4, 5'-TAATTCTTCA-ATCATGTCCGGCAGGTTCTTCATTGGGTAGT TGTTGTAAACGATGAGATATCATGCGTAGTCA-GGCAC-3'. A 54-bp gene fragment (underlined) of the *S. cerevisiae* glycerol phosphate dehydrogenase gene (*GDP*1) was added to each primer used as homologous integration site. After purification, this *gpd1'*-P$_{TPI}$-*BGLII*-Km-*gpd1'* fragment was introduced into the industrial alcoholic yeast by the lithium acetate method [15]. The recombinants were screened on the

YEPD plate containing 300 μg/ml G418. Correct insertion of the gene into the target locus was verified by PCR.

The gene *mel1* was amplified by PCR form the genomic DNA of *S. pombe* using primers P5(5'-CCG*G-GATCC*TTGCCACATTCGCCTCCGTA-3'), and P6 (5'-CCC*GGATCC*ATCATGTGCTAGGTCGATTCTG-GT-3') containing *Bam*H I sit on both ends. This *Bam*H I digested fragment was inserted into the same sit of vector pYX212, resulting in the plasmid pYX-*MEL*. After that, G418 resistance gene was inserted into the downstream of the gene *mel1* and the resulted plasmid was designated pYX-*MEL-Km*. The α-galactosidase expressing cassette including *TPI* promoter, and G418 resistance gene was isolated from the plasmid pYX-*MEL-Km* with primers P7 (5'-ATGTAATAAGCAAA-CAAGCACGAATGGGGAAAGCCTATGTGCAA-TCACCAAGGTAACGGGAGCGTAATGGTGAT-GGAA-3') and P8 (5'-TCGTGAACTTCTCTGCA-TGTGATTATCCCTTGGGCGGATTGACCGTTAA-GCAATGAGATATCATGCGTAGTCAGGCAC-3'). A 54-bp gene fragment (underlined) of the *S. cerevisiae* glycerol phosphate dehydrogenase (*gdp2*) gene was added to each primer used as homologous integration site. After purification, this *gpd2'*-P$_{TPI}$-*Mel*-Km-*gpd2'* fragment was introduced into the industrial alcoholic yeast. The recombinants were screened on the YEPD plate containing 300 μg/ml G418. Correct insertion of the gene into the target locus was verified by PCR.

For co-expressing 2 genes, the recombinant strain expressing β-glucosidase was re-transformed by the α-galactosidase expressing cassette and higher concentration of G418 and nearly 800 μg/ml was used which was determined by the resistance experiment of the initial recombinant. Correct insertion of the gene into the target locus was verified by PCR.

Measurement of enzyme activity. The recombinant strains were cultivated at 30°C for 48 h in YEPD medium and the resulting fermentation fluid was used as enzyme solution. Activities of β-glucosidase and α-galactosidase were determined by measuring pNP (*p*-nitrophenol) concentration derived from pNPG. To assay the β-glucosidase activity, the reaction mixture (final volume, 4.0 ml) containing 0.2 ml of enzyme solution, 1.8 ml of 0.2 M Na$_2$HPO$_4$ and 2.0 ml of 5.0 mM 4-nitrophenyl-β-D-glucopyranoside (Sigma, USA) in 0.1 M citric acid buffer (pH 4.5), was mixed and incubated at 30°C for 10 min. Reaction was stopped by adding 2.0 ml of 1.0 M Na$_2$CO$_3$. The enzyme reaction was monitored by spectrophotometry (400 nm) at room temperature for 5 min [16]. For measuring the activity of α-galactosidase, 4-nitrophenyl-β-D-glucopyrano-side was substituted by 4-nitrophenyl-α-D-galactopy-ranoside used as chromogenic substrate [16]. One unit of pNPGase activity was defined as the amount of enzyme required for releasing total reducing sugar equivalent to 1 μmol pNP min^{-1}.

OD_{600} of the host *S. cerevisiae* 0086 and recombinants during growth in cellobiose/melibiose-containing medium

Time, h	OD_{600}				
	S. cerevisiae 0086	Recombinant strains			
		1	9	15	24
24	0.18 ± 0.01	0.28 ± 0.02	0.21 ± 0.01	0.16 ± 0.02	0.19 ± 0.02
48	0.21 ± 0.01	0.81 ± 0.02	0.54 ± 0.03	0.20 ± 0.02	0.26 ± 0.01
Max. specific growth rate, h^{-1}	0.17 ± 0.01	0.29 ± 0.02	0.24 ± 0.02	0.16 ± 0.02	0.20 ± 0.01
DCW, g l^{-1}	0.19 ± 0.02	7.33 ± 0.02	7.61 ± 0.01	7.82 ± 0.01	7.25 ± 0.02

Note: $\pm$ − the standard deviation.

Aerobic growth of recombinants in cellobiose and melibiose mixed medium. Cultivations were carried out under aerobic conditions in a flask with a working volume of 100 ml. The transformed yeast or the parental yeast were tested for the ability to grow in a medium containing 10.0 g l^{-1} of cellobiose and 10.0 g l^{-1} of melibiose as carbon source supplemented with 7.5 g of $(NH_4)_2SO_4$, 3.5 g of KH_2PO_4, 0.75 g of $MgSO_4 \cdot 7H_2O$ and 0.5 g of yeast extract. The colonies from YPD slant were inoculated in this medium. During the cultivation process, the flasks were kept at 100 rpm at 30°C in a thermostatic chamber. The experiments were performed in triplicate. The optical density at 600 nm (OD_{600}) of the broth was monitored using the fresh medium as control.

Cellulose fermentation. 10 g of microcrystalline cellulose and 100 ml water were mixed in a 500 ml conical flask. The pH was adjusted to 4.8 with 6 M HCl and different amount of cellulase (Novozymes A/S, Denmark, 95 ± 4 filter paper Unit (FPU)/g) was added as follows: 6.0 FPU cellulase/g cellulose added at the beginning of fermentation process (process 1), or 4.0 FPU cellulase/g cellulose was added and the medium was incubated at 50° C for 1−1.5 h and then, another 2.0 FPU cellulase/g cellulose was added at the beginning of fermentation (process 2), or 4.0 FPU cellulase/g cellulose was added at the beginning and after incubated for 1.0−1.5 h at 50° C, another 2.0 FPU cellulase/g cellulose was added at the beginning and 2.0 FPU cellulase/g cellulose was supplemented at every 12 h thereafter during the fermentation process (process 3). For each experiment, 5 g l^{-1} of melibiose and a pre-culture of yeast (15 ml) were added, and the solution was incubated at 30°C with no air supplied. The cellobiose, glucose and melibiose concentrations were determined by HPLC using column HP1100 (Agilent, USA) eluted with 0.01 M H_2SO_4 at 50°C [17]; ethanol concentration was determined by GC [18].

RESULTS AND DISCUSSION

β-glucosidase and α-galactosidase activities of extracellular solution. Ethanol is a renewable energy source produced through the fermentation of the sug-

ars and is widely used as a partial gasoline replacement in many countries. However, the high production cost of ethanol makes the cost of ethanol-based fuels comparably higher than that of fossil fuels. The potential mechanism to reduce the costs of ethanol production is the use of cellulosic raw materials or improvement of the ethanol yield from starchy materials. Since the most of the global ethanol is fermented from corn, it is necessary to improve the utilization rate of the starchy materials. Here, the gene *mel1*, encoding α-galactosidase in *S. pombe*, and the gene *bgl2*, encoding β-glucosidase in *T. reesei*, were co-expressed in the industrial ethanol-producing strain of *S. cerevisiae*. The engineered strain *S. cerevisiae* CG1 was used to incorporate cellulase for simultaneous saccharification and fermentation of cellulose and melibiose to ethanol. The enzymatic activities of β-glucosidase and α-galactosidase were measured from the enzyme solution of transformed yeast (Materials and Methods), and one unit of β-glucosidase activity was defined as the amount producing 1 μmol pNP in 1 ml of crude cell extracts per min. The results had shown that the highest activity of β-glucosidase of the transformants was 0.47 u/ml compared with the wild type which produced no detectable β-glucosidase activity. Meanwhile, the transformant showed much higher activity of α-galactosidase (1.58 u/ml) than the original strain (0.33 u/ml).

Characteristics of the recombinants under aerobic growth conditions. The ability of the industrial *S. cerevisiae* 0086 and its recombinant strains expressing β-glucosidase and α-galactosidase were tested during the growth in a medium with cellobiose and melibiose as carbon source. *S. cerevisiae* 0086 or positive recombinant colonies (1, 9, 15, and 24) were inoculated in cellobiose/melibiose-containing medium and the OD_{600} was measured after 24 and 48 h (Table).

Recombinants 1, 9, and 24 had OD_{600} at 24 and 48 h higher than those of the host yeast, indicating enhanced growth compared to wild-type. Recombinant 15 had a lower OD_{600} compared to wild-type at both time points. These results indicated that recombinants 1, 9, and 24 had enhanced growth in medium containing cellobiose and melibiose as carbon source com-
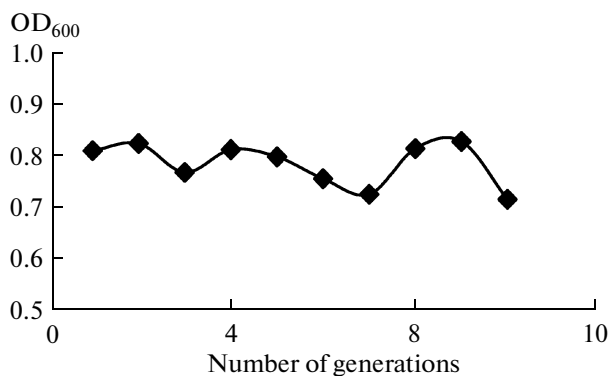
OD$_{600}$

Fig. 1. OD$_{600}$ of successive generation of *S. cerevisiae* CG1 using cellobiose and melibiose as carbon source in the medium of growth.

pared to host organisms. In contrast, recombinant 15 had reduced growth compared to wild-type. As recombinant 1 had the most marked increase in OD$_{600}$ of the recombinants, it was used for further analysis and was designated *S. cerevisiae* CG1.

Inheritance capacity of *S. cerevisiae* CG1. We tested the inheritance capacity of the recombinant *S. cerevisiae* CG1. These cells were cultivated in a YEPD slant at 30°C and transferred to another slant every 24 h.

The colonies on every slant were inoculated in medium supplemented with cellobiose and melibiose in a rotary mixer (200 rpm) at 30°C every 48 h. OD$_{600}$ of the broths was measured to determine the ability of the recombinants to use cellobiose and melibiose as the carbon source. OD$_{600}$ was relatively stable after 10 generations (Fig. 1), demonstrating the stable inheritance capacity of *bgl2* in *S. cerevisiae* CG1.

Replication capacity of *S. cerevisiae* CG1. To test the replication capacity of the recombinant, *S. cerevisiae* CG1 and wild type were incubated in YEPD at 30°C with shaking (200 rpm) for 48 h, and then 20 h without shaking. After that the yeast concentration in the broth was counted. The results had shown that the amount of yeast in 1 ml of broth containing *S. cerevisiae* CG1 or wild type were 0.84×10^8 or 0.91×10^8, respectively. This indicated that the replication capacity of the recombinant did not significantly decrease compared to the host strain.

Yeast shape of *S. cerevisiae* CG1. Cell shapes of *S. cerevisiae* wild type and CG1 incubated in YEPD were determined by imaging using electron microscopy. The cells of *S. cerevisiae* CG1 were smaller and self-flocculated in comparison to wild type (Fig. 2). This suggests that the structure of the yeast cell had changed during construction of the cellobiose and melibiose metabolic pathway. However, this shape change had minimal effect on the yeasts' inheritance capacity or replication ability.

Cellulose fermentation by *S. cerevisiae* CG1. The ability of *S. cerevisiae* wild type and CG1 to mediate cellulose fermentation was investigated. In our experiments, three processes (1, 2 and 3) were tested, depending on the amount of cellulase added (see Materials and Methods). The broth was sampled every 12 h and cellubiose, melibiose, glucose, and residual sugar concentrations were measured. The alcohol concentration of the final fermentation broth was also determined. The results showed that alcohol concentration was increased and the cellobiose and melibiose accumulation markedly decreased in the broth fermented with *S. cerevisiae* CG1 compared to wild type, allowing to conclude that the feedback inhibition engendered by cellobiose accumulation could be eliminated by integration of *bgl2* into the chromosomal DNA of the parent yeast, as well as the residual melibiose. Furthermore, in the fermentation broth of *S. cerevisiae* CG1 of process 1, the glucose concentration maintained at a higher level and the cellobiose accumulated at lower level than in the parent yeast (Fig. 3). At the end of fermentation, recombinant yeast produced 32.2 ± 2.3 g l^{-1} ethanol, much higher than 13.1 ± 1.5 g l^{-1} ethanol of the reference strain. In process 2, 2.0 FPUs

(a)   (b)

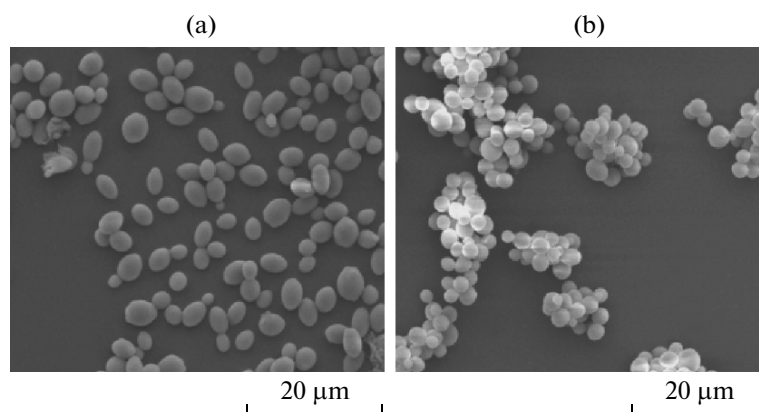20 μm   20 μm

Fig. 2. Electron microscopy of *S. cerevisiae:* a — parental strain of *S. cerevisiae* 0086; b — recombinant strain of *S. cerevisiae* CG1. Images are taken at 2400× magnification. Scale bar — 20.0 μm.
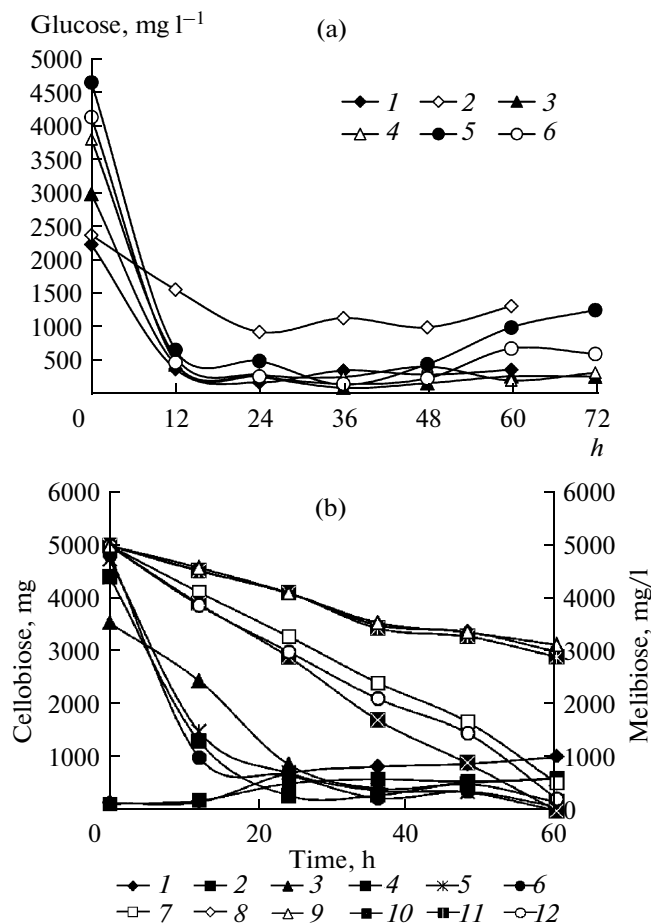
Fig. 3. Comparison of the time curves of fermentation. a – glucose concentration in the course of fermentation for *S. cerevisiae* 0086 wild type in process 1 (line *1*), 2 (line *3*), 3 (line *5*) and for *S. cerevisiae* CG1 in process 1 (line *2*), 2 (line *4*) and 3 (line *6*) respectively; b – cellobiose and melibiose concentrations in the course of fermentation for *S. cerevisiae* 0086 in process 1 (line 1, cellobiose; line 7, melibiose), 2 (line 3, cellobiose; line 9, melibiose), 3 (line 5, cellobiose; line 11, melibiose) and *S. cerevisiae* CG1 in process 1 (line 2, cellobiose; line 8, melibiose), 2 (line 4, cellobiose; line 10, melibiose), 3 (line 6, cellobiose; line 12, melibiose) (see Materials and Methods).

of fresh cellulase/g of cellulose were supplied after the enzymatic reaction had proceeded for 1–1.5 h, so that the fermentation trends of *S. cerevisiae* CG1 and wild type were nearly the same at 50 h. However, thereafter the cellobiose accumulation of *S. cerevisiae* 0086 increased (Fig. 3b), indicating that some cellulase combined with cellulose was not reversible. As a result, 36.5 ± 1.0 g l⁻¹ ethanol was produced by the recombinant strain from 100 g of cellulose supplied with 5 g l⁻¹ melibiose within 60 h. The yield (g of ethanol produced/g of carbohydrate consumed) was 0.44 g/g, which corresponds to 88.0% of the theoretical yield. In contrast, only 13.8 ± 0.8 g l⁻¹ ethanol was produced by the parent strain during the same process. For process 3, the fermentation trend of *S. cerevisiae* CG1 was

the same as that of wild type (Fig. 3). This was due to the continuous supplementation of the broth with cellulase, including small amounts of β-glucosidase, which resulted in cellobiose hydrolyzation. However, recombinant strain CG1 could produce 31.4 ± 1.6 g l⁻¹ ethanol as compared to 18.5 ± 1.9 g l⁻¹ of the parent strain. This demonstrates that addition of an adequate amount of β-glucosidase can be used to overcome the feedback inhibition of cellobiose. Although the recombinants could grow in the medium with cellobiose as the sole carbon source, the cellobiose was not well utilized to produce ethanol. Probably, the enzyme activity expressed in our system was not sufficient to hydrolyze cellulose. Future research will need to focus on designing yeast vectors with a high-level of *bgl* expression and a high mitotic stability under non-selective conditions. We demonstrated that cellobiose and melibiose accumulation decreased and alcohol productivity increased. It allows to conclude that the feedback inhibition engendered by cellobiose accumulation was partially relieved and the residual melibiose could be effectively utilized by the new strain. In future, more efforts should be made to enhance the usage of other kinds of unfermentable sugars for *S. cerevisiae* to improve the ethanol productivity.

REFERENCES

1. Lynd, L.R., Weimer, P.J., Van Zyl, W.H., and Pretorius, I.S., *Microbiol. Mol. Biol. Rev.*, 2002, vol. 66, no. 3, pp. 506–577.

2. Tolan, J.S. and Foody, B., *Adv. Biochem. Eng. Biot.*, vol. 65, pp. 41–67.

3. Sternberg, D., Vijayakumar, P., and Reese, E.T., *Can. J. Microbiol.*, 1997, vol. 23, no. 2, pp. 139–147.

4. Yan, T., Lin, Y., and Lin, C., *J. Agric. Food. Chem.*, 1998, vol. 46, no. 2, pp. 431–437.

5. Hahn-Hägerdal, B., Wahlbom, C.F., Gàrdonyi, M., Van Zyl, W.H., Cordero Otero, R.R., and Jönsson, L.J., *Adv. Biochem. Eng. Biotechnol.*, 2001, vol. 73, pp. 53–84.

6. Bhatia, Y., Mishra, S., and Bisaria, V.S., *Crit. Rev. Biotechnol.*, 2002, vol. 22, no. 4, pp. 375–407.

7. Adam, A.C., Rubio-Texeira, M., and Polaina, J., *Yeast*, 1995, vol. 11, no. 5, pp. 395–406.

8. Misawa, N. and Nakamura, K., *Agr. Biological. Chem.*, 1989, vol. 53, no. 3, pp. 723–727.

9. Morana, A., Moracci, M., and Ottombrino, A., *Biotechnol. Appl. Biochem.*, 1995, vol. 22, no. 3, pp. 261–268.

10. Rajoka, M.I., Bashir, A., and Hussain, S.R., *Folia Microbiol.*, 1998, vol. 43 , no. 2, pp. 129–135.

11. Wong, W.K.R., Ali, A., Chan, W.K., and Lee, N.T.K., *Gene*, 1998, vol. 207, no. 1, pp. 79–86.

12. Ausubel, F.M., Kingston, R.E., and Seidman, J.G., *Short Protocols in Molecular Biology,* New York: John Wiley and Sons., 3th Ed., 1995, pp. 580–581.

13. Esterbauer, H., Steiner, W., and Labudova, I., *Bioresource Technol.*, 1991, vol. 36, no. 1, pp. 51–65.

14. Holtzapple, M., Cognata, M., and Yuancai, S., *Biotechnol. Bioeng.*, 1990, vol. 36, no. 3, pp. 275–287.

15. Ito, H., Fukuda, Y., Murata, K., and Kimura, A., *J. Bacteriol.*, 1983, vol. 153, no. 1, pp. 163–168.

16. Machida, M., Ohtsuki, I., Fukui, S., and Yamashita, I., *Appl. Environ. Microbiol.*, 1988, vol. 54, no. 12, pp. 3147–3155.

17. Khan, A.W. and Trottier, T.M., *Appl. Environ. Microbiol.*, 1978, vol. 35, no. 6, pp. 1027–1034.

18. Felipe, M.S.S., Rogelin, R., and Azevedo, M.O., *Biotechnol. Techniques,* 1993, vol. 7, no. 9, pp. 639–644.

РАЗРАБОТКА И ОПТИМИЗАЦИЯ ИММУНОХРОМАТОГРАФИЧЕСКИХ ТЕСТОВ ДЛЯ ВЫЯВЛЕНИЯ БОТУЛИНИЧЕСКИХ ТОКСИНОВ

© 2012 г.   А. А. Титов, И. В. Шиленко, А. А. Морозов, С. П. Ярков, В. Н. Злобин

Государственный научно-исследовательский институт биологического приборостроения Москва, 125424
e-mail: niibp@dol.ru

Разработаны иммунохроматографические монопараметрические тесты для выявления ботулинических токсинов типов А, В, а также мультипараметрический тест для одновременного выявления ботулинических токсинов типов А и В. Показано, что на чувствительность тестов влияют размеры наночастиц коллоидного золота, использованных в качестве маркеров антител, величины нагрузки антител на наночастицы коллоидного золота в конъюгатах, тип аналитических мембран, а также химический состав буферных растворов для хранения конъюгата и проведения иммунохроматографического анализа. Предел обнаружения монопараметрических иммунохроматографических тестов составляет 0.5 нг/мл, а мультипараметрических — 5.0 нг/мл. Разработанные иммунохроматографические тесты могут быть использованы для экспресс-анализа качества продуктов питания, контроля содержания ботулинических токсинов в фармацевтических препаратах, контроля окружающей среды.

Восемь типов ботулинических токсинов (А, В, C_1, C_2, D, E, F, G), обладающих нейротоксическим действием, могут продуцироваться токсикогенными штаммами анаэроба *Clostridium botulinum*. Ботулинические токсины могут присутствовать в консервах, копченостях, рыбе, грибах, представляя опасность для человека [1, 2]. Максимальной токсичностью для человека обладает ботулинический токсин типа А (**БТА**). Важным фактором лечебно-профилактических мероприятий при пищевых отравлениях является определение типа ботулинических токсинов (**БТ**) с целью дальнейшего лечения антитоксическими сыворотками. В медицине препараты "Ботокс", "Диспорт", на основе высокоочищенных препаратов БТА и БТ типа В (**БТВ**), применяются как средства для стойкой хемоденервации мышечных волокон, а химически инактивированные препараты БТ в виде анатоксинов используют для индукции иммунного ответа крупных животных с целью получения лечебных антитоксических сывороток. Наконец, ввиду высокой токсичности и устойчивости во внешней среде БТ рассматриваются, как одни из наиболее вероятных поражаю-

щих биологических агентов, пригодных для осуществления террористических актов [3].

Разработка высокочувствительных методов обнаружения, идентификации БТ в продуктах питания, объектах окружающей среды, определение концентрации в медицинских препаратах, в т.ч. для контроля их качества, является актуальной задачей. В настоящее время для идентификации типа БТ широко применяется биологический тест — реакция нейтрализации на мышах [2]. Иммунохимические методы анализа, такие, как иммуноферментный анализ (**ИФА**) [4], иммунохроматографический анализ (**ИХА**) [5], реакция непрямой гемагглютинации эритроцитов (**РНГА**), применяются, в основном, для контроля продуктов питания и выявления БТ в окружающей среде. Среди иммунохимических методов выявления БТ иммунохроматография выделяется не только малой длительностью анализа, но и высокой чувствительностью [6].

Современные представления о корреляции между размерами и аффинностью поливалентных конъюгатов антител и наночастиц коллоидного золота (**НКЗ**) [7], а также данные о влиянии размеров конъюгатов НКЗ на чувствительность иммунохроматографических тестов при выявлении поливалентных антигенов с повторяющимися эпитопами, на примере вирусов растений [8], открывают новые возможности для оптимизации ИХА. В частности, представляется интересным сравнить закономерности ИХА при выявлении "корпускулярных" антигенов (вирусы) и белковых растворимых антигенов (БТ) при использовании конъюгатов НКЗ различного размера. Од-

---

Сокращения: БА — буфер для проведения иммунохроматографического анализа; **БСА** — бычий сывороточный альбумин; **БТ** — ботулинический токсин; **БТА** — ботулинический токсин типа А; **БТВ** — ботулинический токсин типа В; **БХ** — буфер хранения конъюгата; **ВЦР** — видеоцифровая регистрация; **ИК** — индекс контрастности; **ИХА** — иммунохроматографический анализ; **ИФА** — иммуноферментный анализ; **КрАМ** — антитела кролика к иммуноглобулинам мыши; **МКА** — моноклональные антитела; **НКЗ** — наночастицы коллоидного золота; **ФБ** — фосфатный буферный раствор.

ним из преимуществ ИХА является возможность как визуальной, так и приборной регистрации результатов. В частности, видеоцифровая регистрация (**ВЦР**) иммунохроматограмм может повысить чувствительность аналитической системы и исключить субъективность при интерпретации результатов ИХА [9, 10].

Цель исследования — разработка оптимизированных по своим аналитическим характеристикам моно- и мультипараметрических иммунохроматографических тестов для выявления БТА и БТВ, а также изучение влияния на чувствительность тестов размера маркерных НКЗ, состава конъюгата НКЗ с моноклональными антителами, типа аналитической мембраны, состава буферов хранения конъюгата (**БХ**), буфера для проведения иммунохроматографического анализа (**БА**), а также условий ВЦР данных анализа.

МЕТОДИКА

Реактивы. Применяли золотохлористоводородную кислоту ($HAuCl_4$), сахарозу, бычий сывороточный альбумин (**БСА**), Трис, Твин-20, цитрат натрия дигидрат, аскорбат натрия, NaCl, Na_2HPO_4, KH_2PO_4, K_2CO_3 ("Sigma", США), азид натрия, динатриевую соль ЭДТА ("ДиаэМ", Россия), натрийборгидрид ($NaBH_4$) ("Merck", Германия). Все растворы готовили на деионизованной воде, полученной при помощи установки Nanopure II ("Sybron-Barnstead", США).

Иммунокомпоненты. В качестве рабочих моделей БТА и БТВ использовали паспортизованные очищенные препараты соответствующих анатоксинов, полученные из филиала "Микроген" (Россия). Для изучения перекрестных реакций иммунохроматографических тестов с другими типами БТ использовали ботулинический анатоксин типа Е, дифтерийный и столбнячный анатоксины этого же производителя. Концентрация анатоксинов принималась равной концентрации белкового азота в препарате. МКА к БТА клоны ВТА151 и ВТА232, МКА к БТВ клоны ВТВ 224, КВВ18 ("Импакт", Россия). Примененные нами МКА к БТ были типоспецифичны. Кроличьи антитела к IgG мыши (**КрАМ**) фирмы "Sigma" (США).

Получение наночастиц коллоидного золота. НКЗ с номинальным диаметром 13 нм (НКЗ-1) получали восстановлением $HAuCl_4$ натрийборгидридом [11]. К 98.4 мл 0.3мМ динатриевой соли ЭДТА при перемешивании добавляли 0.4 мл 0.2 M K_2CO_3 и 1 мл 1%-ного $HAuCl_4$, затем быстро при интенсивном перемешивании вносили 250 мкл 0.5%-ного $NaBH_4$. НКЗ с номинальным диаметром 16 нм (НКЗ-2) получали восстановлением $HAuCl_4$ аскорбатом натрия [12]. К 25 мл охлажденной до 4°C деионизованной воды добавляли 1 мл 1%-ного $HAuCl_4$ и 1 мл 0.1 M K_2CO_3.

Смесь помещали в ледяную баню и быстро при перемешивании вносили 0.25 мл 7%-ного аскорбата натрия, перемешивали, пока окраска не становилась пурпурно-красной. Объем смеси доводили до 400 мл деионизованной водой, кипятили до появления красной окраски. НКЗ диаметром 25—47 нм получали по методу Френса [13] восстановлением $HAuCl_4$ цитратом натрия. К 100 мл деионизованной воды добавляли 1 мл 1%-ного $HAuCl_4$, доводили до кипения и при перемешивании добавляли 1%-ный цитрат натрия. Для НКЗ 25 нм (НКЗ-3) — 2 мл, НКЗ 31 нм (НКЗ-4) — 1.25 мл, НКЗ 47 нм (НКЗ-5) — 1 мл 1%-ного раствора цитрата натрия. Растворы кипятили еще 5 мин и охлаждали до комнатной температуры. Препараты НКЗ хранили при +4—6°C в темноте.

Получение конъюгатов антител с препаратами НКЗ. Определяли количество МКА, оптимальное для конъюгации с НКЗ [14]. Растворы НКЗ доводили до pH 9.0 добавлением 0.1 M K_2CO_3. К 1 мл НКЗ добавляли 120 мкл раствора МКА в воде с концентрацией 0—120 мкг/мл, перемешивали и инкубировали 5 мин при комнатной температуре. Затем в каждую пробу добавляли 1 мл 2%-ного раствора NaCl, перемешивали, через 5 мин определяли оптическую плотность при 580 нм (D_{580}). Строили зависимости D_{580} от концентрации конъюгируемых МКА, т.н. кривые флокулляции. Величины стабилизирующих золь концентраций МКА лежали в диапазоне от 10 до 70 мкг/мл для различных препаратов НКЗ и клонов МКА.

Конъюгаты НКЗ с МКА к БТА, клон ВТА151 и НКЗ с МКА к БТВ, клон ВТВ224 получали следующим образом. К НКЗ с pH 9.0 при перемешивании добавляли выбранное количество МКА. Через 5 мин добавляли БСА до концентрации 0.25%. Конъюгат осаждали центрифугированием в течение 40 мин при 25000 g для НКЗ-1, для остальных НКЗ — в течение 25 мин при 12000 g. Осадки отмывали два раза 0.25%-ным раствором БСА и суспендировали в БХ. Оптическую плотность НКЗ и конъюгатов определяли в 1 см кювете на спектрофотометре СФ-102 (НПО "Интерфотофизика", Россия).

Электронная микроскопия. Для проведения электронной микроскопии образцы НКЗ наносили на медные сеточки, покрытые пленкой-подложкой из поливинилформаля. Снимки препаратов НКЗ получали на электронном трансмиссионном микроскопе JEM-1011 ("Jeol", Япония) при ускоряющем напряжении 80 кВ и увеличении 320000. Изображение фиксировали с помощью цифрового фотоаппарата ES500W ("Gatan", Германия). Величина выборки гранулометрического анализа варьировала в диапазоне 50—220 частиц для различных препаратов золя золота.

Расчет объема, диаметра НКЗ. Номинальный объем частицы V_{HK3}, нм^3, рассчитывали по фор-

муле: $V_{НКЗ} = 4\pi a^2 b/3$, где a, b (нм) — длины большой и малой полуосей эллипсоида вращения. Расчет диаметра частиц (d, нм), поученных цитратным методом, проводили по формуле: $d = 38.2V^{-0.855}$, где V (мл) объем 1%-ного раствора цитрата натрия в расчете на 100 мл НКЗ [11].

Приготовление буферных растворов. Готовили БХ следующего состава: (БХ-1) — водный раствор 10%-ной сахарозы и 0.25%-ного БСА; (БХ-2) — 0.05 М Трис, рН 8.5, с 10% сахарозы и 0.25% БСА; (БХ-3) — 0.05 М K-Na Фосфатный буфер (**ФБ**), рН 8.0, с 10% сахарозы и 0.25% БСА; (БХ-4) — 0.05 М Трис, рН 8.5, с 20% сахарозы и 0.25% БСА; (БХ-5) — 0.05 М Трис, рН 8.5, с 10% сахарозы и 1.0% БСА; (БХ-6) — 0.05 М Трис, рН 8.5, с 20% сахарозы и 1.0% БСА. Для проведения иммунохроматографического анализа готовили БА следующего состава: 0.1 М ФБ, рН 7.8, с 0.4% твин-20 и 0.25% БСА.

Получение иммунохроматографических тестов. Для получения иммунохроматографических тестов формировали мультимембранные коньюгаты, представляющие собой последовательно размещенные на единой подложке жесткости — мембрану из целлюлозной бумаги (CFSP) с нанесенным и высушенным конъюгатом НКЗ и МКА к определяемому соединению, аналитическую нитроцеллюлозную мембрану (HF120 или HF240), конечную впитывающую мембрану (CFSP). Указанные мембраны плотно прилегали друг к другу. Внесение определяемого соединения в БА на мембрану для нанесения образца обеспечивало регидратацию конъюгата, перенос капиллярными силами жидкости определяемого образца и иммунореагентов к аналитической и контрольной зоне теста, где были нанесены МКА к определяемому соединению и антивидовые, по отношению к АТ конъюгата, иммуноглобулины соответственно. Все использованные в работе мембраны были производства "Millipore" (США).

Конъюгат НКЗ с D 3.0 наносили на стекловолоконную мембрану GFSP (далее в тексте конъюгатная мембрана) в количестве 0.05 мл на 1 см подложки и высушивали. Для мультипараметрических тестов на конъюгатную мембрану последовательно наносили в равных количествах конъюгаты НКЗ с МКА ВТА151 и ВТВ224 либо проводили конъюгацию НКЗ определенного номинального размера со смесью МКА ВТА151 и МКА224, взятых в отношении 2 : 1 минимальных стабилизирующих концентраций, с последующим нанесением на мембрану и высушиванием.

При изготовлении монопараметрических тестов в аналитическую и контрольную зону нитроцеллюлозных мембран HF120 и HF240 наносили антитела с помощью диспенсера IsoFlow ("Imagene Technology", США). В аналитическую зону — растворы МКА ВТА232 против БТА или МКА КВВ18 против БТВ в 0.01М ФБ, рН 7.4, в количестве 50—150 нг антител на 1 мм² мембраны. В контрольную зону — КрАМ в количестве 100 нг/мм. В случае получения мультипараметрических тестов на нитроцеллюлозной мембране HF120 формировали две аналитические зоны из МКА ВТА232 и КВВ18.

Полученный мультимембранный коньюгат в условиях контролируемой влажности резали с помощью программируемой гильотины Matrix 2360 ("Kinematic Automation", США) на полоски размером 5 × 60 мм, которые помещали в пластиковые оправы с отверстиями для нанесения образца и считывания результата ("Advanced Microdevices", Индия). Полученные иммунохроматографические тесты до использования хранили в газонепроницаемых фольгированных пакетах в присутствии активированного силикагеля при комнатной температуре.

Условия проведения ИХА и регистрация результатов. ИХА проводили при комнатной температуре. В отверстие для нанесения образца пластиковой оправы иммунохроматографического теста вносили 120—150 мкл раствора определяемого соединения в БА. Регистрацию результата проводили визуально по появлению окрашенных полос в аналитической и контрольной зонах. Для получения количественных данных об интенсивности окрашивания линий иммунохроматограмм использовали видеоцифровые рефлектометры Рефлеком (ООО "Синтэко-Комплекс", Россия) и Зондаж (разработка ФГУП "ГосНИИ БП"). Показания прибора Рефлеком выше 0.3 усл. ед. достоверно указывали на положительный результат ИХА. Рефлектометр Зондаж позволял проводить регистрацию иммунохроматограмм и их последующую обработку при освещении в различных спектральных диапазонах — зеленом, красном, синем, а также освещении белым светом. Ширина спектральных линий светодиодных источников света прибора на полувысоте максимума эмиссии составляет 30, 28, 25 нм соответственно. Коэффициент вариации при измерении прибором Зондаж интенсивности окрашивания аналитической зоны иммунохроматограмм не превышал 6%, а при измерении окрашивания контрольной зоны — 1%. Индекс контраста (**ИК**) иммунохроматограмм [15] рассчитывали по формуле: ИК = $(S - S_0)/S_0$, где S_0 (отн. ед.) — показания рефлектометра вне области аналитической зоны при внесении БА (фоновый сигнал), S (отн. ед.) — показания рефлектометра в области аналитической зоны при различных концентрациях определяемого соединения (полезный сигнал).

Таблица 1. Характеристика препаратов НКЗ и их конъюгатов с МКА

Параметр	Препарат золя золота				
	НКЗ-1	НКЗ-2	НКЗ-3	НКЗ-4	НКЗ-5
Средний диаметр по длинной оси, ± стандартное отклонение, нм	13 ± 1	16 ± 3	23 ± 2	31 ± 5	47 ± 7
Средний диаметр по короткой оси, ± стандартное отклонение, нм	10 ± 1	12 ± 3	19 ± 2	26 ± 4	40 ± 6
Степень эллиптичности, ±стандартное отклонение	1.30 ± 0.13	1.27 ± 0.13	1.19 ± 0.12	1.20 ± 0.10	1.16 ± 0.10
Средний номинальный объем частицы, нм^3	0.93×10^3	1.58×10^3	5.32×10^3	1.30×10^4	4.62×10^4
Расчетный средний диаметр частицы, нм	–	–	25	31	40
Длина волны максимума поглощения НКЗ, нм	510	516	518	522	526
Длина волны максимума поглощения конъюгата с МКА, нм	520	526	528	528	532

РЕЗУЛЬТАТЫ И ИХ ОБСУЖДЕНИЕ

Гранулометрические и спектральные характеристики препаратов НКЗ и конъюгатов НКЗ с МКА. Представленные в табл. 1 данные демонстрируют, что полученные в результате восстановления $HAuCl_4$ боргидридом, аскорбатом или цитратом натрия НКЗ имеют сферическую форму или форму эллипсоида вращения с невысокой степенью эллиптичности. Распределение НКЗ по размерам в каждом из полученных препаратов было асимметричным, близким к нормальному.

Спектры поглощения НКЗ демонстрируют красный сдвиг положения максимума по мере увеличения средних размеров НКЗ. То же самое можно сказать и о конъюгатах с МКА. Образование белковых слоев (полислои) на поверхности НКЗ приводит к небольшому, но закономерному сдвигу максимума поглощения по сравнению с НКЗ. Такой же спектральный сдвиг наблюдали при конъюгации НКЗ с овомукоидом в работе [11].

Таблица 2. Влияние состава буфера хранения конъюгата и pH БА на интенсивность окрашивания аналитической зоны в отсутствие специфического соединения

Буфер хранения	Интенсивность окраски аналитической зоны, усл. ед.		
	pH БА		
	4.9	6.0	7.8
БХ-1	9.3	2.3	0
БХ-2	4.2	1.2	0
БХ-3	3.1	1.5	0
БХ-4	3.1	1.1	0
БХ-5	3.8	0.9	0
БХ-6	2.1	0.3	0

Расчетные значения средних диаметров частиц, полученных восстановлением цитратом натрия, практически совпадали с экспериментальными.

Разработка монопараметрических тестов для выявления БТ. Полученные конъюгаты НКЗ различных номинальных размеров использовали для построения иммунохроматографических тестов. Применили "сэндвич" формат иммунохроматографического теста, в котором использовали МКА, специфичные к различным антигенным эпитопам белковых цепей токсина. Одно из МКА было конъюгировано с НКЗ, а второе — наносилось в аналитическую зону теста. Образовавшийся окрашенный комплекс определяемого соединения, конъюгата и МКА формировал аналитический сигнал, который был пропорционален концентрации определяемого соединения. Для поиска наиболее оптимальной, с точки зрения уменьшения предела обнаружения, конфигурации теста варьировали следующие параметры: номинальный размер НКЗ для получения конъюгатов, нагрузка антител на НКЗ, плотность нанесения антител в аналитическую зону аналитической мембраны, состав БХ и БА. Основные экспериментальные результаты по подбору состава БХ и БА приведены в табл. 2. Смещение pH БА из кислой в щелочную область позволило полностью избежать неспецифической сорбции конъюгатов в аналитической зоне при прохождении пробы, не содержащей определяемого соединения. Явление неспецифической сорбции может привести к появлению ложноположительных результатов ИХА. Замена БХ-2, содержащего фосфатный буфер с 10% сахарозы и 0.25% БСА, pH 8.0, на буфер БХ-6, содержащий 0.05 M Tris с 20% сахарозы и 1.0% БСА, pH 8.5, также уменьшало явление неспецифической сорбции конъюгата в аналитической зоне.
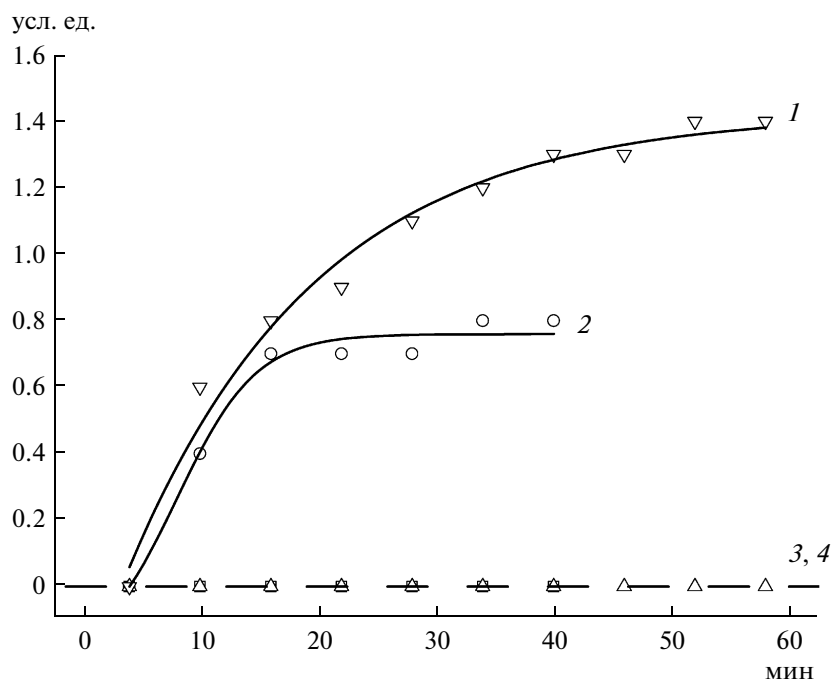
Рис. 1. Зависимость интенсивности окрашивания (усл. ед.) аналитической зоны иммунохроматограммы от времени анализа (мин) и типа применяемых аналитических мембран. *1* — мембрана HF240, *2* — мембрана HF120, *3* — отрицательный контроль для мембраны HF240, *4* — отрицательный контроль для мембраны HF120. Концентрация определяемого соединения 2.5 нг/мл БТА.

На возможное появление неспецифической сорбции конъюгата в аналитической зоне значительно влиял состав БХ. Наименее подвержены влиянию pH оказались иммунохроматографические тесты, построенные с использованием БХ-6. При сравнении пределов обнаружения БТ наилучший результат показал тест, где использовался БХ-1, но этот тест оказался наиболее чувствителен к изменению величины pH БА, что, возможно, объясняется отсутствием солей в составе данного БХ. Поэтому, при выборе БХ в процессе оптимизации иммунохроматографических тестов, в большей степени руководствовались целью уменьшения неспецифической сорбции конъюгата в аналитической зоне. В итоге использовали, как компромиссный вариант, тесты, построенные на основе конъюгатов в БХ-6 и применяли БА с величиной pH 7.8.

Предел обнаружения БТ уменьшался при увеличении концентрации МКА в аналитической зоне с 50 до 150 нг/мм и увеличении нагрузки конъюгатов по белку антител до величины, в 2 раза превышающей минимальную стабилизирующую концентрацию. Дальнейшее увеличение нагрузки конъюгатов приводило к появлению неспецифической сорбции конъюгатов в аналитической зоне. Наименьший предел обнаружения БТ — 0.5—1.0 нг/мл достигался на мембранах HF120 (скорость латерального течения жидкости — 120 ± 30 с/4 см) за время 30 мин.

Применение более "медленных" аналитических мембран HF240 (скорость латерального течения жидкости — 240 ± 75 с/4 см) не приводило к уменьшению предела обнаружения, но увеличивало время анализа до 50 мин (рис. 1). Причем у иммунохроматографических тестов с НКЗ-5 и аналитической мембраной HF240 наблюдали появление неспецифической сорбции конъюгата к 30 мин времени анализа.

Сравнение предела обнаружения тестов, построенных с использованием НКЗ различного размера, при прочих равных условиях (рис. 2), показало, что применение НКЗ с номинальным диаметром 31 и 47 нм приводило к уменьшению предела обнаружения. Это явление может быть связано с увеличением аффинности конъюгатов НКЗ большого размера, как это было показано в работе [7].

Разработка и аналитические свойства мультипараметрических тестов. Мультипараметрические тесты отличались от монопараметрических наличием двух аналитических зон (A_1 и A_2), в которые были нанесены МКА, специфичные к БТА и БТВ соответственно, и одной контрольной зоны, сформированной из КрАМ. Для получения конъюгата использовали НКЗ-5 с номинальным размером частиц 47 нм. Наблюдаемая картина при анализе индивидуальных токсинов или их смеси мультипараметрическими тестами приведена на рис. 3. Предел обнаружения мультипараметриче-
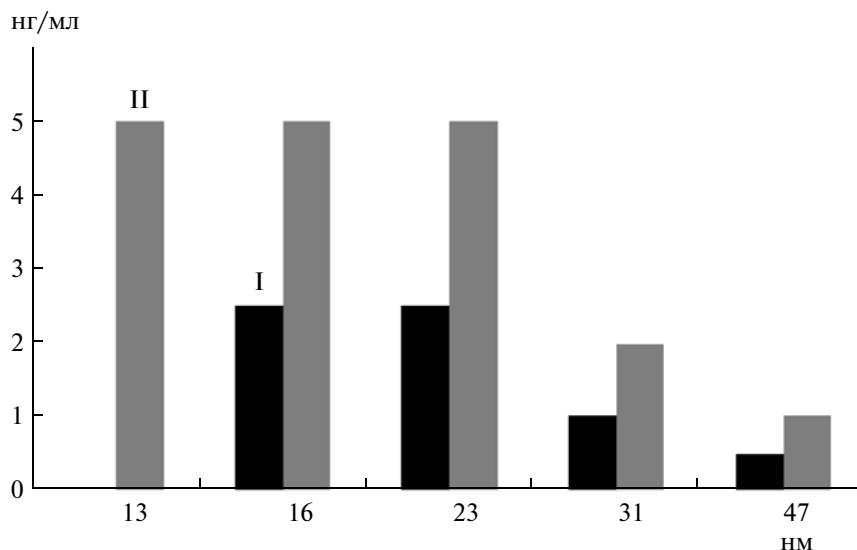
Рис. 2. Зависимость определяемого обнаружения БТ (нг/мл) от номинального размера НКЗ конъюгатов (нм) при прочих равных условиях. I — БТА; II — БТВ. Нагрузка конъюгата равна стабилизирующей концентрации МКА. Концентрация МКА в аналитической зоне 100 нг/мм. Тип мембраны HF120.
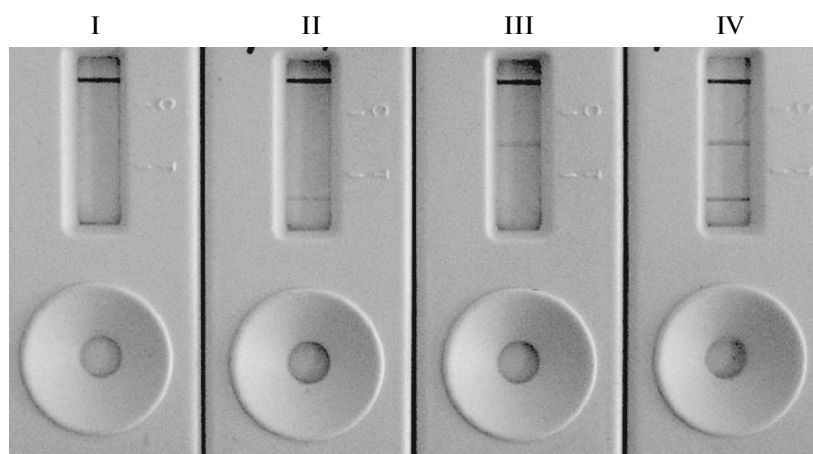

Рис. 3. Внешний вид иммунохроматограмм при мультианализе БТ. I — 0 нг/мл БТА и БТВ (отрицательный контроль), II — 10 нг/мл БТА, III — 10 нг/мл БТВ, IV — смесь, содержащая 10 нг/мл БТА и 10 нг/мл БТВ.

ского теста был несколько выше, чем у монопараметрических тестов как в режиме определения индивидуальных соединений, так и их смесей. Исследовали два способа формирования конъюгатной подложки для мультипараметрического теста. Первый — получение конъюгата из смеси антител (см. методику), второй — получение двух конъюгатов с индивидуальными антителами и их последующее смешивание в равных пропорциях на конъюгатной мембране.

Предел обнаружения тестов, в которых использовался второй способ формирования конъюгатной подложки, составил 10 нг/мл по БТА и

БТВ, в то время как применение первого способа позволило уменьшить его до 5 нг/мл.

Специфичность разработанных нами моно — и мультипараметрических тестов была проверена на модельных растворах, содержащих 500—10 000 нг/мл БТА, БТВ или БТЕ, а также 1.0 мкг/мл дифтерийного и столбнячного анатоксинов. Ни для одного из перечисленных выше определяемых соединений не наблюдалось ложноположительных реакций при проведении ИХА с помощью разработанных тестов.

Приведенные данные по пределу обнаружения моно- и мультипараметрических тестов относят-

ся к модельным растворам в БА. Известно, что матрикс, в котором содержится определяемое соединение, может существенно влиять на предел обнаружения. Представляло интерес определить предел обнаружения разработанных иммунохроматографических тестов при выявлении БТ в других матриксах. Учитывая, что продуцентом БТ являются анаэробные микроорганизмы, БТ вносили в овощные, рыбные и мясные консервы с последующим проведением ИХА. Чтобы уменьшить влияние матрикса, перед ИХА проводили процедуру пробоподготовки, которая заключалась в гомогенизации и суспендировании образца консервов в БА, удалении твердых частиц и жиров центрифугированием и ультразвуковой обработкой, доведении уровня pH образца до 7.0—8.0. Работу проводили с использованием монопараметрических тестов, для построения которых использовали препарат НКЗ-3 и БХ-6. В качестве экстрагирующего буфера использовали БА. Эксперименты показали, что предел обнаружения БТА повышался от 7 раз (овощные консервы) до 13 раз (мясные консервы), а при выявлении БТВ повышение предела обнаружения составило от 10 до 20 раз, по сравнению с модельными образцами. Однако подробное изучение влияния матрикса и процедуры пробоподготовки на предел обнаружения ИХА БТ не входило в цели данной статьи.

В наших исследованиях для получения количественных данных широко использовалась ВЦР результатов ИХА. ВЦР основана на анализе цифровых снимков иммунохроматограмм специализированными программами, позволяющими определять интегральную интенсивность поглощенного света аналитической и контрольной зоны, сформированных окрашенными частицами конъюгата. Для достижения наибольшей чувствительности регистрации должен существовать максимальный контраст между фоном мембраны и окрашенными зонами иммунохроматограммы. Учитывая, что НКЗ и его конъюгаты имеют широкие бесструктурные полосы поглощения в диапазоне 500—600 нм, контраст должен зависеть от спектрального состава освещения иммунохроматограммы. С помощью прибора Зондаж, позволяющего осуществлять освещение иммунохроматограмм в различных диапазонах видимого света, изучили значения ИК для иммунохроматографического теста при выявлении БТВ (рис. 4), в котором использовали НКЗ-3 с размером частиц 23 нм. Наибольшие значения ИК были получены при освещении зеленым светом, а наименьшие — красным. Освещение белым светом дало промежуточные значения ИК. Аналогичная картина наблюдалась и для НКЗ-5 с размером частиц 47 нм. Таким образом, использование зеленого освещения понижало предел обнаружения ВЦР иммунохроматограмм, в которых использовались НКЗ. Соответственно, при применении в каче-
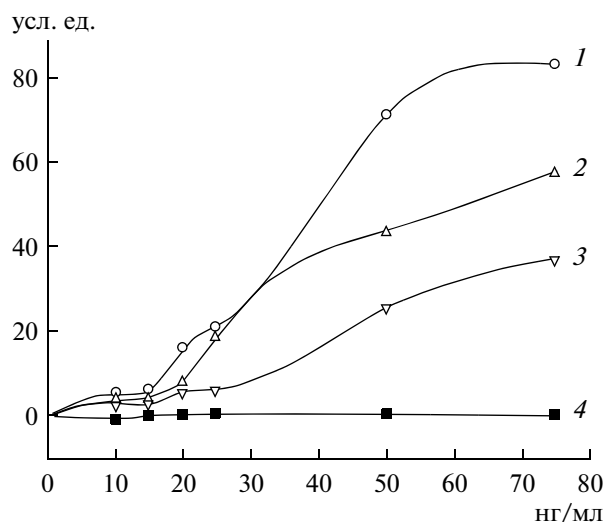

Рис. 4. Зависимость ИК аналитической зоны иммунохроматограмм от концентрации БТВ (нг/мл) и спектрального диапазона освещения при ВЦР на приборе Зондаж. *1* — зеленый свет (525 нм), *2* — синий свет (470 нм), *3* — белый свет, *4* — красный свет (630 нм).

стве дисперсной фазы в иммунохроматографических тестах, окрашенных в различные цвета латексных частиц или золей для повышения ИК, целесообразно использовать освещение в разных спектральных диапазонах.

Разработаны иммунохроматографические моно- и мультипараметрические тесты для определения БТ, которые имеют предел обнаружения 0.5—5.0 нг/мл, сравнимые по порядку величины с ИФА — 0.1 нг/мл. Мультипараметрический тест для выявления двух типов БТ разработан впервые нами. Выбор объектов исследования (БТА и БТВ) из всей гаммы нейротоксинов, продуцируемых токсикогенными штаммами *Clostridium botulinum* для построения иммунохроматографических тестов, обусловлен их наибольшей токсичностью, широкой распространенностью и практическим применением в медицинских препаратах.

Тесты имеют определенные преимущества по сравнению с ИФА, а именно: процедура проведения анализа более проста и менее длительна по времени (десятки минут), не включает стадий промывания и сенсибилизации планшетов, равно как и необходимости использования субстратов для проведения ферментативной реакции.

Использование инструментальных методов регистрации, в частности ВЦР, расширяет возможности ИХА за счет более объективной регистрации результата и получения количественных данных. Разработанные иммунохроматографические тесты могут быть использованы для экспресс-анализа качества продуктов питания, контроля содержания БТ в фармацевтических препаратах, контроля окружающей среды.

СПИСОК ЛИТЕРАТУРЫ

1. *Тимаков В.Д.* Микробиология. М.: Медицина, 1973. 432 с.

2. *Ракова И.Д., Гуржей С.Н., Сметанин Н.Н.* // Медицина экстремальных ситуаций. 2010. Т. 33. № 3. С. 71—73.

3. *Arnon S.S., Schechter R., Inglesby T.V., Henderson D.A., Bartlett J.G., Ascher M.S.* // JAMA. 2001. V. 285. № 8. P. 1059—1070.

4. *Ferreira J.L., Maslanka S., Johnson E., Goodnough M.* // J. Assoc. Off. Agric. Chem. Int. 2003. V. 86. № 2. P. 314—331.

5. *Sharma S.K., Eblen V.S., Bull R.L., Burr D.H., Whiting R.C.* // Appl. Environ. Microbiol. 2005. V. 71. № 7. P. 3935—3941.

6. *Wong R.C., Tse H.Y.* Lateral Flow Immunoassay. N. Y.: Humana Press, 2009. 223 p.

7. *Safenkova I.V., Zherdev A.V., Dzantiev B.B.* // J. Immunol. Methods. 2010. V. 357. № 1—2. P. 17—25.

8. *Бызова Н.А., Сафенкова И.В., Чирков С.Н., Жердев А.В., Блинцов А.Н., Дзантиев Б.Б, Атабеков И.Г.* // Прикл. биохимия и микробиология. 2009. Т. 45. № 2. С. 225—231.

9. *Старовойтова Т.А., Зайко В.В., Волощук С.Г., Стериополо Н.А., Мартынкина Л.П., Савина М.И., Зайцева Н.А., Тогузов Р.Т., Венгеров Ю.Ю.* // Клиническая лабораторная диагностика. 2005. № 9. С. 24—25.

10. *Ярков С.П., Третьяков С.И., Башарова Л.А., Злобин В.Н.* // Вестник РАМН. 2007. № 12. С. 22—26

11. *Хлебцов Н.Г., Богатырев В.А., Дыкман Л.А., Мельников А.Г.* // Коллоидный журнал. 1995. Т. 57. № 3. С. 412—423.

12. *Hermanson G.T.* Bioconjugate Techniques. London: Acad. Press, 1996. 785 p.

13. *Frens G.* // Nature Phys Sci. 1973. V. 241. № 1. P. 20—22.

14. *Horisberger M., Rosset J.* // J. Histoch. Cytochem. 1977. V. 25. № 4. P. 295—305.

15. *Qian S., Bau H.H.* // Anal. Biochem. 2003. V. 322. № 1. P. 89—98.

Development and Optimization of Immunoassays for the Detection of Botulinum Toxins

A. A. Titov, I. V. Shilenko, A. A. Morozov, S. P. Yarkov, and V. N. Zlobin

State Research and Development Institute of Biological Engineering, Moscow, 125424 Russia

e-mail: niibp@dol.ru

Abstract—Monoparametric immunoassay tests for detecting botulinum toxins types A and B and multiparametric assays for simultaneous detection of botulinum toxins type A and B have been developed. It is shown that the sensitivity of assays is affected by the size of nanoparticles of colloidal gold used as a marker of antibodies, load intensity of antibodies of colloidal gold in conjugates, the type of analytical membranes, as well as the chemical composition of buffer solutions used for the storage of conjugates and immunoassay analysis. The detection limit of monoparametric immunoassay tests is 0.5 ng/ml; that of multiparametric assays, 5.0 ng/ml. The developed immunoassay can be used for rapid assay of product quality, for grade control of botulinum toxins in pharmaceuticals, and environmental monitoring.